Model-based assessments of freshwater ecosystems and species under climate change

Doctoral dissertation

Oskar Kärcher
Osnabrück University

Model-based assessments of freshwater ecosystems and species under climate change

Dissertation thesis
for the degree of
Doctor of Natural Sciences (Dr. rer. nat.)

Institute of Environmental Systems Research
Division of Mathematics/ Computer Science
Osnabrück University

Submitted by

Oskar Kärcher

Osnabrück, 2019

Abstract

Climate change, global warming and anthropogenic disturbances are threatening freshwater ecosystems globally. The protection and preservation of freshwater environments, its biodiversity and all of its services for human well-being requires comprehensive knowledge of the impacts that climate change and anthropogenic disturbances have on freshwaters and freshwater species. In-depth knowledge needed for conservation strategies can be established through versatile assessments. Quantitative assessments and the investigation of prevailing environmental relationships within ecosystems constitute the basis for sustaining freshwater systems. However, it is a great challenge to quantify the multifaceted effects of climate change and to broaden the understanding of complex environmental relationships.

This thesis aims at contributing to an extension of the understanding of climate change impacts on freshwater ecosystems and environmental relationships, which implies the provision of useful guidelines for the protection and preservation of freshwaters. For this, various statistical approaches based on comprehensive data sets are applied at different scales, ranging from local to global assessments. In particular, five research studies investigating the (1) water quality-nutrient and temperature relationships in European lakes, (2) drivers of freshwater fish species distributions across varying scales in the Danube River delta, (3) globally derived thermal response curves and thermal properties of native European freshwater species, (4) differences between thermal properties derived from native and global range data, and (5) thermal performances of freshwater fish species for different life stages and different global future dispersal scenarios are presented to address the effects of environmental change.

Main results of this thesis comprise various aspects of conservation implications and planning. (i) The first study outlines drivers influencing water quality through studying multi-dimensional relationships and compares different modelling techniques in order to outline models that are suitable for the identification of complex driver interactions. (ii) The second study addresses scale effects on the performance of species distribution models, which are commonly used for assessments of climate change impacts, and identifies key predictors driving distributions for the varying scales and studied species. (iii) The third study parameterizes thermal responses of species from different taxonomic groups and assesses the potential resilience in terms of warming tolerance and additional thermal properties as well as the influence of future rising temperatures on current distributions. (iv) The fourth study quantifies the differences in thermal response curves and thermal properties for freshwater fishes derived from global and continental data in order to clarify the need for using global range data in studies making suggestions for conservation planning. (v) The last study estimates the impact of changing climatic conditions on species distribution ranges of two fish species for different time periods by including biotic information about thermal performances for various life stages.

Overall, this thesis contributes to the broad field of studying consequences and impacts of climate change on freshwater ecosystems. By applying statistical methods tailored to the underlying investigations, useful implications for conservation planning are derived.

Contents

PART I

Introduction, Methodology and Data

Chapter 1

Introduction

Background and challenges

Global challenges of ecosystems

Changes in ecosystems are accumulating globally. Marine, terrestrial and freshwater ecosystems are affected in various ways. Covering around 71% of the Earth's surface (Hoegh-Guldberg and Bruno, 2010), marine ecosystems show increased disease outbreaks, spreading of invasive species, novel species assemblages, shifting fauna, acidification, primary production decreases, mass coral bleaching and mortality as well as loss of dissolved oxygen (Hoegh-Guldberg and Bruno, 2010; Lejeusne et al., 2010; Deutsch et al., 2015). Terrestrial biota faces distributional shifts, phenological shifts, changes in species morphology, population size decreases and even population extinctions (Parmesan et al., 2000; Pereira et al., 2010; Burrows et al., 2011). For freshwater ecosystems, which cover less than 1% of the Earth's surface, but are home to around 6% of all known species (Strayer and Dudgeon, 2010), also shifts in species distributions and phenology as well as eutrophication of lakes, changes in population assemblages, extinctions and plastic shifts of various species traits are observed (Nussey et al., 2005; Parmesan, 2006; Durant et al., 2007; Deutsch et al., 2008; Woodward et al., 2010; Poikane et al., 2014).

These exemplary alterations in ecological systems have multiple causes; however, one of the greatest stressors is climate change and especially global warming. It is expected that the global surface temperature increase for the end of the 21st century is likely to exceed 2°C compared to 1850 to 1900 (IPCC, 2013). Due to their characteristics, such as being fragmented habitats, and additional multiple anthropogenic stressors from the surrounding landmasses, global freshwaters are particularly vulnerable to warming temperatures (e.g. Woodward et al., 2010; Markovic et al., 2017).

Freshwater ecosystems under climate change

Freshwater ecosystems provide various ecosystem services for humans, e.g. recreational possibilities, clean water and food resources (Daily, 1997; Science for Environment Policy, 2015; Green et al., 2015). Preserving these benefits is among other things intrinsically linked to monitoring and improving water quality across freshwater environments. Specifically, lakes as vital resources for freshwater biodiversity and human needs require actions to sustain the functional structure. However, progressing eutrophication is observed across many lake ecosystems and threatening their integrity (e.g. Albrecht and Wilke, 2008). Major factors of water quality degradation are climate change and anthropogenic pollution originating from growth in tourism, rapid urbanization, land use intensification and water uptake (e.g. Matzinger et al., 2006; Kraemer et al., 2017). It is thus of high importance to understand the prevailing connections and relationships that influence water quality in order to adjust sustainable management actions, which aim at preserving the benefits provided by lake ecosystems.

Beside the indirect influence of climatic stressors on biodiversity and species distributions through water quality (e.g. Verberk et al., 2016), a direct influence of climate change on freshwater species is, for example, associated with the key environmental driver temperature (Krenek et al., 2011; Schulte et al., 2011; Kärcher et al., 2019). Temperature as abiotic factor is known to influence species on different levels. It is influencing species' traits and thus its physiological performance such as the rate of development, growth, metabolic processes and the seasonal timing of life history events (Jonsson and d'Abée-Lund, 1993; Wootton, 1998; Krenek et al., 2011; Scranton and Amarasekare, 2017). Furthermore, temperature has different effects on different life stages of a species. For example, the life stage "eggs" of fish species is the most vulnerable to climate change (e.g. Elliott and Elliott, 2010). The comprehensive influence of temperature and climatic factors in general on biodiversity and single species within freshwater ecosystems underlines the necessity of various investigations and the usage of proper approaches for understanding the impacts of climate change and global warming.

Previous studies have identified transitions from cold-water to warm-water species, called thermophilisation, which implies the increasing dominance of warm-water species (Jeppesen et al., 2012; De Frenne et al., 2013), poleward and altitudinal shifts, population declines, range losses and changes in abundance based on climatic changes (Henle et al., 2010; D'Amen et al., 2011; Isaak et al., 2011; Comte et al., 2013; Domisch et al., 2013a; Markovic et al., 2014). Several conservation actions have been developed in order to reduce these biodiversity threatening impacts across current species habitats (e.g. Lassalle et al., 2008). However, changing climatic conditions might alter the current habitat structures and reduce their suitability in the future. Given the result of range shifts and the ongoing climate change, species will track their niche throughout the freshwater network (Comte et al., 2013; Domisch et al., 2013a). Niche tracking of strictly aquatic species can be severely disturbed by the fragmentation of most large rivers due to constructed dams and artificial barriers (Limburg and Waldman, 2009; Lassalle et al., 2008, 2010). Anthropogenic disruption of the habitat network was shown to be a major factor reducing climate change resilience (Markovic et al., 2017), as this distribution constraint might force the species to adapt to changing environmental conditions or eventually lead to extinction (Angilletta, 2009). For preventing the latter scenario, assessments of future distributions have to include information on dispersal possibilities and different scenarios in order to provide guidelines for potential adjustments of already implemented conservation actions.

In regard of the ample evidence for climate change impacts on freshwater ecosystems, many questions about future states of these ecosystems and the species within arise. For this reason, it is of high importance to evaluate the impact of climate change by investigating freshwater ecosystems in various comprehensive ways and to provide a useful insight into the prevailing relationships within ecosystems in order to understand the complexity and to preserve the precious gifts of ecosystems and its biodiversity.

Objectives

This thesis aims at investigating complex relationships of water quality and climatic influences on freshwater species distributions at different scales. Water quality is studied at the scale of European lake ecosystems while climatic impacts on freshwater biodiversity are investigated at scales ranging from local to global. The following research questions are addressed:

1) How can the water quality relationships in European lake ecosystems be described for different modelling techniques?

Studying water quality relationships has already a long history (Sakamoto, 1966; Dillon and Rigler, 1974) and many different modelling methods were used to derive information about water quality drivers and the corresponding dependencies (e.g. Bachmann et al., 2012; Magumba et al., 2013). It is, however, unclear which modelling category is the most suitable for investigating water quality influences. Moreover, comparisons of derived water quality relationships using the same data basis are missing.

2) Are there differences in the model performance and the identification of drivers of freshwater fish species distributions across varying spatial scales?

Scale effects on the performance of niche-based species distribution models have commonly been studied using grid cell data of, for example, bird, plant and vertebrate species (Guisan et al., 2007; Lauzeral et al., 2013). In regard of climate change threats to freshwater ecosystems and data availability at different scales, it is of fundamental importance to address scale effects on the performance of species distribution models and climatic/ non-climatic drivers of species distributions. Comparable studies that use multiple grain-size resolutions at the catchment-scale and species distribution models for freshwater species do not exist.

3) What are the thermal properties of native European freshwater species in regard of climate change?

Investigations of macroecological patterns, thermal properties and thermal responses of species to temperature have been commonly restricted to single taxonomic groups and bounded spatial scales (Hickling et al., 2005; Buisson et al., 2010; D'Amen et al., 2011). Comparative studies delineating responses of species to temperature from various taxonomic groups at global scales are missing. Current data availability allows for overcoming previous restrictions.

4) How strong are the differences between thermal properties derived from native and global range data of freshwater species?

Many recent studies have used local to continental species occurrence data and bioclimatic models to derive species' thermal niches (e.g. Lassalle et al., 2008, 2010; Logez et al., 2012; Domisch et al., 2013a). Those are then used towards evaluating climate change impacts on species distributions and conservation planning. However, com-

parisons of thermal properties inferred from native and global occurrence data are rarely quantified.

5) How will the species' performance of freshwater fish for different life stages change in the future based on different dispersal scenarios?

Only a few studies have confronted species distribution model predictions with species functional traits (e.g. Wittmann et al., 2016). The inclusion of species traits in niche modelling techniques under consideration of different life stages and dispersal scenarios is missing. Thus, it is unclear how species' performances will develop in the future and how distribution patterns may look like.

Overall, this thesis seeks to provide several examples of climate change influences, drivers of species distributions and drivers of water quality. Throughout the investigations, different modelling frameworks are used, which aim at describing the complex relationships and which are tailored to the given data.

Structure of the thesis

This thesis is composed of three parts. The first part (Part I) introduces the knowledge gap and objectives (Chapter 1) and gives a brief overview of the methodology and data (Chapter 2). The second part (Part II) includes five individual research studies (Chapters 3-7). Chapter 3 applies different modelling approaches to a water quality database of European lakes. The performances of the modelling approaches are compared and multi-dimensional water quality relationships are derived. Model performance is additionally tested for mountain lakes. In Chapter 4, performance of fish species distribution models is tested across different scales. Occurrence data from the Danube River Basin, hierarchical catchment ordering and multiple environmental factors are used to identify scale effects for freshwater fish. Chapter 5 identifies thermal response curves of several taxonomic groups at the global scale. Species distributions along thermal gradients are then used to assess future climatic impacts for Europe. In Chapter 6, the utilization of native and global range data is compared. The comparison includes thermal responses, thermal properties and future impacts of temperature increases. Chapter 7 investigates species thermal performance for three main life stages (adults, juveniles, eggs) based on collected species traits data. Thermal performance is assessed for current and future scenarios. Future scenarios include model predictions of different statistical techniques and several dispersal possibilities, which incorporate habitat connectivity. The third part (Part III) comprises a general discussion and the main conclusions of the overall results of this thesis (Chapter 8). Methodological frameworks are discussed in terms of model limitations and future perspectives.

Chapter 2

Methodology and data

Modelling approaches and tools

Various statistical models are used for the investigations and predictions in this thesis. Statistical modelling techniques have in general a broad application range. Models that particularly address the explanation of species distribution ranges are called species distribution models (SDMs) (e.g. Buisson and Grenouillet, 2009; Markovic et al., 2012; Comte and Grenouillet, 2013; Domisch et al., 2013a; Filipe et al., 2013). By relating current environmental conditions as predictor variables across the study area to the target variable, here water quality or species distributions, the models are able to uncover prevailing relationships and to project the target variable. Identification of relationships and predictions, however, are limited to the given data used for model calibration. For example, derived from observed presences SDMs assume that species will track current habitat conditions, i.e. its current climatic niche, in the future (Thuiller, 2003; Franklin, 2009). Statistical approaches have been extensively studied in ecological applications. Previous studies demonstrate statistical models as valuabe tools for studying biogeography, ecology and impacts of climate change. Found relationships are providing suggestions for ecosystem conservation and management (e.g. Wittmann et al., 2016). However, the importance of attributes of individual methods, choice of a well-founded predictor set, and sources of uncertainty have to be considered for useful inferences (e.g. Araújo and Guisan, 2006; Marmion et al., 2009; Grenouillet et al., 2011; Markovic et al., 2012).

In this thesis, a broad set of statistical approaches written for R (R Development Core Team, 2018) is used for deriving conservation relevant inferences (Table 1). Panel Data Models (PDM) are linear regression methods that can account for fixed individual/time effects, random individual/ time effects or that can simply pool the data to obtain a multiple linear regression (e.g. Magumba et al., 2013). In order to uncover certain effects, a panel structure of the data must be given. Generalized Additive Models (GAM) are non-parametric methods, which use a sum of smooth functions to model non-linear relationships between the predictor and target variables (Hastie and Tibshirani, 1986). Boosted Regression Trees or Gradient Boosting Machines (BRT/ GBM) are a group of decision trees, which are built and combined by the gradient boosting algorithm, i.e. each single tree within the group of trees of the BRT model is determined successively by fitting the residuals at each step. BRTs/ GBMs are able to express non-linear relationships and interactions between predictors due to the structure of decision trees (Hastie et al., 2001; Elith et al., 2008). Artificial Neural Networks (ANN) are complex, non-linear model systems. ANNs resemble the biological brain in the sense that they include a certain number of nodes called neurons that are connected via different types of so-called activation functions like synapses in a brain in order to transmit information (Bishop, 1995; Jain et al., 1996; Duda et al., 2001; Hastie et al., 2001; Li and Wang, 2013; Lee et al., 2016). Random Forest (RF) consists of a certain number of decision trees. Each tree of the forest is built by using a random sample of the training data set and predictor variables, respectively (Breiman, 2001a). Multivariate Adaptive Regression Splines (MARS) are based on piecewise splines that are smoothly connected at the transitions. They are able to model linear and non-linear relationships (Friedman, 1991; Zhang and Goh, 2016). Maximum Entropy Method (MAXENT) is a principle from statistical mechanics and information theory, which can

be applied generally (Phillips et al., 2006). As SDM, MAXENT uses only presence data for calibration. Under the constraint of the calibration data, it estimates the target probability distribution by finding the probability distribution of maximum entropy (Phillips and Dudík, 2008). Elastic Net (ELNET) consists of a Generalized Linear model (GLM) with additional penalty terms for coefficient determination. These penalty terms are associated with Lasso and Ridge regularization, which refer to L1- and L2-regularization (Friedman et al., 2010).

In order to adjust the statistical methods to the given data situation and research questions, parameter tunings were conducted if required.

Table 1 Statistical modelling techniques and corresponding R packages used for analyses in the thesis.

Method	Abbreviation	R package	Version	Reference
Panel Data Models	PDM	plm	1.6-5	Croissant and Millo, 2008
Generalized Additive Models	GAM	mgcv	1.8-17	Wood, 2011
		gam	1.15	Hastie, 2016
Boosted Regression Trees/ Gradient Boosting Machines	BRT/ GBM	gbm	2.1.3	Ridgeway, 2017
		h2o	3.20.0.8	The H2O.ai team, 2018
Artificial Neural Networks	ANN	h2o	3.20.0.8	The H2O.ai team, 2018
Random Forest	RF	h2o	3.20.0.8	The H2O.ai team, 2018
Multivariate Adaptive Regression Splines	MARS	earth	4.4.7	Milborrow, 2018
Maximum Entropy Method	MAXENT	dismo	1.1-1	Hijmans et al., 2017
Elastic Net	ELNET	h2o	3.20.0.8	The H2O.ai team, 2018

Data strategy

Study areas

This thesis comprises various study areas from local to global ranges (Table 2). Chapter 3 (Part II) investigates water quality relationships at the scale of 157 European lakes. In Chapter 4, the Danube river basin with hierarchical catchment ordering is used as study area. Scale effects in the Danube river basin are investigated by considering five different catchment levels with the number of catchments ranging from 126 to 1,363. For deriving thermal properties and responses of freshwater species, the whole currently known and available global range is used in Chapter 5 with in total 209,659 catchments. Thermal property results are afterwards used for assessing future climatic impacts in Europe (16,689 catchments). Chapter 6 compares inferences from native and global range data of European freshwater species at the catchment scale. At the global and European scale, 228,064 and 18,767 catchments are utilized, respectively. For model calibration of the SDMs, global distribution data mapped to 11,695 catchments is used in Chapter 7.

Table 2 Scales used in the application studies.

Study	Scale	Specification
Chapter 3	Europe	157 lakes
Chapter 4	local	Danube river basin, 126-1,363 catchments
Chapter 5	global; Europe	209,659; 16,689 catchments
Chapter 6	global; Europe	228,064; 18,767 catchments
Chapter 7	global	11,695 catchments

Species data

Species distribution data of several taxonomic groups (crayfish, fish, molluscs, odonates, plants) consisted of presence and absence data in Part II (Table 3). In Chapter 4, species occurrence data in the Danube River Basin were provided by the EU-funded project Biofresh (www.freshwaterplatform.eu, Schinegger et al., 2016). Fish occurrence data were mapped to the different catchment scales. Species data in Chapter 5 were obtained from the IUCN Global Species Programme (IUCN, 2013, 2014). Presence and absence data on freshwater species distribution ranges were provided in polygon shape files corresponding to global watershed boundaries. Afterwards, freshwater species data were mapped to the catchment scale. Global data of 577 freshwater species native to Europe (5 crayfish, 220 fishes, 99 molluscs, 75 odonates, 178 plants) were used in the final analysis. Analogously, for Chapter 6, distribution data were derived from the IUCN Global Species Programme for four fish species native to Europe (*Coregonus sardinella*, *Pungitius pungitius*, *Rutilus rutilus* and *Salvelinus alpinus*). Chapter 7 comprised the investigations of two freshwater fish species, namely *Salmo trutta* and *Salmo salar*. Distribution data were obtained from the Global Biodiversity Information Facility (GBIF). Occurrences were mapped to the corresponding catchment scale. Additionally, laboratory experiment data on species thermal traits for *Salmo trutta* and *Salmo salar* at different life stages from various studies were collected (see Table S3 and S4 in Appendix 5).

Table 3 Species occurrence data sources of the application studies.

Study	Taxonomic group	Species number	Source
Chapter 3	NA	NA	NA
Chapter 4	fish	8	Biofresh project www.freshwaterplatform.eu
Chapter 5	crayfish, fish, molluscs, odonates, plants	577	IUCN Global Species Programme https:// www.iucn.org/theme/species/our-work/iucn-red-list-threatened-species
Chapter 6	fish	4	IUCN Global Species Programme https:// www.iucn.org/theme/species/our-work/iucn-red-list-threatened-species
Chapter 7	fish	2	Global Biodiversity Information Facility https://www.gbif.org/

"Critical minimum temperature for survival" (CT_{min}), "optimum temperature" (T_{opt}) and "critical maximum temperature for survival" (CT_{max}) for the life stages adults, juveniles, and eggs were extracted.

Environmental data

Due to the dependence of statistical models on the data quality, reliable and validated sources had to be selected in Part II. Environmental data strategy focused on collecting comprehensive and up to date data for the respective research questions (Table 4). Therefore, Chapter 3 did not only include *in situ* observations of physical and chemical water quality parameters from the Waterbase-Lakes database provided by the European Environment Agency but also satellite-based data on lake surface water temperature derived from the Riffler et al. (2015) data set and from the ARC-Lake data set (see Table 4). In Chapter 4, predictor variables from various sources were used to explain species distributions. Topographic data were obtained from the CCM2 pan-European catchments database (de Jager and Vogt, 2010); climatic data were obtained from the gridded Worldclim 30 arc-second (approximately 1 km × 1 km) database (Hijmans et al., 2005); land cover information was extracted from the CORINE land cover database (EEA, 2011), and data on the number of inhabitants per area (human population) were based on the Global Rural-Urban Mapping Project (GRUMP, version1) (see Table 4). For deriving thermal responses of freshwater species in Chapter 5, global climatic data was used from the WorldClim 30 arc-second data set (Hijmans et al., 2005). Future climatic impacts were assessed by utilizing various projections for the middle of the 21st century from the CIAT (International Center for Tropical Agriculture) 30 arc-seconds gridded data set (see Table 4). Chapter 6 has the same data basis as Chapter 5. Data for Chapter 7 was based on the WaterGAP3 hydrology model (Brauman et al., 2016; Eisner, 2016; Schneider et al., 2017). WaterGAP3 provides data on natural river discharge and is a well-performing and state-of-the-art global freshwater model (Beck et al., 2016; Eisner et al., 2017; Schneider et al., 2017). Various current and future predictor variables for species distributions could be computed from the gridded input and output data of WaterGAP3 at the 5 by 5 arc-minute resolution

(~ 9 × 9 km at the Equator). Additionally, land cover variables from the Global Land Cover Characterization map (GLCC; USGS, 2008) and the CORINE Land Cover map (CLC2000; EEA, 2004) were included for modelling species distributions. To account for distribution opportunities and restrictions, the Global Reservoir and Dams database (GRanD), containing information on 6,862 georeferenced reservoirs (Lehner et al., 2011) was included in future scenarios.

Table 4 Environmental data sources of the application studies.

Study	Category	Source
Chapter 3	physical and chemical water quality parameters	Waterbase-Lakes database provided by the European Environment Agency (EEA) http://www.eea.europa.eu/data-and-maps/data/waterbase-lakes-10, accessed on April 2017
	satellite-based lake surface water temperature	Riffler et al. (2015) doi:10.1594/PANGAEA.831007, accessed on April 2017
		ARC-Lake http://www.laketemp.net/home//, accessed on April 2017
Chapter 4	topographic	de Jager and Vogt (2010) CCM2 pan-European catchments database (CCM version 2.1) http://data.jrc.ec.europa.eu/dataset/fe1878e8-7541-4c66-8453-afdae7469221
	climatic	Hijmans et al. (2005) Worldclim 30 arc-second (approx. 1 × 1 km) grids (version 1.4) www.worldclim.org, accessed on March 2018
	land cover	EEA (2011) CORINE land cover map https://land.copernicus.eu/pan-european/corine-land-cover, accessed on June 2018
	human population	Global Rural-Urban Mapping Project (GRUMP, version1) http://sedac.ciesin.columbia.edu/gpw, accessed on June 2018
Chapter 5	climatic (current)	Hijmans et al. (2005) Worldclim 30 arc-second (approx. 1 × 1 km) grids (version 1.4) www.worldclim.org, accessed on March 2018
	climatic (future)	CIAT (International Center for Tropical Agriculture) 30 arc-seconds gridded data set www.ccafs-climate.org, accessed on March 2018
Chapter 6	climatic (current)	Hijmans et al. (2005) Worldclim 30 arc-second (approx. 1 × 1 km) grids (version 1.4) www.worldclim.org, accessed on March 2018
	climatic (future)	CIAT (International Center for Tropical Agriculture) 30 arc-seconds (approx. 1 × 1 km) gridded data set www.ccafs-climate.org, accessed on March 2018
Chapter 7	climatic (current and future)	e.g. Brauman et al. (2016); Eisner (2016); Schneider et al. (2017) WaterGAP3 global hydrology model at 5 by 5 arc-minute resolution (approx. 9 × 9 km at the Equator) http://www.watergap.de/
	land cover	USGS (2008) Global land cover characterization map (GLCC) provided within WaterGAP3 data delivery
		EEA (2004) CORINE land cover map (CLC2000) https://land.copernicus.eu/pan-european/corine-land-cover provided within WaterGAP3 data delivery
	dams	Lehner et al. (2011) Global Reservoir and Dams database (GRanD) http://sedac.ciesin.columbia.edu/data/set/grand-v1-dams-rev01, accessed on January 2019

PART II

Application Studies

Chapter 3

Chlorophyll *a* – nutrient and temperature relationships, and predictions for lakes across mountain regions

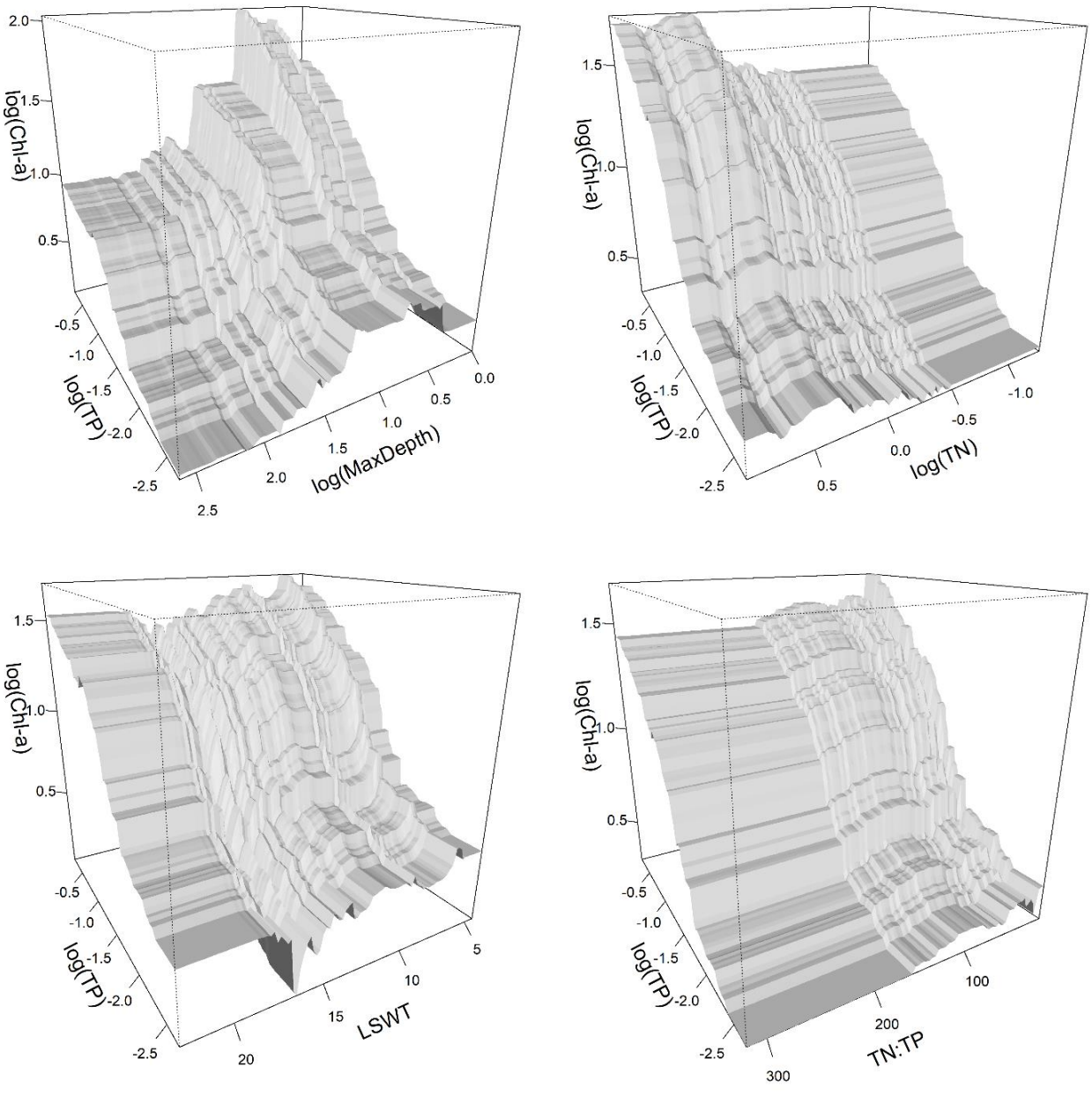

Supporting information can be found in Appendix 1 of the thesis.

Abstract

Model-derived relationships between chlorophyll *a* (Chl-a), nutrients and temperature have fundamental implications on understanding complex interactions among water quality measures used for lake classification, yet accuracy comparisons of different approaches are scarce. Here, we 1) compared Chl-a model performances across linear and non-linear statistical approaches, 2) evaluated single and combined effects of nutrients, depth and temperature as lake surface water temperature (LSWT) or altitude on Chl-a, and 3) investigated the reliability of the best water quality model across 13 lakes from perialpine and central Balkan mountain regions. Chl-a was modelled using *in situ* water quality data from 157 European lakes, elevation data and LSWT *in situ* data complemented by remote sensing measurements. Non-linear approaches performed better, implying existences of complex relationships between Chl-a and explanatory variables. Boosted regression trees, as best performing approach, were able to accommodate interactions among predictor variables. Chl-a – nutrient relationships were characterized by sigmoidal curves with total phosphorus having the largest explanatory power for our study region. In comparison with LSWT, utilization of the often-used temperature surrogate altitude led to different influence directions but similar predictive performances. These results support utilizations of altitude in models for Chl-a predictions. Compared to Chl-a observations, Chl-a predictions of the best performing approach for mountain lakes (oligotrophic-eutrophic) led to minor differences in trophic state categorizations. Our findings suggest that both models with LSWT and altitude are appropriate for water quality predictions of lakes in mountain regions and emphasize importance of incorporating variable interactions in facing lake management challenges.

Introduction

Despite water quality improvements in many European lakes, eutrophication is still the most serious threat to lake water quality (cf. Poikane et al., 2014). Eutrophication and water quality status are often evaluated by using phytoplankton biomass as one indicator. Specifically, chlorophyll *a* (Chl-a) is used as a measure of primary producer biomass (cf. Kasprzak et al., 2008) and for defining ecologically relevant lake water quality targets (Poikane et al., 2014). Understanding Chl-a – total nitrogen (TN) and Chl-a – total phosphorus (TP) relationships is critical to understanding lake ecosystem health and management (Rapport et al., 1998). Studies on Chl-a – nutrient relationships have a long history (Sakamoto, 1966; Dillon and Rigler, 1974) and emphasize a need for accurate models. The majority of empirical studies have shown TP to be a better predictor of Chl-a than TN, supporting the view that phosphorus limits the production of phytoplankton biomass in lakes (cf. Abell et al., 2012), but TN may co-limit phytoplankton biomass under certain conditions (Elser et al., 2007; Bracken et al., 2015). Also, in McCauley et al. (1989), there was a significant interaction term between TN and TP when predicting Chl-a, in which TN has a large influence on Chl-a at high TP. Filstrup and Downing (2017) found a similar importance of TN on predicting Chl-a depending on TP concentration emphasizing modelling approaches that can incorporate interactions among predictor variables.

Most previous studies have documented relationships between Chl-a and TN or TP (Phillips et al., 2008; Abell et al., 2012) with

different linear approaches on log-transformed axes ranging from ordinary least squares (Bachmann et al., 2012) to panel data models (Magumba et al., 2013). Linear methods can be limited in describing complex interactions between exogenous and endogenous variables because only one influence direction for each variable is possible. Non-linear methods, however, can account for varying responses along environmental gradients. Few studies have considered non-linear modelling approaches. For example, McCauley et al. (1989) pointed out sigmoidal Chl-a – TP relationships by using non-linear regression which was subsequently supported by Filstrup et al. (2014), Hollister et al. (2016) modelled the trophic state with random forest (Breiman, 2001a), and Lu et al. (2016) developed an artificial neural network model (e.g. McCulloch and Pitts, 1943) to predict Chl-a for a lake in the United States. Although there is a growing tendency to model these relationships by using non-linear approaches, there are still many questions remaining regarding model form and the accuracy of predictions, especially across mountain regions.

Temperature can strongly influence Chl-a concentrations observed at given nutrient concentrations (e.g. Kraemer et al., 2017); however, water quality – temperature relationships are commonly inferred from LSWT surrogates. Magumba et al. (2013), for example, used altitude to control the effect of temperature on the Chl-a concentration. Comparisons between Chl-a – altitude and Chl-a – lake surface water temperature (LSWT) relationships are insufficiently explored. Thus, the Chl-a – temperature vs. Chl-a – altitude relationships need to be further investigated. The latter is particularly important for mountain lakes and lakes in the foothills of mountains, regarded as highly susceptible towards environmental perturbations such as warming (Huber et al., 2005; Battarbee et al., 2009; Markovic et al., 2017). Preserving and improving the ecosystem services provided by lakes requires information on the level of ongoing changes as well as scenarios to estimate possible future developments.

Here, we investigated Chl-a concentrations of European lakes across a broad trophic gradient (from ultra-oligotrophic to hyper-eutrophic) using linear and non-linear statistical modelling approaches: Panel Data Models (PDMs), Generalized Additive Models (GAMs) and Boosted Regression Trees (BRTs). Different statistical approaches ensure the consistency of resulting parametrized relationships. In addition to *in situ* measurements of the nutrients (TN, TP) and lake morphometric parameters (maximum depth), Chl-a models included LSWT *in situ* measurements supplemented by remote sensing based LSWT data (MacCallum and Merchant, 2013; Riffler et al., 2015). Subsequently, we aimed at identifying the statistical approach and variable set yielding the best model performance. For the best performing statistical method, water quality drivers were identified by calculating the variable importance. Comparisons of predicted and observed Chl-a concentrations were used to test the prediction ability of the best performing statistical method for perialpine and central Balkan mountain lakes.
In summary, the objectives of this study were to: 1) model Chl-a concentration in lakes (with the focus on performance comparisons across multiple statistical models and on the identification of water quality drivers), 2) investigate the Chl-a – nutrient relationships and Chl-a – temperature relationships inferred

from altitude and LSWT using multivariate modelling, and 3) test the best performing model for predicting trophic state of lakes in European mountain regions.

Materials and methods

Water quality data

In situ observations of physical and chemical water quality parameters were mainly obtained from the Waterbase-Lakes database provided by the European Environment Agency (http://www.eea.europa.eu/data-and-maps/data/waterbase-lakes-10, accessed on April 26, 2017). Waterbase contains timely, reliable and policy-relevant data collected from EEA member countries through the WISE-SoE data collection process managed by the EEA (for more details see http://dd.eionet.europa.eu/datasets/3163, accessed on April 2017). Due to a lower number of observations for the aggregation period "summer" in the Waterbase-Lakes data set, we focussed on the annual mean values between 1989 and 2012 of chlorophyll *a* (Chl-a), total phosphorus (TP), total nitrogen (TN), Secchi depth, and lake surface water temperature (LSWT). Annual mean values resulting from an *in situ* aggregation length of less than 10 months were excluded from the analyses due to high uncertainty. For lakes with multiple monitoring stations, only stations with the longest series of observations of the parameters of interest were included. Lake maximum depth (MaxDepth) and surface elevation (altitude) were considered as static parameters. Information on altitude gathered from Google Earth was added if lake observations were missing altitude data. For Lake Ohrid, we additionally used water quality data obtained from the Hydrobiological Institute in Ohrid.

Since LSWT of many lakes was not monitored or was monitored on an irregular basis, remote sensing data was used to complement and extend traditional lake sampling methods, facilitating the understanding of recent trends and the current state of lake ecosystems (Peterson and Parker, 1998; Turner et al., 2003; McPhearson and Wallace, 2008). Specifically, *in situ* observations of LSWT were complemented by the satellite-based LSWT data derived from the Riffler et al. (2015) data set (doi:10.1594/PANGAEA.831007, accessed on April 2017) and from the ARC-Lake data set (http://www.laketemp.net/ home/, accessed on April 2017). The data are mainly based on (Advanced) Along Track Scanning Radiometers (A)ATSRs and the Advanced Very High Resolution Radiometer (AVHRR) and were maximally available from 1989 to 2013.

The data set used for calibration of the Chl-a models included 721 sets of annual mean values of the parameters Chl-a, TP, TN and LSWT. The variables used for modelling are summarized in Table 1. The data set (n = 721) covered 157 lakes with various trophic states. Consequently, lakes with low Chl-a (min = 0.4 µg/l), TN (min = 50 µg/l) and TP (min = 2 µg/l) concentrations as well as lakes with Chl-a concentrations above 500 µg/l were included. The highest number of annual data was available *inter alia* for Lake Vesterborg (24 years). The lakes in the data set were distributed across Europe, ranging from southern (~37 °N) to northern (~60 °N) and western (~9 °W) to eastern (~29 °E) Europe (Fig. 1a).

Table 1 Summary statistics of Chl-a, the explanatory variables and geographical characteristics of the 157 European lakes in the modelling data set.

Variable	Unit	Minimum	Mean	Maximum	Standard deviation
Chl-a	µg/l	0.40	26.45	551.74	48.13
TN	mg/l	0.05	1.72	8.17	1.37
TP	mg/l	2·10-3	0.08	0.59	0.09
TN:TP (by weight)		0.59	42.11	316.67	43.66
MaxDepth	m	1.00	37.76	410.00	70.50
LSWT	°C	4.37	10.99	22.70	2.59
Altitude	m	0.00	145.54	2432.00	275.53
Longitude	°E	-8.69	11.57	28.61	4.27
Latitude	°N	37.67	53.13	59.45	4.43

Chlorophyll *a* modelling

Chl-a was modelled by using two different variable sets. Each variable set included TN, TP, TN:TP (by weight), and MaxDepth, with all variables except TN:TP being $\log_{10}$-transformed prior to analysis (hereafter only log). To identify variations resulting from the utilization of LSWT and LSWT surrogates, we extended the basic variable set with either LSWT or altitude.

The variable selection for modelling Chl-a was based on previous studies, which found that TP and TN influence Chl-a concentration, either in isolation or together (Gunkel and Casallas, 2002; Abell et al., 2012). Furthermore, TN:TP was included for the identification of limiting nutrients (Bachmann and Hoyer, 2003) and its influence on Chl-a – nutrient relationships (Prairie et al., 1989). The utilization of MaxDepth accounts for the residence time of water (Kalff, 2002; Londe et al., 2016) and the proportion of water column that is vertically mixed, which can influence Chl-a – nutrient relationships (e.g. Weithoff et al., 2000). Increasing temperature has been demonstrated to positively affect Chl-a concentration, yet temperature surrogates are generally used (e.g. Carvalho et al., 2009). Although water transparency influences a wide range of biogeochemical processes, Secchi depth was not included as a predictor due to the high influence of chlorophyll concentration on water transparency.

Relationships between Chl-a and the two investigated variable sets were parametrized with three different modelling approaches: Panel Data Models (PDMs), Generalized Additive Models (GAMs) and Boosted Regression Trees (BRTs). The statistical approaches are available in the R packages "plm" (Croissant and Millo, 2008) (PDM), "mgcv" (Wood, 2011) (GAM) and "gbm" (Ridgeway, 2017) (BRT). PDMs account for possible linear relationships. Three PDM

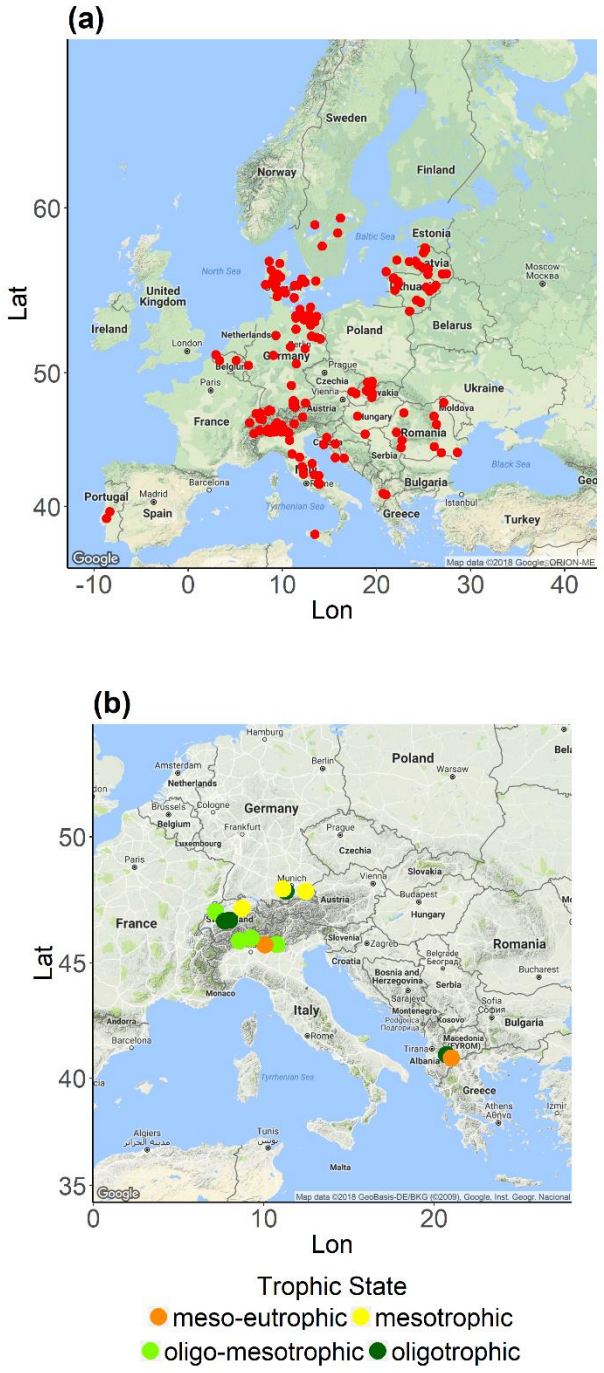

Figure 1 Locations of the (a) 157 European lakes used for modelling water quality and the (b) 13 perialpine and central Balkan mountain lakes including trophic states. For the 13 selected lakes the trophic state assessment was based on combinations of annually averaged values of Chl-a, TP and Secchi depth from 2005 to 2008.

types were used: 1) fixed individual effects, 2) random individual effects, and 3) pooled. Therefore, we compared the performance of these PDM types for the two variable sets and used the best performing PDM for the respective variable set for further analyses. For the final PDMs, the standard errors of the coefficients were computed with a robust covariance matrix estimator to address potential heteroscedasticity (Long and Ervin, 2000; Greene, 2012). In contrast to PDMs, GAMs are able to account for non-linear relationships between the explanatory and dependent variables, consequently they do not assume a linear influence of each explanatory variable on Chl-a. The third approach (BRT) takes into account the possibility of relationships among the exogenous variables. BRTs are non-parametric and able to express non-linear relationships and interactions between predictors due to the structure of decision trees (Elith et al., 2008). The single trees of the BRT model are determined successively by fitting the residuals at each step. For this procedure, four parameters in the BRT model have to be defined manually: the learning rate (*lr*, defines the contribution of each tree to the whole model), tree complexity (*tc*, indicates the final number of nodes), bag fraction (*bf*, introduces randomness into the model) and the number of trees (*nt*). We determined the number of trees for different combinations of *lr*, *tc* and *bf* with the R function 'gbm.step' of the R package "dismo" (Hijmans et al., 2017). Following Elith et al. (2008), combinations leading to fewer than the recommended optima of at least 1,000 trees were excluded from further examination. Subsequently, the four parameters yielding the smallest average testing mean squared error (MSE), which was determined by randomly dividing the data set 10 times into a calibration (80%) and a testing data set (20%), were set as optimal model values. The calibrated BRT model can be viewed as a sum of *nt* trees, each multiplied by *lr* and including variable interactions if *tc* >1, whereas *bf* represents the

random fraction of the data used to propose the next tree.

The determination of the best performing approach was based on indices that compare predicted and observed Chl-a values, i.e. R^2 and root mean squared error (RMSE). Standard model selection criteria, such as the Akaike Information Criterion (AIC), are unsuitable for non-parametric models. Here, the performance evaluation was conducted via bootstrapping, with random data splitting into calibration (80%) and validation (20%) data sets, repeated 100 times. Based on the bootstrapping data samples, the mean R^2 and mean RMSE from the calibration and the validation data set were assessed. The model resulting in the highest validation mean R^2 and lowest mean RMSE is hereafter referred to as the "best performing approach".

For all models, we identified the influence direction (partial dependence curves) of each explanatory variable, whereas the variable importance and the multi-dimensional partial dependence plots were computed only for the best performing approach. The influence direction (partial dependence) for non-linear models is depicted as a function of an individual explanatory variable displaying the response variable while all remaining variables are either fixed or kept at their mean value. The variable importance for BRTs is based on the number of selections for splitting, weighted by the squared improvement to the model as a result of each split, and averaged over all trees (Friedman and Meulman, 2003). Uncertainty estimation additionally included the testing of the variable importance accuracy by computing the average variable importance from 100 repetitions with the calibration data set for the best performing approach. The variable importance of each explanatory variable for the best performing approach was used to identify Chl-a concentration drivers. After identifying the variables with the highest importance, we additionally investigated multi-dimensional partial dependence plots by using the gbm.plot function integrated in the gbm-package (see also Friedman and Meulman, 2003; Friedman and Popescu, 2008; Lampa et al., 2014).

Predicting chlorophyll *a* concentration in perialpine and central Balkan mountain lakes

Our study included major lakes located in or near the European Alps (cf. Riffler et al., 2015) and the two major freshwater biodiversity hotspots – the Balkan lakes Ohrid and Prespa (Fig. 1b). The lakes had significantly different morphometric and trophic characteristics. The surface areas varied from 29.8 km^2 (Lake Brienz) to 369.9 km^2 (Lake Garda), with maximum depths ranging from 73 m (Lake Chiem) to over 400 m (Lake Como; Table S1). The trophic status spanned from oligotrophic to meso-eutrophic (Table 2). Specifically, four lakes were classified as oligotrophic (Brienz, Ohrid, Starnberg, Thun), four lakes as oligo-mesotrophic (Biel, Como, Garda, Maggiore), three lakes as mesotrophic (Ammer, Chiem, Zurich), and two lakes as meso-eutrophic (Iseo, Prespa). Lake selection was guided by the availability of *in situ* water quality observations and satellite-based lake surface water temperature data.

To evaluate the prediction ability for perialpine and central Balkan mountain lakes, we predicted Chl-a and the trophic state lake-by-lake for the 13 lakes occurring in the modelling data set with the best performing approach. For the Chl-a prediction of a studied lake, the respective lake was excluded beforehand in the model calibration.

Table 2 OECD lake classification.

Lake	Chl-a (µg/l)	TP (mg/l)	Secchi depth (m)	Trophic state
Ammer	3.22 – 4.29	0.008 – 0.008	4.0 – 4.0	mesotrophic
Biel	1.00 – 1.95	0.015 – 0.017	-	oligo-mesotrophic
Brienz	0.55 – 0.93	0.004 – 0.009	-	oligotrophic
Chiem	4.42 – 4.60	0.008 – 0.011	3.7 – 4.8	mesotrophic
Como	1.60 – 7.20	0.005 – 0.026	4.2 – 12.2	oligo-mesotrophic
Garda	1.69 – 3.75	0.019 – 0.030	6.2 – 12.5	oligo-mesotrophic
Iseo	2.73 – 6.35	0.051 – 0.099	4.4 – 5.4	meso-eutrophic
Maggiore	0.83 – 4.67	0.003 – 0.014	4.5 – 10.6	oligo-mesotrophic
Ohrid	0.53	0.008	-	oligotrophic
Prespa	4.87 – 7.97	0.044 – 0.060	-	meso-eutrophic
Starnberg	1.83 – 1.91	0.006 – 0.006	5.9 – 7.0	oligotrophic
Thun	1.15 – 1.65	0.003 – 0.006	-	oligotrophic
Zurich	4.68 – 6.33	0.034 – 0.035	-	mesotrophic

The classification of the trophic status was conducted following OECD fixed boundary recommendations (Premazzi and Chiaudani, 1992). Chlorophyll *a* (Chl-a), total phosphorus (TP) and Secchi depth represent the minimum and the maximum of the annual averages based on observations collected between 2005 and 2008. "-" indicates that the required water quality parameters were missing.

Subsequently, the Chl-a prediction was assessed by comparing predicted and observed trophic states for 2005-2008 and used to calculate the RMSE.

Results

Chlorophyll *a* modelling

log(Chl-a) concentration was positively related to log(TP) ($R^2 = 0.64$, $p < 0.001$) and log(TN) ($R^2 = 0.40$, $p < 0.001$) concentration (Fig. 2a-b). log(TN) and log(TP) were positively correlated ($R^2 = 0.44$, $p < 0.001$; Fig. 2c). LSWT, however, was not significantly correlated with log(Chl-a) (Fig. 2d).

Among the studied Panel Data Models (fixed individual effects, random individual effects, and pooled), adjusted R^2 was highest for the pooled modelling data (Table S2). Therefore, we continued our analysis using the pooled data without including any lake specific individual effects. For both variable sets, the coefficients and thus influence directions of the pooled data model showed significant positive influences of TN and TP on Chl-a, whereas MaxDepth had a significant negative influence (Table S3). For individual variable sets, altitude showed a significant negative influence on Chl-a, whereas LSWT did not have a significant effect (Table S3).

In general, all models had moderate to good mean validation R^2 (Table 3). Compared to the model using LSWT, the use of altitude as LSWT surrogate resulted in a marginal improvement of validation mean R^2 and

Table 3 Summary statistics of the predictive accuracy of PDMs, GAMs and BRTs including the mean R^2 and mean RMSE for the calibration (80%) and validation data set (20%).

Method	Model	Calibration		Validation	
		Mean R^2	Mean RMSE	Mean R^2	Mean RMSE
PDM	LSWT variable set	0.72	0.29	0.72	0.30
	Altitude variable set	0.73	0.30	0.72	0.30
GAM	LSWT variable set	0.79	0.26	0.76	0.28
	Altitude variable set	0.81	0.25	0.77	0.28
BRT	LSWT variable set	0.92	0.15	0.82	0.24
	Altitude variable set	0.92	0.17	0.84	0.23

The validation was conducted by bootstrapping 100 times. Predictive accuracy was determined for the calibration (80%) and validation data set (20%). Afterwards averages of the R^2 and RMSE were calculated.

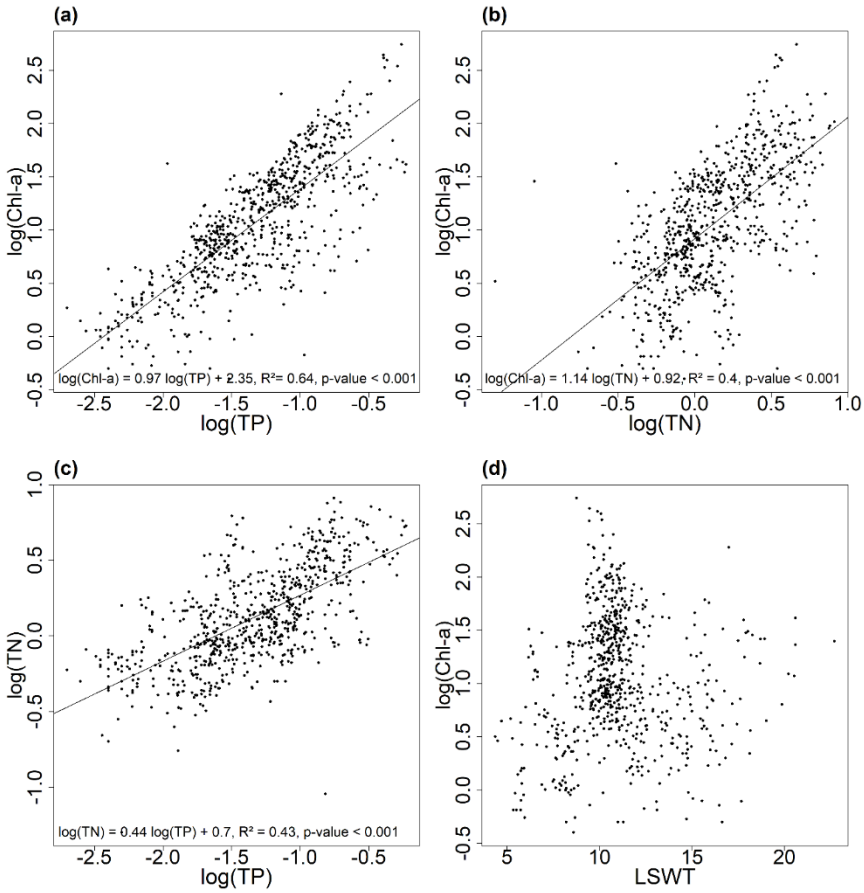

Figure 2 Bivariate scatterplots of (a) log(Chl-a) and log(TP), (b) log(Chl-a) and log(TN), (c) log(TN) and log(TP), (d) log(Chl-a) and LSWT (°C) and the corresponding R^2 and p-value for significant relationships only.

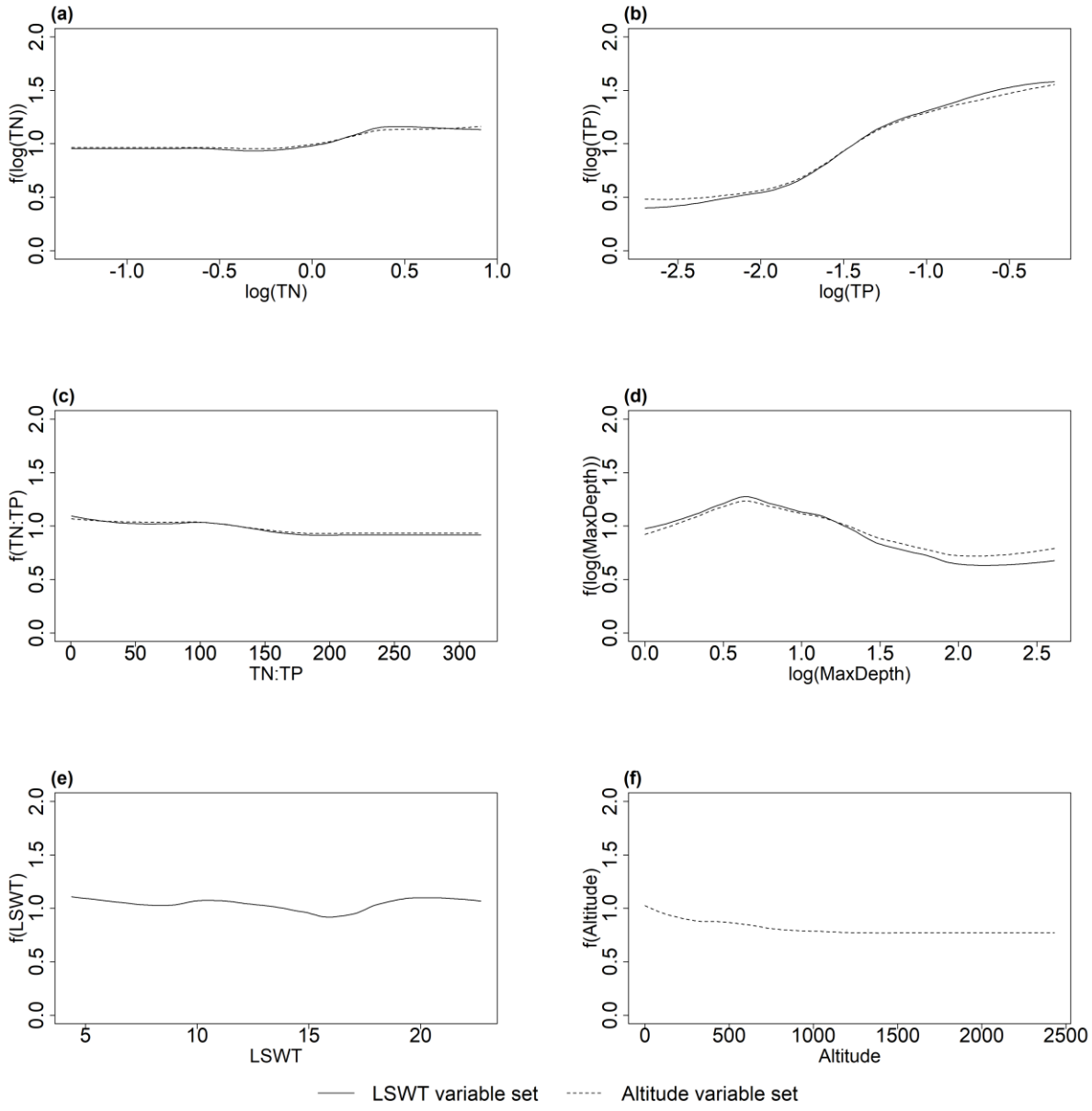

Figure 3 Smoothed partial dependence curves of each exogenous variable for the two BRT models. log(Chl-a) is depicted as a function of (a) log(TN), (b) log(TP), (c) TN:TP, (d) log(MaxDepth), (e) LSWT (°C) and (f) altitude (m) while all remaining variables are kept at their mean values.

RMSE by 0.02 and 0.01 maximum, respectively. Furthermore, with a mean validation R^2 of 0.82 – 0.84 and a mean validation RMSE of 0.23 – 0.24 for LSWT and altitude models, BRTs emerged as the best performing approach. The corresponding BRT model parameter specifications are listed in Table S4. Lowest performance was attributed to PDMs suggesting that the uses of non-linear models and models that allow for interactions among exogenous variables improve the prediction accuracy for modelling Chl-a. The highest differences between the summary statistics for the calibration and the validation samples were present for the BRTs.

Overall, the partial dependence curves, i.e. influence directions, for the two best performing approaches, BRTs (Fig. 3) and GAM (Fig. S1), indicated similar relationships between Chl-a and the explanatory variables.

However, the uncertainty of the GAM based estimates increased near extreme predictor values. The relationship between TN and Chl-a in BRT models was non-linear and showed a slight increase of Chl-a with increasing TN concentration until a certain peak was reached (at log(TN) = 0.4, i.e. TN = 2.5 mg/l) (Fig. 3). Chl-a and TP displayed a sigmoidal relationship with an acceleration of the positive slope at log(TP) = -1.9 (0.013 mg/l) and a deceleration at around log(TP) = -1.3, i.e. TP = 0.05 mg/l (Fig. 3). The partial dependence for TN:TP showed a slight decrease with increasing TN:TP. For TN:TP ratios above approximately 170 (by weight), no particular influence direction was observable. However, GAMs identified a strictly negative relationship for TN:TP with increasing uncertainty for greater TN:TP ratios (Fig. S1). For MaxDepth, both GAM and BRT suggested a positive influence until log(MaxDepth) = 0.6 (~4 m), and a negative influence afterwards (Fig. 3 and S1). We note that lakes with a maximum depth above 100 m (log(MaxDepth) > 2) were scarcely included in the modelling data set, implying influence directions with higher uncertainty (Fig. S1). Similarly, both GAMs and BRTs identified a non-linear interaction between LSWT and Chl-a (Fig. 3 and S1). The BRT models showed an alternating influence direction for LSWT with a slightly negative tendency followed by an increase from 16°C until 20°C (Fig. 3). The BRT based Chl-a – altitude relationship showed a decrease in Chl-a concentration with increasing altitude (Fig. 3), while GAM showed more variation in the Chl-a – altitude relationship, accompanied by increasing uncertainty for lakes with an altitude above ~700 m (Fig. S1).

As the validation and calibration of the best performing BRT models confirmed nearly identical results in regard of the variable importance (Table 4 and S5), we consider the results from the calibrations with the whole data set in the following (Table 4). TP appeared to have the strongest influence (> 50%) on Chl-a concentration in European lakes for the BRT LSWT and altitude models (Table 4). The lake characteristic MaxDepth (26.8% and 22.3% for the LSWT and altitude model, respectively) was identified as second most important variable, followed by TN (9.2%) for the LSWT and by altitude (15.2%) for the altitude model. TN (7.8%) had an even lower variable importance in the altitude model compared to the LSWT model. LSWT, however, had a calculated variable importance of 5.8%. Both BRT models assigned TN:TP the smallest variable importance with 3 – 4%.

Table 4 Relative variable importance (normalized to 100%) resulting from the calibration of BRT models with the whole data set.

Variable	BRT Model	
	LSWT variable set	Altitude variable set
log(TN)	9.2%	7.8%
log(TP)	53.9%	51.4%
TN:TP	4.3%	3.3%
log(MaxDepth)	26.8%	22.3%
LSWT	5.8%	-
Altitude	-	15.2%

Two-dimensional partial dependence plots were considered for combinations of the variable with the highest variable importance (TP) and the remaining predictor variables. For the same variable combinations, the BRT LSWT and altitude model yielded similar two-dimensional partial dependence plots (Fig. 4 and Fig. S2). The combination of the two variables with the highest calculated variable importance, i.e. TP and MaxDepth, suggested a high Chl-a concentration for lakes with higher TP concentrations (> 0.1 mg/l) and lower maximum depth (2 – 4 m) (Fig. 4a and

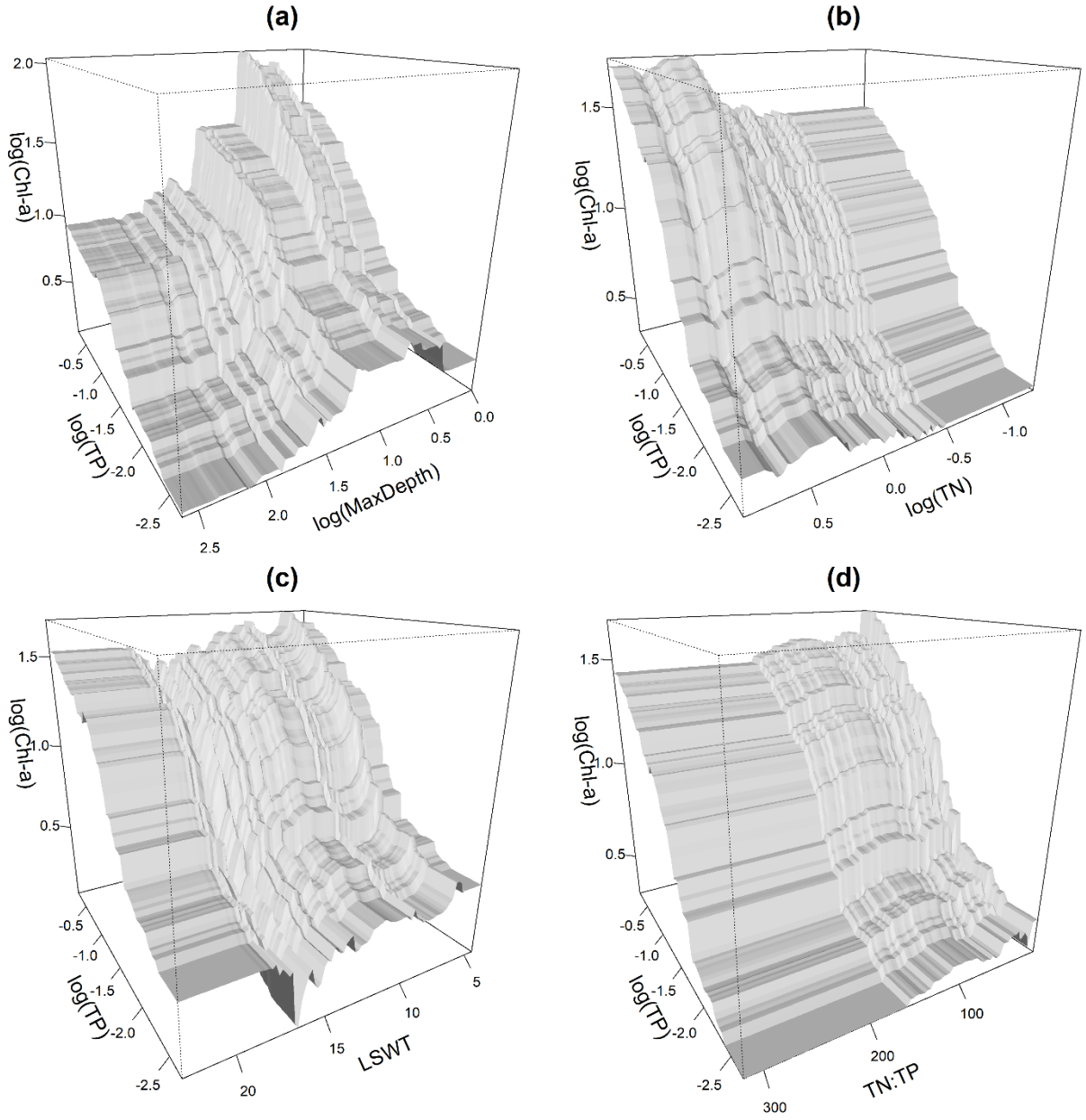

Figure 4 Two-dimensional partial dependence plots for combinations of TP and each remaining exogenous variable for the BRT LSWT model. log(Chl-a) is depicted as a function of (a) log(TP) and log(MaxDepth), (b) log(TP) and log(TN), (c) log(TP) and LSWT (°C), and (d) log(TP) and TN:TP, accounting for the averaged effects of the other variables.

Fig. S2a). With increasing maximum depth, the maximum Chl-a concentration decreased for a given TP concentration. The sigmoidal structure of the dependence curve and the magnitude of change along the nutrient gradient is similar regardless of depth, however the Chl-a concentration is shifted to higher values at low lake depths (Fig. 4a). Furthermore, increases in nutrient loadings were accompanied by increases in Chl-a (Fig. 4b and Fig. S2b), displaying high Chl-a concentration resulting from the combination of high TN and TP concentrations, with rising TN having a slightly stronger effect if TP is already high. However, a high TN and low TP concentration was connected to a notably lower Chl-a concentration than vice versa. Variable combinations with variables that were characterized by a lower computed variable importance (i.e., TP and LSWT, TP and altitude, or TP and TN:TP) appeared to have no clearly discernible trend (Fig. 4c-d and

Fig. S2c-d). For TP and LSWT, and TP and TN:TP, the two-dimensional partial dependence plots were mainly driven by the sigmoidal structure manifested by TP with no strong influences of the second variable on the Chl-a concentration. For TP and altitude, however, lakes with high TP concentration at lower elevations appeared to have a positive effect on Chl-a (Fig. S2c).

Three-dimensional partial dependence plots visualizing three-way variable interactions of TN, TP and MaxDepth in the BRT LSWT and altitude model showed high Chl-a concentrations for lakes with low maximum depths combined with high TN and TP concentrations (Fig. S3-S4). As the maximum depth increased, the maximum Chl-a concentration decreased. The maximum Chl-a concentration (around log(Chl-a) = 1.1 ~ 13 µg/l) in lakes deeper than log(MaxDepth) = 1.3 ~ 20 m was only reached with a combination of high TN and TP concentrations, i.e. TN and TP being greater than log(TN) = 0.3 ~ 2 mg/l and log(TP) = -1.0 ~ 0.1 mg/l, respectively. In regard of the relationships between the temperature variables and nutrients, the three-way interactions between TN, TP and LSWT as well as TN, TP and altitude did not vary along the respective gradients of the temperature variables (Fig. S5-S6).

Table 5 Chl-a observations and predictions (min-max) of the BRT LSWT and altitude models, and the corresponding trophic state categorizations using the Chl-a observations and predictions for 2005-2008. We note that for lakes with a single prediction value, only one complete variable set necessary for a model prediction was available.

Lake	Observation		Prediction		
	Chl-a (µg/l)	Trophic state	BRT LSWT (µg/l)	BRT Altitude (µg/l)	Trophic state
Ammer	3.22 – 4.29	mesotrophic	1.39	1.27	oligo-mesotrophic
Biel	1.00 – 1.95	oligo-mesotrophic	3.38 – 4.00	3.44 – 3.91	mesotrophic
Brienz	0.55 – 0.93	oligotrophic	1.18 – 1.92	1.37 – 1.96	oligotrophic
Chiem	4.42 – 4.60	mesotrophic	1.54	1.90	oligo-mesotrophic
Como	1.60 – 7.20	oligo-mesotrophic	1.54 – 3.53	1.45 – 3.17	oligo-mesotrophic
Garda	1.69 – 3.75	oligo-mesotrophic	1.8 – 4.05	2.34 – 3.37	oligo-mesotrophic
Iseo	2.73 – 6.35	meso-eutrophic	6.59 – 8.86	4.92 – 6.97	meso-eutrophic
Maggiore	0.83 – 4.67	oligo-mesotrophic	1.14 – 2.09	1.05 – 1.70	oligo-mesotrophic
Ohrid	0.53	oligotrophic	2.15	1.27	oligotrophic
Prespa	4.87 – 7.97	meso-eutrophic	3.34	2.51	meso-eutrophic
Starnberg	1.83 – 1.91	oligotrophic	1.07	1.01	oligotrophic
Thun	1.15 – 1.65	oligotrophic	1.09 – 1.32	1.08 – 1.35	oligotrophic
Zurich	4.68 – 6.33	mesotrophic	2.36 – 3.34	2.70 – 2.97	mesotrophic

The classification of the trophic status was conducted following OECD fixed boundary recommendations (Premazzi and Chiaudani, 1992).

Predicting chlorophyll *a* concentration in perialpine and central Balkan mountain lakes

For lakes in European mountain regions, the best performing approach – the BRTs – was used to predict the Chl-a concentration and classify the resultant predictions into trophic states. Specifically, the prediction accuracy of the BRTs was evaluated by calculating the RMSE in μg/l and comparing predicted and observed trophic states for 13 selected lakes. Differences in the average RMSE between the LSWT and altitude models were only marginal with values of 1.76 μg/l and 1.62 μg/l, respectively (Table S6). Maximum RMSE was observed for Lake Iseo with the LSWT variable set (2.74 μg/l). In addition, for Lake Iseo the RMSE difference between the two variable sets was the biggest (2.74 μg/l – 1.23 μg/l = 1.51 μg/l); however, for the remaining lakes the difference was below 0.38 μg/l. Overall, lowest RMSE was present for Lake Starnberg and Lake Thun (0.57 – 0.71 μg/l). We note that for Lake Prespa the RMSE could not be calculated because more than one observation/prediction for the calculation is needed.

In comparison with the respective lake's annual mean Chl-a values, varying overestimations and underestimations of Chl-a concentrations were present (Table 5). However, the overestimations and under-estimations led only to minor or no variations in the trophic state assessment for the period 2005-2008 including TP and Secchi depth. For 10 of the 13 lakes, the predicted trophic state agreed with the observed water quality status. Only for Lake Biel the observed trophic state was underestimated by the prediction (oligo-mesotrophic vs. meso-trophic), whereas it was overestimated for Lake Ammer and Chiem (mesotrophic vs. oligo-mesotrophic) (Table 5).

Discussion

Chlorophyll *a* modelling

Boosted regression trees (BRTs) resulted in the overall best performance in modelling water quality for both variable sets. Therefore, further investigations of Chl-a – nutrient and temperature relationships and predictions for lakes from mountain regions were based on the results of the gradient boosted model. Due to a tree complexity of >1 in both the BRT LSWT and altitude model variable interactions were fitted in our water quality models (Elith et al., 2008). Thus, we were able to examine multi-dimensional partial dependence plots, which reflect the different interactions of two or more predictor variables (Friedman and Meulman, 2003) and allow studying the detailed nature of interaction effects (Friedman and Popescu, 2008).

In general, the computed variable importance (see Elith et al., 2008) as indicator of the explanatory power could be seen as a determinant of the influence extent, which is displayed by the partial dependence plots, i.e. greater changes in Chl-a are expected if changes of more important variables are present. As such, for the most important variable TP (~53%) we observed a sigmoidal Chl-a – TP relationship, indicating increasing Chl-a concentrations for increasing TP until an upper Chl-a maximum was reached (Filstrup et al., 2014). Multi-dimensional partial dependence plots underlined the computed variable importance and dominance of TP in the variable interactions by showing greater changes in Chl-a concentration for increases in TP compared to the other considered variables. However, all interaction analyses showed higher Chl-a concentrations when TN and TP concentration were high. The influence

of TN (~8%) could be characterized by smaller expected changes in Chl-a for varying TN concentrations in the analyzed lakes, but still having a positive influence on phytoplankton biomass with a sigmoidal partial dependence curve and a peak around TN = 2.5 mg/l. This threshold is similar to the threshold identified in Filstrup and Downing (2017), whereas after the threshold (TN > 2.5 mg/l) in our study the relationship is flat and not negative. This is likely because the data presented here do not include high TN values (> 10 mg/l) that were present in the study of Filstrup and Downing (2017). The influence of TN, however, can vary with respect to TP concentrations. The two-dimensional interaction analysis with TP showed increases in Chl-a when TN concentration increased in lakes with already high phosphorus concentrations. Accordingly, Filstrup and Downing (2017) have detected a markedly stronger effect of TN in TP-rich and especially hypereutrophic lakes than in mesotrophic or eutrophic lakes, implying different Chl-a – TN relationships in nutrient-rich lakes. In addition, for mesotrophic and eutrophic lakes a similar sigmoidal relationship was found (Filstrup and Downing, 2017). Thus, our findings support previous studies demonstrating the non-linear response of Chl-a to nutrients (McCauley et al., 1989; Filstrup et al., 2014) and suggest that Chl-a may display greater responses to phosphorus reductions in the European lakes considered in this study.

Guildford and Hecky (2000) pointed out that the nutrient ratio TN:TP constitutes an important indicator of nutrient limitation with phytoplankton growth becoming increasingly phosphorus-limited for rising nutrient ratio. Here, the influence extent and directions of the least important variable TN:TP (~4%) implied only marginal negative effects on Chl-a for increasing TN:TP ratio and thus increasing phosphorus limitation. TN:TP is known to have little effect when the system is strongly P-limited but becomes more important under more balanced resources (see e.g. Cardinale et al., 2009). Multi-dimensional interaction analyses also did not reveal any further discernible effects on water quality. Our data mainly consisted of phosphorus-limited lakes (high TN:TP). Low (< 10) TN:TP ratios were present for 62 out of 721 observations. Prairie et al. (1989) found that TP explained more variance in Chl-a than TN with increasing TN:TP. This finding matches our detected influence direction of TN:TP and high relative importance of TP in our data. The higher predictive ability of TP, however, does not imply lower correlation of TN with Chl-a for high TN:TP compared to TP (Prairie et al., 1989). In addition, according to the BRT models, lakes with a MaxDepth up to ~4 m had a positive influence on Chl-a. This positive influence direction was also supported in the two- and three-dimensional interaction analysis but might be biased by the high number of hypereutrophic lakes (Chl-a > 25 µg/l) (Premazzi and Chiaudani, 1992) with low depths in the data set (118 out of 196 observations with MaxDepth ≤ 4 m had Chl-a > 25 µg/l). A decreasing partial dependence curve afterwards indicated a negative effect on Chl-a for increasing maximum depth and consequently in general increasing water residence time (Carvalho et al., 2009). This negative influence can also be explained by lower nutrient loadings per volume and the well-established positive relationship between phytoplankton biomass and light availability (Sakamoto, 1966; Scheffer, 1998). The computed variable importance for MaxDepth (~25%) underlines the strong influence of lake morphometry on Chl-a concentration and

indicates interactions among explanatory variables.

The BRT model with a negative linear partial dependence curve for the temperature surrogate altitude (e.g., Carvalho et al., 2009) confirmed previously found positive Chl-a – temperature relationships, which are defined as the inverse of Chl-a – altitude relationships. In contrast, the Chl-a – temperature relationship found by the BRT LSWT model in general did not confirm such a positive linear influence of temperature on Chl-a. Slightly alternating influence directions with only small impacts on Chl-a concentration characterized the Chl-a – LSWT relationship. The non-linear relationship may be explained by the reduced effect of water temperature change when nutrient levels are low (Elliott et al., 2006) or different responses to warming in phytoplankton-rich lakes, where warming tends to increase Chl-a, and phytoplankton-poor lakes, where warming leads to a Chl-a decrease (Kraemer et al., 2017). However, further analyses of variable interactions with nutrients did not show any significant increases or decreases along the temperature gradient. Thus, combinations of LSWT with other predictors, especially nutrients, and their influence on phytoplankton communities should be further investigated. We note that the variable importance of altitude (~15%) and LSWT (~6%) in our study implied rather small influences of temperature on Chl-a.

There is a need to evaluate interaction effects on water quality, as previous studies found different relationships among essential predictors for different lake settings (McCauley et al., 1989; Elliott et al., 2006; Filstrup and Downing, 2017; Kraemer et al., 2017). Our performance results suggest that non-linear models incorporate the existing coherences among explanatory variables more precisely. As such, the non-linear gradient boosted regression method (BRT) was able to identify interactions among predictor variables (Elith et al., 2008) and to perform better than other regression approaches such as GAMs and PDMs. A better performance of BRTs compared to non-linear GAMs indicates that models with abilities to accommodate interactions among predictors in multi-dimensional settings are necessary to understand the complex interactions among water quality variables in lakes. We therefore recommend using further non-linear modelling and learning techniques that can incorporate possible variable interactions.

Predicting chlorophyll *a* concentration in perialpine and central Balkan mountain lakes

Prediction performances of BRTs were evaluated for 13 selected perialpine and central Balkan mountain lakes. The RMSE differences between using LSWT or altitude seem minor (1.62–1.76 µg/l). This conclusion can also be inferred from the comparison of the predicted and observed trophic states. Three out of 13 lakes (Ammer, Biel and Chiem) had minor differences between the observed and predicted trophic state, which may be related to absences of lakes with similar characteristics in the calibration data set. Further reasons for lower accuracy of predictions can come from models focusing rather on better generalization abilities, i.e. better data coverage, than precise predictions for very low or very high Chl-a concentrations (see also Suleiman et al., 2016). Similarly, other well performing water quality modelling approaches such as the artificial neural network model of Lu et al. (2016) led to underestimations of high values and

overestimations of low values. However, e.g. for the unusual lake system formed by Lake Ohrid and Prespa, which is characterized by a connection of the lakes through karst channels (Matzinger et al., 2006), the predicted trophic states agreed with the observations. As such, the regression tree approach was able to make accurate predictions for unique lake systems, which usually can set limits to the transferability of general water quality models. Nonetheless, we emphasize the need for further studies on applications of general water quality models for unique lakes from mountain regions. Although the dataset included some lakes, which covered longer time periods than others, overall Chl-a predictions of BRT models for perialpine and central Balkan mountain lakes in general provided satisfactory results. Further improvement potential is in balancing data availability across space and time.

Chapter 4

Scale effects on the performance of niche-based models of freshwater fish distributions

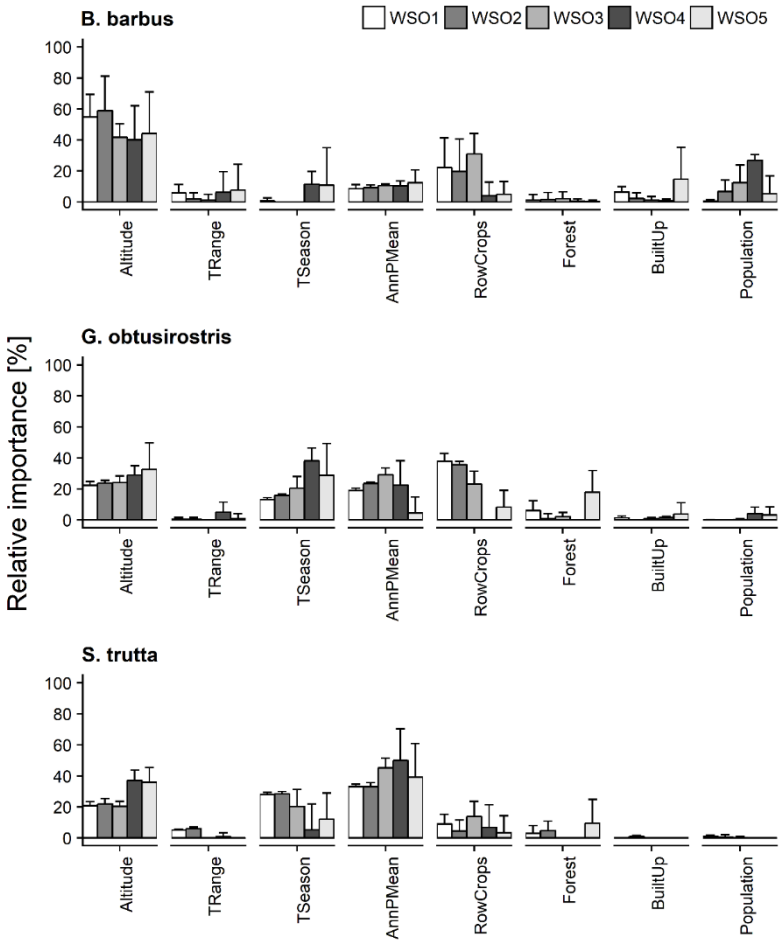

This chapter has been published as Kärcher, O., Frank, K., Walz, A., and Markovic, D. (2019). Scale effects on the performance of niche-based models of freshwater fish distributions. *Ecological Modelling*, **405**, 33–42. https://doi.org/10.1016/j.ecolmodel.2019.05.006

Supporting information can be found in Appendix 2 of the thesis. The full version of the Appendix is available at:
https://www.sciencedirect.com/science/article/pii/S0304380019301711?via%3Dihub#sec0075

Abstract

Niche-based species distribution models (SDMs) have become an essential tool in conservation and restoration planning. Given the current threats to freshwater biodiversity, it is of fundamental importance to address scale effects on the performance of niche-based SDMs of freshwater species' distributions. The scale effects are addressed here in the context of hierarchical catchment ordering, considered as counterpart to coarsening grain-size by increasing grid-cell size. We combine fish occurrence data from the Danube River Basin, the hierarchical catchment ordering and multiple environmental factors representing topographic, climatic and anthropogenic effects to model fish occurrence probability across multiple scales. We focus on 1st to 5th order catchments. The spatial scale (hierarchical catchment order) only marginally influences the mean performance of SDMs, however the uncertainty of the estimates increases with scale. Key predictors and their relative importance are scale and species dependent. Our findings have useful implications for choosing proper species dependent spatial scales for river rehabilitation measures, and for conservation planning in areas where fine grain species data are unavailable.

Introduction

Niche-based species distribution models (SDMs) play a central role in studying species habitat preferences, conservation and restoration planning at global, regional and local scales (e.g. Franklin, 2009). Multitudes of different algorithms now exist, and new methods and algorithms are developed continuously (e.g. Efron and Hastie, 2016). Methodological aspects of SDMs have been thoroughly studied from many perspectives, demonstrating reasons for differing performances (see Elith and Graham, 2009) including the sampling patterns (presence/absence or presence only data, Brotons et al., 2004), choice of single algorithm vs. consensus methods (Marmion et al., 2009), the length of studied future time periods and used predictors (Morán-Ordóñez et al., 2017), collinearity (Dormann et al., 2013), prevalence (Lawson et al., 2014) and the choice of grain-size (resolution) of environmental layers (Guisan et al., 2007). While the superior performance of consensus SDM methods has been repeatedly demonstrated increasing the reliability of the projections and reducing the model uncertainties (e.g. Thuiller, 2004; Marmion et al., 2009; Grenouillet et al., 2011), the influence of spatial scales on predictive power was less frequently studied. A study by Guisan et al. (2007) has shown that a 10-fold increase of the grid cell size does not have a substantial effect on the performance of SDMs describing distributions of bird, plant and vertebrate species. Similarly, Lauzeral et al. (2013) have shown a minor decrease in the performance of SDMs for five virtual species with coarsening grain-size from 30′′×30′′ to 32′′×32′′. Comparable studies that use multiple grain-size resolutions and SDMs for freshwater species do not exist; however, a study by Domisch et al. (2013b) has shown that the choice of stream network or landscape as study area does not affect the performance of SDMs of stream biota.

Hierarchical catchment ordering provides a valuable framework to address scale effects on niche-based SDMs of freshwater species' distributions (cf. Allan et al., 1997) and was thus considered as counterpart to coarsening grain-size by increasing grid-cell size, which is

commonly used in modelling distributions of virtual or terrestrial species. Specifically, the hierarchical structure of catchments is considered to be one of the key challenges in the application of SDMs in freshwater ecosystems (Domisch et al., 2015). Given that SDMs are central to both fundamental and applied research in biogeography (Araújo and Guisan, 2006), in particular conservation and restoration planning, the need for an improved understanding of the effects of grain-size on the overall performance of freshwater species SDMs becomes apparent.

Studies of freshwater species' distributions using multiple spatial scales are rare and generally limited to the comparison of the relative importance of reach- and sub-catchment-related environmental factors for the variation in species local composition (e.g. Hopkins and Burr, 2009; Esselman and Allan, 2010) using exploratory data analysis techniques. However, Domisch et al. (2013b) studied the effects of the extent of the modelled area (stream network vs. landscape) and the choice of predictors on SDMs of stream macroinvertebrates. As the lack of data constrains freshwater conservation strategies in many regions of the world, in particular less-developed countries, catchment scale data hold great promise where fine grain survey data on freshwater species occurrence or environmental factors are unavailable. Our study aims to accommodate the need for clarity on the predictive performance of freshwater SDMs based on catchment scale data, i.e., for SDMs lacking fine grain survey data. Given the current threats to freshwater biodiversity including high anthropogenic stress levels, habitat fragmentation, climate change (Woodward et al., 2010; Markovic et al., 2017) and the tremendous efforts for improvements (Knowler et al., 2003; Bernhardt et al., 2005), it is of fundamental importance to understand what environmental factors at what spatial scales (grain-size) are suitable predictors of which freshwater species' distributions.

The grain-size change is based on the most widely used hierarchical catchment ordering, the Strahler system (Strahler, 1964). Strahler order reflects the hierarchical level of each reach in the whole river network, with 1st order assigned to all reaches with no tributaries, 2nd order to the confluences of two first-order reaches, and so on. We focus on the "reach scale" (here, the catchment area of the river reach where an occurrence of the freshwater fish was observed) and the corresponding 2nd to 5th order catchments (following the catchment nomenclature of the CCM2 pan-European catchments database; CCM version 2.1, de Jager and Vogt, 2010; for further details see http://ccm.jrc.ec.europa.eu, accessed on 10.11.2018). The study area includes the Danube River Basin. The aims of the present study are: (1) to test whether there is a decrease in the performance of SDMs with coarsening grain-size (i.e., catchment order) and (2) to quantify what environmental factors at what catchment orders are important predictors of which fish species' distributions.

Materials and methods

Study area

The Danube is Europe's second largest river basin (801,463 km^2) and is shared among more than 80 million people from 19 countries. It extends from Central Europe through the Balkans and drains to the Black Sea (Fig. S1). The Danube River delta is one of the world's largest wetlands, rich in rare fauna and flora and inscribed on UNESCO's World Heritage

List in 1991. Due to its large spatial extent and diverse relief, the Danube River Basin also shows great differences in climate. The summed annual precipitation ranges from more than 2,300 mm in the high mountains to less than 400 mm in the delta region, while the mean annual discharge reaches 6,460 m^3s^{-1} at the Danube delta in Romania (ICPDR, 2009). The Danube River Basin hosts over 2,000 plant species, 40 mammals species and approximately 100 fish species, and is subject to increasing pressure including pollution from agriculture, industry and municipalities (ICPDR, 2009).

Environmental data

Choice of environmental factors was based on recent studies of fish species distributions (Buisson et al., 2008; Lassalle et al., 2010; Markovic et al., 2012; Isaak et al., 2017). To provide information on the performance of freshwater SDMs at multiple scales, and in particular for the potential applications where fine resolution survey data are not available, all environmental data were gathered from publicly available databases. A total of 22 environmental variables emerged representing topographic, climatic and anthropogenic effects on ecosystems (Table 1). Topographic data were extracted from the CCM2 pan-European catchments database (CCM version 2.1, de Jager and Vogt, 2010). Climatic data were extracted from the Worldclim 30 arc-second (approx. 1km×1km) gridded information (Hijmans et al., 2007). As a measure of anthropogenic pressure, we used land cover information extracted from the CORINE land cover database (EEA, 2011) and the number of inhabitants per area (Population) based on the Global Rural-Urban Mapping Project (GRUMP, version1) (available at http://sedac.ciesin.columbia.edu/gpw, accessed on 10.11.2018). Although different aspects of the hydrologic regime, such as flow magnitude, frequency, timing and variability may impair ecological success of particular life stages of freshwater species (Domisch et al., 2015; Markovic et al., 2017), the availability of the discharge data is restricted even in the developed countries. The hydrologic predictors were not used as the aim of the study was to undertake performance assessment for SDMs that lacked fine grain survey data.

Hierarchical catchment orders

The analyses and modelling were conducted for five different catchment orders (WaterShed Order WSO1 to WSO5, Fig. S1) based on the Strahler order of the river reaches from the CCM2 pan-European catchments database (CCM version 2.1, de Jager and Vogt, 2010). The 1st order catchments (WSO1) were defined according to the drainage areas of the individual river reaches, while higher order catchments (WSO2 – WSO5) result from groupings of the lower-order catchments in a hierarchical way. The "WSO1" to "WSO5" nomenclature originated from the CCM2 pan-European catchments database and was kept here for consistency. Catchment order increase was reflected in an increasing catchment size, with an average ranging from 12 km^2 for the WSO1 to 2,148 km^2 for the WSO5. For each WSO, environmental factors were calculated by averaging gridded data across the corresponding catchment areas (Fig. S1).

Table 1 Initially considered environmental variables.

Category	Variable	Abbreviation	Description
Topographic	Altitude	Altitude	Mean catchment elevation
	Gradient	Gradient	Relief energy of the river segment
	Length	Length	Cumulative length of the upstream flow network
	Slope	Slope	Mean slope in percent
Climatic	Mean temperature	AnnTMean	Mean annual temperature
	Maximum temperature	AnnTMax	Max temperature of warmest month
	April-September temperature	TAprSep	Mean annual April to September temperature
	May-August temperature	TMaiAug	Mean annual May to August temperature
	Temperature range	TRange	Temperature annual range
	Annual temperature seasonality	TSeason	Standard deviation
	Wettest quarter temperature	WettTMean	Mean temperature of wettest quarter
	Precipitation	AnnPMean	Mean annual precipitation
	April-September precipitation	PAprSep	Mean annual April to September precipitation
	May-August precipitation	PMaiAug	Mean annual Mai to August precipitation
	Precipitation seasonality	PSeason	Coefficient of variation
Anthropogenic	Agricultural area	Agriculture	% of catchment area used for agriculture
	RowCrops	RowCrops	% of catchment area under row crops
	Forest	Forest	% of catchment area under forest
	Grassland	Grassland	% of catchment area under grasslands
	Pastures	Pastures	% of catchment area under pastures
	Built-up area	BuiltUp	% of catchment area under artificial surfaces
	Population	Population	Number of inhabitants per catchment

Fish data

Species occurrence data for the Danube River Basin were provided by Biofresh (www.freshwaterplatform.eu, Schinegger et al., 2016) for 1,364 sites (Fig. S1). Fisheries data were sampled by either single-pass or double-pass electrofishing between 1985 and 2002. To ensure an accurate estimate of the species distributions, only species with a minimum of 50 occurrences at the largest analyzed scale, the WSO5, were included into the analysis (cf. Coudon and Gégout, 2007). Eight fish species were included in the study and ecological

characterization followed Kottelat and Freyhof (2007): the bleak (*Alburnus alburnus*) is a small cyprinid and prefers open waters of lakes and medium to large rivers. The stone loach (*Barbatula barbatula*) is usually found in medium-sized rivers with gravel to stone bottom. *Barbus barbus* is a fish of the cyprinid family preferably inhabiting faster flowing, summer-warm, medium to large-sized rivers. Gudgeons of the genus Gobio, here represented by *Gobio obtusirostris*, are riverine cyprinids, too, which tolerate – in contrast to barbels – lower flow velocities and finer spawning substrates. The bullhead (*Cottus gobio*) inhabits cold, clear and fast-flowing water of small streams to medium-sized rivers. The roach (*Rutilus rutilus*) is a small fish of the cyprinid family mainly found in nutrient-rich large to medium sized lowland rivers and backwaters. The trout (*Salmo trutta*) is a species of salmonid fish preferring cold, well-oxygenated streams in the mountainous areas. The chub (*Squalius cephalus*) is a fish of the cyprinid family found in slow-flowing lowland rivers, very small mountain streams, and in large streams of barbel zone.

For each of the five WSOs, fish occurrence data were aggregated to presence/absence information (hereafter called "catchment-scale mapping"). The final number of catchments of each particular order and their spatial arrangement was thus directly constrained by fish data availability. With the WSO increase, the number of catchments under consideration decreased (from 1,363 for the WSO1 to 126 for the WSO5), with a corresponding increase in species prevalence (Table 2). We note here that, because of the dendritic structure of river networks, catchment-scale mapping is more appropriate for freshwater species than the point-to-grid mapping, used for mapping terrestrial species' occurrences (see Fagan, 2002). In addition, given that catchments serve as units for freshwater management and conservation (commonly referred to as the Catchment Based Approach – CaBA, see DEFRA, 2013), catchment-scale mapping of freshwater species' occurrences ensures compatibility between the management and the analysis scales (Lévêque et al., 2008; Markovic et al., 2017).

Table 2 Freshwater fish species and their prevalence. The total number of catchments for the studied scales (WSO1-WSO5) is indicated in parentheses.

Name	Code	WSO1 (1,363)	WSO2 (1,059)	WSO3 (681)	WSO4 (350)	WSO5 (126)
Alburnus alburnus	Albual	0.20	0.22	0.29	0.38	0.62
Barbatula barbatula	Barbbr	0.31	0.33	0.34	0.35	0.45
Barbus barbus	Barbba	0.20	0.21	0.23	0.28	0.45
Cottus gobio	Cottgo	0.44	0.42	0.43	0.48	0.51
Gobio obtusirostris	Gobris	0.31	0.33	0.36	0.37	0.51
Rutilus rutilus	Rutiru	0.22	0.25	0.30	0.38	0.58
Salmo trutta	Saltta	0.71	0.70	0.72	0.74	0.69
Squalius cephalus	Squace	0.44	0.46	0.49	0.53	0.72

Data analysis and modelling

Univariate strength of the environmental predictor variables was quantified using the weight of evidence (WOE) and information value (IV) concepts as implemented in the R (R Development Core Team, 2018) library "Information" (Larsen, 2016). While WOE describes the relationship between a predictor variable X (here environmental predictors listed in Table 1) and a binary dependent variable Y (here species occurrence in a particular catchment), information value measures the strength of the Y-X relationship. Specifically, if $b_i, i = 1, \dots, k$, denote k discrete bins for the predictor X, then, the strength of the predictor in describing Y can be quantified as

$$\sum_i (P(X \in b_i|Y = 1) - P(X \in b_i|Y = 0)) \times WOE_i \quad (1)$$

(cf. Larsen, 2016). As such, information value is suitable for the initial predictor selection, i.e., for comparing the predictive power of the environmental factors. The information value was used to reduce the parameter number used in the modelling and thus avoid possible overfitting. Specifically, among several strongly correlated parameters (with pairwise correlations above $|0.75|$), the parameter with the largest information values was used in the modelling.

Species distribution modelling was performed using Generalized Additive Models (GAM) (R library "gam"; Hastie, 2016). GAM is a non-parametric extension of generalized linear methods and is widely used for modelling current and future distribution patterns of fish species. Previous investigations using various SDMs have shown that GAM-, GLM- (Generalized Linear Models) and regression tree based SDMs have similar validation performance. The first two kinds of models had also similar calibration performance, while regression tree based SDMs tended to overfit during the calibration phase (Markovic et al., 2012). The improved performance of consensus or ensemble methods in providing more accurate and robust projections of species distribution have been already demonstrated (Marmion et al., 2009; Buisson et al., 2010; Lauzeral et al., 2013). However, the main objective of this study was determining the effect and importance of variation in spatial scale rather than the performance of different SDMs. Moreover, GAMs are very flexible models, and in contrast to the majority of SDMs, have well performance at high collinearity (Dormann et al., 2013). Therefore, we focussed only on GAM based SDMs, but acknowledge the importance of using multiple SDMs when the study goal is predicting future species distribution patterns (see Markovic et al., 2012; Meller et al., 2014).

Species occurrence probabilities resulting from GAM application were transformed to presence/absence information using the thresholds, which maximize both sensitivity (the true positive rate) and the specificity (the true negative rate). We applied random splitting of the fish data ten times into calibration (70%) and validation (30%), i.e., each of the ten models was calibrated using a different 70% data sample and validated using the remaining 30%. The repetitive modelling procedure allowed for quantifying the uncertainty of the estimates. Agreement between the observed and modelled species distribution patterns was quantified by sensitivity and specificity, while the performance of the calibrated models was estimated using the Area under the Receiver Operator Curve (AUC) and the True Skill

Statistic (TSS) (Allouche et al., 2006). The use of the different statistical measures (here, sensitivity, specificity, AUC and TSS) was necessary to ensure that sensitivities of the individual measures to prevalence and scale (see Lobo et al., 2007) were not misleading. An AUC of 0.5 and a TSS of 0 indicate that a model has no discriminatory power, while an AUC or TSS of 1 indicate that presences and absences are perfectly discriminated. The search for a parsimonious model involved analyses of the model improvement based on the Akaike Information Criterion (AIC) through simultaneous forward and backward predictor selection.

To quantify the relative predictor importance, the variance partitioning method by Lindeman et al. (1980), implemented within the R library "relaimpo" (Grömping, 2006) was used. The advantage of the variance partitioning method by Lindeman et al. (1980) is that it considers sequential sums of squares over all predictor permutations, and thus considers the inter-correlation effects among the individual predictors, with high predictor relative importance not necessarily implying causation.

Results

Information value and correlations

The mean catchment elevation (Altitude) manifested the highest univariate strength in describing distributions of the studied fish species across the studied spatial scales (Table S1 and Fig. S2f). Specifically, for WSO1, WSO2 and WSO5, Altitude had by far the highest information value (IV), and at WSO4 the second highest. At WSO3, eight predictors (including Altitude) had almost equally high IV. Consequently, Altitude had to be retained as the predictor at all scales, while predictors with either marginal IV (Length, PSeason, Grassland and Pastures) or extremely high correlations (-0.99 – -0.93) with Altitude (Slope, Gradient, AnnTMean, AnnTMax, TAprSep, TMaiAug and WettTMean) were omitted from the analyses for parsimony reasons (Table S1 and Fig. S2). It is noteworthy that the pairwise correlation between Altitude and several variables describing temperature (AnnTMean, AnnTMax, TAprSep, TMaiAug and WettTMean) increased with scale. The remaining temperature variables TRange (mean IV = 0.52) and TSeason (mean IV = 1.21) (Table S1), however, were included in order to account for direct temperature effects and not solely indirect given by the often-used temperature surrogate Altitude, whereby correlations between Altitude and TRange as well as TSeason were still high for catchment scales above WSO2 (-0.90 – -0.74) (e.g. Fig. S3). We note that GAMs are very flexible models and still have well performance at high collinearity. For WSO1 and WSO2, however, pairwise correlations of these variables with Altitude were below |0.75| (-0.74 – -0.54). Mean information values of further climatic variables, i.e. PMaiAug, PAprSep and AnnPMean, were close to each other (1.30 – 1.42) (Table S1). High pairwise correlations among the three precipitation parameters and a lower correlation for WSO1 – WSO5 between AnnPMean and each of the already chosen variables, especially Altitude, led to the exclusion of PAprSep and PMaiAug. A low mean information value led also to the exclusion of the last precipitation variable PSeason (0.43) (Table S1).

Among the anthropogenic variables, the area under row crops (RowCrops) emerged as the most valuable in describing distributions

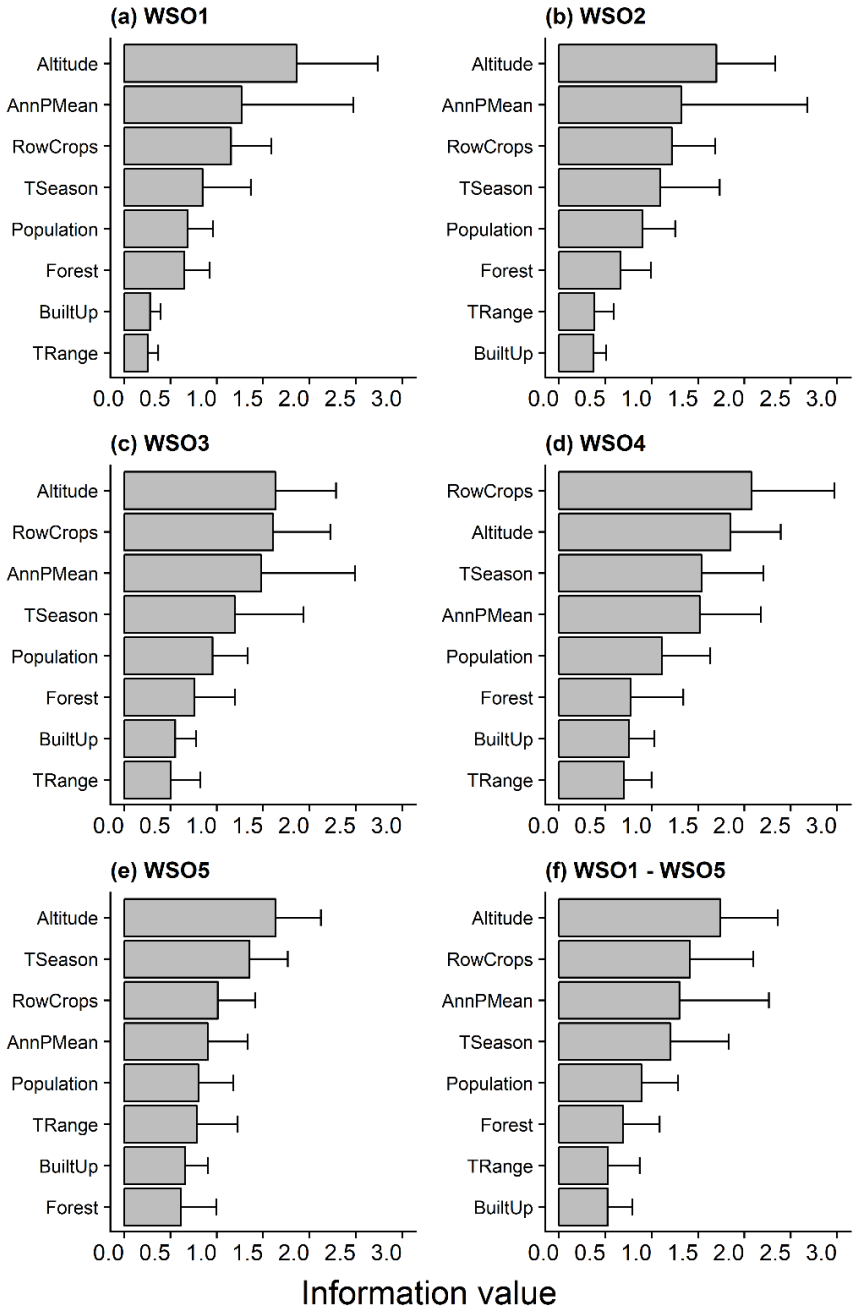

Figure 1 Information value as a measure of the univariate strength of the environmental predictor variables. For convenience, the environmental predictors are ordered according to their information value. (a)-(e) For each of the five spatial scales the information value was calculated as an average predictive strength of the environmental predictor across all studied species; (f) the overall information value of an environmental predictor was calculated as an average predictive strength across all scales and all considered species. Error bars represent one standard deviation of the estimates.

of the studied fish species. The high correlation between RowCrops and the second most valuable anthropogenic variable Agriculture (0.78 – 0.95) (e.g. Fig. S3) has led to the omission of Agriculture. While the remaining anthropogenic variables BuiltUp, Forest and Population were included in the final variable set because of low pairwise correlations among the included variables and high information values within the anthropogenic category, the variables Grassland and Pastures were excluded due to low information values (Table S1).

The final variable set consequently consisted of the topographic variable Altitude, the climatic variables TRange, TSeason and AnnPMean, and the anthropogenic variables RowCrops, Forest, BuiltUp, and Population (Fig. 1 and Table S2).

Model performance

Using the selected eight predictor variables (Table S2), we pursued two distinct model fitting approaches across all catchment scales and species: Modelling species distributions with GAM by (a) keeping the predictor number (n = 8) constant across the scales, and (b) using simultaneous forward and backward predictor selection in order to obtain a parsimonious model. When keeping all predictors across all scales, the overall validation performance was highly accurate with a mean AUC of 0.88 and a mean TSS of 0.63 across all catchment scales and species (Table S3). Similar results held for the models

Table 3 Mean and standard deviation (sd) for validation AUCs and TSSs of the multivariate SDMs with simultaneous forward and backward predictor selection across all studied scales (WSO1-WSO5). Performance was assessed by using repeated random splitting (10 times) of the fish data into calibration (70%) and validation (30%).

Species	Accuracy measure		WSO1	WSO2	WSO3	WSO4	WSO5
A. alburnus	AUC	mean	0.90	0.90	0.91	0.91	0.91
		sd	0.01	0.02	0.02	0.03	0.05
	TSS	mean	0.61	0.65	0.68	0.71	0.69
		sd	0.04	0.04	0.04	0.08	0.10
B. barbatula	AUC	mean	0.83	0.86	0.87	0.87	0.77
		sd	0.02	0.02	0.01	0.02	0.05
	TSS	mean	0.53	0.58	0.60	0.59	0.47
		sd	0.05	0.04	0.04	0.03	0.12
B. barbus	AUC	mean	0.86	0.85	0.84	0.83	0.76
		sd	0.02	0.03	0.03	0.04	0.07
	TSS	mean	0.57	0.51	0.53	0.46	0.37
		sd	0.07	0.05	0.06	0.06	0.15
C. gobio	AUC	mean	0.83	0.86	0.86	0.90	0.85
		sd	0.01	0.01	0.02	0.02	0.05
	TSS	mean	0.53	0.57	0.56	0.67	0.57
		sd	0.02	0.03	0.04	0.05	0.13
G. obtusirostris	AUC	mean	0.89	0.89	0.89	0.89	0.81
		sd	0.02	0.01	0.02	0.02	0.08
	TSS	mean	0.64	0.64	0.60	0.63	0.46
		sd	0.03	0.05	0.06	0.07	0.19
R. rutilus	AUC	mean	0.90	0.91	0.90	0.91	0.85
		sd	0.01	0.02	0.02	0.02	0.06
	TSS	mean	0.66	0.69	0.69	0.71	0.64
		sd	0.03	0.05	0.04	0.05	0.15
S. trutta	AUC	mean	0.94	0.95	0.97	0.98	0.96
		sd	0.01	0.01	0.01	0.01	0.04
	TSS	mean	0.75	0.76	0.82	0.89	0.82
		sd	0.03	0.02	0.04	0.04	0.10
S. cephalus	AUC	mean	0.87	0.87	0.87	0.87	0.83
		sd	0.01	0.02	0.02	0.03	0.07
	TSS	mean	0.60	0.59	0.56	0.57	0.49
		sd	0.03	0.04	0.05	0.08	0.15

with simultaneous forward and backward predictor selection where a mean validation AUC of 0.88 and a mean validation TSS of 0.62 (Table 3) were obtained. The highest performance values for both model fitting approaches were observed for *S. trutta* at WSO4 (AUC = 0.98) (Table 3 and Table S3). Overall, when coarsening the grain size (i.e. increasing catchment order), both a slight model degradation and a slight model improvement was observed (Fig. S4 and S5). In addition, the increasing catchment order was accompanied by an uncertainty increase manifested by an increase in the

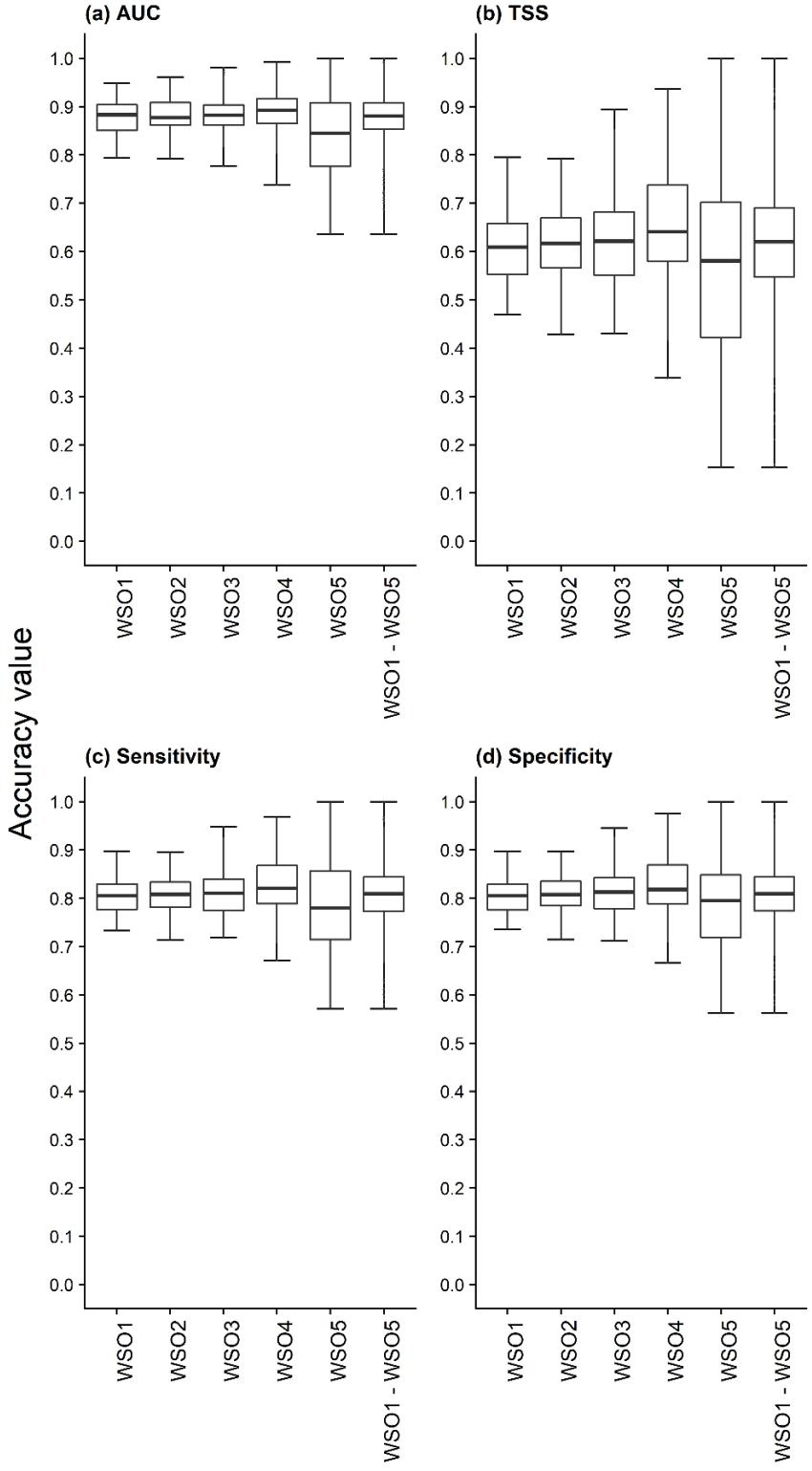

Figure 2 Mean performance measures of the multivariate SDMs with simultaneous forward and backward predictor selection across the five studied scales (WSO1 – WSO5). Performance was assessed by using repeated random splitting (10 times) of the fish data into calibration (70%) and validation (30%) and calculating the (a) AUC, (b) TSS, (c) sensitivity and (d) specificity.

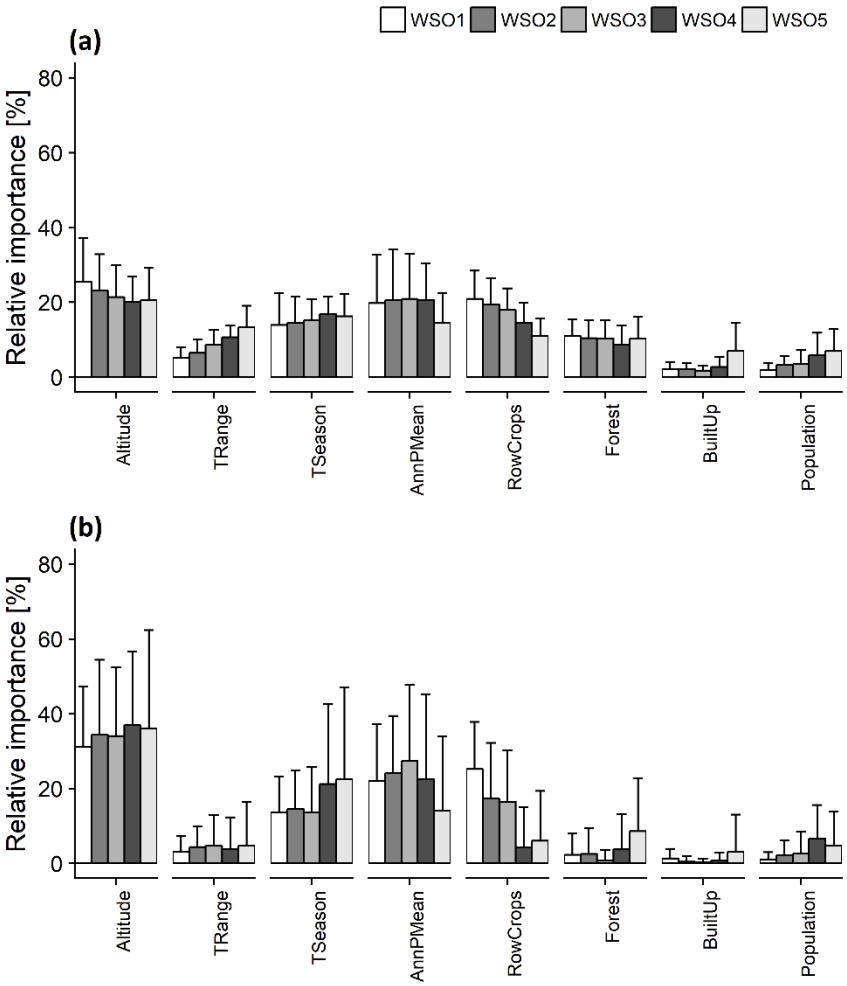

Figure 3 Mean relative predictor importance resulting from the SDMs across all studied species and all studied scales (WSO1-WSO5) for two distinct model fitting approaches: (a) with keeping the predictor number constant across the scales, and (b) with simultaneous forward and backward predictor selection. Error bars represent one standard deviation of the estimates. We note that the figure represents the mean relative predictor importance based on all model runs per species and catchment order.

standard deviation of the validation sensitivity, specificity, AUC and TSS (Fig. 2 and Fig. S6).

Predictor importance per species and catchment order

Predictor importance patterns varied across species and catchment orders (Fig. 3-4, Table S4-S5, Fig. S7-S14). High variation throughout species is shown in Fig. 3 by high standard deviations for all variables. For both model fitting approaches and all species, highest predictor importance was distributed among the variables Altitude (20.1% – 37%), TSeason (13.5% – 22.5%), AnnPMean (14.1% – 27.5%) and RowCrops (4.3% – 25.3%) (Fig. 3). In general, lowest predictor importance was present for TRange, Forest, BuiltUp and Population. However, TRange was shown to have an increasing overall mean importance with increasing catchment order (5.1% – 13.4%) and Forest an overall nearly constant importance across all scales at around 10%, both inferred from the first model fitting approach, which keeps the predictor number constant. Using simultaneous forward and backward predictor selection implied a mean predictor importance below 9% for the four least important variables across all scales (Fig. 3). Trends in the predictor importance for the four most important variables across the five catchment orders varied depending on whether the predictors were kept constant across scales or automatically selected. The first approach identified a downward trend of the importance for Altitude with increasing scale, whereas the second approach

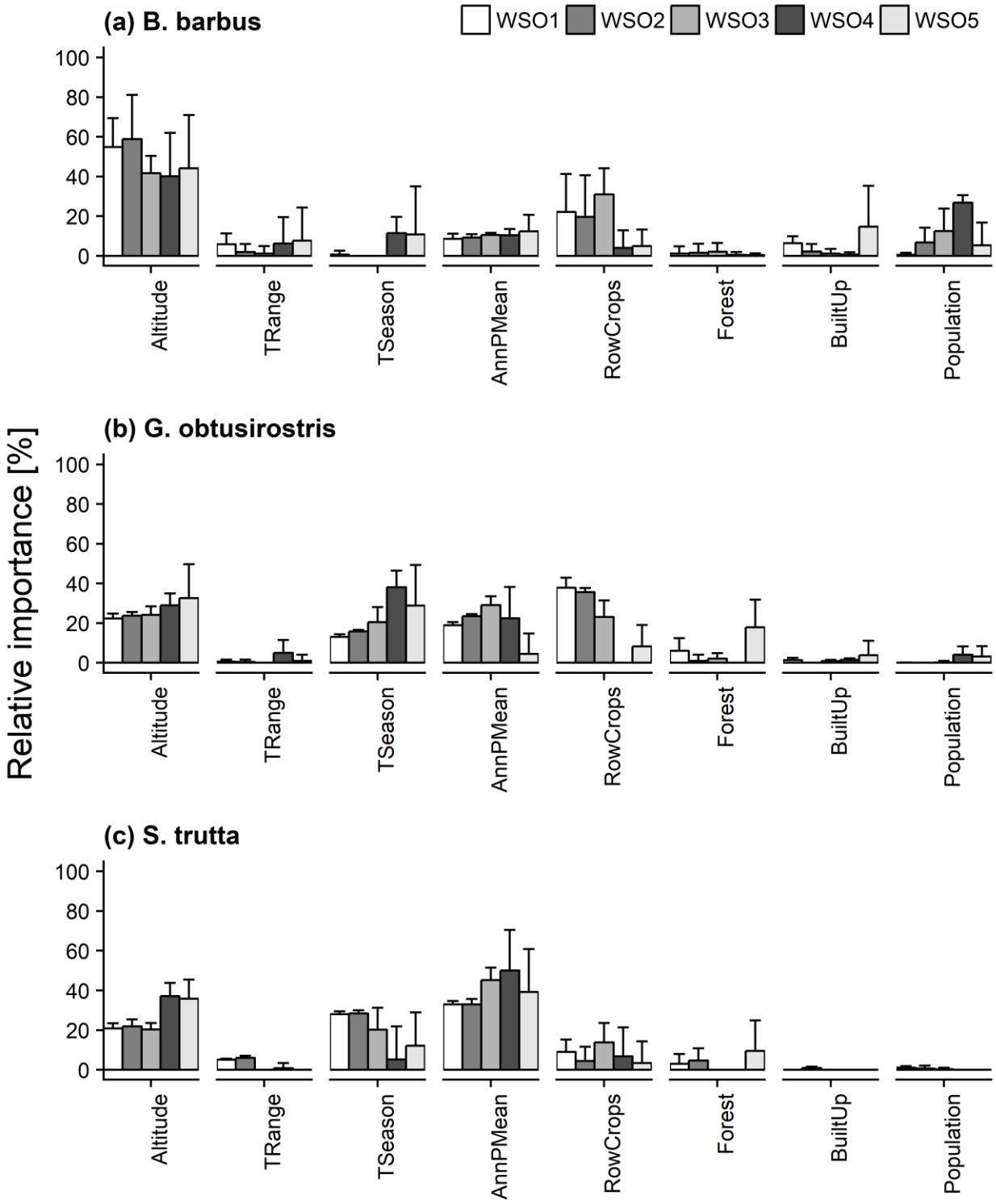

Figure 4 Relative predictor importance in describing distribution patterns of (a) *B. barbus*, (b) *G. obtusirostris* and (c) *S. trutta* across the studied scales (WSO1-WSO5) inferred from the multivariate SDMs with simultaneous forward and backward predictor selection. Error bars represent one standard deviation of the estimates. We note that the figure represents the mean relative predictor importance based on all model runs per catchment order.

delineated an increasing importance with increasing scale. Trends of predictor importance along the studied scales inferred from both approaches were similar for TSeason, which could be described by an upward trend, whereas the importance for WSO4 and WSO5 deduced from the second approach was higher. Both model fitting

approaches assigned high importance to AnnPMean from WSO1 to WSO4 and lower importance at WSO5. The second approach, however, showed greater variation for AnnPMean. The predictor importance of RowCrops for both approaches revealed highest explanation power at local scales and lower importance at WSO4 and WSO5 (Fig. 3). Overall, at least one variable of the three considered categories ("topographic", "climatic", "anthropogenic"), respectively, was identified as important in describing fish species distributions.

On the single species level, most important variables consisted in general of a subset of the overall identified four most important variables (Altitude, TSeason, AnnPMean, RowCrops) (Fig. 4, Table S4-S5, Fig. S7-S14). Few exceptions were for example *B. barbus* or *G. obtusirostris* where higher predictor importance with increasing scale of TRange for the first model fitting approach was observable (Fig. S9 and S11). Moreover, some of the four most important predictors were only selected at certain catchment orders. As such, TSeason as explanatory variable for the distribution of *B. barbus* had a predictor importance above 10% only for WSO4 and WSO5, whereas for WSO2 and WSO3 the variable was not selected as predictor (Fig. 4a and Table S5). However, Altitude was dominating the predictor importance pattern of *B. barbus* from WSO1 to WSO5 and the distribution of *B. barbus* at the local levels WSO1 to WSO3 was strongly influenced by RowCrops (Fig. 4a and Table S5). This pattern was also identified by the first modelling approach (Fig. S9a and Table S4). In addition, the anthropogenic variable Population, here generally identified as variable with low importance, had an importance of 26.8% at WSO4 for models with automatic predictor selection. Such occasional high importance of variables with generally low importance could also be observed for other considered species. For *G. obtusirostris*, Altitude, TSeason, AnnPMean and RowCrops emerged as the key factors (Fig. 4b, Fig. S11 and Tables S4-S5). Similarly, for *S. trutta*, Altitude, TSeason, AnnPMean and RowCrops were most often selected as predictors across all scales (Fig. 4c, Fig. S13 and Tables S4-S5).

Discussion

The majority of models of fish distribution patterns across the studied spatial scales were highly accurate for both used model fitting approaches. The negligible effect of the catchment order on the mean performance of freshwater SDMs is in line with the results of Guisan et al. (2007) who have shown that coarsening study grain-size through grid-cell size increase, does not have substantial effects on the performance of terrestrial SDMs. However, our study additionally shows that the variance of the validation performance measures increases with increasing scale. The high accuracy of the SDMs across all studied catchment orders confirms the overall appropriateness of the considered environmental factors and is also a reflection of the predictive ability of the applied statistical methodology, i.e. GAM. As such, we note that adding new parameters to our models would rather result in an overfitting than in a meaningful improvement in the model accuracy.

When looking at the predictive ability of each individual environmental factor, the topographic variable Altitude, the climatic variables TSeason and AnnPMean, and the anthropogenic variable RowCrops tend to be the most important predictors irrespective

whether or not an automatic predictor selection was used. Altitude, which can be seen as a surrogate for temperature, and climatic factors are well known to influence fish species distributions (e.g. Kuemmerlen et al., 2014). The identification of RowCrops as important predictor aligns with previous studies stressing the importance of surrounding landscape on the in-stream ecosystem structure and function (Fausch et al., 2002; Linke et al., 2008). The link between the area covered by RowCrops and fish distribution patterns was argued by Strayer et al. (2003) as high nitrate flux leading to a high level of aquatic plant cover which in turn leads to low fish species richness. Similarly, intensely used crop lands with its bare soils free of weeds suffer from surface erosion and thus, provide a continuous source of fine sediments leading to clogging and siltation of coarse substrates followed by the decline of gravel-spawning riverine fish species (Soulsby et al., 2001; Lapointe et al., 2004; Greig et al., 2005; Jensen et al., 2009). Overall, our results, especially the differences in predictor importance trends across scales of the two approaches and the corresponding variable selection, suggest species dependent selection of factors describing species distributions, paired with appropriate monitoring of effects and management of mitigation activities tailored to ensure species' long-term persistence.

The relative importance of the factors used to describe species distribution patterns is known to vary across spatial scales (Jackson et al., 2001; Blackburn and Gaston, 2002; Tudesque et al., 2014). At the same time, the relative importance of the spatial scale and the environmental factors used in species distribution modelling is largely determined by a combination of species range and species prevalence (Hopkins and Burr, 2009). Our results indicate that for *B. barbus* the relative importance of anthropogenic pressure – manifested by RowCrops, Population and BuiltUp – is similar to or higher than the importance of the considered three climatic factors. *B. barbus* is known to be especially sensitive to damming, river regulation and fine sediment input indicating that the results of the SDMs well align with the ecological classification of this species (Kottelat and Freyhof, 2007). Also, *B. barbus* seems more susceptible to the effects of land-use on water quality and spawning habitat than *S. trutta* (which has similar environmental requirements). However, this seeming relation simply results from higher cumulative anthropogenic pressure at the lower elevated river reaches preferably colonized by barbel. This is further confirmed by the finding that the influence of RowCrops at local scales better describes the distribution of gudgeons of the genus Gobio, which prefer cold and clean water. Our finding of the dominant role of climatic variables in shaping distribution patterns of the fish species studied for all catchment orders, contradicts the suggestions that climate related factors may be good predictors of species distributions only at the macro-scale (e.g. Pearson and Dawson, 2003). However, for robust conclusions to be made further integrated climate impact modelling would be needed.

Although it contributes significantly to the understanding of freshwater fish patterns at various scales, our modelling framework has a number of limitations. One limiting aspect of our study framework lies in the fact that the selected set of catchment orders and the predictor data set used do not account for the effects of spatial arrangements of local habitats and spatial autocorrelation effects, as well as

habitat peculiarities with respect to species requirements at different life stages. Specifically, proximal environment experienced by a species is not necessarily reflected in the geographic scales used to calculate the environmental factors. As such, the probability of species' occurrence resulting from the calibrated models provides the information on the potential habitat suitability of catchments at different hierarchical levels. This suitability does not consider the accessibility of habitats required for particular life stages, or temporal resource availability and adequateness.

Another weakness is the use of multi-decadal averages of climatic factors in the model calibration process. Climate information for the last 30-50 years may not adequately reflect species environmental tolerance ranges. Moreover, the tolerance limits are rarely rigidly fixed, as they might depend on lifetime experience, the developmental stage of individuals within species and the combined effect of various abiotic and biotic factors. Consequently, in order to account for temporal and spatial aspects of species distribution patterns, researchers will need to disentangle species information according to life stages, the life strategy and temporal mismatch of predictors to response, as well as environmental information according to temporal variability scales of the physical processes governing individual environmental properties. Time, space and hierarchical level are the fundamental axes of scale, and since many physical and ecological phenomena are related in space versus time (Wu and Li, 2006) temporal information should be accounted for in models of species distributions (see also Soranno et al., 2014).

Conclusion

Coarsening study grain-size through catchment order increase are shown to be of minor influence on the mean performance of freshwater fish SDMs. However, the uncertainty of the estimates increases with scale. We highlight the importance of using anthropogenic effects as population and land cover related predictors when addressing species sensitive to pollution such as *B. barbus*. Specifically, our results indicate that the model complexity and the importance assigned to environmental drivers of fish distributions are both catchment order dependent and species dependent. The latter emphasizes importance of compatibility between the scale of factor importance and species conservation management scale.

With the current threat to freshwater biodiversity and lack of information on which to base freshwater conservation strategies in many regions of the world, in particular less-developed countries, our results have useful implications for predicting distributions of species and conservation planning in areas where fine grain survey data on species occurrence are unavailable. In particular, our results indicate that the use of broader scale species and environmental data (i.e. up to WSO5 catchment scale data), does not significantly affect the performance of SDMs. We remind here that the ecological scales of relevance of species and environmental variables should be matched (Hurlbert and Jetz, 2007), although the increased availability of high-resolution environmental data is tempting towards studying species distributions at finer resolutions than the species survey data, to avoid misleading conservation assessments. In addition, in view of the extreme global pressure of climate

change on freshwater ecosystems and the importance of the climatic factors on distribution patterns of the studied freshwater fish species even at the smallest studied scale (reach scale), our findings underline the necessity of efforts to continuously re-assess the potential effects of climate change on suitability of catchments for freshwater fish species. Given the high vulnerability of freshwater ecosystems paired with limited dispersal ability of strictly aquatic species such as fish, addressing environmental effects across multiple (spatial and temporal) scales is central to effective species conservation and timely identification of potentially detrimental changes in habitat suitability.

Chapter 5

Freshwater species distributions along thermal gradients

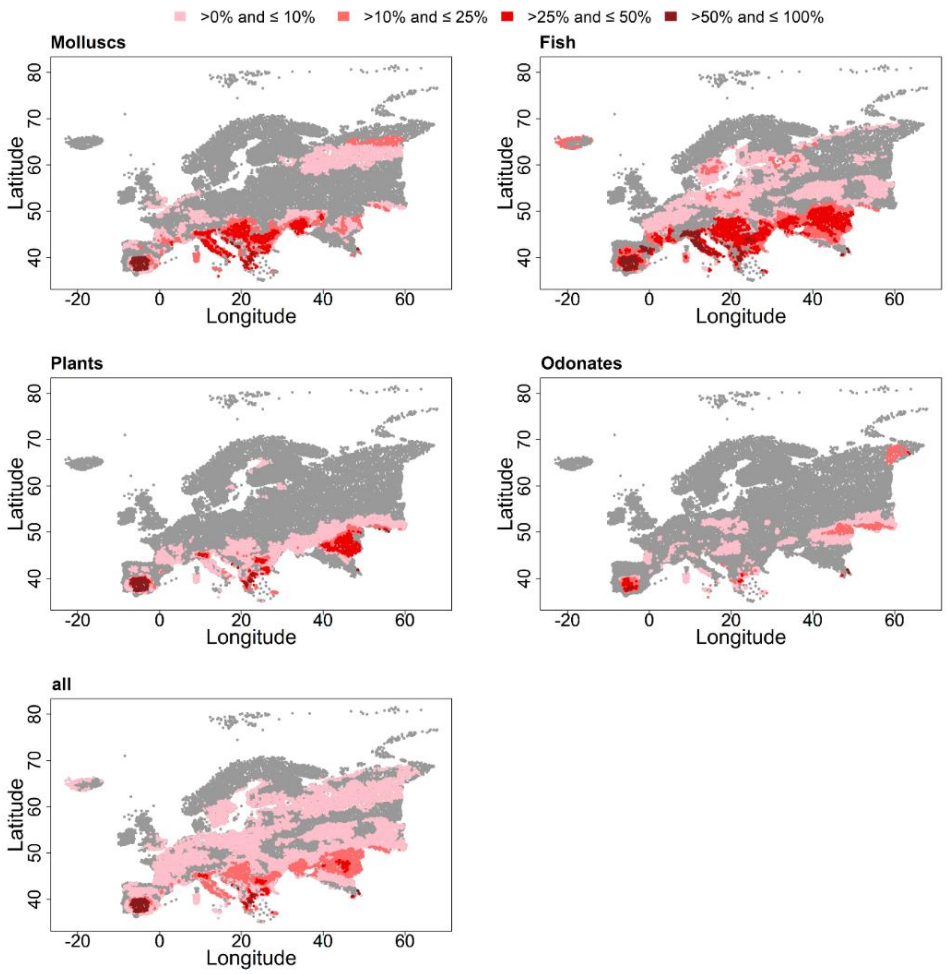

This chapter has been published as Kärcher, O., Hering, D., Frank, K., and Markovic, D. (2019). Freshwater species distributions along thermal gradients. *Ecology and Evolution*, **9**(1), 111–124. https://doi.org/10.1002/ece3.4659

Supporting information can be found in Appendix 3 of the thesis. The full version of the Appendix is available at:
https://onlinelibrary.wiley.com/doi/full/10.1002/ece3.4659

Abstract

The distribution of a species along a thermal gradient is commonly approximated by a unimodal response curve with a characteristic single optimum near the temperature where a species is most likely to be found and a decreasing probability of occurrence away from the optimum. We aimed at identifying thermal response curves (TRCs) of European freshwater species and evaluating the potential impact of climate warming across species, taxonomic groups, and latitude. We first applied generalized additive models using catchment-scale global data on distribution ranges of 577 freshwater species native to Europe and four different temperature variables (the current annual mean air/water temperature and the maximum air/water temperature of the warmest month) to describe species TRCs. We then classified TRCs into one of eight curve types and identified spatial patterns in thermal responses. Finally, we integrated empirical TRCs and the projected geographic distribution of climate warming to evaluate the effect of rising temperatures on species' distributions. For the different temperature variables, 390–463 of 577 species (67.6%–80.2%) were characterized by a unimodal TRC. The number of species with a unimodal TRC decreased from central toward northern and southern Europe. Warming tolerance (WT = maximum temperature of occurrence—preferred temperature) was higher at higher latitudes. Preferred temperature of many species is already exceeded. Rising temperatures will affect most Mediterranean species. We demonstrated that freshwater species' occurrence probabilities are most frequently unimodal. The impact of the global climate warming on species distributions is species and latitude dependent. Among the studied taxonomic groups, rising temperatures will be most detrimental to fish. Our findings support the efforts of catchment-based freshwater management and conservation in the face of global warming.

Introduction

Freshwater ecosystems cover less than 1% of the Earth's surface but are home to around 6% of all known species (Strayer and Dudgeon, 2010). The warming rates of recent decades combined with the multitude of anthropogenic stressors threaten the biological diversity, structure and function of freshwater ecosystems (Woodward et al., 2010; Strayer and Dudgeon, 2010; Mantyka-Pringle et al., 2014). Habitat fragmentation and the limited ability of many species to track spatial shifts towards suitable habitats cause freshwater biodiversity to be highly vulnerable to climate warming (cf. Markovic et al., 2017).

The magnitude of the already observed temperature alterations plays a fundamental role for determining the future climatic suitability of current species' ranges. Temperature has strong impacts on the physiology (Vornanen et al., 2014), growth (Elliott and Allonby, 2013) and behaviour of certain species (Frost et al., 2013). According to the Fifth Assessment Report of the Intergovernmental Panel on Climate Change (IPCC, 2013), the linear trend of the globally averaged combined land and ocean surface temperature data show a warming of 0.85°C (0.65 to 1.06°C), over the period 1880–2012 (IPCC, 2013). Recent warming was shown to drastically shift the ranges of different taxonomic groups (Chen et al., 2011; Domisch et al., 2013a; Markovic et al., 2017), leading to a decline of many populations (Parmesan, 2006). Especially for strictly aquatic species, temperature may set environmental tolerance

range limits (Wiens, 2011). Accordingly, already minor shifts in water temperature lead to considerable changes of species assemblages.

The typical assumption for a thermal response curve of a species is the Gaussian curve (Gauch and Whittaker, 1972), with the preferred temperature at its peak. For freshwater species, responses along thermal gradients are sparsely explored, providing the opportunity to investigate current thermal response shapes. Most previous studies on the thermal responses of freshwater species have been constrained to single taxonomic groups or to single stream networks. For example, using the logistic generalized linear regression models (GLMs), Logez et al. (2012) have identified thermal responses for 21 native European fish species, while Isaak et al. (2017) identified thermal responses for 14 fish and amphibian species for a mountain stream network in the U.S. Rocky Mountains. Similarly, Pyne and Poff (2017) identified insect taxon response curves for temperature and streamflow. Comparative studies delineating response curves of species from various taxonomic groups are missing.

Assessing species responses along environmental gradients commonly involves the use of various statistical approaches that estimate the probability of a species' occurrence as a function of the environmental conditions across the current species' geographic range, i.e., the environmental response curves. GLMs are among the most widely used approaches for identifying response curves. However, there are numerous alternative approaches such as 95%-quantile regressions (Carrascal et al., 2016) or Huisman-Olff-Fresco models (HOF) (Huisman et al., 1993). The latter are considered one of the best statistical tools for response modelling, because of their predictive performance (Oksanen and Minchin, 2002; Jansen and Oksanen, 2013). It was shown that HOF models perform better than GLMs or beta functions (Oksanen and Minchin, 2002; Lawesson et al., 2003). Generalized additive models (GAMs) provide response curves that coincide with the shape of those resulting from the HOF models (Jansen and Oksanen, 2013). Specifically, Jansen and Oksanen (2013) have shown that the HOF models were mostly located in the range of the 95% confidence interval of GAMs. Additionally, according to Oksanen and Minchin (2002) GAMs and HOF models usually were consistent, but GAM has a greater flexibility regarding the response shape than HOF models, which are restricted to a limited number of shapes.

This study explores and compares the thermal responses of 577 European freshwater species of molluscs, fish, plants, odonates and crayfish. Thermal properties derived from global species ranges (209,659 catchments) are transferred to the European scale (16,689 catchments). We use GAMs to link the species occurrence data to the annual mean air/water temperature and to the maximum air/water temperature of the warmest month, respectively, to parameterize species' thermal response curves (TRCs). Specifically, we examine and compare the TRC types for the different temperature variables and the thermal properties across the individual species, taxa groups and latitudes. The TRCs link the species occurrence probability to temperature patterns and are thus of fundamental importance for the conservation of freshwater biodiversity given the current warming rates and the likelihood of further temperature increases (cf. Isaak et al., 2017). Finally, we match the empirical thermal response curves with the projected

temperature for the middle of the 21st century to evaluate the impacts of temperature alterations on freshwater species distributions throughout Europe.

Materials and methods

Species data

The IUCN Global Species Programme, as part of the Red List assessment process (IUCN, 2013, 2014), compiled presence and absence data on freshwater species distribution ranges in polygon shape files corresponding to global watershed boundaries. To capture the whole range of freshwater species native to Europe, the global species data from the IUCN Global Species Programme were used. Global data were available for 1,402 freshwater species native to Europe including 609 molluscs, 473 fishes, 209 plants, 106 odonates, and five crayfish (see https://www.iucn.org/theme/species/our-work/iucn-red-list-threatened-species for more details). Freshwater species data were mapped to 209,659 catchments at the HydroBasins level 8 resolution (Lehner and Grill, 2013) (see Appendix 3, Fig. S1.1). Only species that occurred in at least 50 catchments were part of the analysis to guarantee an accurate estimate of the TRCs (Coudon and Gégout, 2007). Due to the dendritic structure of river networks, catchment mapping is more appropriate for freshwater species than the point-to-grid mapping used for mapping terrestrial species' occurrences (see Fagan, 2002). In addition, given that catchments serve as units for freshwater management and conservation (commonly referred to as the Catchment-Based Approach—CaBA, see DEFRA, 2013), catchment-scale mapping of freshwater species' occurrences ensures compatibility between the management and the analysis scales (Lévêque et al., 2008; Markovic et al., 2017).

Climate data

Global climatic data were ascertained for the second half of the 20th century (1960–1990, hereafter referred to as baseline) from the WorldClim (version 1.4) 30 arc-second (approximately 1 km × 1 km) data set (Hijmans et al., 2005, www.worldclim.org, accessed on March 19, 2018). Due to a lack of *in situ* and satellite-retrieved water temperature data given the large spatial extent of our study (209,659 river catchments), parameterization of species' thermal response curves was based on the catchment-specific annual mean air temperature ($Tmean_{air}$) and the maximum air temperature of the warmest month ($Tmax_{air}$) of the baseline period. However, given a strong correlation between water and air temperature (Markovic et al., 2013; Mohseni et al., 1998), we used a global relationship model to transform air temperature to stream water temperature on a monthly basis (Punzet et al., 2012). Thus, we estimated the annual mean water temperature ($Tmean_{water}$) and the maximum water temperature of the warmest month ($Tmax_{water}$). The annual mean water temperature was derived by averaging the transformed monthly average air temperatures. Areas without appreciable flows, that is, lakes, reservoirs, and lagoons, were excluded from the analysis. Pairwise Pearson correlations among the four used variables ranged from 0.81 to 0.98 (Table S1.1).

Future climate projections for Europe (16,689 river catchments) were gathered for the middle of the 21st century (hereafter referred to as 2050s) from the CIAT (International Center for Tropical Agriculture) 30 arc-

seconds gridded data set (www.ccafs-climate.org). The projections in the CIAT data set were obtained by three climate models (MOHC, IPSL, and MPI), each considering the RCP4.5 (Representative Concentration Pathways) emission scenario. RCP4.5 follows a medium-low mitigation of greenhouse gas emission and represents intermediate scenarios (van Vuuren et al., 2011). The gridded layers of the 20th and 21st century $Tmean_{air}$ and $Tmax_{air}$ were mapped to HydroBasins level 8 resolution catchments using the ESRI ArcGIS zonal statistics tool and afterwards transformed to projections of $Tmean_{water}$ and $Tmax_{water}$ using the derived global relationships model (Punzet et al., 2012).

Modelling thermal response curves

Statistical model

Global distributions of freshwater species native to Europe were modeled using GAMs (Hastie, 2016). GAMs are useful to model nonlinear relationships and for relating binary data to probabilities by an adequate transformation of the fit. The evaluation of the species' thermal response curves for the four different temperature variables $Tmean_{air}$, $Tmax_{air}$, $Tmean_{water}$, and $Tmax_{water}$ (four models per species) was based on a univariate modeling approach, that is, $Tmean_{air}$, $Tmax_{air}$, $Tmean_{water}$, or $Tmax_{water}$ was the only explanatory variable, respectively. Furthermore, a smoothing by spline functions with three degrees of freedom, that is, a piecewise interpolation by polynomials of maximal order two, was applied in order to get a smooth representation of the probability.

Based on the probability results from the statistical model, a threshold for separating presences and absences of a species was determined by minimizing the absolute difference between specificity (the rate of correctly predicted absences) and sensitivity (the rate of correctly predicted presences) (Fielding and Bell, 1997). Minimizing the difference between the sensitivity and specificity generally leads to accurate predictions (Jimenez-Valverde and Lobo, 2007).

To evaluate the models' performance, two main measures were calculated: the area under the receiver operating characteristic (ROC) curve, AUC (Hosmer and Lemeshow, 2000), and the true skill statistic (TSS = sensitivity + specificity − 1), whereas specificity and sensitivity are the result of the probability threshold determination (Allouche et al., 2006). AUC values can range from 0 to 1, with values of 0.5–0.7 demonstrating poor performance, 0.7–0.9 moderate, and >0.9 high performance (Manel et al., 2001; Swets, 1988). An AUC value of 0.5 indicates a random prediction while an AUC value of 0 means that every presence is incorrectly predicted. TSS values range from −1 to +1, where values ≤0 indicate a random and +1 a perfect performance (Allouche et al., 2006). Consequently, only species with thermal modeling results fulfilling AUC ≥0.7 and TSS ≥0.4 for all four temperature variables were included in further investigations.

To account for accuracy of the predictive performance, the data were split into a training (80%) and validation (20%) data set. The random data splitting into the training and the validation data sets procedure was repeated 100 times, leading to 100 individual values of the main performance measures for the calibration and validation phase, respectively, which were averaged afterwards (Dormann et al., 2008). The average AUC and TSS values of

the validation were used for the assessment of the predictive performance.

Uncertainty was depicted by calculating 95% confidence intervals (CIs) around the modeled probabilities of occurrence, that is, around the thermal response curves, for each observation. CIs give an impression of the scattering and the preciseness of statistically calculated key figures (De Jong and Heller, 2008).

Thermal response curve types

The resulting thermal response curves for each of the four temperature variables, illustrating the probability of occurrence along the thermal gradient, were classified into eight different curve types (see Table 2). Type I corresponds to a Gaussian distribution, that is, a unimodal symmetric response, showing a uniform distribution of the species' occurrence around the temperature with the highest probability of occurrence (here termed as "preferred temperature"). Type II represents a unimodal right skewed response and thus a tendency toward warmer regions. Type III describes a unimodal left skewed response, representing the tendency toward colder regions, that is, regions below the preferred temperature. Type IV represents no response, that is, the response curve is approximately a constant line at some probability. Type V describes an increasing probability of occurrence up to a certain threshold and an afterwards nearly constant response at the height of the respective threshold, showing a constant probability for higher temperatures. Type VI corresponds to a mirror image of the Type V response. Type VII response is characterized by a monotonic growth and Type VIII by a monotonic decline, indicating higher or lower probabilities along cold to warm temperatures, respectively (see Table 2).

Responses were automatically identified as Type IV, that is, no response, if the maximum probability of occurrence was smaller than 0.01, because for these low probability TRCs no reliability can be assumed. In cases of a maximum probability greater than or equal to 0.01, all types were taken into consideration in order to determine the type via an automatic identification that makes use of the slope properties of each thermal response curve.

Assessment of species' thermal properties

The global thermal range of each single species is defined as the current temperature range. Thus, the thermal range is the difference between the maximum temperature and the minimum temperature of occurrence. Thermal ranges or breadths facilitate the understanding of the vulnerability to extinction and of the rarity of a species (Slatyer et al., 2013). Additionally, for each of the four statistical models, a thermal preference for species of Types I-III, that is, for species with unimodal responses, was specified. The preferred temperature (T_{pref}) is the temperature with the highest probability of occurrence. T_{pref} was determined by using the function "optimize" implemented in R (R Development Core Team, 2017), which searches for the maximum probability. The maximum temperature at which the species was registered for each temperature variable was set as critical temperature (CT).

Species sensitivity to global warming is closely related to species' thermal range, thermal distribution and preferred temperature (cf. Markovic et al., 2017). For example, species with a small thermal range and low CT are more likely to be sensitive to rising temperatures. The potential exposure to global warming at the European scale was quantified using the difference between the

average of the respective projected temperature variables of the three climate models and the corresponding species-specific CT. The difference was considered "critical" if the projected temperature exceeded CT (i.e., the current baseline maximum temperature of occurrence of the species). "Warming tolerance" (WT) was calculated as the difference between CT and T_{pref} of the statistical model (WT = CT − T_{pref}). For each temperature variable, "safety margin" (SM) was calculated as the difference between T_{pref} and the average temperature of the species' current temperature range (T_{av}) (SM = T_{pref} – T_{av}). WT and SM values were derivable only for species with a unimodal response curve (Types I-III). Geographical variations at the European scale of these tolerance measures were depicted by averaging across latitude. We note that the critical temperature (CT), safety margin (SM), and the warming tolerance (WT) are the common terms used to describe the species thermal performance curves (TPCs) (see Deutsch et al., 2008). Here, we used the latter terms to provide comparable descriptors of the TRCs, but underline that the interpretation of the CT, SM, and WT in the context of TRCs and TPCs is different. Specifically, while TPCs address the question of the species' performance within a certain thermal range, the TRCs address the question of the likelihood of species occurrence.

Results

Results from transformed temperature variables, that is, annual mean water temperature and maximum water temperature of the warmest month, led to similar patterns in thermal response curves and thermal properties of the considered species. Therefore, the focus of the results and the following discussion will be on the non-transformed temperature variables, that is, annual mean air temperature and maximum air temperature of the warmest month. However, results for the water temperature variables are presented in the Appendix 3 (Table S1.2, Fig. S1.7 – S1.16, Tables S2.3 and S2.4).

Species' thermal range

The current thermal ranges based on the global species ranges varied greatly across the taxa groups (see Fig. 1a,b, Tables S2.1 and S2.2; for convenience, in figures and tables taxa groups are ordered according to the number of initially available species). The globe wanderer (*Pantala flavescens*), the freshwater snail big-ear radix (*Radix auricularia*), the widely distributed pea clam (*Pisidium casertanum*), and the water-starwort (*Callitriche brutia*) with thermal ranges above 47°C and 45°C for $Tmean_{air}$ and $Tmax_{air}$, respectively, were among the species with the highest thermal ranges. The mollusc species *Turricaspia lindholmiana*, restricted to the estuarine waters of the Dnieper River system (Ukraine) and the Don River system (Russia), had the smallest realized thermal range regarding both air temperature variables (1.5°C for $Tmean_{air}$ and 2.3°C for $Tmax_{air}$). While for $Tmean_{air}$ the second smallest realized thermal range was assigned to the fern *Marsilea batardae* (2.2°C) endemic to the Iberian Peninsula, for $Tmax_{air}$ the fish species *Percarina maeotica* had the second smallest thermal range for $Tmax_{air}$ (2.5°C). The median of the realized thermal ranges was smallest for fish and molluscs (Fig. 1a,b).

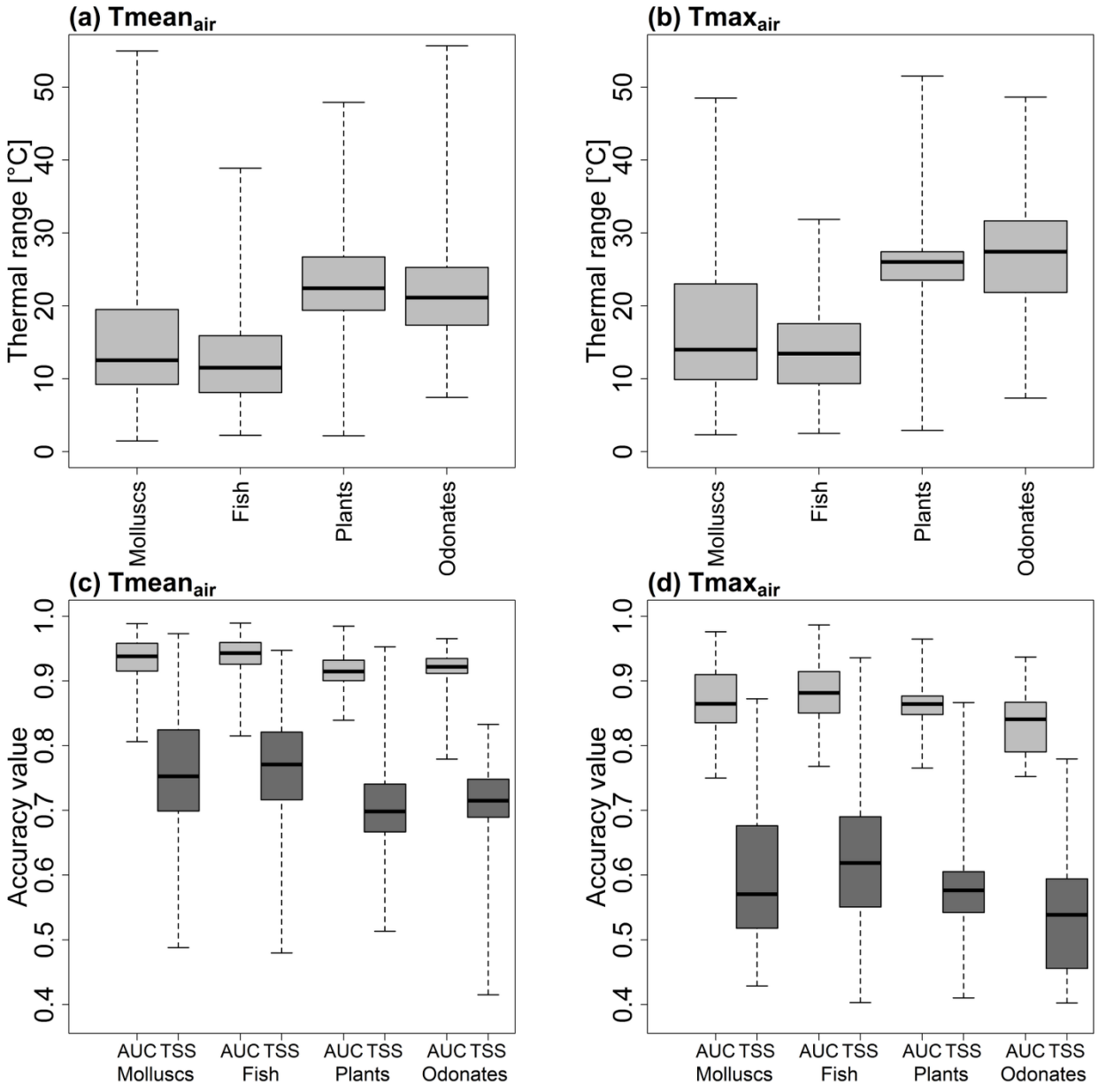

Figure 1 Thermal ranges of the species and the distribution of the accuracy measures per taxonomic group for the respective temperature variable, that is, for (a, c) Tmean$_{air}$ and (b, d) Tmax$_{air}$. The boxplots illustrate the distribution of the minimum, 25% quantile, median, 75% quantile, and maximum of the thermal ranges. The minimum and maximum are displayed by the end of the corresponding whiskers. Note that crayfish were excluded because of the low frequency of analyzed species.

Models' performance and uncertainty

Of the initially 1,402 considered European freshwater species, 649 species occurred in more than 50 catchments and were thus suitable for the species distribution modeling. Of the 649 species whose spatial distributions were modeled using GAM, validation model performance was moderate to high ($0.7 \leq AUC \leq 1$ and $0.4 \leq TSS \leq 1$) across the temperature variables for 577 species (see Table 1, Fig. 1c,d, Tables S2.1 and S2.2). Models with AUC <0.7 and TSS <0.4 were considered insufficiently accurate, which led to an elimination of the corresponding species from the further analysis (n = 72). The validation AUC and TSS values were highest for fish ($0.94 \geq AUC$

Table 1 Development of the species number per taxonomic group. The table includes the initial number of species, the number of species, which occurred in at least 50 catchments, and the number of species, which fulfilled the statistical model accuracy criteria for all four temperature variables, that is, the AUC and TSS values of the species' statistical thermal response curve model were ≥0.7 and 0.4, respectively.

Taxonomic group	No. species	No. species with n ≥50	No. species with AUC & TSS ≥ limit
Molluscs	609	106	99
Fish	473	243	220
Plants	209	196	178
Odonates	106	99	75
Crayfish	5	5	5
Sum	1,402	649	577

median ≥0.88 and 0.77 ≥ TSS median ≥0.61) and lowest for plants and odonates (0.92 ≥ AUC median ≥0.84 and 0.71 ≥ TSS median ≥0.54). The uncertainty of the modeled occurrence probabilities was low.

Thermal response curve types

Considering all categorizations of the air temperature variables the most common TRC types for molluscs, fish, plants, odonates (Table 2) and crayfish (Tables S2.1 and S2.2) were Type I (unimodal symmetric response, 374 ($Tmax_{air}$) and 437 ($Tmean_{air}$) species) and Type IV (no response, 107 ($Tmean_{air}$) and 179 ($Tmax_{air}$) species) (Table 2). For example, for $Tmean_{air}$, 58.6% (molluscs) to 89.3% (plants, odonates) had Type I as thermal response curve (Fig. S1.2; Fig. S1.3 for $Tmax_{air}$; Table 2, Table S2.1 and S2.2). The Type IV response was mainly found for endemic and restricted-range species. However, for *Marsilea batardae* endemic to the Iberian Peninsula we found a Type I response for the annual mean air temperature ($Tmean_{air}$), suggesting that a Type IV response cannot be generalized for all endemic and restricted-range species. A Type IV response consequently represents species with statistically no identifiable thermal preference.

With regard to the species' TRCs spatial distribution, the number of species with a unimodal thermal response curve type, that is, Type I-III, decreased from central toward northern and southern Europe (Fig. S1.4).

Assessment of species' thermal properties

Thermal responses were unimodal (Type I-III) for 463 (80.2%) and 390 (67.6%) species using $Tmean_{air}$ and $Tmax_{air}$ to model species distributions, respectively (Table 2, Tables S2.1 and S2.2). For these species, the preferred temperature (T_{pref}), warming tolerance (WT) and safety margin (SM) could be determined. Since high latitude analyses are based on a small number of species, high latitude WTs and SMs should be treated with caution. WT—latitude relationships were characterized by a WT increase with increasing latitude until around 55°N (Fig. 2 and 3). As mentioned, for latitudes above 55°N, no reliable trend can be outlined because of the low number of species representing the higher latitudes. The SMs of all considered species were located around 0°C for 40°–55°N with species having either positive or negative SMs (Fig. 2j and 3j). Both, WT and SM, were generally below 5°C for species with an average latitude of occurrence below 45°N for $Tmean_{air}$ (e.g., the around −7°C (e.g., the pea clam *Pisidium casertanum* with a safety margin of −7.4°C and −7.2°C for $Tmean_{air}$ and $Tmax_{air}$, respectively) (Fig. 2b and 3b; Table S2.1 and S2.2). Of those

Table 2 Thermal responses according to the univariate GAM using the annual mean air temperature ($Tmean_{air}$) and the maximum air temperature of the warmest month ($Tmax_{air}$). n is the total number of species with the respective TRC and the corresponding percentage. Note that crayfish were excluded because of the low frequency of analyzed species.

No.	Thermal response curve type		Taxonomic groups							
			Molluscs		Fish		Plants		Odonates	
			$Tmean_{air}$	$Tmax_{air}$	$Tmean_{air}$	$Tmax_{air}$	$Tmean_{air}$	$Tmax_{air}$	$Tmean_{air}$	$Tmax_{air}$
I	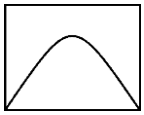	n	58	43	148	109	159	156	67	61
		%	58.6	43.4	67.3	49.5	89.3	87.6	89.3	81.3
II	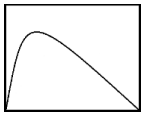	n	0	1	0	0	0	0	1	2
		%	0.0	1.0	0.0	0.0	0.0	0.0	1.3	2.7
III	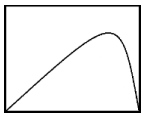	n	5	1	13	6	7	6	0	0
		%	5.1	1.0	5.9	2.7	3.9	3.4	0.0	0.0
IV	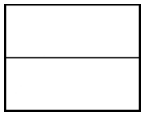	n	36	54	59	105	9	12	3	8
		%	36.4	54.5	26.8	47.7	5.1	6.7	4.0	10.7
V	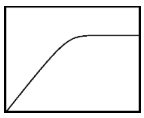	n	0	0	0	0	0	0	1	1
		%	0.0	0.0	0.0	0.0	0.0	0.0	1.3	1.3
VI	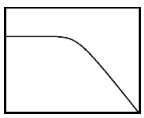	n	0	0	0	0	0	4	0	0
		%	0.0	0.0	0.0	0.0	0.0	2.2	0.0	0.0
VII	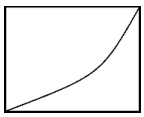	n	0	0	0	0	0	0	3	3
		%	0.0	0.0	0.0	0.0	0.0	0.0	4.0	4.0
VIII	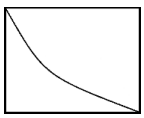	n	0	0	0	0	3	0	0	0
		%	0.0	0.0	0.0	0.0	1.7	0.0	0.0	0.0
$\sum$			99		220		178		75	

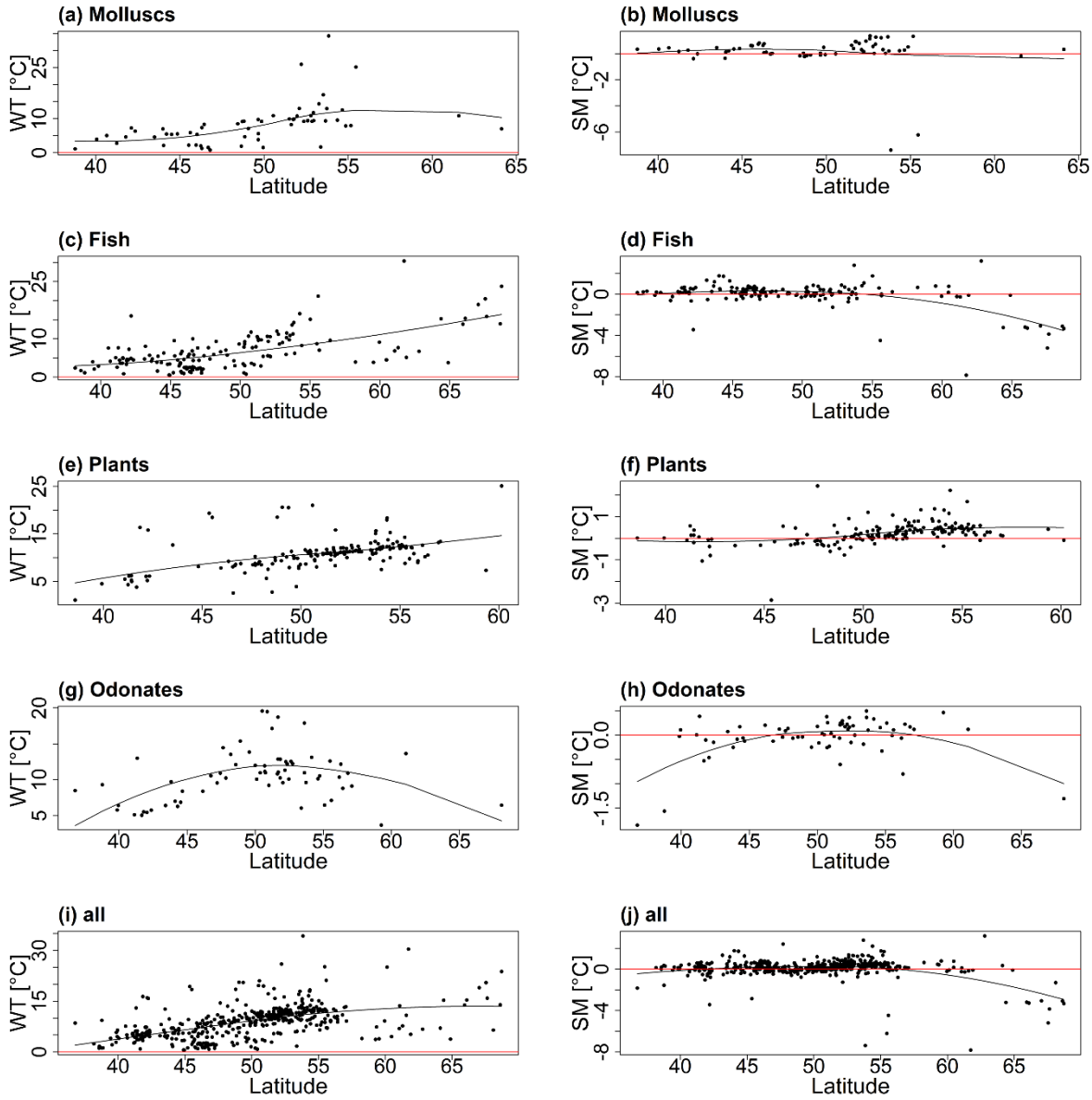

Figure 2 Latitudinal distributions and nonlinear trend lines of warming tolerance (WT = CT − T_{pref}) and safety margin (SM = T_{pref} − T_{av}) for freshwater species inferred from the temperature variable $Tmean_{air}$. CT represents the maximum temperature of a species' occurrence, T_{pref} the temperature corresponding to the highest probability of occurrence and T_{av} the average temperature of the current distribution range. WT and SM were only computed for species with a unimodal response, that is, responses for which a temperature that maximizes the probability of occurrence could be determined. Here, latitude values correspond to the average latitude of each species' European latitudinal range. WT, SM, and average latitude values were determined for (a, b) molluscs, (c, d) fishes, (e, f) plants, (g, h) odonates, and (i, j) all taxonomic groups with unimodal response curves combined. Note that crayfish were excluded because of the low frequency of analyzed species. Each dot represents the WT and SM of one species in the respective figure.

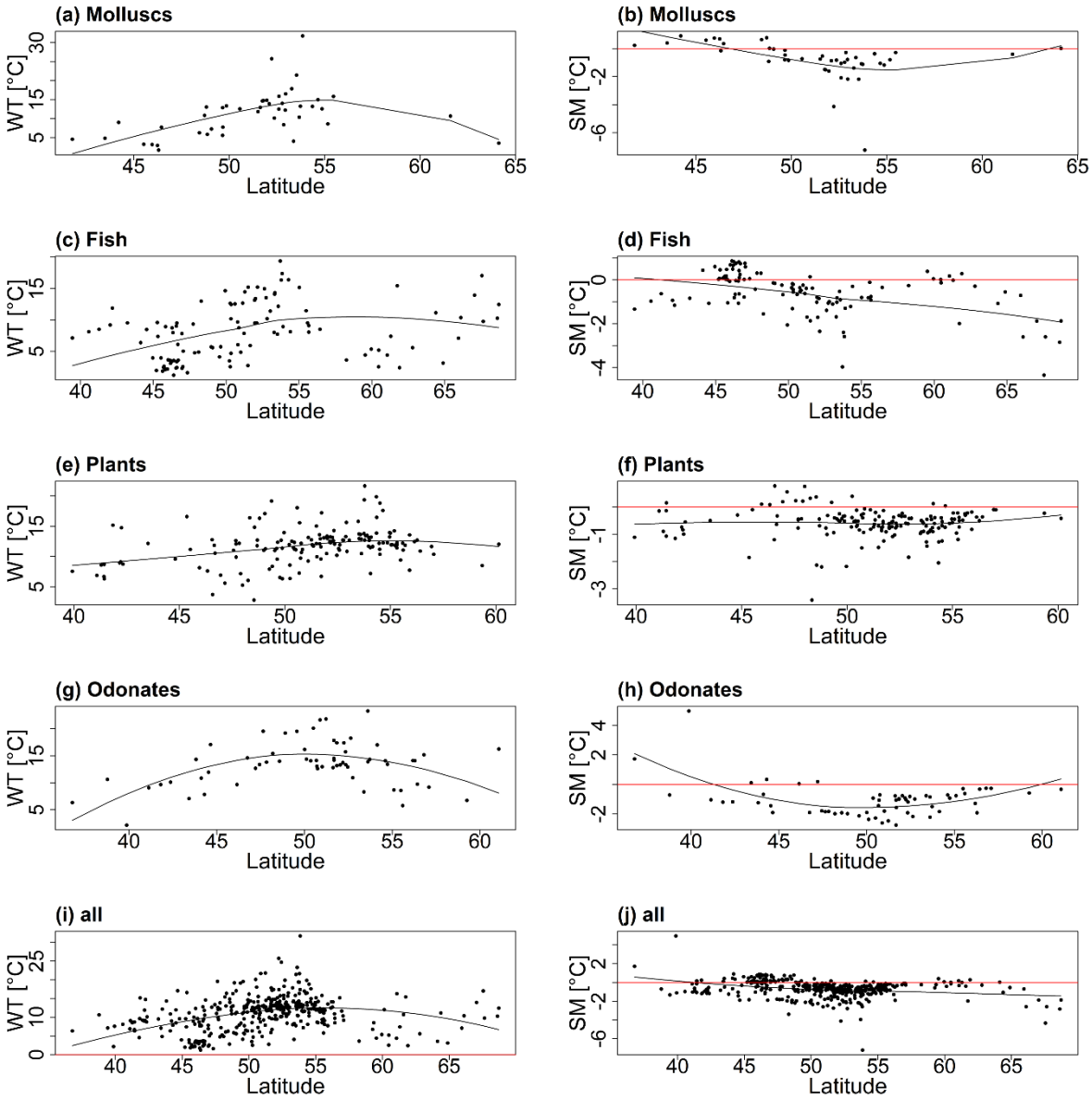

Figure 3 Latitudinal distributions and nonlinear trend lines of warming tolerance (WT = CT − T_{pref}) and safety margin (SM = T_{pref} − T_{av}) for freshwater species inferred from the temperature variable $Tmax_{air}$. CT represents the maximum temperature of a species' occurrence, T_{pref} the temperature corresponding to the highest probability of occurrence and T_{av} the average temperature of the current distribution range. WT and SM were only computed for species with a unimodal response, that is, responses for which a temperature that maximizes the probability of occurrence could be determined. Here, latitude values correspond to the average latitude of each species' European latitudinal range. WT, SM, and average latitude values were determined for (a, b) molluscs, (c, d) fishes, (e, f) plants, (g, h) odonates, and (i, j) all taxonomic groups with unimodal response curves combined. Note that crayfish were excluded because of the low frequency of analyzed species. Each dot represents the WT and SM of one species in the respective figure.

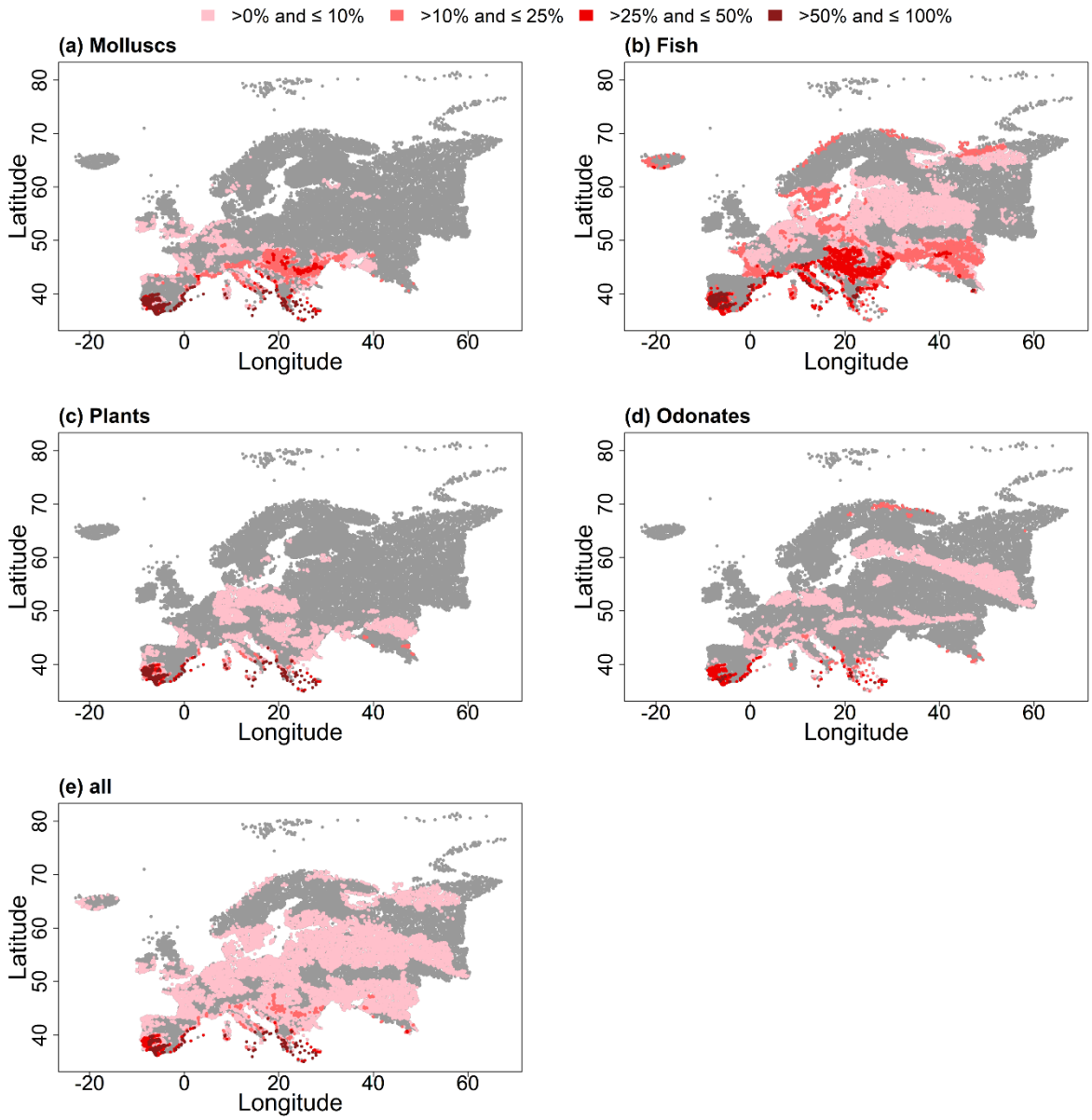

Figure 4 Relative frequency per catchment of species with the critical maximum temperature (CT) inferred from $Tmean_{air}$ that is exceeded by the averaged projected temperature of the three climate models MOHC, IPSL, and MPI for the 2050s for (a) molluscs, (b) fishes, (c) plants, (d) odonates, and (e) all taxonomic groups combined. The grey area represents either no occurrence or catchments in which the CT, that is, the maximum temperature of a species' occurrence, is not exceeded by the projected temperatures. Note that crayfish were excluded because of the low frequency of analyzed species.

species with a unimodal response, the proportions of species with a negative safety margin per taxa group were between 22% (molluscs) and 44% (odonates) (Fig. S1.5). We note that for $Tmax_{air}$ the proportion of species with negative SMs was higher than for $Tmean_{air}$, ranging from 70% (fish) to 91% (plants) (Fig. S1.6).

For both air temperature variables, the analyses showed that areas in Spain and Mediterranean coastlines will be affected the most by rising temperatures (Fig. 4e and 5e). Regarding the CT deduced from $Tmax_{air}$, regions in Eastern Europe, especially in the coastal area of the Caspian Sea and the Danube region will likely suffer from temperature

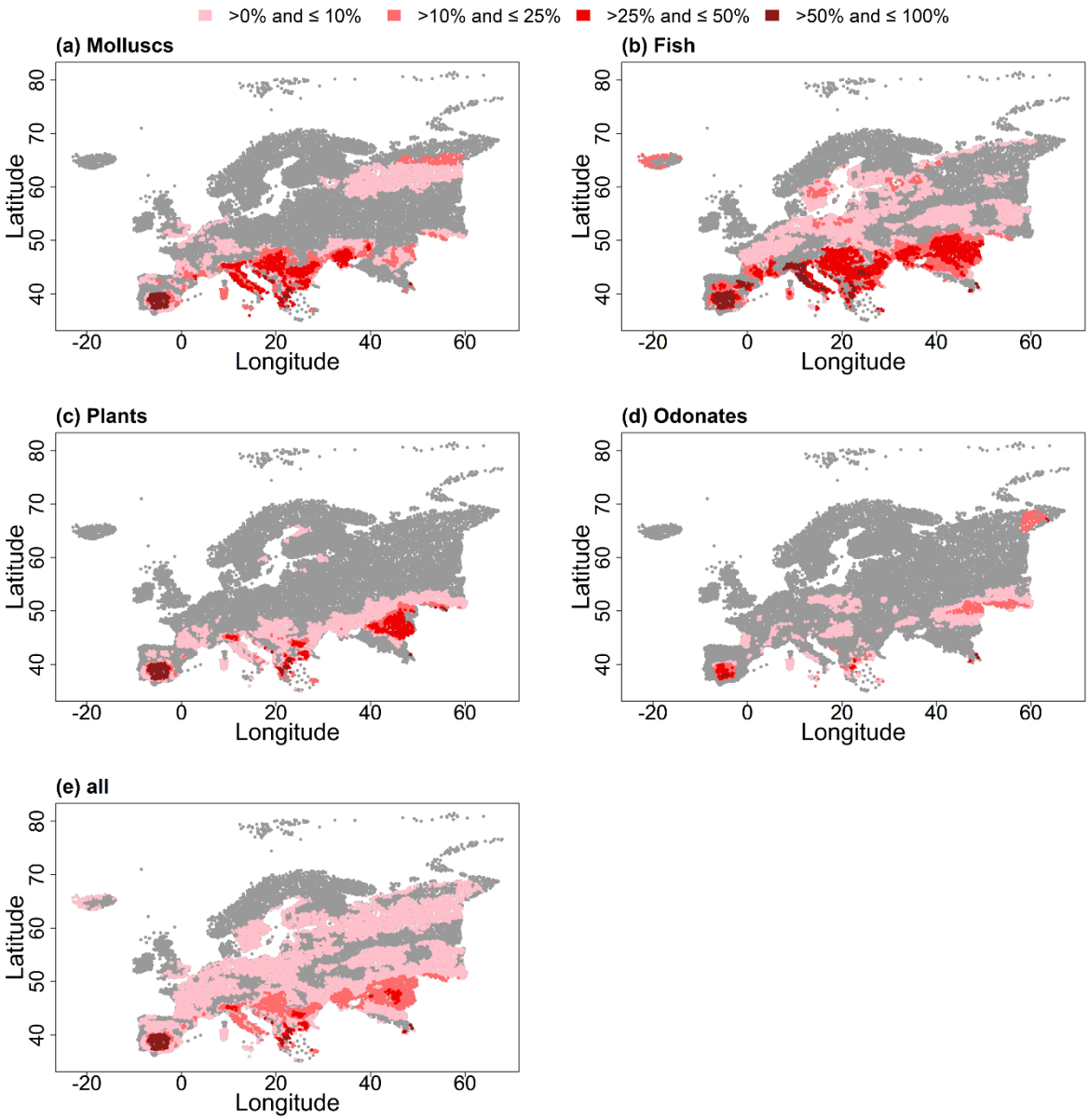

Figure 5 Relative frequency per catchment of species with the critical maximum temperature (CT) inferred from $Tmax_{air}$ that is exceeded by the averaged projected temperature of the three climate models MOHC, IPSL, and MPI for the 2050s for (a) molluscs, (b) fishes, (c) plants, (d) odonates, and (e) all taxonomic groups combined. The grey area represents either no occurrence or catchments in which the CT, that is, the maximum temperature of a species' occurrence, is not exceeded by the projected temperatures. Note that crayfish were excluded because of the low frequency of analyzed species.

increases (Fig. 5e). Among the studied taxonomic groups rising temperatures will be most detrimental to fish with more than 25% of the species in the respective catchments having a CT below the predicted temperatures mostly in the southern areas of Europe, reaching from the coastlines of Portugal and Spain to the coastlines of the Caspian Sea (Fig. 4 and 5). Overall, the relative frequency of species with a critical difference between the projected and current maximum temperature of occurrence in a catchment was mainly below 10% (Fig. 4e and 5e). These numbers were generally exceeded in the coastal areas of Spain and Italy, in south-west Portugal, in coastal areas of Greece, in the Alpine region, the Balkans, and the western areas of the Caspian Sea.

Discussion

Since decades, the classical Gaussian response curve, which has a single optimum and a decreasing probability of occurrence away from the optimum along the thermal gradient, is a well-accepted assumption for a species' thermal response (Gauch and Whittaker, 1972). Thermal response curves of the European freshwater species did not vary greatly among taxonomic groups and the species within a group. Our results highlighted that the unimodal response curves (Type I–III) were most frequent among all considered taxonomic groups and all four temperature variables ($Tmean_{air}$—annual mean air temperature, $Tmax_{air}$—maximum air temperature of the warmest month, $Tmean_{water}$—annual mean water temperature, $Tmax_{water}$—maximum water temperature of the warmest month) that were used to model the thermal response (390–463 of 577 species, i.e., 67.6%–80.2%). High pairwise correlations of the temperature variables (above 0.8) explain the similarities of the results. For species with spatial distribution ranges characterized by substantially differing thermal gradients across the used temperature metrics, the corresponding thermal response types (TRCs) also varied. Species with unimodal response types were most common in central Europe, following thus the species richness patterns. Namely, the species density was higher in central than in northern and southern Europe.

Despite the "overarching importance of thermal regimes to aquatic life" (Isaak et al., 2017), thermal niches of freshwater species are only scarcely studied. For example, Lassalle et al. (2008) found unimodal responses using annual temperature for *Acipenser gueldenstaedtii*, *Acipenser stellatus*, *Alosa alosa*, *Alosa tanaica*, *Vimba vimba*, and *Osmerus eperlanus*, corresponding to our response type categorization for $Tmean_{air}$. The response type of the cold-water specialist brown trout (*Salmo trutta*, Type III for $Tmax_{water}$) coincides with the findings of Isaak et al. (2017), where both the multivariate and univariate (using August stream temperature as explanatory variable) models showed a unimodal response. For the fish species investigated by Logez et al. (2012) using the mean air temperature in July, response curves for $Tmax_{air}$ are different for three fish species (*Alburnus alburnus*, *Rhodeus amarus*, *Salmo trutta*). Differences may have resulted from consideration of native portions of species ranges by Logez et al. (2012), whereas our study considers global species ranges.

Warming tolerances and safety margins for the different temperature variables showed only marginal differences in the latitudinal trends. The species-based warming tolerance increased by moving northwards until 55°N, indicating that on average species in central Europe had a greater difference between the critical and preferred temperature than southern species and thus a greater capacity to cope with warming. For high latitude species, no reliable latitudinal relationships above approximately 55°N could be given due to a low species number as compared to much larger data availability for southern to central Europe. In addition, due to the statistical barrier of 50 occurrences at the analyzed scale, many endemic species of the Italian, Iberian, and Balkan Peninsulas with few catchment occurrences could not be included for southern parts of Europe. Most species in central Europe have a high colonization capability, wider distribution ranges and experience greater intra-annual variability than species at lower latitudes, which explains their warming

tolerance. Furthermore, while some specialists of cold climates in the far north had also a low warming tolerance comparable to species in the south (e.g., *Gasterosteus islandicus* native to Iceland with WT = 3.8°C and WT = 3.1°C inferred from $Tmean_{air}$ and $Tmax_{air}$, respectively), other species with average latitudes located in colder climates (>60°N) had higher warming tolerances. High warming tolerance at these latitudes may be an indication of species occurrences in areas different from the European ranges. For example, the fish species *Osmerus dentex* (WT = 19°C and WT = 14°C inferred from $Tmean_{air}$ and $Tmax_{air}$, respectively) occurs at the European scale at an average latitude of 67°N, but is also found at lower latitudes, for example, in Japan or Korea. Despite the fact that WT increased with latitude up to about 55°N, one has to be cautious with the interpretation of this result as the preferred temperature, T_{pref}, might have been already exceeded for some species (negative safety margin).

Shuter and Post (1990) and Brazner et al. (2005) found that temperature is one of the main drivers of the spatial distribution of stream fish, suggesting high vulnerability to future temperature rise. In our study, future temperature predictions showed that especially fish will be affected critically by rising temperatures. Fishes spend their entire life cycle in the water. Consequently, they depend on the water temperature throughout all life stages, in contrast to merolimnic species (e.g., odonates) that are connected to the waters only in early stages of their life cycle, having the ability to escape water temperature rises in critical periods. Additionally, sensitivity of fishes to temperature changes (Magnuson et al., 1979), in terms of survival and growth, underline the threat fishes are facing in the future. Potential movement is connected with a maximization of the growth rate (Jobling, 1981) and metabolic power available for reproduction and activity (Kelsch, 1996) and may vary by life-history strategies, for example, migratory and sedentary fish. Considering all taxonomic groups, especially the Balkans, the western area of the Caspian Sea and the coastal areas of the Mediterranean Sea like southern Portugal and Spain or Italy and Greece will be affected according to the temperature projections. Additional changes in the marine realm (Lejeusne et al., 2010) demonstrate the ongoing and upcoming changes in the Mediterranean area. More than 25% of the considered species in the catchments of these regions had a CT below the predicted temperature of the 2050s. Some species can adapt, more or less fast, to a certain extent by physiological adjustment (Johnson and Kelsch, 1998) or behavioral thermoregulation (Heggenes et al., 1993), while another option for escaping or mitigating these threatening conditions is movement to suitable areas. However, especially in the regions of the Iberian Peninsula and the Mediterranean area, where thermal alteration impacts will be the strongest, endemic, or restricted-range species prevail. The latter suggest an urgent need for further research on species' sensitivity to climate warming; in particular, effects of rising temperatures have to be investigated in the context of species thermal properties, with the focus on species with currently small thermal ranges, and dispersal traits paired with habitat suitability and connectivity.

Strengths and weaknesses of statistical models describing species distributions have been extensively evaluated in the literature (see, e.g., Franklin, 2009). Considering our study, the thermal response curves and thus

the occurrence probabilities along thermal gradients resulting from GAMs should be viewed in the context of the analyzed scale (catchments) and statistical approach. Consequently, different thermal responses may result from local scale data and for species with few occurrences (n < 50) thermal responses could not be captured. Thus, high-endemism areas (peri-Mediterranean region and Balkans) are in need of additional extensive analyses at finer scales. Furthermore, our thermal response curves do not consider the above discussed possibility of adaption to environmental changes. We considered annual mean water temperature and the maximum water temperature of the warmest month as a transformation of the corresponding air temperature via a global relationships model (Punzet et al., 2012). The key shortcoming of the latter model is that it solely depends on air temperature and thus ignores effects such as catchment heterogeneity, shading, or dissolved oxygen concentration. Although thermal responses give a quantification of thermal habitats (Hester and Doyle, 2011) and a necessary assessment of the impact of future global warming (Vetaas, 2000), they do not account for other environmental and community influences. It is important to keep in mind that species do not respond to a single environmental factor (Økland, 1992). Therefore, our results on thermal properties and responses should be viewed in the context of complex interactions of different factors. For example, Verberk et al. (2016) outlined effects of stream oxygenation on thermal tolerances, while Arismendi et al. (2012) found that the combination of flow reduction and temperature increase could lead to an exacerbation of the reduction in cold-water species habitat. The latter leads to a process known as "thermophilization," describing the increasing dominance of warm-water species (De Frenne et al., 2013). As such, amplifications of climate change related impacts caused by anthropogenic pressures, for example, intensified eutrophication of lake catchments and especially the disappearance of water bodies and modification of habitats (Nowakowski et al., 2017) should be further considered in the context of the potential future species distributions. New generations of species distribution models aim at combining abiotic and biotic factors but need detailed and thus rarely available ecological information about species for reliable projections (Singer et al., 2016; Urban et al., 2016).

In summary, future temperatures are expected to exceed the current maximum temperature of occurrence of species living in coastal areas of the Mediterranean Sea, the Balkans, and the western area of the Caspian Sea. Synergetic effects of rising temperatures and other influencing factors, such as restricted catchment connectivity or anthropogenic disturbances in these areas, will additionally aggravate the viability of populations, but the whole scope of climate change impacts remains difficult to grasp. However, given the high vulnerability of freshwater ecosystems to climate change, re-assessments of the existing conservation areas and integrated management practices that facilitate species migration are urgently needed. Furthermore, for keeping the thermal habitat suitability of European catchments within species tolerance limits, a renewed effort to slow down the pace of climate change is essential.

Chapter 6

European vs. global analyses of species' thermal response curves: pessimistic or optimistic regarding species' future?

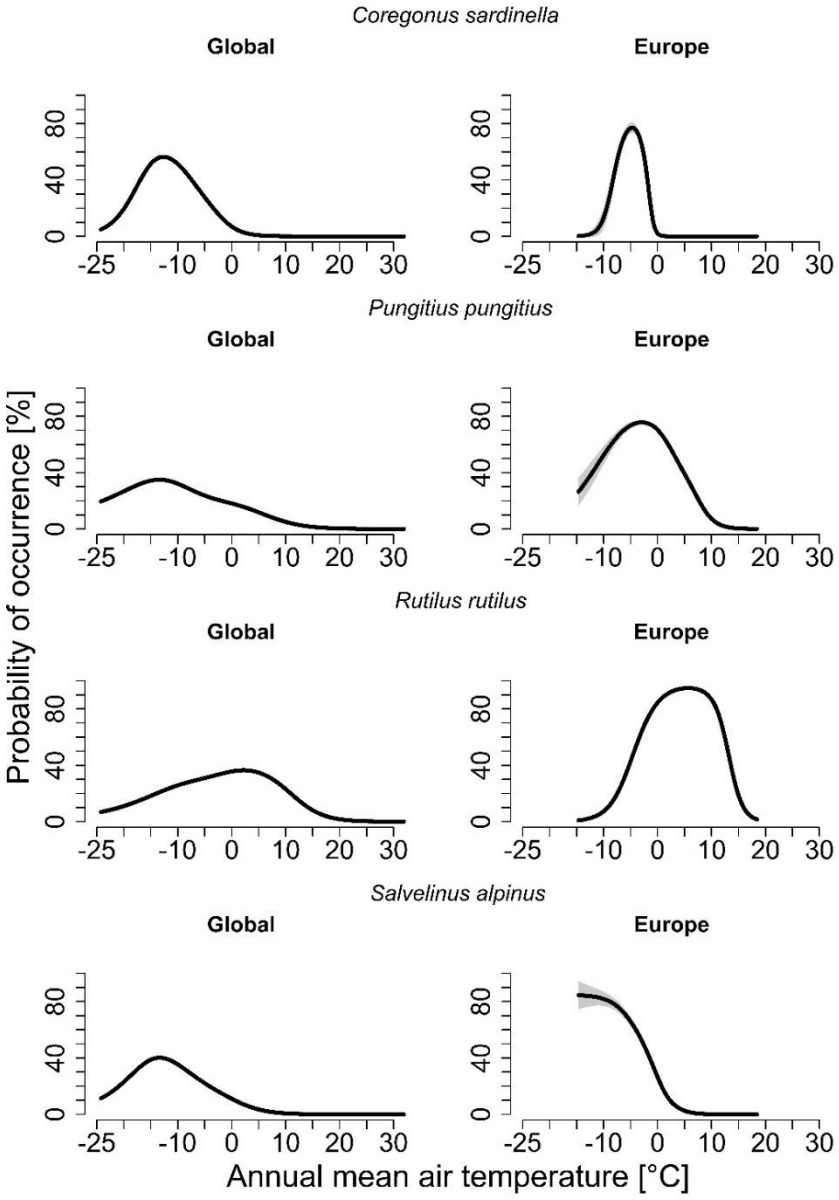

Supporting information can be found in Appendix 4 of the thesis.

Abstract

Thermal responses are used to derive species' thermal properties and abilities to cope with warming. However, different distributions of species along thermal gradients can be expected for different range portions. We identify differences in thermal response curves (TRCs) and thermal properties for four selected freshwater fishes (*Coregonus sardinella*, *Pungitius pungitius*, *Rutilus rutilus*, *Salvelinus alpinus*) native to Europe at the global and European catchment level. Global TRCs for all four species were different from European TRCs. European ranges captured only a portion of the global thermal range with, in great part, major differences in the minimum (T_{min}), maximum (T_{max}) and average temperature (T_{av}) of the respective distributions. Further investigations of the model-derived preferred temperature (T_{pref}), warming tolerance ($WT = T_{max} - T_{pref}$), safety margin ($SM = T_{pref} - T_{av}$) and the future climatic impact showed substantially differing results. All considered thermal properties either were under- or overestimated at the European level, implying that even the consideration of continental ranges is not sufficient for studying thermal responses. Management actions should thus rely on models that consider the whole species niche. Studies should favour global distribution data for analyzing species responses to environmental gradients.

Introduction

Thermal response curves describe the relationship of species occurrence in relation to values of a temperature variable (Franklin, 2009). Those response curves are often depicted graphically, e.g. displaying the probability of occurrence along a thermal gradient. Many studies have analyzed species responses along thermal gradients in order to describe current and predict future species distributions according to climate change scenarios (Lassalle et al., 2008; Logez et al., 2012; De Frenne, 2013; Filipe et al., 2013; Markovic et al., 2013). Such assessments are often considered in order to quantify the effect of temperature on species distributions (Carrascal et al., 2016; Isaak et al., 2017) or to identify specialists or generalists by classifying whether species have narrow or broad thermal responses (Barnagaud et al., 2012; Logez et al., 2012). However, most studies consider only portions of the whole species range for deriving species-specific thermal characteristics, although responses may vary greatly with the geographical extent of the data (Thuiller et al., 2004; Filipe et al., 2013).

Here we would like to remind on the importance of using the full species ranges to describe species thermal niches and evaluate future climate change impacts by providing examples of substantially differing species' thermal characteristics at the global (whole species range) and European scale (native species range). Using niche-based species distribution models, we analyzed distributions of four selected freshwater fish species native to Europe and quantified differences between global and European range data in (i) thermal response curves, (ii) the associated thermal properties, and (iii) future climatic impacts in Europe.

Results and discussion

The variation in the geographical extent for parameterizing thermal response curves was manifested in shifts and significant shape

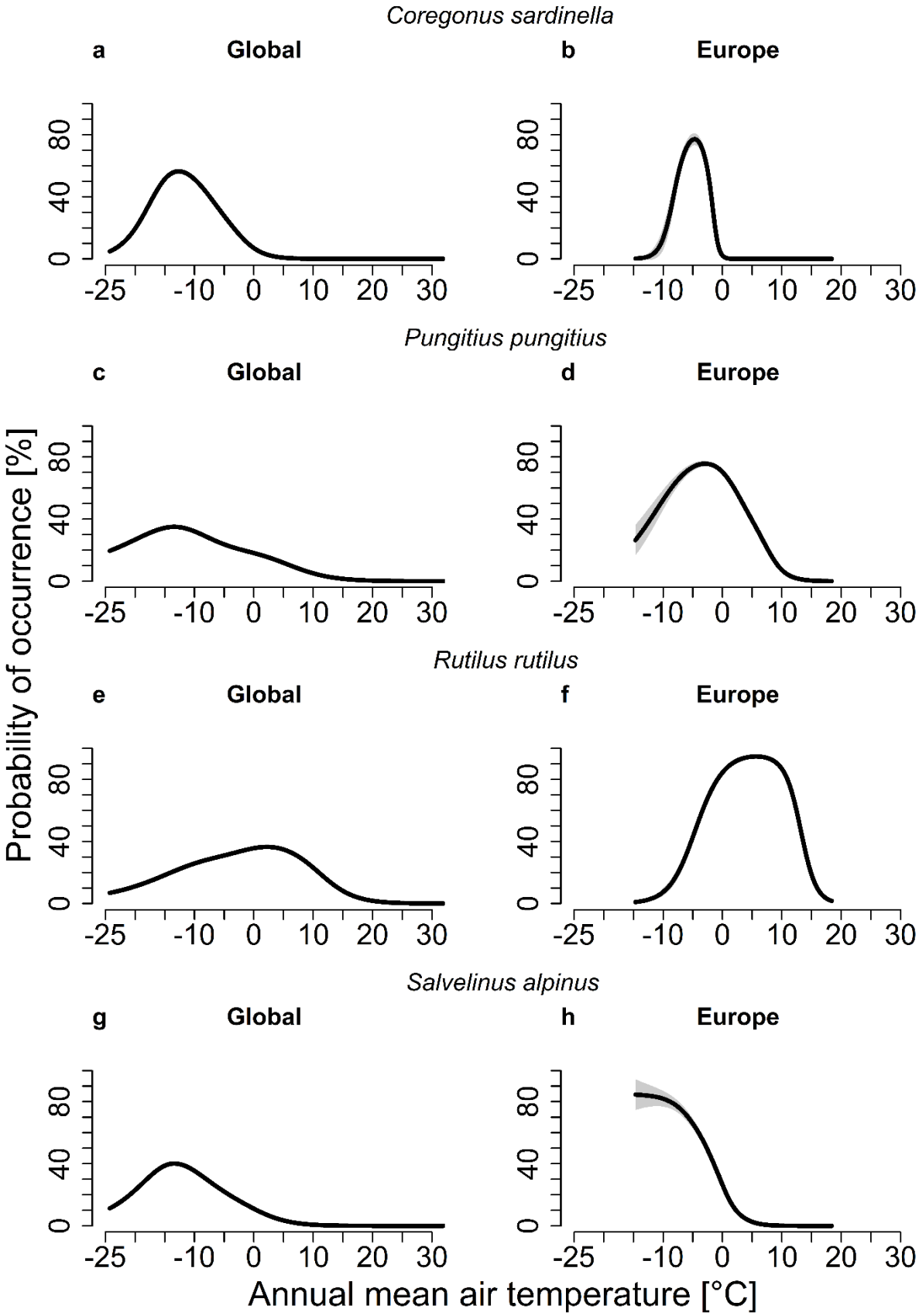

Figure 1 Thermal response curves along the annual mean air temperature gradient. Thermal response curves are displayed for (a, b) *Coregonus sardinella*, (c, d) *Pungitius pungitius*, (e, f) *Rutilus rutilus*, and (g, h) *Salvelinus alpinus* at the global and European scale, respectively. The grey area around the response curves represents the 95% confidence interval.

differences of the curves (e.g. Filipe et al., 2013). For *Coregonus sardinella*, *Pungitius pungitius* and *Rutilus rutilus* at both scales a unimodal thermal response curve was present, whereas the global response curves were characterized by a shift towards lower temperatures (Fig. 1). The European response curve of *Salvelinus alpinus* suggests a monotonic decreaser (i.e., the occurrence probability decreases with temperature increase), while the global thermal response curve was unimodal.

The quantification of different thermal properties of the species at both scales such as the thermal range, the preferred temperature, warming tolerance and safety margin reflected varying implications for the respective species. In particular, comparisons with globally derived thermal properties showed that each of the named property dimensions was either more optimistic or pessimistic when quantified with native range data (see Bush et al., 2018). Global thermal ranges for each of the four species were greater than European thermal ranges (e.g. Lee-Yaw et al., 2016). Differences between the thermal ranges inferred from the global and European extents ranged from 6.5°C (*Salvelinus alpinus*) to 20.1°C (*Pungitius pungitius*) (Table 1). For all species, global minimum temperature (T_{min}) was significantly lower than European T_{min} and global maximum temperature (T_{max}) exceeded European T_{max} for all species, except for *Salvelinus alpinus* (Table 1).

Preferred temperatures (T_{pref}) at both spatial scales could be determined for *Coregonus sardinella*, *Pungitius pungitius* and *Rutilus rutilus* because of unimodal thermal response curves where a temperature that maximizes the probability of occurrence is uniquely determinable (Table 2). T_{pref} inferred from the global scale analyses was 3.5-10.5°C lower than the preferred temperature

Table 1 Comparison between the thermal characteristics inferred from global and European species distributions.

Scale	Annual mean air temperature (°C)	Species			
		Coregonus sardinella	*Pungitius pungitius*	*Rutilus rutilus*	*Salvelinus alpinus*
Global	T_{min}	-21.2	-21.5	-19.9	-20.6
	T_{max}	2.9	17.4	17.9	7.5
	Thermal range	24.1	38.9	37.8	28.1
	T_{av}	-9.3	-5.0	0.5	-8.0
	Median	-10.0	-5.7	1.3	-9.2
	Standard deviation	4.8	7.9	7.7	6.1
European	T_{min}	-8.9	-8.9	-8.0	-14.1
	T_{max}	-0.6	9.9	15.9	7.5
	Thermal range	8.3	18.8	23.9	21.6
	T_{av}	-3.5	2.3	5.4	-1.1
	Median	-2.8	2.1	5.5	-0.6
	Standard deviation	2.1	3.6	4.0	3.6

Table 2 Different thermal properties of the analyzed species for the two considered spatial extents.

Scale	Annual mean air temperature (°C)	Species			
		Coregonus sardinella	*Pungitius pungitius*	*Rutilus rutilus*	*Salvelinus alpinus*
Global	T_{pref}	-12.7	-13.4	2.2	-13.4
	WT	15.6	30.8	15.7	20.9
	SM	-3.4	-8.4	1.7	-5.4
European	T_{pref}	-4.7	-2.9	5.7	NA
	WT	4.1	12.8	10.2	NA
	SM	-1.2	-5.2	0.3	NA

T_{pref} – preferred temperature, WT – warming tolerance, and SM – safety margin.

determined at the European level for *Coregonus sardinella*, *Pungitius pungitius* and *Rutilus rutilus*. In particular, T_{pref} for *Coregonus sardinella* and *Pungitius pungitius* inferred from the global analysis was more than 8°C lower than European T_{pref}. For *Rutilus rutilus* the difference was smaller with T_{pref} = 2.2°C and T_{pref} = 5.7°C at the global and European scale, respectively. Global T_{pref} = -13.4°C of *Salvelinus alpinus* was in the range of European T_{min} = -14.1°C. Due to the non-unimodal European TRC of *Salvelinus alpinus*, T_{pref} could not be determined for this species.

Warming tolerances (WT = T_{max} – T_{pref}) of *Coregonus sardinella* and *Pungitius pungitius* deduced from the global analysis were more than 11°C greater than the WTs obtained by the European analysis (e.g. Vetaas, 2002) (Table 2). For *Rutilus rutilus*, the global WT showed a smaller increase (+5.5°C) compared to the European WT. *Salvelinus alpinus* had a global WT that approximately corresponded to the European thermal range (global WT = 20.9°C and European thermal range = 21.6°C). European WT for *Salvelinus alpinus* could not be determined, because of the absence of a uniquely determinable T_{pref}. Additional comparisons of catchment-specific global and European WTs are provided in the Appendix 4 (Fig. S1-S4).

For *Coregonus sardinella* and *Pungitius pungitius* the global safety margin (SM = T_{pref} – T_{av}) was 2-3°C lower than at the European scale (Table 2), i.e. the exceeding of the preferred temperature (T_{pref}) by the current average habitat temperature (T_{av}) was underestimated with European data. For *Rutilus rutilus* the European SM was 1.4°C lower than the global SM. European SM for *Salvelinus alpinus* could not be determined, however, the species had a negative global SM. Further catchment-specific comparisons are provided in the Appendix 4 (Fig. S5-S8).

Differences between the average future projection for each catchment and species-specific T_{max} outlined that European analyses convey a more pessimistic view of the future climatic impact as T_{max} of the global range was higher than T_{max} of the European range for all species, except for *Salvelinus alpinus* (see also Thuiller et al., 2004) (Table 1, Fig. S12). Greater differences of the future climatic impact assessment between the global and European scale were observable for *Coregonus sardinella*

(Fig. S9) and *Pungitius pungitius* (Fig. S10). For *Rutilus rutilus* (Fig. S11), both scales indicated mainly future temperatures below T_{max}, with few exceptions for catchments in the southern ranges of the respective species distribution at the European scale.

Focussing only on native portions of species ranges and not on the whole range can result in substantially different thermal response curves (TRCs) and thermal properties. TRCs among the four analyzed species at the European and global scale varied greatly. All species indicated broader thermal ranges at the global level resulting in clearly shifts of the TRCs towards colder temperatures that were not captured by the European data set for three out of four species (Bush et al., 2018). Thus, European response analyses may create pessimistic views of allegedly specialists with small thermal ranges. Furthermore, species' thermal properties deduced from the European analyses either were under- or overestimated. Regions where a species is likely to suffer from future climatic impacts will be different for global and European scale analyses, unless the European scale already includes the whole known species distribution range (Thuiller et al., 2004; Fitzpatrick & Hargrove, 2009; Lee-Yaw et al., 2016). However, factors such as new distribution possibilities (Kletou et al., 2016), biotic interactions, future anthropogenic responses to environmental change and thermal adaptations (Angiletta, 2009) may enable species to cope with environments in regions outside their native distribution range (Vetaas, 2002; Bush et al., 2018). Management actions should thus rely on models that consider the whole species niche. Specifically, studies should favour whole range distribution data for analyzing species responses along thermal gradients.

Materials and methods

Species data

Global distribution data of four fish species native to Europe (*Coregonus sardinella*, *Pungitius pungitius*, *Rutilus rutilus* and *Salvelinus alpinus*) were derived from the IUCN Global Species Programme containing the known range of each species (IUCN, 2013,2014) (see https://www.iucn.org/theme/species/our-work/iucn-red-list-threatened-species for more details). Species selection was based on a previous study where thermal responses for 577 species from different taxonomic groups were investigated (Kärcher et al., 2019) and focussed on outlining species with significant differences in thermal properties depending on spatial scales. At the global scale (Table S1), species data were mapped to 228,064 HydroBasins level 8 catchments (Lehner and Grill, 2013). Occurrence numbers at the global scale ranged from 17,055 (*Salvelinus alpinus*) to 33,756 (*Rutilus rutilus*) (Table S2). European distribution data was defined as a subset of the global distribution data; overall covering 18,767 catchments (Table S1). Occurrence numbers at the European scale ranged from 745 (*Coregonus sardinella*) to 15,478 (*Rutilus rutilus*).

Climate data

Global climatic data were ascertained for the second half of the 20th century (1960-1990, "baseline") from the WorldClim (version 1.4) 30 arc-second data set (Hijmans et al., 2005) (www.worldclim.org, accessed on March 19, 2018). Due to a lack of water temperature data given the large spatial extent of our study (228,064 catchments) and the focus on the species' major thermal properties, parameterization of species' thermal response

curves was based on the catchment-specific annual mean air temperature ($Tmean_{air}$).

Future climate projections for Europe (18,767 catchments) were gathered for the middle of the 21st century ("2050s") from the CIAT (International Center for Tropical Agriculture) 30 arc-seconds gridded data set (www.ccafs-climate.org). We focussed on three climate models (MOHC, IPSL and MPI), each considering the RCP4.5 (Representative Concentration Pathways) emission scenario. RCP4.5 follows a medium-low mitigation of greenhouse gas emission and represents intermediate scenarios (Van Vuuren et al., 2011). The gridded layers of the 20th and 21st century $Tmean_{air}$ were mapped to HydroBasins level 8 resolution catchments using the ESRI ArcGIS zonal statistics tool.

Statistical model

Global and European distributions of the four fish species were modelled using GAMs (Hastie, 2016) were run in R language version 3.3.124 (R Development Core Team, 2018). The probability of occurrence along the thermal gradient represents the thermal response curve (TRC). Since our focus was on the species' thermal properties, the evaluation of the species' TRC was based on a univariate modelling approach, i.e. $Tmean_{air}$ was the only explanatory variable.

Model performance was evaluated by calculating two performance measures: the area under the receiver operating characteristic (ROC) curve, AUC (Swets, 1988; Hosmer & Lemeshow, 2000; Manel et al., 2001), and the true skill statistic (TSS = specificity+sensitivity–1), whereas specificity and sensitivity were the result of a probability threshold determination (Allouche et al., 2006). Here, the threshold for separating presences and absences of a species was determined by minimizing the absolute difference between specificity and sensitivity (Fielding & Bell, 1997; Jimenez-Valverde & Lobo, 2007). Accuracy of the performance measures was validated by splitting the data into a training (80%) and validation (20%) data set 100 times. The average AUC and TSS values of the validations were used for the assessment of the predictive performance (Dormann et al., 2008).

For the depiction of the uncertainty, we computed 95% confidence intervals (CIs) around the modelled probabilities of occurrence for each observation (De Jong & Heller, 2008).

Assessment of thermal properties

Comparisons of TRCs between the global and European scale included analyses of: (1) Thermal range, defined as the difference between the maximum (T_{max}) and minimum temperature (T_{min}) of occurrence; (2) Preferred temperature (T_{pref}), determined if the thermal response was unimodal, i.e. if a temperature that maximizes the probability of occurrence was uniquely determinable; (3) 'Warming tolerance' (WT), calculated as the difference between T_{max} and T_{pref} ($WT = T_{max} – T_{pref}$); (4) 'Safety margin' (SM), calculated as the difference between T_{pref} and the average temperature across the species' distribution range (T_{av}) ($SM = T_{pref} – T_{av}$); (5) Exposure to future global warming across the species' range, assessed by calculating the difference between the average of the projected temperatures of the three climate models and the species specific T_{max}.

Chapter 7

Combining species distribution modelling techniques with species thermal performance curves

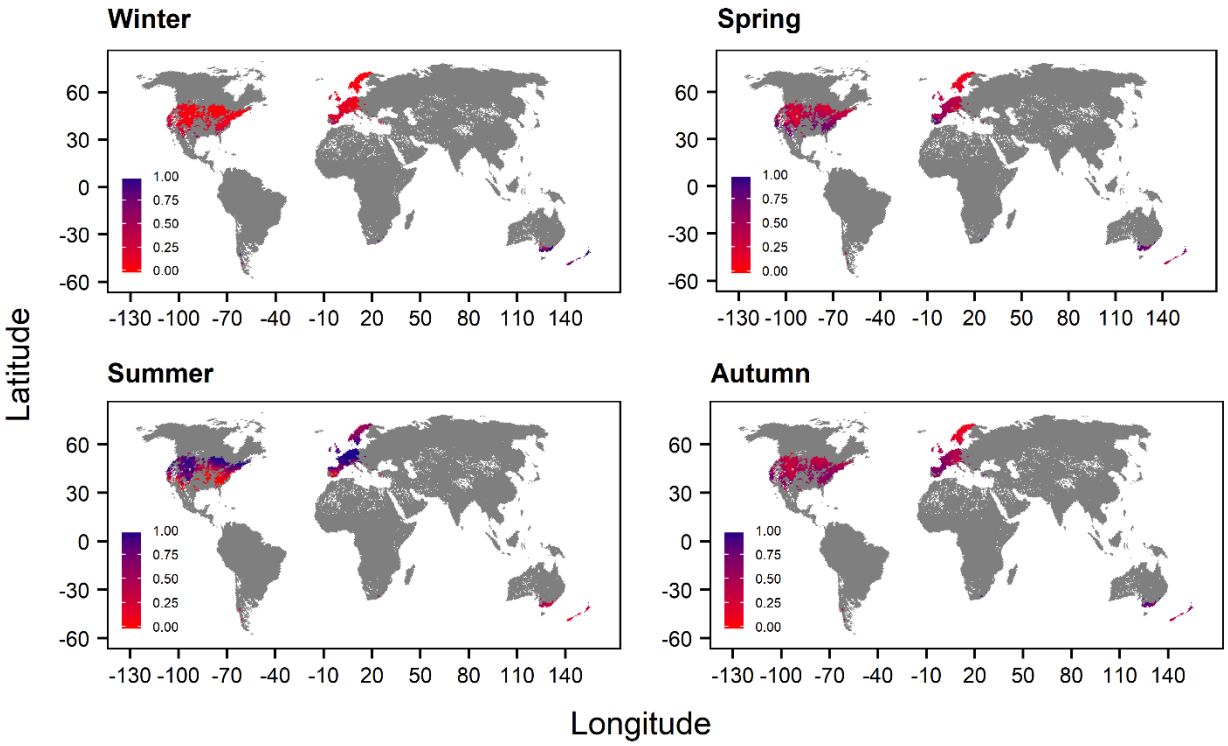

Supporting information can be found in Appendix 5 of the thesis.

Abstract

Extending assessments of climate change induced range shifts via statistical species distribution models by including species traits is crucial for conservation planning. However, comprehensive assessments of future distribution scenarios incorporating responses of biotic factors are poorly investigated. In this study, we combine global model predictions for the 2050s and thermal performances of *Salmo trutta* and *Salmo salar* under consideration of different life stages (adults, juveniles, eggs), timeframes (monthly, seasonal, yearly) and dispersal scenarios (no dispersal, free dispersal, restricted dispersal). We demonstrate that thermal performances of different life stages will either increase or decrease for certain time periods. Model predictions and thermal performances imply range declines and poleward shifts. Dispersal to suitable habitats will be an important factor mitigating warming effects; however, dams are blocking paths to areas linked to high performances. These results emphasize enhanced inclusion of critical periods for species and dispersal solutions in conservation planning.

Introduction

Accumulating evidence for increases in the mean temperature, in heat events and cold extremes emerges (Field et al., 2014; Scranton and Amarasekare, 2017). Temperature rises may be further aggravated through globally changing factors such as increases in irrigation and water extraction for human consumption, which also lead to reductions in river discharge (Jatteau et al., 2017). Locally, urbanization, increases of built-up areas, dams and the decreasing riparian cover disrupt thermal regimes within freshwaters (Souchon and Tissot, 2012). With temperature being one of the major abiotic drivers of ectothermic species, observed changes in temperature will transfer to the species' distribution, abundance and physiological performance (Krenek et al., 2011; Schulte et al., 2011). Water temperature influences the rate of biochemical reactions in ectothermic species (Rome et al., 1992; Angiletta et al., 2002; Hochaka and Somero, 2002; Angiletta, 2009; Childress and Letcher, 2017) and consequently growth, development, behaviour, metabolic processes as well as timing and duration of life-history events (Huey and Stevenson, 1979; Jonsson and d'Abée-Lund, 1993; Wootton, 1998; Jonsson and Jonsson, 2009; Scranton and Amarasekare, 2017). Especially fishes as poikilothermic species will be affected by global warming because their metabolic rates increase with water temperature, which however increases mortality and shortens the life span (Glebe & Legett, 1981; Pried, 1985; Enders et al., 2005; Jonsson and Jonsson, 2009). Stronger temperature increases are expected over land compared to the ocean (Pachauri et al., 2015), implying larger physiological changes of fishes in the freshwaters (e.g. Jonsson and Jonsson, 2009).

Thermal tolerance depends on the physiological sensitivity of the fish to temperature changes (Jonsson and Jonsson, 2009). Species' responses to climatic changes already include plastic shifts in traits such as phenology and behaviour (Nussey et al., 2005; Parmesan, 2006; Durant et al., 2007). Prior incorporation of functional traits into the analysis of climate change impacts enables the reliable assessment of thermal tolerance to environmental conditions, range shifts,

upcoming risks and new conservation opportunities (Floury et al., 2017; MacLean and Beissinger, 2017; Vasconcelos et al., 2017). Furthermore, in regard of niche tracking, species traits can be fundamental components for investigating spatially explicit impacts of climate change (MacLean and Beissinger, 2017). Responses of functional traits along thermal gradients can be parameterized with thermal performance curves (TPCs) (Jonsson and Jonsson, 2009; Childress and Letcher, 2017). Angiletta (2009) defines performance as any measure of an organism's capacity to function. Measures of performance can include, for example, growth, locomotion or survivorship, which are usually expressed as a rate or probability (Angiletta, 2006; Angiletta, 2009; Schulte et al., 2011). Thermal performance curves (TPCs) are generally used for predicting performance for different thermal environments and indexing the direct effect of temperature on the species' fitness (Huey and Stevenson, 1979; Frazier et al., 2006; Deutsch et al., 2008; Childress and Letcher, 2017). Thus, the incorporation of functional traits through TPCs may be promising for exploring range dynamics and species-specific variation in range shifts under climate change (MacLean and Beissinger, 2017).

Thermal tolerance and performance of fish species also depend on the current life stage, with the youngest life phase, i.e. the egg stage, being the most susceptible to high and low temperatures and temperature fluctuations as consequences of climate change (Brett, 1952; Elliott, 1994; Jonsson and Jonsson, 2009; Elliott & Elliott, 2010; Jatteau et al., 2017). Embryonic development is influenced by the surrounding temperature conditions, which additionally affects later species traits and life-history events (e.g. Jonsson and Jonsson, 2009). Thus, changes in climatic conditions in one life stage can have substantial consequences for later life stages (Jonsson and Jonsson, 1993; Fleming et al., 1997). For example, in early life stages warm temperatures might be favorable for rapid growth whereas in later life stages they might limit growth (Angiletta, 2009). Including different life stages of species with complex life cycles becomes essential in regard of assessing the comprehensive effects of climate change on species. However, studies that additionally investigated climate change influences on different life stages of species are missing.

Assessments of future impacts of climatic change on freshwater species mostly rely on statistical species distribution models (SDMs). There are only a few studies that have combined species functional traits with model predictions for fish species (e.g. Wittmann et al., 2016). Wittmann et al. (2016) found correlations between the probability predictions of the models for habitat suitability and growth rates for the Grass Carp (*Ctenopharyngodon idella*), indicating that SDMs may be able to provide scenarios which incorporate more than just the climatic envelope of the considered species in an indirect manner.

This study combines species distribution modelling and species' functional traits to assess future climatic impacts. The salmonid fish species *Salmo trutta* and *Salmo salar* are analyzed in regard of their current and future thermal performance, here defined as survivorship (Angiletta, 2009), based on the species-specific derived thermal performance curves (TPCs) (Deutsch et al., 2008). Future thermal performance is deduced from SDM predictions under three different scenarios ("no dispersal", "free dispersal", "restricted dispersal"). For example, "restricted dispersal" accounts for habitat fragmentation due to artificial barriers. SDMs are calibrated with

global distribution and environmental data at the catchment scale. Specifically, we examine the changes in performance based on the current and predicted distributions across latitude, months, seasons, years and life stages. Performance parameters are evaluated for the life stages adults, juveniles and eggs for both considered fish species. Eventually, we test whether the probability predictions of the calibrated SDMs in this study are correlated with the performance rates of the TPCs (see Wittmann et al., 2016).

Materials and methods

Study area

Global land masses were divided into African, Asian, Australian, European, North American and South American regions (Fig. S1). Each region was additionally differentiated into sub-watershed basins based on the utilization of the integrated water resources model WaterGAP3 (Brauman et al., 2016; Eisner, 2016; Schneider et al., 2017). To reduce uncertainty of environmental data calculations only catchments with an area of > 3,000 km² were included. The total global catchment number was 11,695 (Table S1).

Species data

Global species occurrence data for *Salmo trutta* and *Salmo salar* were obtained from the Global Biodiversity Information Facility (https://www.gbif.org/, accessed November 2018), which provides occurrence data via longitudinal and latitudinal specifications. We considered only presences from 1971 onwards with a coordinate uncertainty of ≤ 5 km and with "human observation" as basis of record. Freshwater species data were mapped to the considered catchment scale leading in total to 730 and 199 catchment occurrences for *Salmo trutta* and *Salmo salar*, respectively (Table S1). In comparison with point-to-grid mapping used for mapping terrestrial species' occurrences, catchment mapping is more appropriate for freshwater species due to the dendritic structure of river networks (see Fagan, 2002). Additionally, catchment assessments are used for large-scale freshwater management strategies (commonly referred to as the Catchment Based Approach – CaBA, see DEFRA, 2013), enabling the compatibility between the management and the analysis scales as well as the optimization of ecological restoration efforts (Lévêque et al., 2008; Markovic et al., 2017; Kuemmerlen et al., 2019).

Environmental data

Modern-day (1971 – 2000, hereafter referred to as baseline) and future (2041 – 2070, hereafter referred to as 2050s) data on natural river discharge were obtained from the WaterGAP3 model (Brauman et al., 2016; Eisner, 2016; Schneider et al., 2017). WaterGAP3 is a state-of-the-art global water model showing well performance (Beck et al., 2016; Eisner et al., 2017; Schneider et al., 2017). Grid-based monthly water balance calculations of WaterGAP3 at the 5 by 5 arc-minute resolution (~ 9 × 9 km at the Equator) were mapped to the studied catchment scale and used for calculations of various discharge statistics for the baseline and 2050s (Table S2). Future flow statistics were computed as multi-model ensemble means of five different general circulation models (GCMs), namely GFDL-ESM2M, HadGEM2-ES, IPSL-CM5A-LR, MIROC-ESM-CHEM, and NorESM1-M, provided by ISI-MIP (Hempel et al., 2013). Each GCM followed the medium-high emission Representative Concentration Pathway 6.0 (RCP6.0) scenario, which

comprises a radiative forcing of 6.0 W/m² in the year 2100 and a global mean temperature increase of 2.2 °C until the end of the century compared to 1986 – 2005 (Riahi et al., 2011). Accordingly, the five integrated GCMs were used to derive water temperature by transforming air temperature to stream water temperature on a monthly basis for the baseline and 2050s via a global relationship model (Punzet et al., 2012) (Table S2).

We used the Global Land Cover Characterization map (GLCC; USGS, 2008) and the CORINE Land Cover map for EU countries (CLC2000; EEA, 2004) for obtaining landscape variables (Table S2). Land cover data were kept constant for the future scenarios (see also Schneider et al. (2017) for detailed description).

In order to model species distribution opportunities and restrictions, we included the Global Reservoir and Dams database (GRanD), which contains information on 6,862 georeferenced reservoirs (Lehner et al., 2011).

Species traits data

We collected laboratory experiment data on species thermal traits for *Salmo trutta* and *Salmo salar* at different life stages from various studies (Table S3 and S4). Data could be collected for the traits "critical minimum temperature for survival" (CT_{min}), "optimum temperature" (T_{opt}), and "critical maximum temperature for survival" (CT_{max}) for the life stages adults, juveniles, and eggs. The thermal optimum (T_{opt}) was defined as the upper limit of the optimum temperature range following Comte et al. (2014). The maximum/ minimum temperature for survival was determined using different experimental approaches, such as the incipient lethal temperature (ILT) method or the critical thermal methodology (CTM). The incipient upper/ lower lethal temperature (IULT/ ILLT) is defined as the temperature that is lethal to 50% of a fish sample estimated over various exposure time intervals whereas for CTM the critical maximum/ minimum temperature is determined by exposing species to a constant linear increase or decrease in temperature until the fish loses its locomotion control (e.g. Beitinger et al., 2000). The maximum and minimum of the experimentally observed CT_{min} and CT_{max}, respectively, were set as final CT_{min} and CT_{max}.

Species distribution modelling

The predictor variables selection was based on a combination of three main criteria: (1) the univariate area under the receiver operating characteristic curve being at least fair (rounded AUC ≥ 0.7), (2) avoidance of multi-collinearity (pairwise correlations of < |0.7|, see Fig. S2) and (3) variable selections in previous studies. Univariate prediction strength was determined by using generalized additive models (GAMs) of the R (R development Core Team, 2018) package "mgcv" (Wood, 2011) as modelling approach. Often-used variables incorporated in scientific literature were only included if at least the second criterion was fulfilled.

Fish distributions were modelled using Artificial Neural Networks (ANN), Random Forest (RF), Gradient Boosting Machines (GBM), Multivariate Adaptive Regression Splines (MARS), Generalized Additive Models (GAM), Maximum Entropy Method (MAXENT) and Elastic Net (ELNET). ANNs are complex, non-linear model systems resembling the biological neural system, i.e. ANNs include neurons with a specified number of layers that are linked by different activation functions (Bishop, 1995; Jain et al., 1996; Duda et al., 2001; Hastie et al., 2001; Li and Wang, 2013; Lee et al., 2016). Commonly, a

three-layer feedforward model is used, which consists of the input layer, the hidden layer, and the output layer (Bishop, 1995) and which can approximate any smooth, finite non-linear function with high accuracy (Thuiller et al., 2009; He et al., 2011). We used the R package "h2o" (The H2O.ai team, 2018) for training ANNs as it provides many opportunities to adapt the model to the specific problem. RF is a combination of a certain number of decision trees where each tree is created by considering a random sample of the training data set and features (Breiman, 2001b). The number of votes of each tree of the forest determines the final prediction. High performances in species distribution modelling can be achieved by using this learning algorithm (e.g. Grenouillet et al., 2011). For building RF we used the R package "h2o" (The H2O.ai team, 2018). GBMs consist of a group of decision trees, which are built and combined by the gradient boosting algorithm (Hastie et al., 2001; Elith et al., 2008). Here, the R package "h2o" (The H2O.ai team, 2018) was used for analyses. MARS is a flexible regression method based on piecewise splines that are smoothly connected and thus able to model linear and non-linear relationships (Friedman, 1991; Zhang and Goh, 2016). The R package "earth" was used for MARS modelling (Milborrow, 2018). GAM is a non-parametric method that is able to account for non-linear relationships between the explanatory and dependent variables by using smoothing functions (Hastie and Tibshirani, 1986). For GAM, we applied the function of the R package "mgcv" (Wood, 2011). MAXENT as a general-purpose machine learning method is a principle from statistical mechanics and information theory (Phillips et al., 2006). It uses only presence data to estimate a target probability distribution by finding the probability distribution of maximum entropy under the constraint of the original data properties (Phillips and Dudik, 2008). The package "dismo" of Hijmans et al. (2017) was employed for the utilization of MAXENT. ELNET, which consists of a generalized linear model with a Lasso and Ridge regularization (L1- and L2-regularization) (Friedman et al., 2010), was used from the R package "h2o" (The H2O.ai team, 2018).

In order to tailor the models to our specified modelling problem we conducted a parameter tuning for the statistical methods ANN, RF, GBM, MARS and ELNET. The "h2o" package offers many tuning options for ANN with the possibility of manual tuning of the learning rates and momentum as well as the possibility of using the ADADELTA method (adaptive learning rate method) of Zeiler (2012). Manual and ADADELTA parameter tuning followed the instructions of the "h2o" manuals (https://www.h2o.ai/resources/, accessed October 2018). Parameter tunings for RF, GBM and ELNET from the R package "h2o" (The H2O.ai team, 2018) were carried out analogously. For MARS, only the maximum number of terms was tuned (Zhang and Goh, 2016; Milborrow, 2018). All tuning parameters are summarized in Table S5. The hyper-parameter optimization strategy for manual and ADADELTA ANN, RF, GBM and ELNET was random grid search (n = 300), since random parameter combination search was shown to find good or even better models compared to pure grid search within a small fraction of the computation time (Bergstra and Bengio, 2012). However, all parameter possibilities were tested for MARS due to significantly less computational cost. For each model that required parameter tuning, we estimated the best parameter combination using the threshold independent performance measure "AUC" resulting from 5-fold cross-

validation of 80% of the data (e.g. Bergstra and Bengio, 2012; El-Gabbas and Dormann, 2017). The remaining 20% were withheld to simulate performance testing on an unseen and independent data set (Bergstra and Bengio, 2012). For the two ANNs, only the model with better performance on the test data set was used in further analyses.

Accuracy of various predictive performance measures after final parameter determination was tested via bootstrapping (n = 100), i.e. the data was randomly split into 80% calibration and 20% validation data 100 times. A threshold for the probability predictions, i.e. for separating presences and absences of a species, was determined by minimizing the absolute difference between specificity (the rate of correctly predicted absences) and sensitivity (the rate of correctly predicted presences) (Fielding & Bell, 1997). Minimizing the difference between the sensitivity and specificity generally leads to accurate predictions (Jimenez-Valverde & Lobo, 2007). Therefore, we also considered the threshold-dependent performance measure "true skill statistic" (TSS = sensitivity + specificity − 1). Validation performance results for AUC, sensitivity, specificity and TSS were computed each time, whereas the average validation performance was used for the assessment of the predictive performance (Dormann et al., 2008).

For species distribution predictions, we applied the consensus method by averaging the resulting probabilities of occurrence in order to reduce uncertainty of using a single modelling approach (Marmion et al., 2009). To ensure reliability and robustness of our statistical approaches, only those models with a mean validation AUC > 0.85 were included. Additionally, we also conducted a validation of the performance measure accuracy for the ensemble model.

We studied three different scenarios in the future spatial distribution patterns of the considered species in terms of distribution possibilities. The first possibility considers no change in future distribution patterns ("no dispersal"), i.e. the 2050s distribution pattern corresponds to the pattern of the baseline in order to identify affected areas in the future of current distributions. The second possibility comprises a free distribution of the species on condition that the predicted presence in a catchment is connected to a catchment with a presence in the baseline pattern ("free dispersal"). The third possibility is defined by a restricted distribution of the species, which considers dams as dispersal barriers ("restricted dispersal"), in order to outline the effects of habitat fragmentation on future species distributions and performance.

Thermal performance curves

Species thermal traits data were used to parametrize thermal performance curves (TPCs), which describe the relationship between temperature and a species' ability to function (Huey and Stevenson, 1979; Angert et al., 2011). Typically, TPCs are bounded at the extreme temperatures (CT_{min}, CT_{max}), possess a single intermediate mode, and appear skewed with a slow performance rise up to the maximum level at T_{opt} and a rapid drop afterwards (Huey and Kingsolver, 1989; Angiletta, 2006; Dell et al., 2011; Sinclair et al., 2016). The skewness of the TPCs arises from slower chemical reactions at low temperatures and constraints of the cellular function capacity due to protein degradation and oxygen limitation at high temperatures (Dell et al., 2011; Childress and Letcher, 2017). Here, performance is defined as survivorship and

related to rates along the thermal gradient (Angiletta, 2009). The model of Deutsch et al. (2008) was used to obtain the performance rates by incorporating the observed data on CT_{min}, T_{opt} and CT_{max} for the life stages adults, juveniles, and eggs, accounting for varying TPCs and stage-specific vulnerability (Sinclair et al., 2016).

Assessment of species' thermal performance

We used the baseline distribution data, the predicted 2050s distribution data based on the three dispersal scenarios ("no dispersal", "free dispersal", "restricted dispersal"), water temperature data and the parametrized TPCs for the different life stages (adults, juveniles, eggs) (see Fig. S3) in order to determine and compare current and future performances of the species. Species performance was studied at a monthly, seasonal and yearly timeframe. Monthly and seasonal analyses were performed for capturing potential phenology shifts either due to enhanced or reduced fitness (Deutsch et al., 2008). Seasons were defined as winter (December to February), spring (March to May), summer (June to August) and autumn (September to November) according to the northern hemisphere. The spawning season (until hatching) for eggs in the northern hemisphere was defined as October – February (Campbell, 1977; Heggberget, 1988; Elliott, 1993; Östergren and Rivinoja, 2008; Jonsson and Jonsson, 2009; Elliott and Elliott, 2010; Jonsson and Jonsson, 2011) and for the southern hemisphere as April – August, being six months out-of-phase with northern conspecifics (Pankhurst and King, 2010). A broad spawning season was chosen to cover phenotypical divergence across populations (Hereford, 2009; Angert et al., 2011). Seasonal and yearly estimates were based on previously calculated monthly performances. Additionally, latitudinal distributions of the performance probabilities were investigated in order to understand how the thermal performance might change (Sinclair et al., 2016).

Relationships between model probability predictions for the baseline and the species' functional trait expressed as the thermal performance were quantified to test the implicit assumption of SDMs that highly suitable sites with high probabilities of occurrence imply higher performance and fitness than poorly suitable sites with lower probabilities of occurrence (Guisan and Thuiller, 2005; Wittmann et al., 2016). Thus, the concept of the environmental niche modelling, which commonly uses abiotic conditions for explaining species distributions, is examined by relating to a biotic factor.

Results

Predictor variables selection

Through synthesis of three variable selection criteria (univariate analysis, correlation analysis, and scientific literature), we selected 8 out of 29 variables representing climatic, topographic and anthropogenic influences from the baseline data set for each species (Table 1, Table S6-S7, Fig. S2). The variable selection accounted for seasonal discharge and water temperature influences in regard of spawning seasons. Discharge variables were all highly correlated with each other, thus limiting the number of discharge variables in the model (Fig. S2). For example, we explained *Salmo trutta* distributions by selecting the Mean autumn water temperature because of the combination of univariate explanatory strength and approaches in scientific literature (Table S2 and S6). Due to high pairwise

Table 1 Variable selection for modelling species distributions of *Salmo trutta* and *Salmo salar*.

Category	Variable	Description	Species	
			Salmo trutta	***Salmo salar***
Climatic	Mean winter discharge	Mean discharge for the months December to February	yes	yes
	Water temperature seasonality	Average of the annual standard deviation of water temperatures	no	yes
	Mean autumn water temperature	Mean water temperature for the months September to November	yes	yes
	Mean diurnal range	Mean of monthly (maximum – minimum water temperature)	yes	no
	Annual water temperature range	Maximum water temperature – minimum water temperature	yes	no
	Isothermality	Mean diurnal range / Annual water temperature range	no	yes
Topographic	Altitude	Mean catchment elevation	yes	yes
Land cover	Cropland	Percentage of catchment area covered by cropland	yes	yes
	Built-up area	Fraction of sealed areas within the catchment	yes	yes
	Forest	Percentage of catchment area covered by forest	yes	yes

correlations of the Mean autumn water temperature with further water temperature variables, only the Annual water temperature range and Mean diurnal range were additionally included. Mean winter discharge was analogously selected because of the combination of univariate explanatory strength and its influence on specific life stages. Factors of anthropogenic and topographic influences were taken into account through Built-up area, Forest, Cropland, and Altitude, whereas especially Cropland and Altitude were included due to scientific literature.

Model performance

Cross-validated AUC values and AUC scores for the test data set during parameter tuning showed well performances (AUC > 0.90) (Table S8 and S9) with only ELNET having lower performance scores (0.80 < AUC < 0.87) for both species. Final parameter tuning results are listed in Appendix 5 (Table S8 and S9). Differences between the AUC test scores, although small, of the manually and ADADELTA tuned ANNs, led to the further inclusion of the manually tuned ANN model for *Salmo trutta* (Table S8) and the ADADELTA ANN for *Salmo salar* (Table S9). The performance validation showed high mean scores (e.g. mean AUC ≥ 0.95) after parameter tuning for all included statistical models except for ELNET (mean AUC ≤ 0.85) (see Table 2). Additionally, threshold-dependent performance measures, i.e. sensitivity, specificity and TSS, attained high values for nearly all statistical approaches. Moderate performance values were only found for ELNET (Table 2). Thus, ELNET was excluded in the consensus modelling for both species. The validation performance values of the consensus models were in the range of the high values of each included statistical model (Table 2).

Table 2 Validation performance results of all considered statistical methods (Artificial Neural Networks (ANN), Random Forest (RF), Gradient Boosting Machines (GBM), Multivariate Adaptive Regression Splines (MARS), Generalized Additive Models (GAM), Maximum Entropy Method (MAXENT), Elastic Net (ELNET), consensus method (CONS)). For *Salmo trutta*, the manually tuned ANN was used for further analyses, while for *Salmo salar* the ADADELTA ANN was used. Due to a mean validation AUC of ≤ 0.85, ELNET was excluded in the consensus model for both species.

Species	Performance measure		Method							
			ANN	RF	GBM	MARS	GAM	MAXENT	ELNET	CONS
Salmo trutta	AUC	min	0.97	0.97	0.97	0.93	0.94	0.95	0.80	0.97
		mean	0.98	0.98	0.98	0.95	0.96	0.96	0.82	0.98
		max	0.99	0.99	0.99	0.96	0.97	0.97	0.84	0.98
	Sensitivity	min	0.91	0.92	0.92	0.85	0.87	0.86	0.72	0.90
		mean	0.93	0.94	0.94	0.88	0.90	0.90	0.74	0.92
		max	0.95	0.95	0.96	0.91	0.92	0.93	0.76	0.94
	Specificity	min	0.91	0.92	0.91	0.85	0.87	0.86	0.72	0.90
		mean	0.93	0.94	0.94	0.88	0.9	0.93	0.74	0.92
		max	0.95	0.95	0.96	0.92	0.92	0.90	0.76	0.94
	TSS	min	0.82	0.84	0.83	0.69	0.75	0.73	0.44	0.81
		mean	0.86	0.87	0.87	0.76	0.79	0.80	0.48	0.84
		max	0.90	0.91	0.92	0.83	0.84	0.85	0.53	0.88
Salmo salar	AUC	min	0.95	0.97	0.95	0.93	0.94	0.96	0.81	0.96
		mean	0.97	0.98	0.98	0.96	0.97	0.97	0.85	0.98
		max	0.99	0.99	0.99	0.98	0.98	0.99	0.89	0.99
	Sensitivity	min	0.86	0.87	0.86	0.85	0.83	0.86	0.74	0.86
		mean	0.91	0.93	0.93	0.90	0.91	0.92	0.78	0.92
		max	0.95	0.97	0.97	0.94	0.95	0.98	0.83	0.97
	Specificity	min	0.87	0.90	0.88	0.85	0.84	0.86	0.73	0.87
		mean	0.91	0.93	0.93	0.90	0.91	0.92	0.78	0.92
		max	0.96	0.97	0.97	0.94	0.95	0.97	0.82	0.96
	TSS	min	0.73	0.79	0.73	0.70	0.67	0.72	0.47	0.73
		mean	0.82	0.87	0.86	0.79	0.82	0.83	0.56	0.84
		max	0.91	0.94	0.94	0.89	0.90	0.95	0.64	0.92

Current and future species' thermal performance

For the thermal performance assessment of the two salmonids, three future dispersal scenarios were considered. While the location and number of presences for the "no dispersal" scenario coincided with the initial baseline situation (n = 730 for *Salmo trutta* and n = 199 for *Salmo salar*), the remaining two future dispersal scenarios showed a reduction of the distribution ranges. For *Salmo trutta*, n = 724 future presences were predicted with the

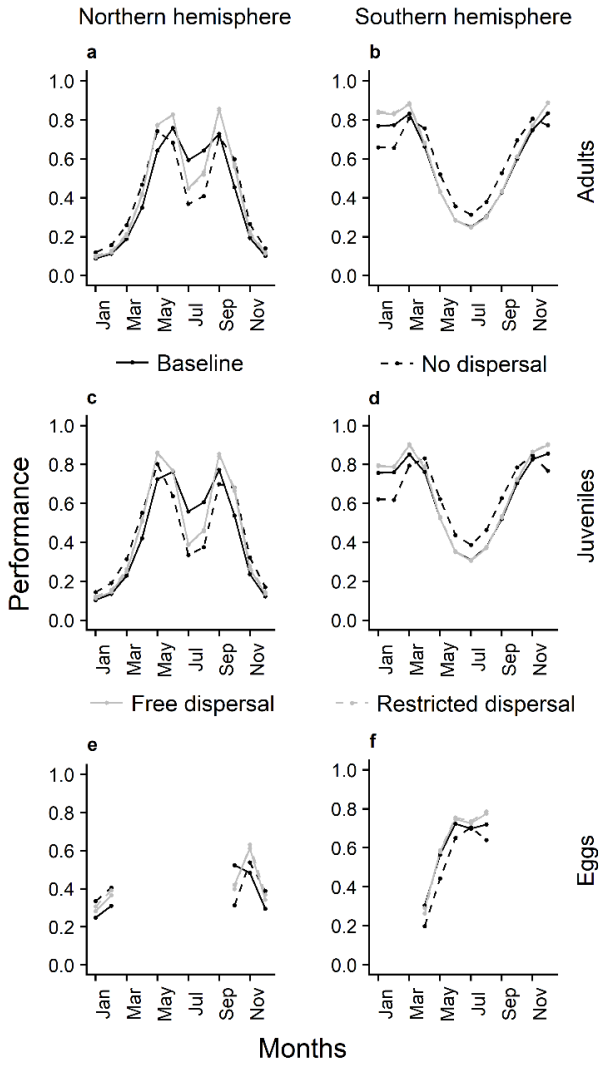

Figure 1 Baseline and 2050s mean monthly performances for the life stages adults, juveniles and eggs of *Salmo trutta* under consideration of different dispersal scenarios.

consensus modelling approach. In regard of the "free dispersal" scenario, which required a connection of the catchment with a predicted presence to a catchment with a baseline presence, the number of predicted presences decreased to n = 582, with 464 out of the 730 currently suitable catchments being suitable in the future (~ 63% of the current area). The integration of the "restricted dispersal" scenario, which included dams as dispersal barriers, indicated a further decline of the distribution range, with n = 475 remaining predicted presences for the 2050s. For *Salmo salar*, the consensus model predicted n = 194 presences for the 2050s. Under the "free dispersal" scenario the predicted number of presences decreased to n = 119 with 89 out of the 199 currently suitable catchments being still suitable in the future (~ 42% of the current area). Similarly, the "restricted dispersal" scenario led to a further decline in the number of predicted presences to n = 102.

Monthly thermal performance trends for the three life stages were considered separately for the northern and southern hemisphere to account for the shifted seasons (Fig. 1 and S4). Mean performances for the life stages adults and juveniles of *Salmo trutta*, respectively, showed similar monthly trends for both hemispheres (Fig. 1). We note that less occurrences were present for the southern hemisphere and that results should be interpreted with caution (see Table S1). Compared to the baseline performance, a slight increase in performance for the "free" and "restricted dispersal" scenarios could be observed from January to June and from September to November, whereas for the remaining months in summer (July, August) all scenarios predicted a drop below the current performance for the populations in the northern hemisphere. The "no dispersal" showed additionally a drop of the performance in May. Future mean performances of the scenarios "free dispersal" and "restricted dispersal" were similar, although the latter scenario led to fewer predicted occurrences. Additionally, both indicated overall higher performance values from May to September compared to those found under the "no dispersal" scenario for northern populations. Monthly performance analysis for the southern hemisphere displayed mean performances of the "free dispersal" and "restricted dispersal" scenarios that were close to the identified

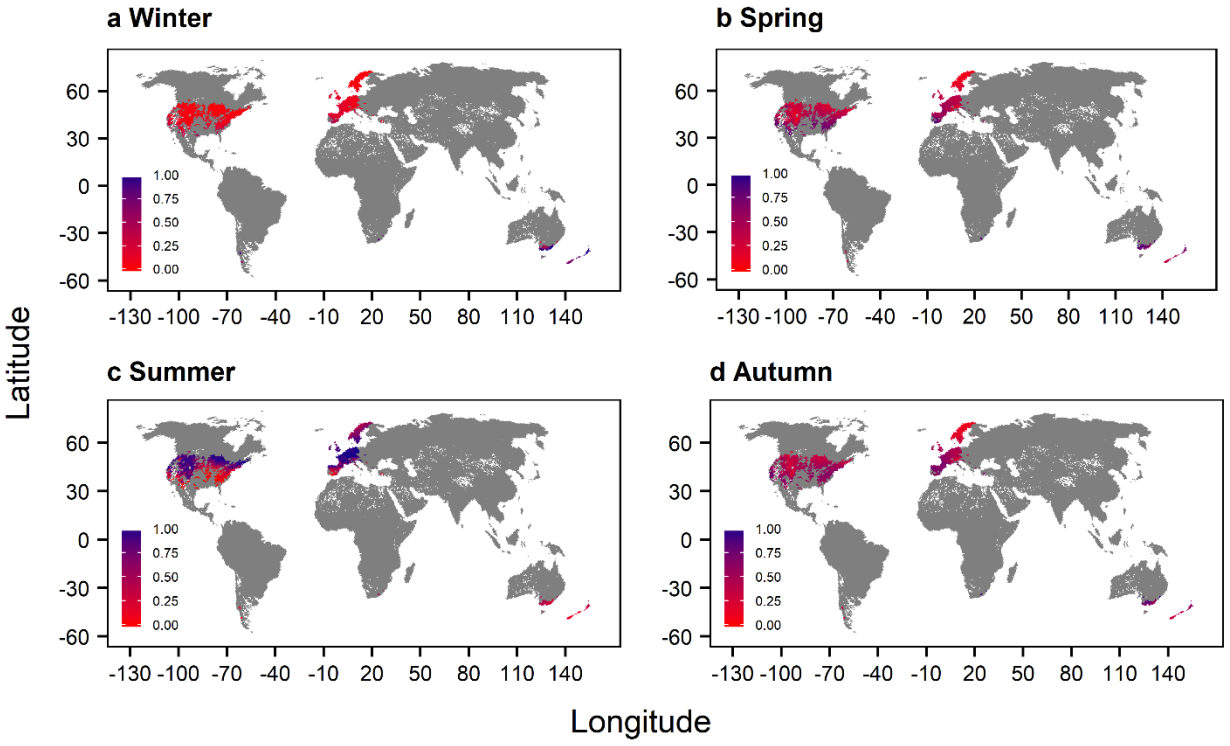

Figure 2 Global map of the seasonal performances of adult *Salmo trutta* for the baseline scenario. Note that seasons were defined according to the northern hemisphere.

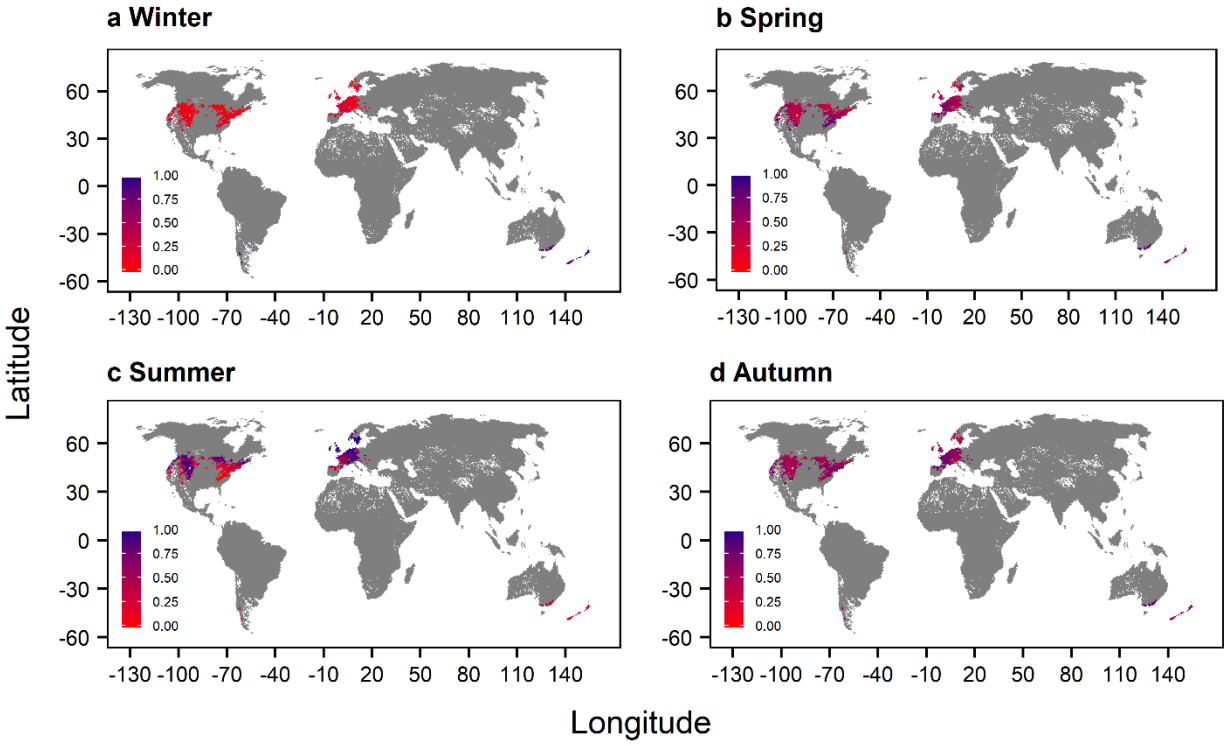

Figure 3 Global map of the seasonal performances of adult *Salmo trutta* for the "restricted dispersal" scenario. Note that seasons were defined according to the northern hemisphere.

Table 3 Comparison of the mean baseline and future performance as rate for different scenarios and timeframes. Performances for populations in the northern (NH) and southern hemisphere (SH) were computed separately. Performance was identified for the life stages adults, juveniles, and eggs, whereas performance of eggs was only considered within the spawning season of the salmonids *Salmo trutta* and *Salmo salar*. Note that values for the southern hemisphere of *Salmo salar* were excluded because of few observations. Seasons were defined according to the northern hemisphere.

Species	Life stage	Timeframe	Scenario							
			Baseline		No dispersal		Free dispersal		Restricted dispersal	
			NH	SH	NH	SH	NH	SH	NH	SH
Salmo trutta	adults	winter	0.10	0.79	0.14	0.70	0.11	0.85	0.12	0.86
		spring	0.39	0.64	0.49	0.70	0.46	0.66	0.47	0.67
		summer	0.66	0.28	0.49	0.35	0.60	0.28	0.60	0.28
		autumn	0.46	0.59	0.53	0.68	0.54	0.60	0.55	0.61
		annual	0.40	0.58	0.41	0.60	0.43	0.60	0.43	0.60
	juveniles	winter	0.12	0.79	0.17	0.67	0.13	0.83	0.14	0.83
		spring	0.46	0.71	0.56	0.75	0.54	0.73	0.54	0.74
		summer	0.64	0.35	0.45	0.43	0.54	0.34	0.54	0.35
		autumn	0.51	0.68	0.57	0.75	0.59	0.70	0.60	0.71
		annual	0.43	0.63	0.44	0.65	0.45	0.65	0.46	0.66
	eggs	spawning	0.37	0.60	0.40	0.53	0.41	0.62	0.42	0.63
Salmo salar	adults	winter	0.08	-	0.11	-	0.11	-	0.11	-
		spring	0.27	-	0.36	-	0.33	-	0.33	-
		summer	0.80	-	0.83	-	0.89	-	0.89	-
		autumn	0.35	-	0.46	-	0.42	-	0.43	-
		annual	0.38	-	0.44	-	0.44	-	0.44	-
	juveniles	winter	0.07	-	0.09	-	0.09	-	0.09	-
		spring	0.21	-	0.29	-	0.25	-	0.26	-
		summer	0.70	-	0.83	-	0.79	-	0.79	-
		autumn	0.28	-	0.38	-	0.34	-	0.34	-
		annual	0.32	-	0.40	-	0.37	-	0.37	-
	eggs	spawning	0.32	-	0.37	-	0.38	-	0.40	-

performances of the baseline scenario from April to November. Higher performance values were identified for the remaining months (January, February, March, December). The "no dispersal" scenario however implied lower performances for these months, underlining the importance of dispersal possibilities. Overall, there were no major temporal shifts of the peak performances of *Salmo trutta* adults in the northern and southern hemisphere, however peak performance of juveniles shifted from June to

May in the northern hemisphere. Future monthly performances of eggs during the spawning season showed in general equal or higher performances with a shift of the peak performance from October to November for the northern species. For all scenarios of the 2050s, a drop below the current performance was observable in October. Performances of eggs in the southern hemisphere were below the current performances solely for the "no dispersal" scenario. Monthly performances for *Salmo salar* were only identified for species in the northern hemisphere (Fig. S4), because low occurrence numbers were present for southern conspecifics (see Table S1). In general, all future scenarios predicted a similar increase in monthly performances for *Salmo salar* adults and juveniles with only "no dispersal" scenario performance slightly dropping below the baseline performance for adult *Salmo salar* in July (Fig. S4). For eggs, the same monthly performance pattern as found for northern *Salmo trutta* eggs emerged.

Seasonal performance patterns of *Salmo trutta* underlined the decrease in the summer performance of adults and juveniles for all scenarios in the southern ranges of the northern hemisphere (Fig. 2-3, Fig. S5-S10 and Table 3). Mean performances were higher for the "free" and "restricted dispersal" scenario (adults: 0.60, juveniles: 0.54) compared to the "no dispersal" scenario (adults: 0.49, juveniles: 0.45) (Table 3). Mean performances of northern populations across the winter, spring and autumn season showed a slight shift from lower to higher performances. In the southern hemisphere, the seasonal mean performances of adults and juveniles for the "free dispersal" and "restricted dispersal" scenario were close to the current performance. Compared to the "no dispersal" scenario (adults: 0.70, juveniles: 0.67), higher mean performances were observable for the "free" and "restricted dispersal" scenarios for the December – February season (adults: 0.85, juveniles: 0.83) (Table 3). Great differences in the seasonal mean performances were not found for the two latter scenarios; however, differences existed at the geographical level for adults and juveniles (Fig. 3 and S6, Fig. S7-S10). For example, the scenario "restricted dispersal" revealed limited distribution possibilities in north-eastern USA and eastern Europe. Thus, northern USA areas where high performance values could be attained in summer of the 2050s could not be reached due to the existence of artificial barriers. Seasonal mean performances of *Salmo trutta* eggs indicated in general increasing performance values for all scenarios. In the southern hemisphere, mean performance of eggs for the "no dispersal" scenario (0.53) was below the performances identified for the other future scenarios (~0.62) (Table 3). Seasonal mean performances of northern *Salmo salar* populations increased similarly for every future scenario and life stage (Table 3, Fig. S11-S18). Non-existing differences between the seasonal mean performances inferred from the "free" and "restricted dispersal" scenario indicated the necessity of geographical inspections. However, for adults and juveniles only the disappearance of single catchments connected to high performances could be observed under "restricted dispersal" especially for the summer season in northern Europe and parts of the USA (Fig. S13 and S14, Fig. S17 and S18), which could be ascribed to the small difference (n = 17) between the numbers of predicted occurrences of the two scenarios.

Latitudinal trends of the annual mean performance revealed a northward trend in the northern hemisphere and a southward trend in the southern hemisphere across all scenarios

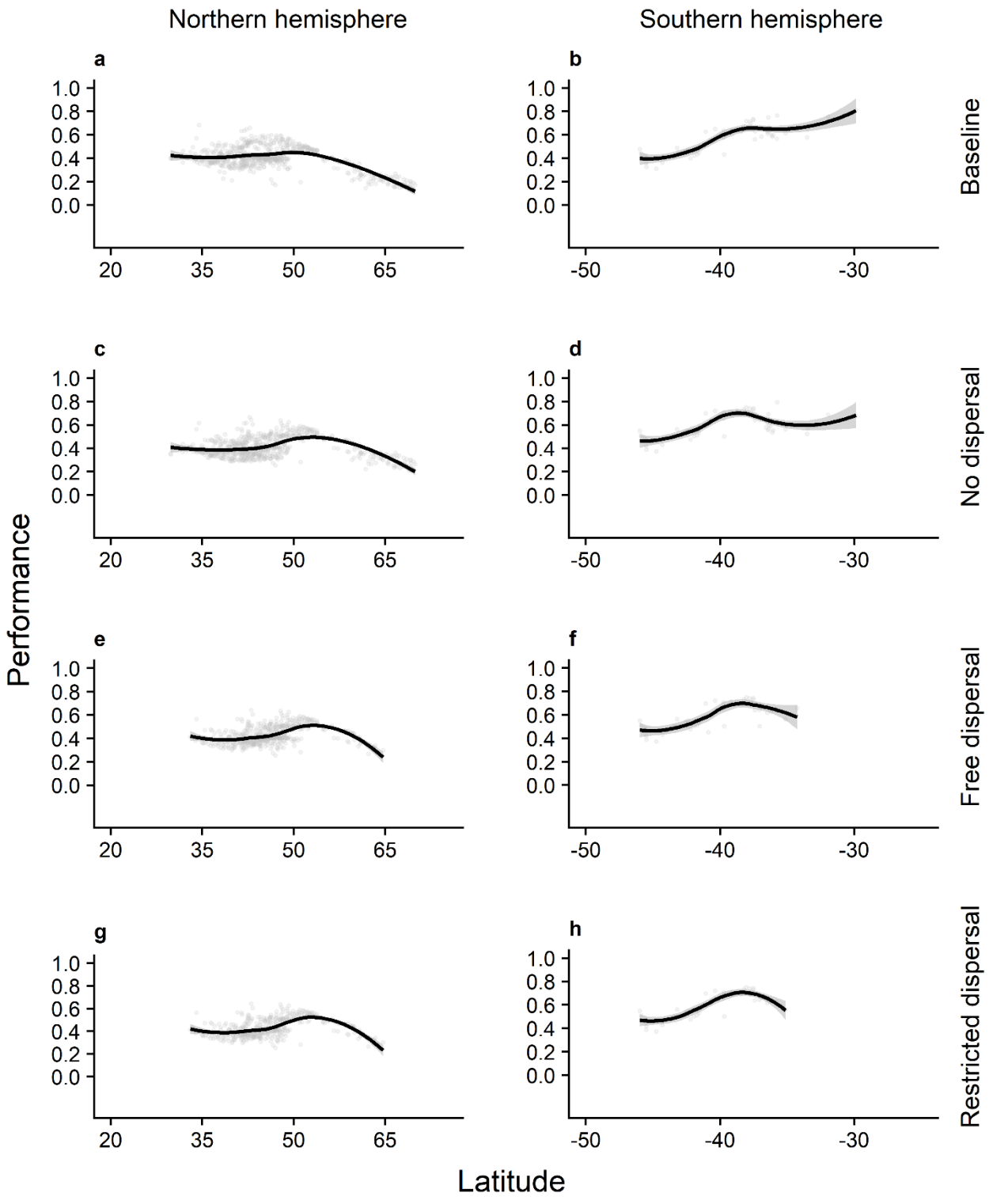

Figure 4 Latitudinal trends of annual mean performance for adult *Salmo trutta* under consideration of different dispersal scenarios. Annual mean performance is based on monthly performance values.

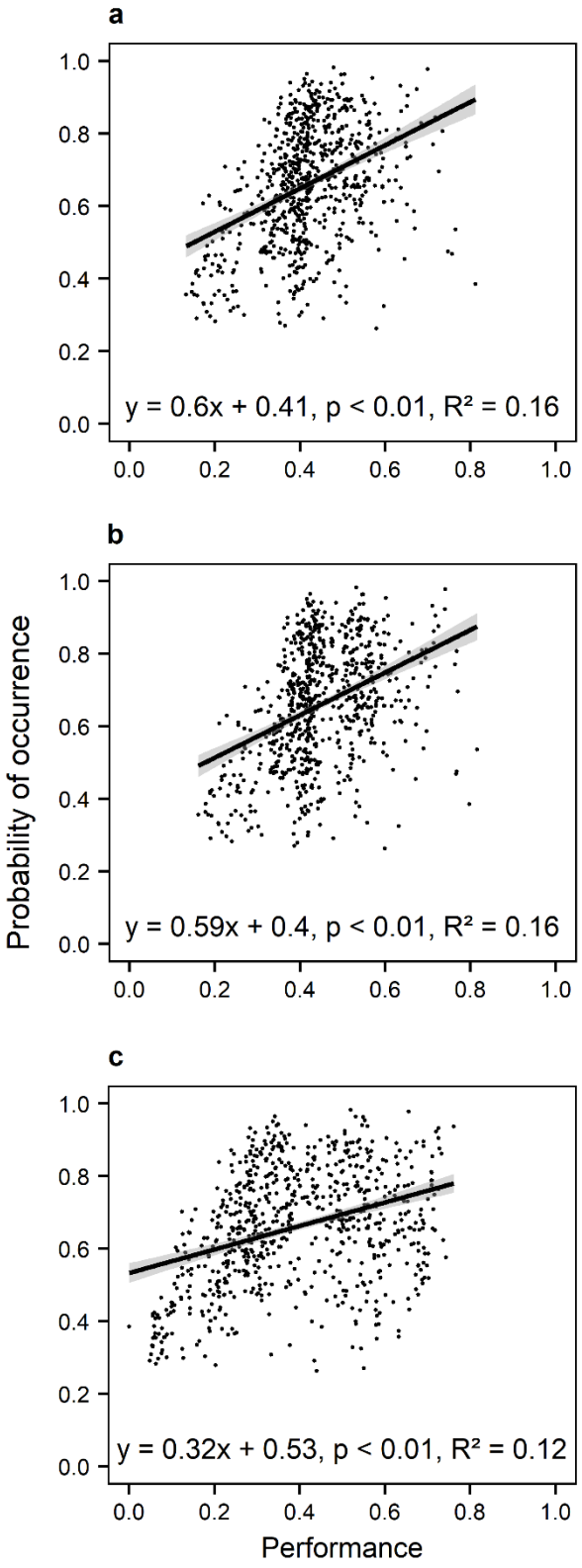

Figure 5 Relationship between the modelled habitat suitability and performance for the life stages (a) adults, (b) juveniles and (c) eggs of *Salmo trutta*. For adults and juveniles, the annual mean performance and for eggs the performance during the spawning season were used for the assessment.

and life stages of *Salmo trutta* (Fig. 4 and Fig. S19-S20). Northward trends were observable due to higher performances around 45° - 55° N (northern USA and central Europe) in the future and range shifts identified through the "free" and "restricted dispersal" scenario (e.g. Fig. 4e, g). However, the increases in performance up to 55° N were followed by declines in the annual mean performance for more northern or polar regions. The spawning season performance of *Salmo trutta* eggs in these regions dropped even stronger than the performance of adults and juveniles (Fig. S20). In general, these observations could be made for the southern hemisphere vice versa. The observed northward trends of the performances and distributions found for *Salmo trutta* in the northern hemisphere could be transferred to all life stages of *Salmo salar* (Fig. S21-S23). Future annual and spawning season mean performances increased around 45° - 55° N and were accompanied by in part steep negative slopes when moving toward higher latitudes. Trends for the southern hemisphere could not be studied because of low occurrence numbers.

Species distribution models and thermal performance

Relationships between the modelled probabilities of occurrence and thermal performances of the two salmonids and the respective life stages were investigated in order to test the ability of SDMs to incorporate biotic characteristics through abiotic predictors. The investigation revealed significant positive relationships for all life stages of *Salmo trutta* ($p < 0.01$; $r = 0.40$ for adults and juveniles; $r = 0.35$ for eggs) (Fig. 5). However, no significant relationships were found for *Salmo salar* adults and juveniles ($p > 0.40$). Only between the performance of *Salmo*

salar eggs in the spawning season and the probability for a species' presence a significant positive relationship was identified in combination with low correlation ($p < 0.01$; $r = 0.28$).

Discussion

Comprehensive assessments of future climate change impacts on species not only require the investigation of abiotic relationships of the species with the environment by using species distribution models (SDMs) but also the consideration of species traits (Jonsson and Jonsson, 2009; Floury et al., 2017; MacLean and Beissinger, 2017). In this study, we assessed climate change impacts by combining predictions of SDMs for three different dispersal scenarios ("no dispersal", "free dispersal", "restricted dispersal") with thermal performance curves for three life stages (adults, juveniles, eggs) of the salmonid species *Salmo trutta* and *Salmo salar*. Thermal performance curves (TPCs) allowed the detailed investigation of performances for different timeframes, i.e. monthly, seasonal and yearly, and thus the identification of periods with potentially higher vulnerability in the future (Deutsch et al., 2008).

Monthly performance analyses showed in general higher future performances for eggs of both studied species with a temporal shift of the peak performance in the northern hemisphere from October to November. Previous studies have stated that spawning times could change quickly under new environmental settings (e.g. Carlson and Seamons, 2008) and Jonsson and Jonsson (2009) have even argued that the time of spawning could be delayed under future conditions, being in accordance with the shift of the peak performance identified in our results. For adults and juveniles of *Salmo trutta* and *Salmo salar*, varying monthly performance changes were observed, implying different reactions of the species to different time periods. For example, there was also a shift of the peak performance from June to May of *Salmo trutta* juveniles in the northern hemisphere. As changes in climatic conditions for a certain life stage can substantially affect later life stages (Jonsson and Jonsson, 1993; Fleming et al., 1997; Angiletta, 2009), identifying responses of different life stages to environmental change is essential. In general, fishes as ectothermic species exhibit phenotypic plasticity and thus plastic responses to temperature variations, implying that life history traits beside survivorship, like fecundity or development, change accordingly (Dawson et al., 2011; Schulte et al., 2011; Scranton and Amarasekare, 2017). Therefore, analyses of species responses on a monthly basis for different life stages enable a more detailed identification of delayed or shifted species' traits.

Mean performances of the "free" and "restricted dispersal" scenario increased for the spawning season as well as winter, spring and autumn in 2050s for both hemispheres and all life stages of *Salmo trutta*. Rising temperatures affected adults and juveniles of *Salmo trutta* especially during the summer season (June – August) in the northern hemisphere, where performance decreases were observable. In summer, the inclusion of different dispersal scenarios outlined the importance of dispersal possibilities in order to escape the increasing temperatures and to reach habitats where higher performances may be possible. In regard of increases in heat events (Field et al., 2014; Scranton and Amarasekare, 2017), movement through the hydrological network will be a major factor influencing survival. For the summer season of

the southern hemisphere (December to February) similar statements could be made, as the "no dispersal" scenario indicated a markedly lower future mean performance than the remaining scenarios. Further on, the ability of dispersal was important for the life stage eggs because higher performances were present under dispersal scenarios accounting for species movements and thus spawning in new habitats, especially in the southern hemisphere. Major differences among the seasonal mean performances of the three dispersal scenarios were absent for *Salmo salar*, which can be ascribed to the lower numbers of presences for each scenario and the catchment-scale used for analysis. However, performances seemed to increase for every season for *Salmo salar* in the northern hemisphere, whereas for the southern hemisphere no analyses could be executed due to low numbers of occurrences. In regard of the geographical distribution of the seasonal performances for both species, the "restricted dispersal" scenarios, which accounted for dams as dispersal barriers, highlighted the negative influences of dams on species distributions, since areas with high thermal performances identified by the "free distribution" scenario could not be reached anymore. Dams are already known to disrupt the hydrological habitat connectivity and thus aggravating climate change influences (e.g. Markovic et al., 2017).

Future distribution patterns retrieved from the SDMs under consideration of the "free" and "restricted dispersal" scenario implied a decline in suitable habitat for the 2050s and northward and southward shifts for both species in the northern and southern hemisphere, respectively. Projections of previous studies finding a reduction in the number of suitable habitats for brown trout *Salmo trutta* are thus confirmed by our results (e.g. Wenger et al., 2011). In addition, northward movements are already projected for *Salmo salar* and highlighting that increases in water temperature may influence species traits, which can lead ultimately to extinctions for southern ranges in the northern hemisphere (Jonsson and Jonsson, 2009). With the summer season being most critical to species in regard of performance in the southern ranges, conservation actions need to focus on providing access to northern habitats within this season to prevent severe impacts for southern populations. Future higher annual mean performances in the northern USA and central to northern Europe and lower performances for the southern distribution ranges for all scenarios and life stages underline the shifts based on the studied biotic factor. However, further investigations have to be carried out to analyze whether the inclusion of other species' traits leads to the same patterns (MacLean and Beissinger, 2017).

Few studies have tested the combination of species functional traits and model-based predictions for species (e.g. Nagaraju et al., 2013; Elmendorf and Moore, 2008; Thuiller et al., 2010; Wittmann et al., 2016). However, these studies have found existing correlations between the model outputs and species traits. In particular, Wittmann et al. (2016) added the first fish example to the correlation analysis, finding a positive relationship ($r = 0.5$) between modelled habitat suitability and growth rates for the Grass Carp (*Ctenopharyngodon idella*). In this study, we investigated the relationship between modelled probabilities of occurrence and the annual mean performances for the different life stages of the salmonids. For *Salmo trutta*, we have found significant positive relationships for all three life stages. However, Bravais-Pearson correlation coefficients were

weak with r ≈ 0.40 for adults and juveniles and r ≈ 0.35 for eggs. For *Salmo salar*, only for eggs a significant positive relationship (r ≈ 0.28) was found. Less studied occurrences of *Salmo salar* (n = 199) compared to *Salmo trutta* (n = 730) at the analyzed catchment scale may have impaired the found relationships. Overall, these results add answers to the question of whether species distribution models are somehow able to account for traits through calibrations with abiotic environmental data. Further studies confronting SDMs with performance data are necessary for deriving a profound answer to this question.

Although we have combined species traits with highly accurate SDMs for assessing climate change impacts by using thermal performance curves (TPCs), such an analysis comes with limitations. Discussions about SDMs and different modelling techniques are broadly covered by literature (e.g. Franklin, 2009), however species trait data have to be considered carefully. TPCs were based on experimentally observed data for different life stages not representing true settings in the field. Acclimation processes in laboratory experiments can substantially modify observed thermal limits and thus the shape of TPCs (Angiletta, 2009). Furthermore, resource limitations in the field can alter the temperature performance relationship as well as the interaction of temperature with a variety of biotic and abiotic factors (Childress and Letcher, 2017; Angiletta, 2009; Schulte et al., 2011). Martin et al. (2016) have found that laboratory data significantly underestimated field-derived thermal mortality. In addition, due to both genetic and non-genetic reasons single individuals in populations may have significantly differing thermal properties (e.g. Kingsolver et al., 2011). As such, the preferred temperature (T_{opt}) may vary from species to species (Angiletta, 2009). Despite these differences, previous studies have found no significant relationships between a species' functional trait or performance and the thermal conditions of different populations (Jonsson et al., 2001; Angiletta, 2009; Forseth et al., 2009; Jonsson and Jonsson, 2009; Elliott and Elliott, 2010). However, T_{opt} is also influenced by further factors such as the amplitude of thermal cycles and variations which species have recently been exposed to or levels of dissolved oxygen (Jobling, 1981; Johnson and Kelsch, 1998). Especially for eggs, a strong relationship between oxygen limitation and thermal tolerance of fish embryos was identified (Martin et al., 2016). The found thermal limits CT_{min} and CT_{max} are also not necessarily survival limits as species may endure short-term exposures to temperatures beyond these limits (Sinclair et al., 2016). Brief exposure to such temperatures can even cause greater tolerance to temperature extremes, which is called hardening (Angiletta, 2009). Consequently, the duration of the exposure to critical temperatures additionally influences the performance, where the performance usually decreases with increasing exposure time (Sinclair et al., 2016). Shifting from static to dynamic TPCs, which incorporate a time component, would enable more comprehensive and realistic studies of climate change impacts (Schulte et al., 2011; Woodin et al., 2013).

In addition, the consideration of different dispersal scenarios for future studies, especially those including dispersal barriers, requires detailed data on species occurrences, the dendritic structure of rivers and the connections between catchments in order to give a more reliable assessment of the distribution possibilities for freshwater fish. Concerning this aspect, this study was limited

due to the scale differences of used data, leading to a more general approach for identifying possible paths of future fish distributions.

In summary, future temperature changes will influence the performance of each life stage of the studied fish species differently according to the analyzed timeframes. Dispersal possibilities will become more important for fish distributions in order to escape warming and reach areas where performance can increase. Dams as dispersal barriers disrupt catchment connectivity and will impede movement to suitable habitats linked to high performance values. Thus, we suggest that conservation management should incorporate a time component enabling the mitigation of severe climate change effects in periods where performances of species might drop critically. Additionally, catchments where dispersal barriers are present and prohibiting movement to places where higher performances could be possible should be reconsidered in further conservation planning.

PART III

Conclusion

Chapter 8

Discussion, synthesis and outlook

Summary of main results

In this thesis, complex relationships between water quality, nutrients and temperature as well as multiple influences of climate change on freshwater species distributions were analyzed with statistical models. All five studies were subject to specific research questions; however, all aimed at providing orientation for decision-making and conservation management in order to sustain the valuable services of freshwater ecosystems.

Water quality relationships in lake ecosystems (Objective 1)

Improving water quality across freshwater environments and preventing progressing eutrophication in lake systems are major aims (cf. Poikane et al., 2014). Thus, providing the right tools for identifying relationships between water quality parameters, drivers of water quality and lake ecosystem health is essential for overall understanding (Rapport et al., 1998). This thesis (see Part II, Chapter 3) contributes to an enhanced understanding of the water quality relationships and the advancement of the modelling framework.

Many studies have investigated water quality relationships with linear approaches so far (Bachmann et al., 2012; Magumba et al., 2013), whereas non-linear methods are underrepresented (e.g. Hollister et al., 2016; Lu et al., 2016). This thesis (Part II, Chapter 3) supports the use of non-linear approaches based on a performance comparison of selected methods from different modelling categories using the same data set. Non-linear models have the ability to uncover complex relationships that significantly differ from linear associations. Especially, methods from the field of machine learning are able to account for predictor variable interactions. The presented results uncovered the potential of Boosted Regression Trees (BRT) for modelling water quality (Elith et al., 2008), indicating the necessity of using models that are able to accommodate interactions among predictors in multi-dimensional water quality settings (Friedman and Popescu, 2008).

Given the abilities of machine learning techniques, water quality relationships of early studies using non-linear statistical methods could be supported. For example, McCauley et al. (1989) found sigmoidal relationships between water quality, measured in terms of chlorophyll *a*, and the nutrients phosphorus and nitrogen, respectively; whereas greater responses were observed for phosphorus in European lakes (cf. Abell et al., 2012). However, the characteristics of BRTs enabled the investigation of interaction effects, which is needed for understanding the complex settings of lakes (e.g. Filstrup and Downing, 2017; Kraemer et al., 2017). Thus, a decrease in water quality was slightly aggravated when nitrogen levels in lakes increased with already high phosphorus concentrations (Filstrup and Downing, 2017). The identification of such variable interactions is important especially with regard to the implementation of conservation actions. Studies have to focus on providing detailed information about water quality relationships to achieve the goal of preventing further degradation of water quality. Since the considered lake systems are influenced by many intertwining factors, the methods aiming at disentangling the relationship network have to be adjusted to the given complexity. As such, the comparison of methods and analysis of relationships conducted in this thesis provide a foundation

for further research studies aiming at deriving useful implications for water quality management.

Another factor on which the derivation of useful implications relies is data availability and quality. Growing availability of remote sensing observations (e.g. MacCallum and Merchant, 2011; Riffler et al., 2015) allows for the complementation of disparately measured *in situ* data and the extension of the data set used for model calibration. In this thesis, a first step of combining *in situ* and remote sensing data on lake surface water temperature (LSWT) was successfully accomplished, leading to well performing models and useful inferences. The data set extension led to the inclusion of additional water quality observations, where *in situ* LSWT was missing, and can be seen as possibility for reducing the uncertainty through data set extensions in deriving implications for lake management. However, no major influence was identified for LSWT in this study.

Scale dependence of species' distribution drivers and model performance (Objective 2)

For modelling species habitat and distributions, niche-based species distribution models (SDMs) are commonly used. The statistical approaches in combination with available data sets thus constitute the basis for deducing conservation plans at various scales. Scale effects on the performance and driver identification of freshwater species distributions, however, were not studied across multiple catchment scales before. Previous studies have only covered, for example, the increases of grid cells for bird, plant, vertebrate or virtual species (e.g Guisan et al., 2007; Lauzeral et al., 2013) rather than multiple catchment scales for fishes (see Part II, Chapter 4). Catchments typically serve as units for freshwater management and conservation (commonly referred to as the Catchment Based Approach – CaBA, see DEFRA, 2013). Analyzing species distribution at catchment scales thus facilitates the synchronization of research results and conservation implementations. For conservation planning, it is additionally of fundamental importance to understand what environmental factors at what spatial scales (grain size) are suitable predictors of what freshwater species' distribution and how various scales influence the predictive power of the models, especially for SDMs lacking fine grain data. This thesis (Part II, Chapter 4) closes the gap of missing cross-scale analyses of freshwater species distributions and outlines useful implications for freshwater rehabilitation.

Being in line with previous results on model performance across spatial scales, this thesis identifies a negligible effect of the considered scales on the mean performance of freshwater fish distribution models (e.g. Guisan et al., 2007). The selected statistical model, generalized additive models (GAM), led to highly accurate predictions across all studied catchment scales. The analysis of multiple scales additionally enabled the observation of increasing variance of the performance values and thus increasing uncertainty during validation with coarsening grain size.

Concerning the importance and selection of environmental factors in explaining fresh-water fish distributions across multiple scales, this thesis outlines that the importance assigned to single determinants of fish distributions and their selection are both catchment scale dependent and species dependent. Varying importance of factors driving species distributions across different spatial scales were also found in previous studies (Jackson et al., 2001; Blackburn and Gaston, 2002; Tudesque et al., 2014). Furthermore, the computed importance of

climatic variables such as temperature was high for all scales and all fish species studied. This contrasts with the suggestion that climatic variables may be only good predictors at the macro-scale (e.g. Pearson and Dawson, 2003). This thesis, therefore, underpins the importance of including climatic variables for explaining species distributions regardless of the spatial scales, which is particularly urgent in face of the ongoing climate change. Variables accounting for non-climatic effects such as anthropogenic influences should be adjusted to the specific species under investigation (e.g. Kottelat and Freyhof, 2007). Future assessments of climate change effects on freshwater fish distributions, especially for regions with limited access to data, can rely on the implications of the results in this thesis, since fine grain data is not necessary for obtaining well performing SDMs. However, variables should be selected according to the considered scale.

Thermal response curves of freshwater species (Objective 3)

With climate being an essential factor influencing freshwater species distributions, responses of species to one of the most important abiotic drivers, temperature, can uncover the impacts of progressing global warming (Chen et al., 2011; Domisch et al., 2013a; Markovic et al., 2017). Studying the distribution of species along the thermal gradient can give additional insights on how species will react to further warming and which populations will be affected in the near future (Deutsch et al., 2008; Slatyer et al., 2013). This thesis (Part II, Chapter 5) overcomes the restrictions of previous studies, i.e. the consideration of only single taxonomic groups and specific spatial scales (Hickling et al., 2005; Buisson et al., 2010; D'Amen et al., 2011), by studying thermal response curves, thermal properties and macroecological patterns for various taxonomic groups (577 European species of crayfish, fish, molluscs, odonates and plants) and temperature variables using global species distribution ranges.

The well-accepted assumption of a unimodal Gaussian thermal response curve was confirmed in this thesis (Gauch & Whittaker, 1972). Unimodal responses among all species of the considered taxonomic groups modelled with the non-linear method GAM (generalized additive models) occurred most frequently for all analyzed temperature variables (annual mean air temperature, maximum air temperature of the warmest month, annual mean water temperature, maximum water temperature of the warmest month). Although previous studies have used only restricted species distribution data, thermal response curve shapes of individual species coincided with response curves derived from restricted range data (e.g. Isaak et al., 2017; Lassalle et al., 2017). However, existing differences can be ascribed to differences in the considered distribution ranges (Logez et al., 2012).

Macroecological patterns of thermal properties in Europe revealed increasing warming tolerance with increasing latitude, thus species in central to northern Europe have a greater capacity to cope with warming than species in southern Europe. The observation that southern species are more susceptible to climate warming than conspecifics in northern regions was also identified in previous studies (e.g. Deutsch et al., 2008; Comte et al., 2017). Based on the global distribution data, the statistically determined preferred temperature, i.e. the temperature for which the peak of the unimodal response is reached, is already exceeded for some species, implying potential decrease in the species' performance with further rising temperatures (Part II, Chapter 5). Projections of future climatic

conditions align with the trends found for the latitudinal patterns of the warming tolerance. The Mediterranean areas, e.g. coastal areas of Spain, Italy and Greece, in southern Europe will be mostly affected by rising temperatures. The uncovered changes in the Mediteranean freshwaters and marine realm (see Lejeusne et al., 2010) show the need for appropriate actions in order to protect the species and enable species movement to more suitable habitats. As such, this thesis provides suggestions for catchment-based freshwater conservation actions.

European vs. global analyses of thermal response curves (Objective 4)

Studying thermal response curves of freshwater species native to Europe in Part II, Chapter 5 outlined several studies focussing on deriving thermal responses based on a restricted distribution data set (e.g. Lassalle et al., 2008; Logez et al., 2012). Those derived response curves are subsequently used to predict future species distributions and assess climate change impacts. Using only a portion of the whole species' distribution can lead to greatly varying responses and thermal properties (Thuiller et al., 2004; Filipe et al., 2013). Thus, this thesis (Part II, Chapter 6) quantifies and clarifies the existing differences in thermal responses derived with GAM and thermal properties deduced from global and European range data for selected freshwater fish species.

Using only distribution data of the native range of the considered fish species led to shifts in the thermal response curves and shape variations. Thermal properties showed major differences for the analyzed species. For example, the globally deduced maximum temperature of occurrence exceeded the European for almost all studied species. These analyses of climate change impacts with European data or in general restricted range data can lead to more either pessimistic or optimistic predictions and can consequently misdirect conservation management decisions (Thuiller et al., 2004). Therefore, studies focussing on climate change impacts using statistical approaches and distribution data should focus on global range data for more reliable assessments.

Thermal performance of freshwater species (Objective 5)

Upcoming increases of extreme thermal events and rising mean temperatures (Field et al., 2014; Scranton and Amarasekare, 2017) will have consequences on species' abilities to function (e.g. Angiletta, 2009; Childress and Letcher, 2017). Ectothermic freshwater species, whose body temperature relies on surrounding temperature conditions (e.g. fish), will be strongly influenced by changes in water temperatures. Thus, the inclusion of species' functional traits becomes more important for reliable climate change assessments (Jonsson and Jonsson, 2009; Floury et al., 2017; MacLean and Beissinger, 2017). Additionally, the combination of species distribution models (SDMs) and measures of functional traits enables a more realistic estimation of future species distributions and consequently climate change impacts. With thermal tolerance of species depending on the current life stage, considerations of trait properties for different life stages are also necessary in regard of comprehensive analyses of climate change effects. However, only few studies have combined SDMs and functional traits (e.g. Wittmann et al., 2016). Combinations of these used for assessments of climate change effects for various life stages are completely missing. This thesis (Part II, Chapter 7) provides a first approach for using SDMs and functional traits parametrized by

thermal performance curves (TPCs) for three life stages (adults, juveniles, eggs) of two fish species (*Salmo trutta*, *Salmo salar*) under three dispersal scenarios ("no dispersal", "free dispersal", "restricted dispersal") to assess climate change impacts.

Using experimentally observed data on life-stage specific thermal limits and optima (see Table S3 and S4 in Appendix 5) for deriving thermal performance curves (TPCs, range: [0, 1]) (Deutsch et al., 2008) and global distribution data as well as environmental data for calibrating SDMs, this thesis compares thermal performances for current and future (2050s) distribution ranges at different timeframes (monthly, seasonal, yearly). For predictions of future distribution ranges, six modelling approaches (Artificial Neural Networks, Random Forest, Gradient Boosting Machines, Multivariate Adaptive Regression Splines, Generalized Additive Models, Maximum Entropy Method) were combined into one consensus model to reduce uncertainty of using only single models (Marmion et al., 2009). Furthermore, three different future scenarios were studied, with "no dispersal" corresponding to current distribution ranges, "free dispersal" accounting for movement from current positions to suitable habitats in the 2050s, and "restricted dispersal" additionally considering artificial barriers, i.e. dams, restricting species movement through the hydrological network.

Future changes in temperatures will have different impacts on each life stage for different time periods. Statements of previous studies such as a delay of spawning could be supported by the monthly analyses of egg performances for both studied species, where a corresponding shift of the peak performances was identified for the 2050s compared to current performances (e.g. Jonsson and Jonsson, 2009). Performance analyses at seasonal timeframes showed increases for all seasons except for summer for *Salmo trutta* adults and juveniles. Future scenarios showed that impacts of temperature changes will be most severe in summer and that dispersal, allowing the escape from rising temperatures and the movement to habitats where higher performances could be possible, will be of high importance. Dispersal played also an important role in mean performances of *Salmo trutta* eggs because performances in suitable habitats of the 2050s under the "free" and "restricted dispersal" scenario were higher than under the "no dispersal" scenario. For *Salmo salar*, such observations were restricted due to lower occurrence numbers. However, performances of *Salmo salar* increased for every season. For both species, the "restricted dispersal" scenario, which included dams as dispersal barriers, prevented movement to areas with high thermal performances, underlining the negative effects of disrupting habitat connectivity (Markovic et al., 2017). Especially, movement to northern regions becomes important. SDMs in accordance with latitudinal annual mean thermal performance patterns of all life stages implied a decline in future suitable habitat accompanied by poleward range shifts. Thus, this study confirms the results of previous studies, where the decline in future suitable habitats for *Salmo trutta* and the northward movements of *Salmo salar* were projected (Jonsson and Jonsson, 2009; Wenger et al., 2011). In order to test the ability of SDMs to incorporate species' functional traits, a correlation analysis between the model output and thermal performance values was conducted. However, no strong relationships were identified for both species and all life stages, joining the results found by Wittmann et al. (2016) for growth rates of Grass Carp (*Ctenopharyngodon idella*) and implying the need of further studies on this topic under consideration of further traits.

This thesis suggests that conservation planning should consider time periods where thermal performances or species traits in general are likely to be severely impacted by changing climate. In addition, in these time periods movement to areas where high performances could be possible must be ensured.

Statistical models

In this thesis, various statistical methods from linear, non-linear to machine learning approaches were applied to gain information about relationships between the independent and dependent variables, and to infer future predictions. All models were evaluated with specific methods to ensure a profound basis for further analyses and to quantify uncertainties of the performance estimates. Consequently, given the variety of alternative options, modelling approaches were used, which ensured a high predictive performance. Parameter tunings were also conducted in order to find the best possible model for the underlying investigation. Overall, the used models showed satisfying results, with certain approaches performing better than others for specific modelling settings.

The statistical models used in Chapter 3 comprised Panel Data Models (PDMs), Generalized Additive Models (GAMs) and Boosted Regression Trees (BRTs). These approaches were used to model water quality relationships based on continuous data. For BRTs, parameter tuning was conducted (Elith et al, 2008). Performance measures for the validation of the models were tailored to the specific data setting, i.e. the R^2 and root mean squared error (RMSE) were used for assessing the predictive ability of the models. Validation and uncertainty estimation of the performance measures were conducted via the commonly applied bootstrapping method, i.e. the data set was split 100 times into 80% calibration and 20% validation data with performance measures being only evaluated for the unseen validation data, which was not used for model calibration. As such, BRTs as a representative of machine learning approaches emerged as best performing approach followed by the non-linear method GAM and the linear PDM, suggesting further usage of methods from the field of machine learning for studying complex water quality relationships.

GAMs, however, were shown to have a good performance in modelling species distributions, where a mixture of continuous and categorical data can be used to explain the dependent binary variable representing presence and absence of a species at the sites within a given region (Markovic et al., 2012; Dormann et al., 2013). In regard of the study goals of Chapter 4, 5 and 6, GAMs were used for the investigations. Performance results in these studies displayed GAMs as reliable method for explaining species distributions, being in accordance with the previously mentioned studies. Performance measures were adapted to the used data type. Thus, the area under the receiver operating characteristic (ROC) curve (AUC), sensitivity, specificity and true skill statistic (TSS) were utilized as performance measures (Hosmer and Lemeshow, 2000; Allouche et al., 2006). Validation was conducted via bootstrapping.

In addition, Chapter 7 (Part II) also highlighted GAMs as well performing model for explaining species distributions that can keep pace with latest versions of machine learning techniques such as Artificial Neural Networks (ANNs), Random Forest (RF), Gradient Boosting Machines (GBMs) and Maximum Entropy Method (MAXENT). Furthermore, Multivariate Adaptive

Regression Splines (MARS) were also among the top performing methods for modelling species distributions for the data setting in Chapter 7. Solely Elastic Net (ELNET) showed rather medium performances during the validation phase via bootstrapping. Prior to validation, a parameter tuning for ANNs, RF, GBMs, MARS and ELNET (Bergstra and Bengio, 2012; Zhang and Goh, 2016; El-Gabbas and Dormann, 2017; Milborrow, 2018) was conducted.

In summary, models belonging to the category of non-linear, non-parametric methods or machine learning tended to perform better than approaches like linear PDMs or ELNET, which is a generalized linear method with additional penalty terms representing L1- and L2-regularization (Friedman et al., 2010). Due to the growing complexity of data settings and relationships among the used variables, this thesis outlines the trend in studying freshwater ecoysystems towards using rather more flexible and machine learning approaches than linear models or generalized linear models.

Data limitations

For investigating the objectives within this thesis, comprehensive data sets were aggregated, partially extended and merged for each study. The included data sets were based on the latest known observations and selected according to the underlying objectives. All data sets were subject to quality checks before the application of statistical models. However, prevailing data uncertainties cannot be ruled out.

Although the data set in Chapter 3 was extended with remote sensing data of lake surface water temperature (LSWT) (e.g. Riffler et al., 2015), which could enable the inclusion of further water quality observations, many *in situ* observations of variables known to influence water quality were erroneous, incomplete or missing. As a result, the size of the data set used for modelling was reduced. Often-times surrogates are selected to deal with missing data on certain variables. Thus, in Chapter 3 the utilization of such surrogates in terms of water temperature by using *in situ* as well as satellite retrieved LSWT and altitude was tested, i.e. modelling was based on two variable sets, one additionally using LSWT and the other altitude. However, in this study major model performance differences between these two variable sets were not found due to weak influences of both variables (see Part II, Chapter 3), but differences in regard of the influence directions on water quality were present, implying the careful selection of surrogates.

Regarding data limitations for species distribution models (Part II, Chapter 4-7), uncertainty lies in the data of species presence and absence at certain sites and respective environmental data used for modelling. For example, species data may not include every known presence of the distribution range at the considered scale. Thus, if areas where a species is present are not considered in the data, the model output will be affected. A similar problem arises for incorrectly identified presences. Uncertainties coming from environmental data can have different sources. Environmental data are typically based on model outputs, so-called global circulation models (GCMs) (see Chapter 4-7), which already comprise uncertainties. These uncertainties are passed on to the statistical models. A reduction of uncertainty is in general achieved by using multi-model predictions of different GCMs (e.g. Part II,

Chapter 7), similar to the case of consensus modelling (Marmion et al., 2009). In addition, certain analyses of freshwater species require the usage of water temperature as explanatory variable. However, global range data of water temperatures for freshwater ecosystems are not available yet, which again suggests the usage of a model transforming air to water temperature and thus producing new sources of uncertainty (Punzet et al., 2012). Other sources of uncertainty are the calculation of mean values for climatic variables over a certain time period, which may not be an adequate representation of a species habitat, and the differences in the grid sizes used for deriving this environmental information for the studied scale.

Moreover, data on species traits in Chapter 7 were limited due to the number of laboratory experiments carried out and different aspects of how the experiments were conducted (more details in Part II, Chapter 7).

In summary, beyond the limitations and uncertainties that arise in analyses based on collected data, useful implications could be derived in this thesis, which added new directions, information and insights to the existing knowledge.

Future perspectives

Freshwater ecosystem analyses will have to keep pace with the ongoing climatic changes to identify areas and species being at high risk of severe climate change impacts early enough so that the valuable services of freshwater ecosystems can be protected (Markovic et al., 2017). With climate change being complex and having different effects on different types of ecosystems, taxonomic groups and species (e.g., see Part II, Chapter 5) further analyses are urgently required to gain more information about the consequences.

Future analyses have to make use of the growing data availability and incorporate additional data sources in order to extend the data set used for the calibration of statistical inferential models (see Part II, Chapter 3). Satellite-retrieved or remote sensing data offer new possibilities for describing species habitats with additional variables and can lead to a better understanding of the relationship between a species and its environment (Leitão and Santos, 2019). Subsequently, statistical models have to be able to infer patterns from these large data sets and be adapted to the underlying investigation. Machine learning approaches are constantly evolving and offering new efficient ways for parameter tuning (e.g. Zeiler, 2012). Usage of state-of-the-art models will thus enable a faster calibration of complex modelling techniques such as artificial neural networks.

Besides the usage of further environmental data and enhanced statistical approaches, the inclusion of biological mechanisms and trait data in analyses of climate change impacts on species will be important for understanding the biotic implications of changing climates (see Part II, Chapter 7; Urban et al., 2016; Floury et al., 2017; MacLean and Beissinger, 2017). Increased uses of combinations of functional trait data on different life stages of various species and distribution models will be able to provide comprehensive assessments of global climatic changes.

Conclusion

This thesis broadened the understanding of ecological relationships in the context of freshwater ecosystems. In particular, factors influencing biodiversity such as water quality,

climate change or anthropogenic pollution were studied in different comprehensive ways. The variety of studies within this thesis is attributed to the versatile effects of these factors on freshwater ecosystems and the associated biodiversity. Accordingly, a variety of methodological frameworks was used to derive estimations of water quality drivers and climate change impacts on freshwater species. Although having differing research aims, all studies provide useful implications for conservation management and planning in order to preserve the benefits of freshwater ecosystems and its biodiversity.

APPENDIX

Appendix 1: Supporting information of Part II, Chapter 3

Chlorophyll *a* – nutrient and temperature relationships, and predictions for lakes across mountain regions

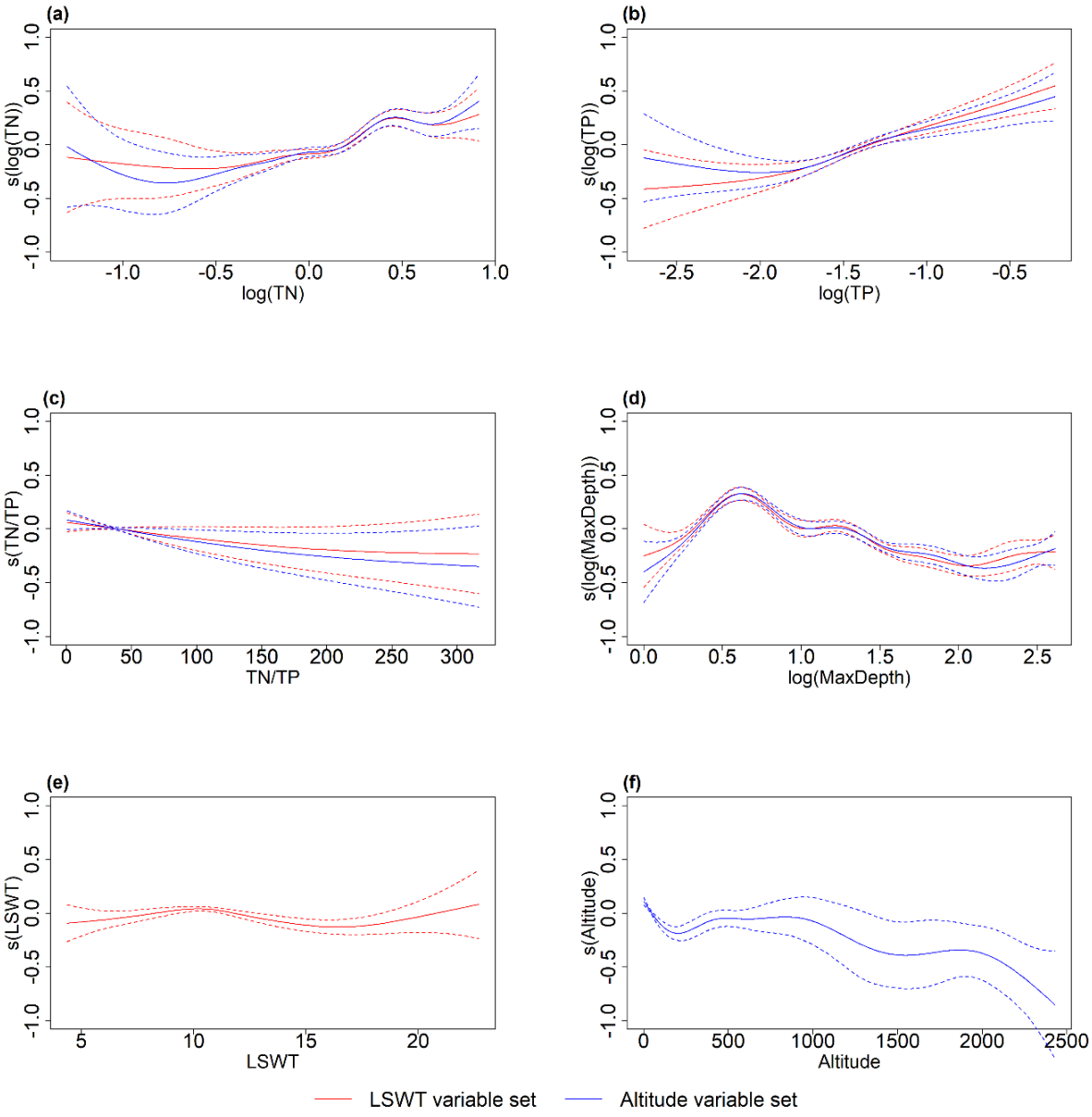

Fig. S1 Relationship between each exogenous variable and log(Chl-a) for GAMs and the respective two variable sets. The plots display the influence on log(Chl-a) as spline functions of (a) log(TN), (b) log(TP), (c) TN:TP, (d) log(MaxDepth), (d) LSWT (°C) and (e) altitude (m) while all remaining variables are fixed. The area around the influence curve depicted by dotted lines represents the uncertainty, i.e. the 95% confidence interval.

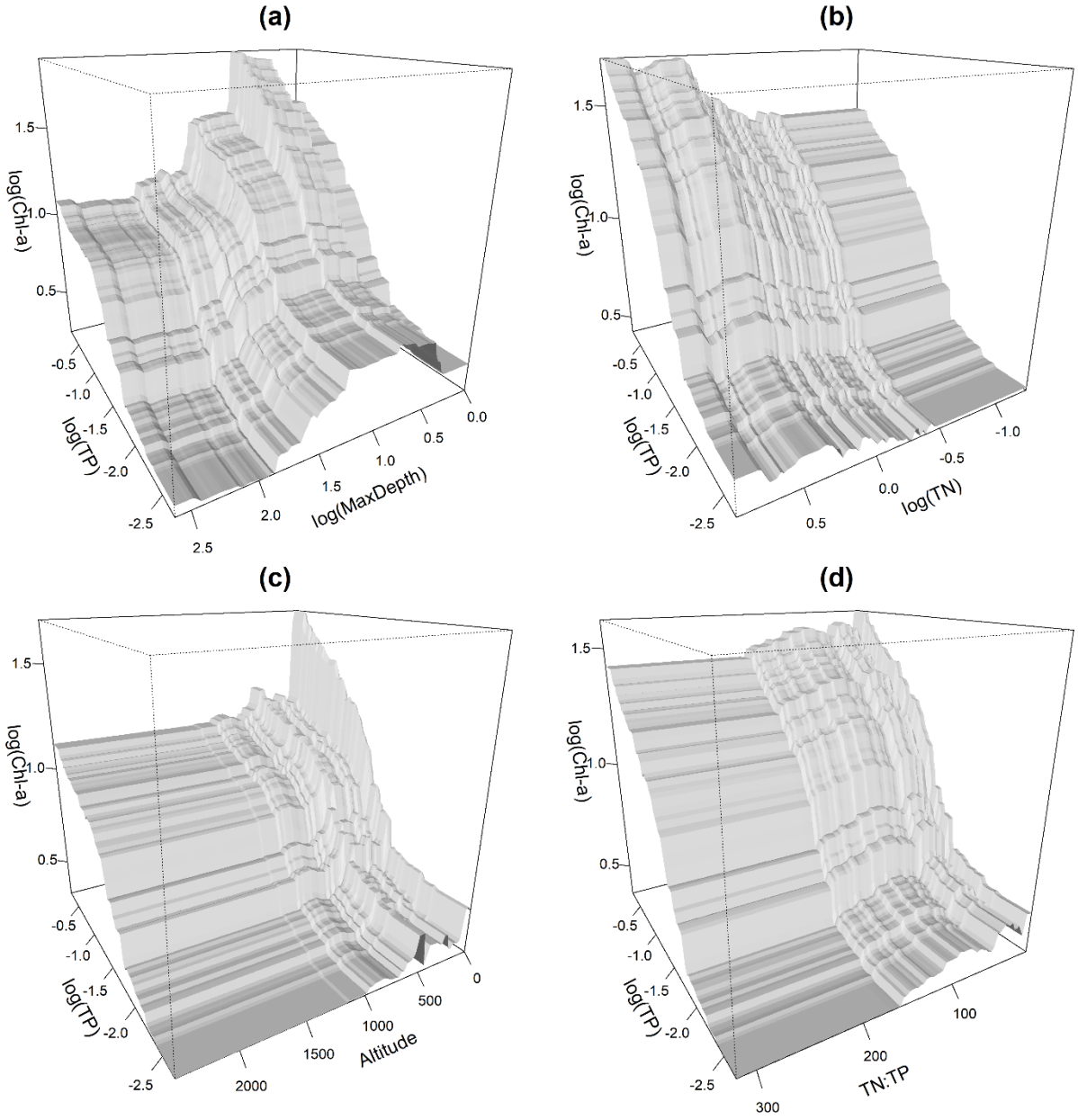

Fig. S2 Two-dimensional partial dependence plots for combinations of TP and each remaining exogenous variable for the BRT altitude model. log(Chl-a) is depicted as a function of (a) log(TP) and log(MaxDepth), (b) log(TP) and log(TN), (c) log(TP) and altitude (m), and (d) log(TP) and TN:TP, accounting for the averaged effects of the other variables.

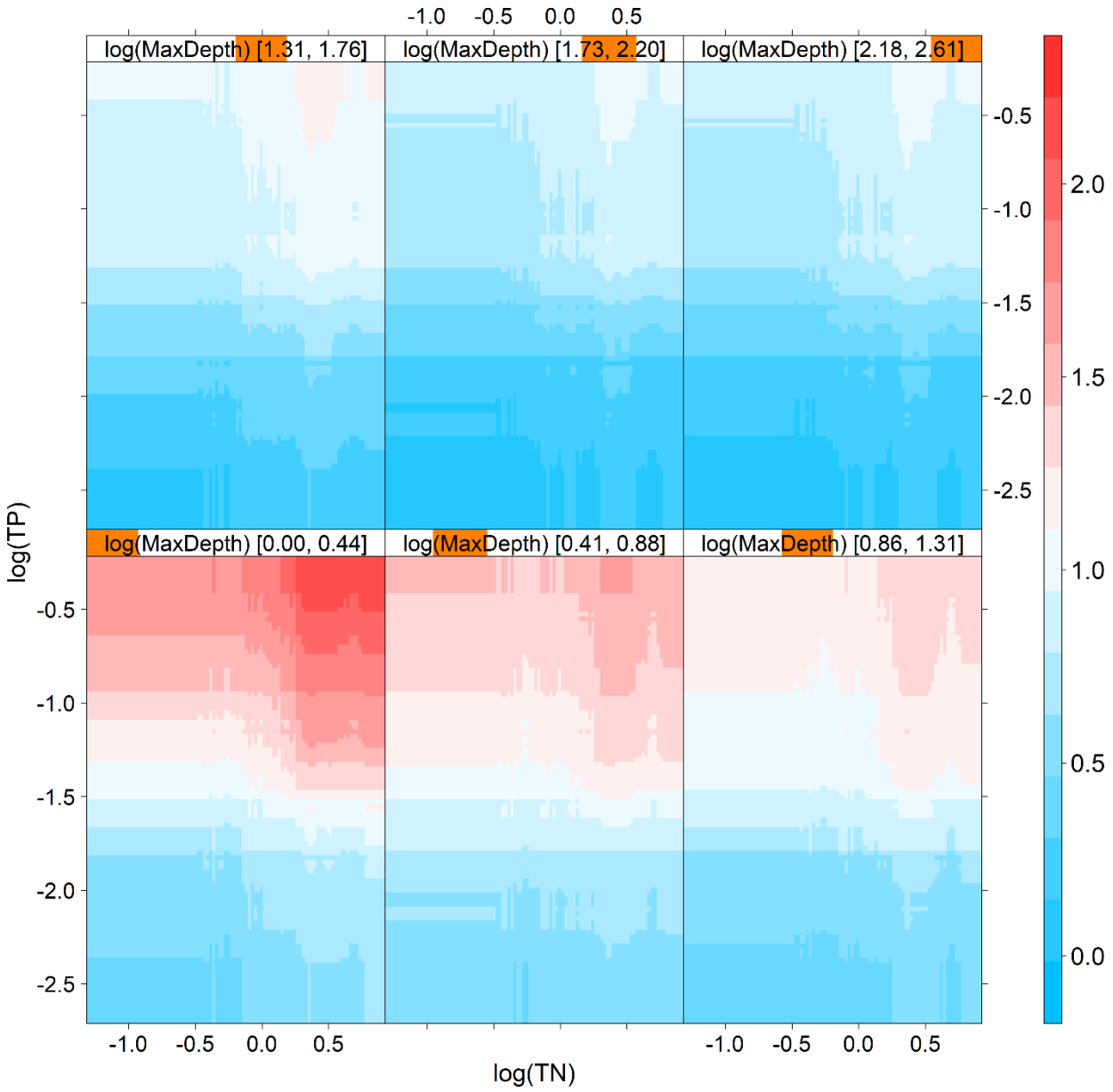

Fig. S3 Three-dimensional partial dependence plot of TP, TN and MaxDepth for the BRT LSWT model. log(Chl-a) is depicted as a function of log(TP), log(TN) and log(MaxDepth) accounting for the averaged effects of the remaining variables. The scale indicates the $\log_{10}$-transformed Chl-a concentration.

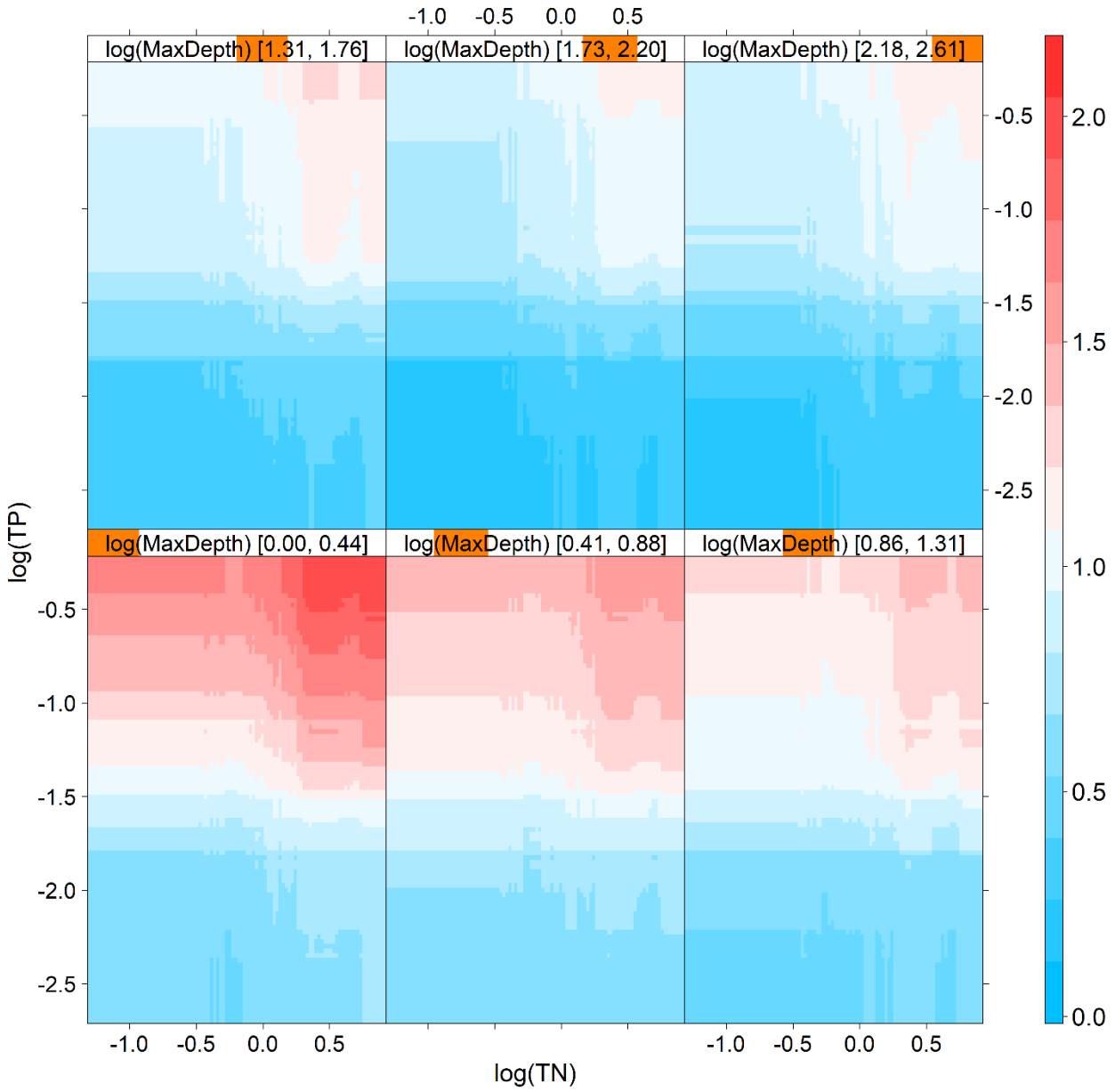

Fig. S4 Three-dimensional partial dependence plot of TP, TN and MaxDepth for the BRT altitude model. log(Chl-a) is depicted as a function of log(TP), log(TN) and log(MaxDepth) accounting for the averaged effects of the remaining variables. The scale indicates the $\log_{10}$-transformed Chl-a concentration.

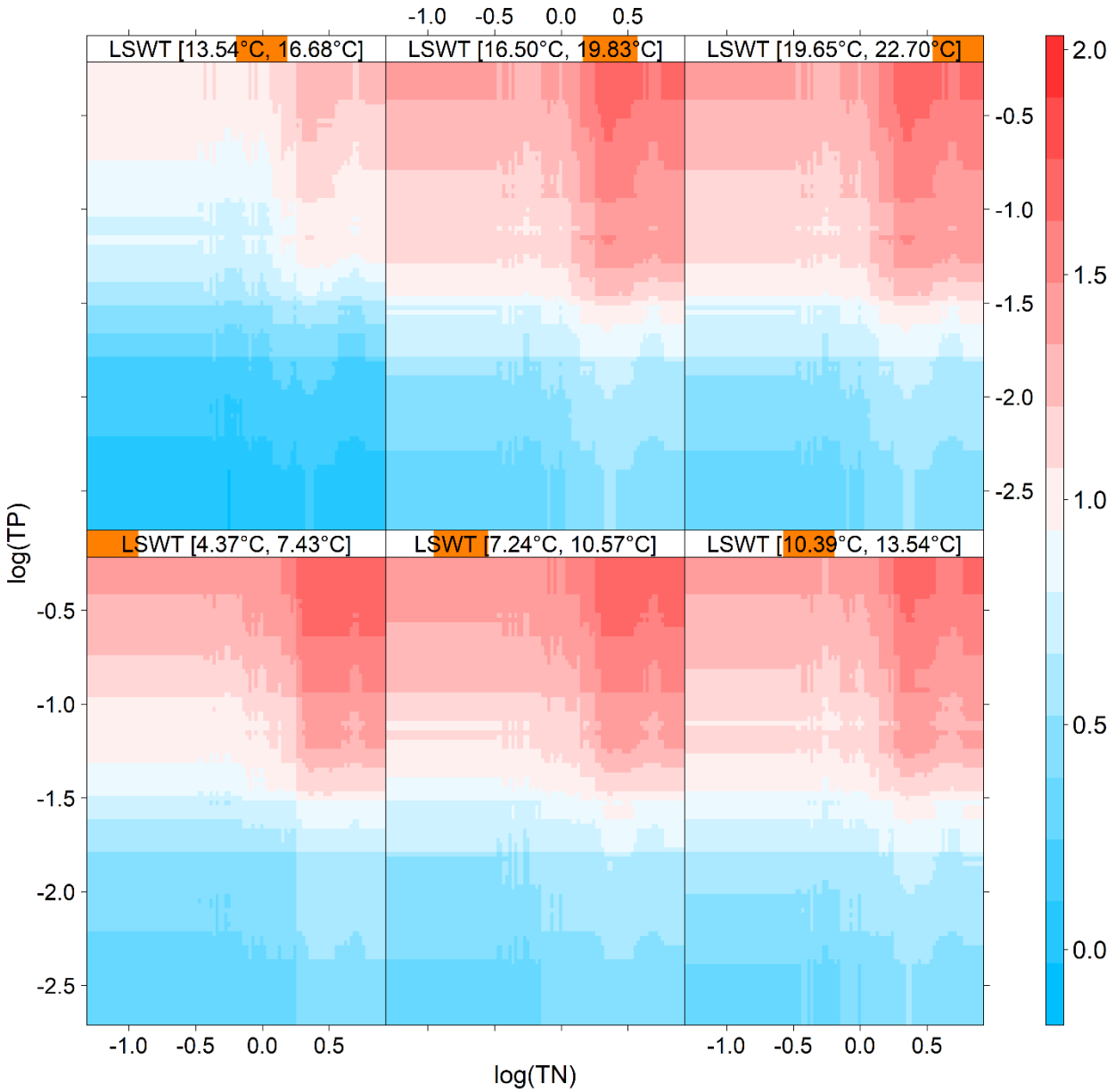

Fig. S5 Three-dimensional partial dependence plot of TP, TN and LSWT for the BRT LSWT model. log(Chl-a) is depicted as a function of log(TP), log(TN) and LSWT (°C) accounting for the averaged effects of the remaining variables. The scale indicates the $\log_{10}$-transformed Chl-a concentration.

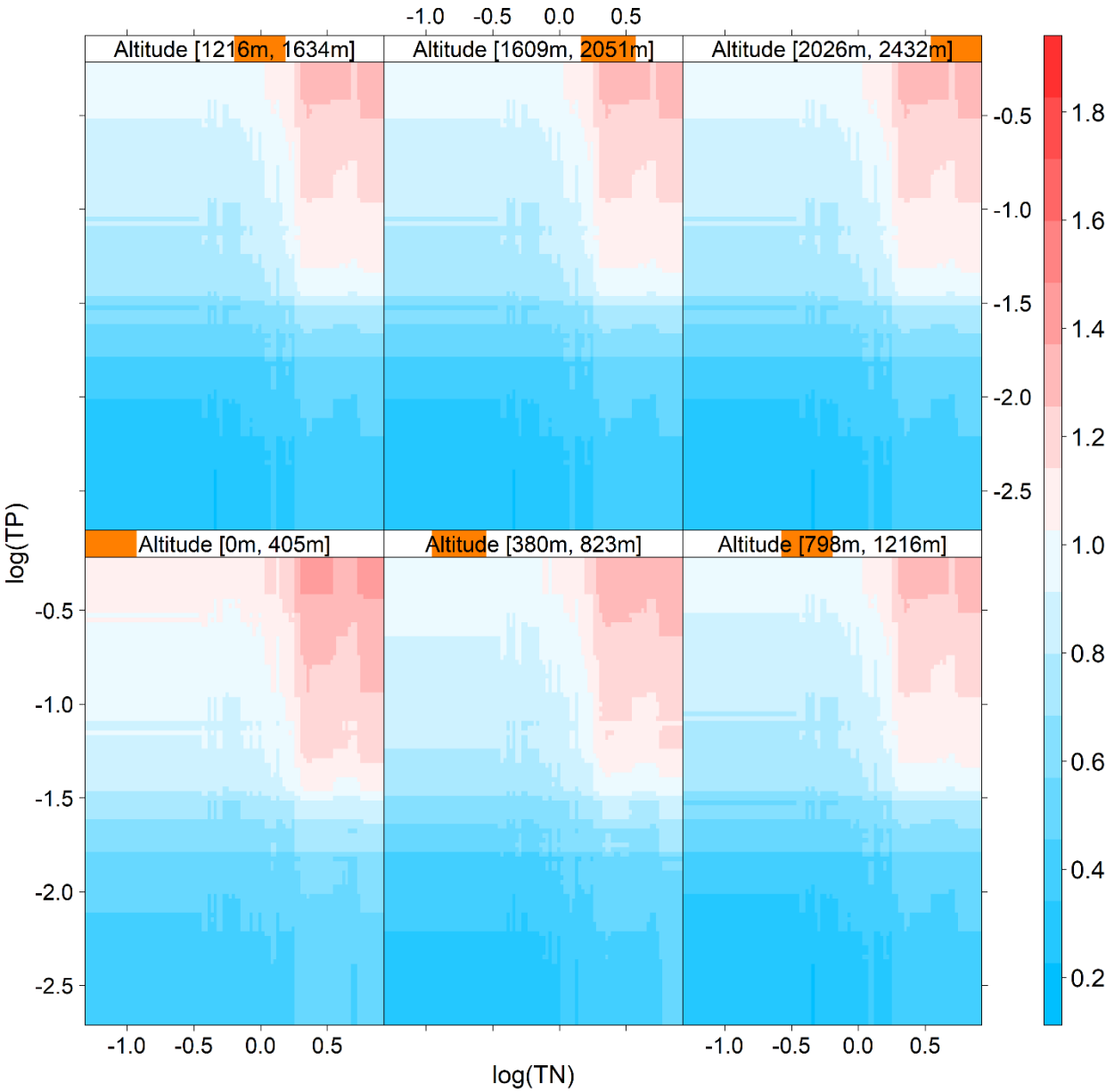

Fig. S6 Three-dimensional partial dependence plot of TP, TN and altitude for the BRT altitude model. log(Chl-a) is depicted as a function of log(TP), log(TN) and altitude (m) accounting for the averaged effects of the remaining variables. The scale indicates the $\log_{10}$-transformed Chl-a concentration.

Table S1 Morphometric characteristics of the studied perialpine and central Balkan mountain lakes.

Lake	Lon	Lat	Altitude (m)	Surface Area (km^2)	Mean depth (m)	MaxDepth (m)	Volume (10^9 m^3)
Ammer	11.13	47.98	533	46.6	38	81	1.75
Biel	7.17	47.08	429	39.3	31	74	1.18
Brienz	8.00	46.74	564	29.8	173	260	5.17
Chiem	12.47	47.89	518	79.9	26	73	2.05
Como	9.26	46.01	198	145.9	154	410	22.5
Garda	10.64	45.54	65	369.9	136	346	50.35
Iseo	10.07	45.74	186	61.8	124	251	8.1
Maggiore	8.57	45.90	194	213.0	177	372	37.5
Ohrid	20.73	41.04	693	358.0	164	288	58.64
Prespa	21.01	40.93	853	274.0	16	54	5.0
Starnberg	11.31	47.90	584	56.4	53	128	2.99
Thun	7.71	46.70	558	48.4	136	217	6.5
Zurich	8.73	47.2	406	67.7	52	143	3.9

Table S2 Adjusted R^2 of GAMs and PDMs with random/fixed individual effects and with pooled data. We note that for BRTs adjusted R^2 could not be computed.

Model	PDM			GAM
	Random individual effects	Fixed individual effects*	Pooled	
LSWT variable set	0.4323	-0.0139	0.7235	0.7823
Altitude variable set	0.4340	-0.0172	0.7280	0.7960

*Note that the usage of fixed individual effects does not incorporate influences of static variables across individuals.

Table S3 Computed coefficients of PDMs and the corresponding statistical significance. Note that for both models the pooled PDM was used. The significance (p-value) of the computed coefficients was determined with heteroscedasticity robust standard errors.

Variables	Model	
	LSWT variable set	**Altitude variable set**
constant	2.2169***	2.0625***
log(TN)	0.3932***	0.4018***
log(TP)	0.5740***	0.5355**
TN:TP	-0.0008	-0.0009
log(MaxDepth)	-0.2697***	-0.2446***
LSWT	-0.0094	-
Altitude	-	-0.0002***

*p<0.1; **p<0.05; ***p<0.01.

Table S4 Modelling parameters (tree complexity – *tc*, learning rate – *lr*, bag fraction – *bf*, number of trees – *nt*) of BRT models.

Model		BRT	
		LSWT variable set	Altitude variable set
modelling parameter	*tc*	4	4
	lr	0.011	0.004
	bf	0.72	0.64
	nt	1,850	3,300

The best combination of the parameters *tc*, *lr*, and *bf*, which generated an optimal tree number *nt* of over 1,000 trees, was determined via randomly dividing the data set 10 times into a calibration (80%) and a testing data set (20%) and by computing the mean squared error (MSE) for the testing data set each time. The smallest average MSE based on the testing data set was used to identify the optimal combination.

Table S5 Mean relative variable importance (normalized to 100%) resulting from the validation of BRT models.

Model		BRT	
		LSWT variable set	Altitude variable set
variable	log(TN)	9.7%	8.8%
	log(TP)	52.8%	51.0%
	TN:TP	4.4%	3.8%
	log(MaxDepth)	26.9%	21.8%
	LSWT	6.2%	-
	Altitude	-	14.6%

The validation was conducted by random sampling of the data, leading to a calibration (80%) and validation (20%) data set. After 100 repetitions, the average variable importance from the calibrations was computed.

Table S6 RMSE (in µg/l) resulting from the best performing approach, BRTs, for the selected perialpine and central Balkan mountain lakes and annual mean Chl-a levels.

Lake	RMSE (µg/l)	
	BRT LSWT	BRT Altitude
Ammer	2.08	2.19
Biel	2.12	2.33
Brienz	1.35	1.34
Chiem	2.43	2.22
Como	2.16	2.14
Garda	1.50	1.33
Iseo	2.74	1.23
Maggiore	1.39	1.64
Ohrid	1.18	0.80
Starnberg	0.57	0.71
Thun	0.59	0.58
Zurich	2.95	2.93
mean	1.76	1.62

To test transferability of the results to the lakes from mountain regions we excluded each of the considered lakes that occurred in the calibration data set and predicted the log-transformed Chl-a value for the excluded lake. Predictions were then transformed back, leading to RMSEs in µg/l. Note that the RMSE could only be calculated if more than one observation was available.

Appendix 2: Supporting information of Part II, Chapter 4

Scale effects on the performance of niche-based models of freshwater fish distributions

---

The full version of the Appendix is available at:
https://www.sciencedirect.com/science/article/pii/S0304380019301711?via%3Dihub#sec0075

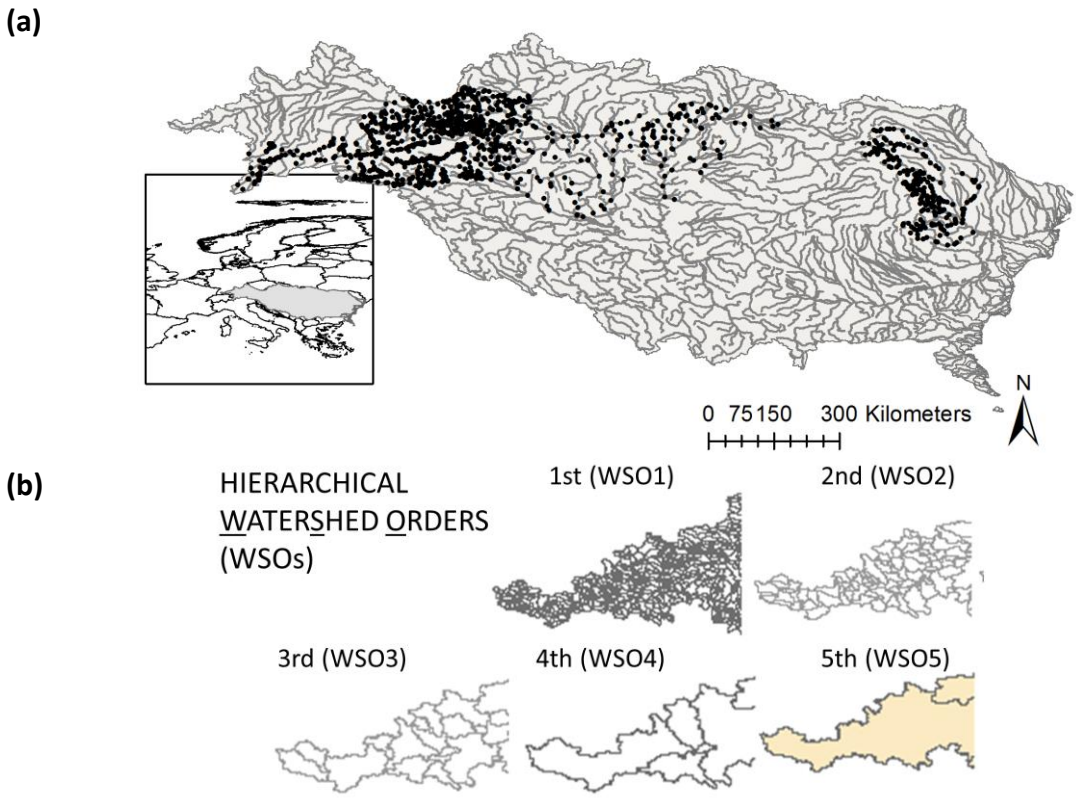

Fig. S1 (a) The study area, Danube Basin (the black circles indicate locations of the sample sites); (b) the different catchment scale resolutions, i.e., the hierarchical watershed orders WSO1 to WSO5 (following the nomenclature of the CCM2 pan-European catchments database; CCM version 2.1, de Jager & Vogt, 2010).

With grain-size coarsening, i.e., an increase in the studied watershed order, there is an increase in the average catchment size (i.e., the polygon size in Fig. S1b).

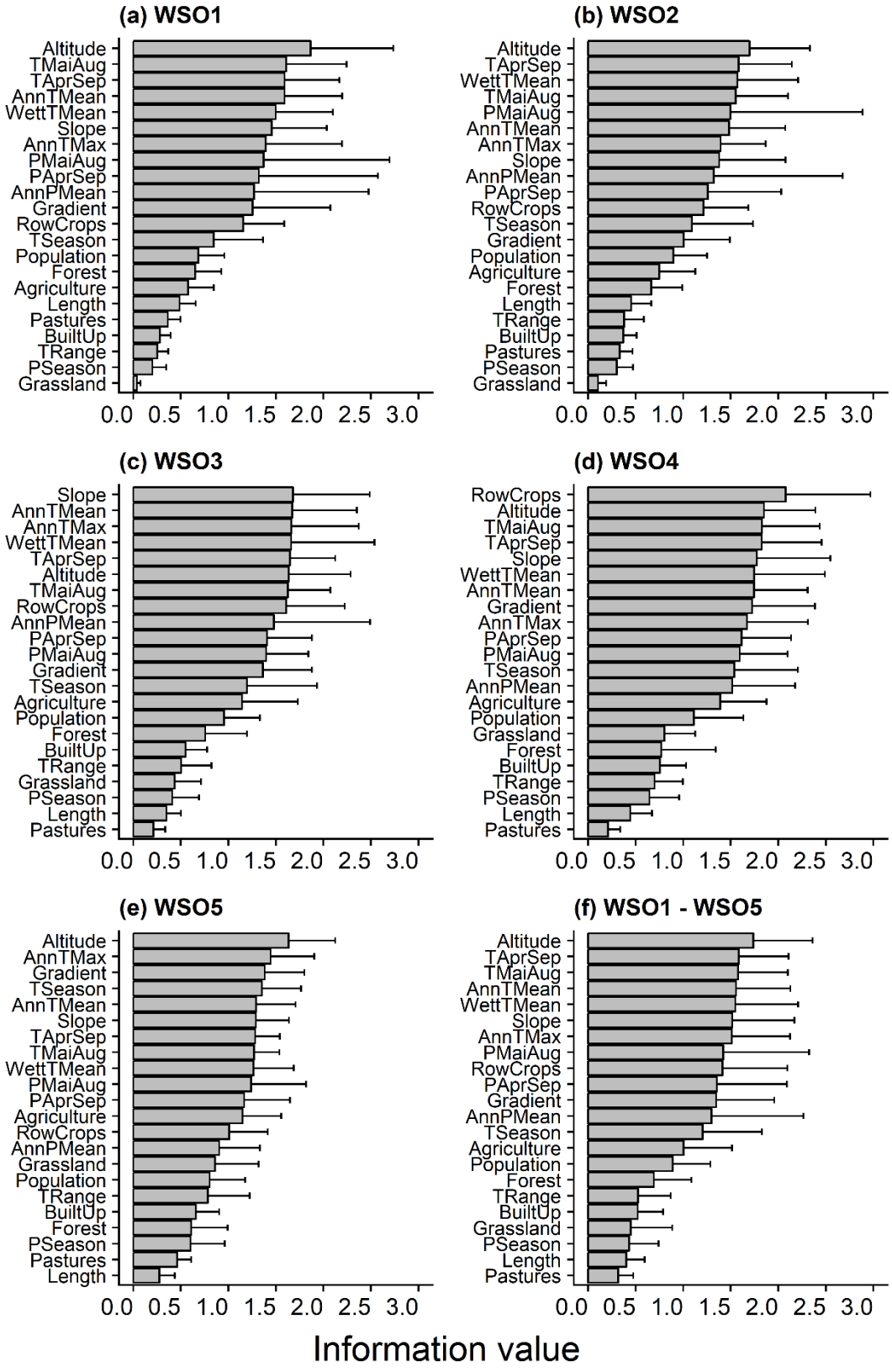

Fig. S2 Information value as a measure of the univariate strength of all environmental predictor variables derived across the corresponding catchment areas. For convenience, the environmental predictors are ordered according to their information value. (a)-(e) For each of the five spatial scales the information value was calculated as an average predictive strength of the environmental predictor across all studied species; (f) the overall information value of an environmental predictor was calculated as an average predictive strength across all scales and all considered species. Error bars represent one standard deviation of the estimates.

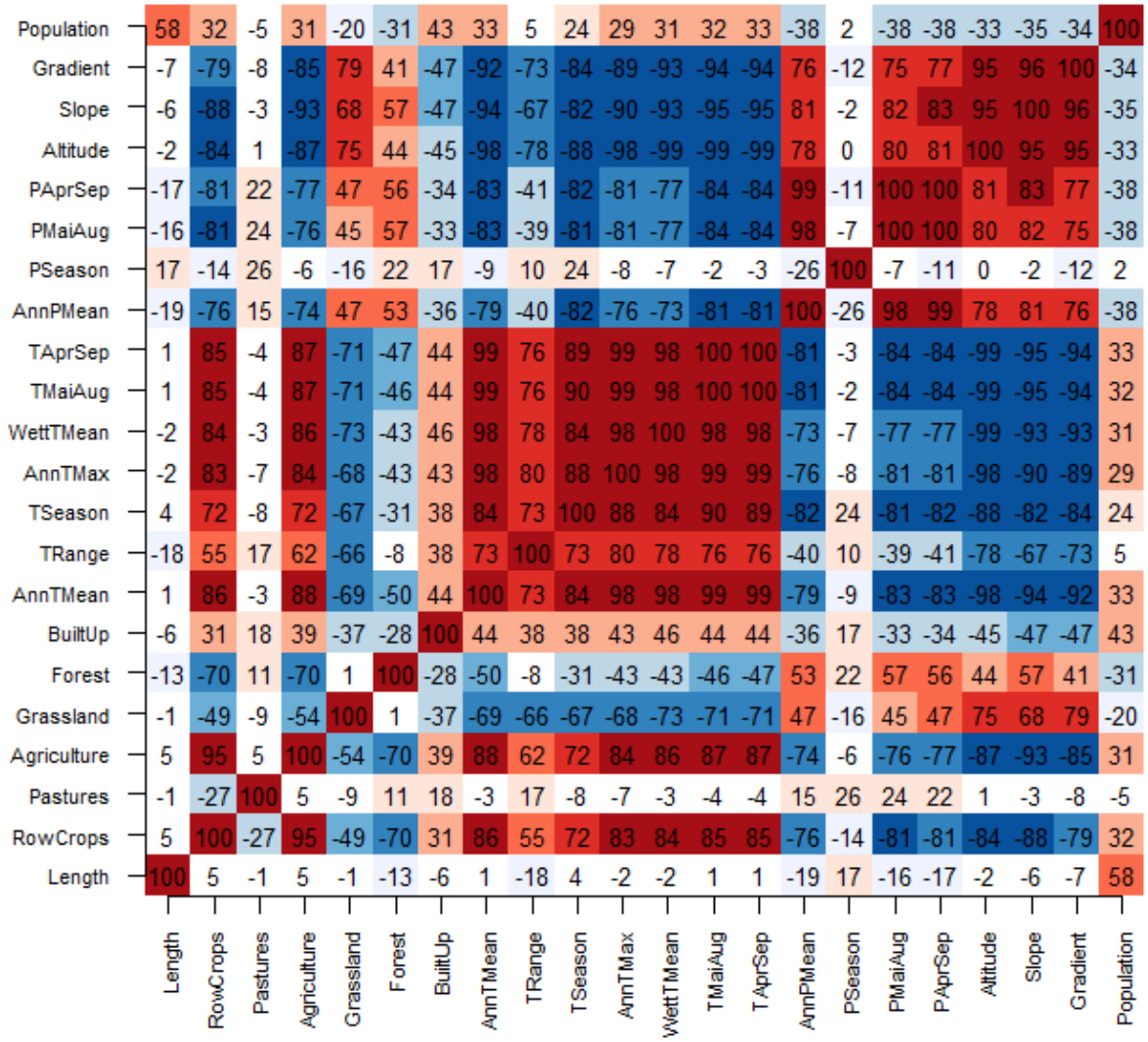

Fig. S3 Correlation matrix indicating the value of the Bravais-Pearson correlation coefficient between the pairs of the environmental predictor variables derived for the catchment order WSO5. For lower catchment orders, the correlations are described in the main text.

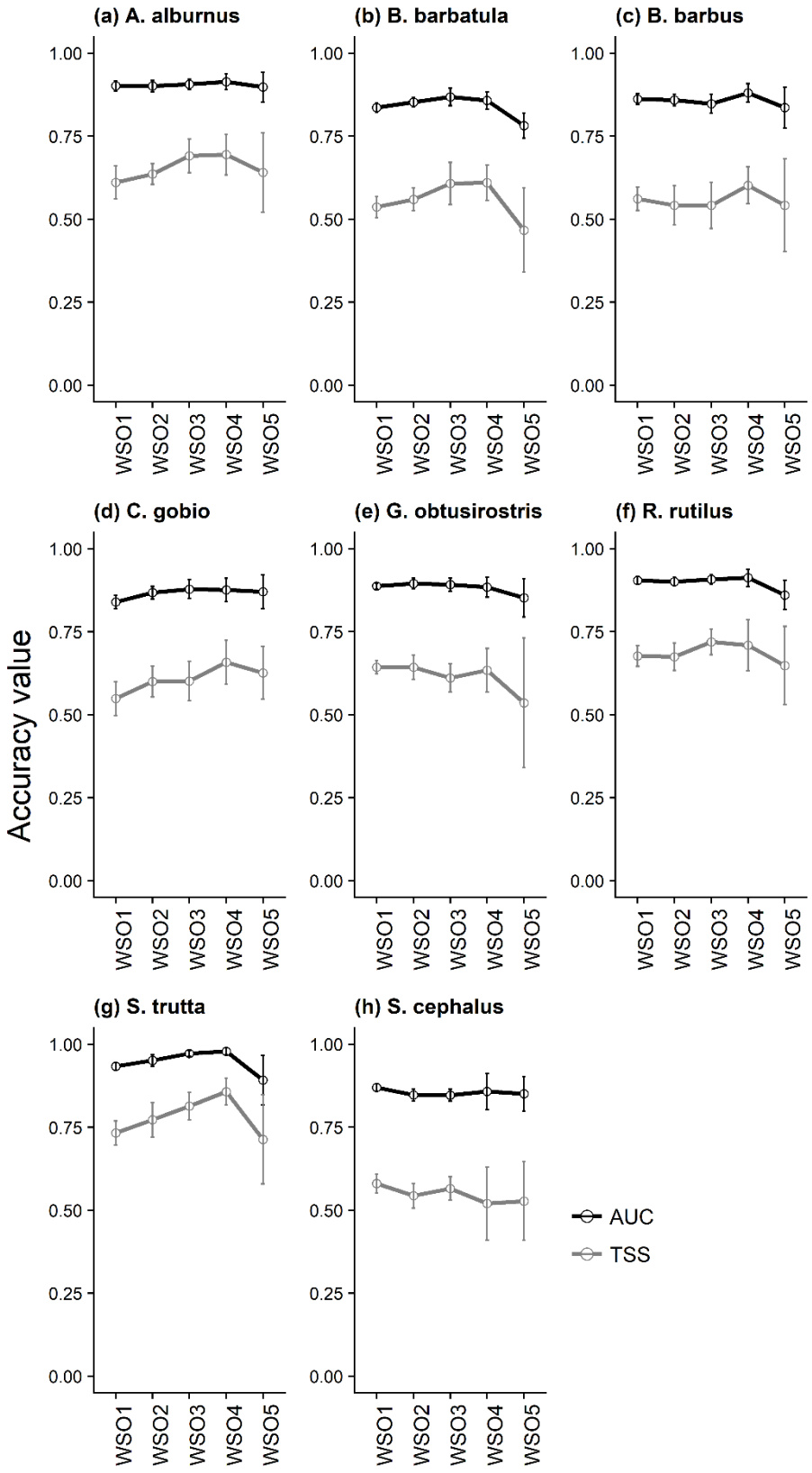

Fig. S4 Mean validation performance AUC and TSS values of the multivariate SDMs with keeping the predictor number constant across the five studied scales (WSO1 – WSO5). Performance was assessed by using repeated random splitting (10 times) of the fish data into calibration (70%) and validation (30%) and validation performance values were calculated for (a) *A. alburnus*, (b) *B. barbatula*, (c) *B. barbus*, (d) *C. gobio*, (e) *G. obtusirostris*, (f) *R. rutilus*, (g) *S. trutta* and (h) *S. cephalus*. Error bars represent one standard deviation of the estimates.

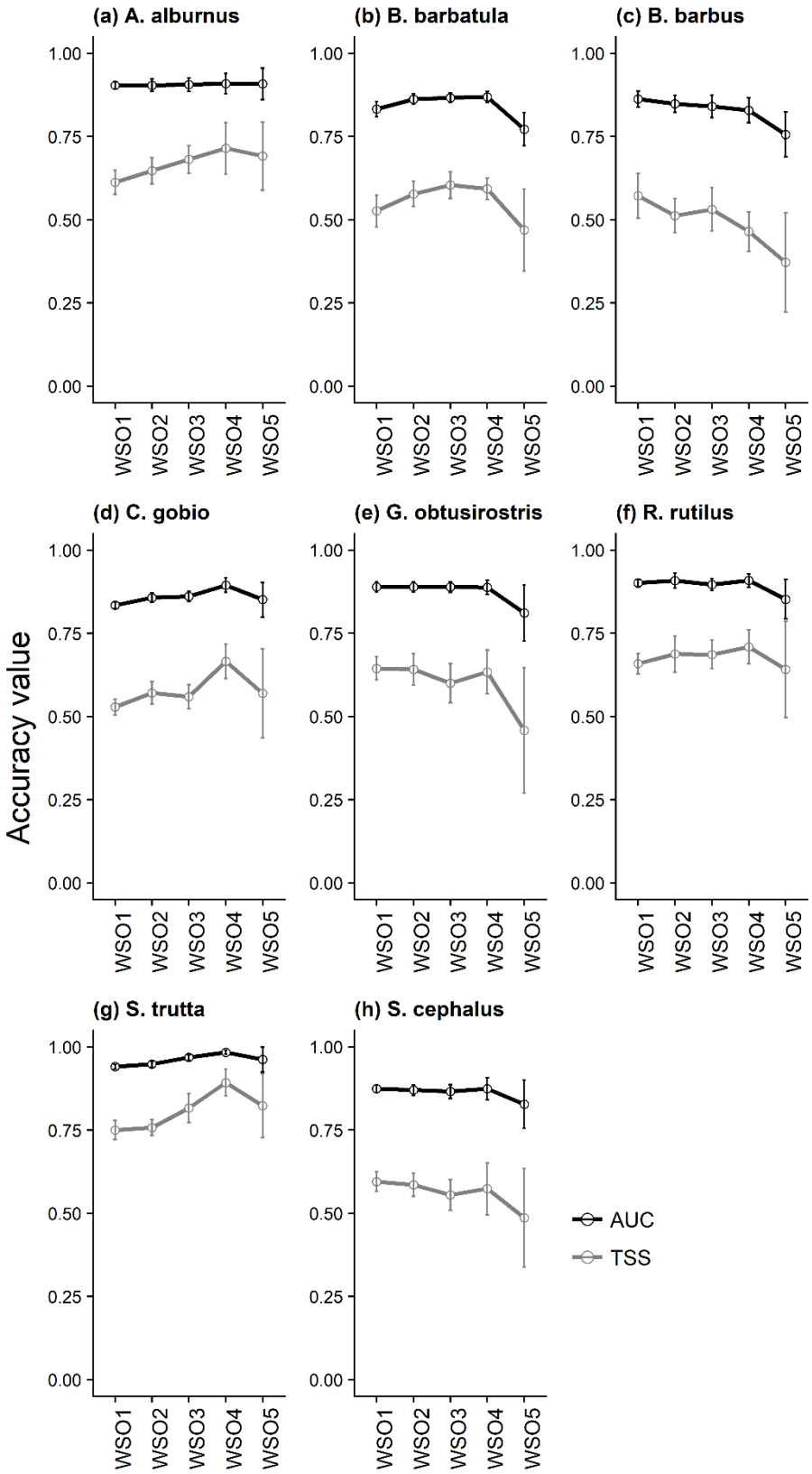

Fig. S5 Mean validation performance AUC and TSS values of the multivariate SDMs with simultaneous forward and backward predictor selection across the five studied scales (WSO1 – WSO5). Performance was assessed by using repeated random splitting (10 times) of the fish data into calibration (70%) and validation (30%) and validation performance values were calculated for (a) *A. alburnus*, (b) *B. barbatula*, (c) *B. barbus*, (d) *C. gobio*, (e) *G. obtusirostris*, (f) *R. rutilus*, (g) *S. trutta* and (h) *S. cephalus*. Error bars represent one standard deviation of the estimates.

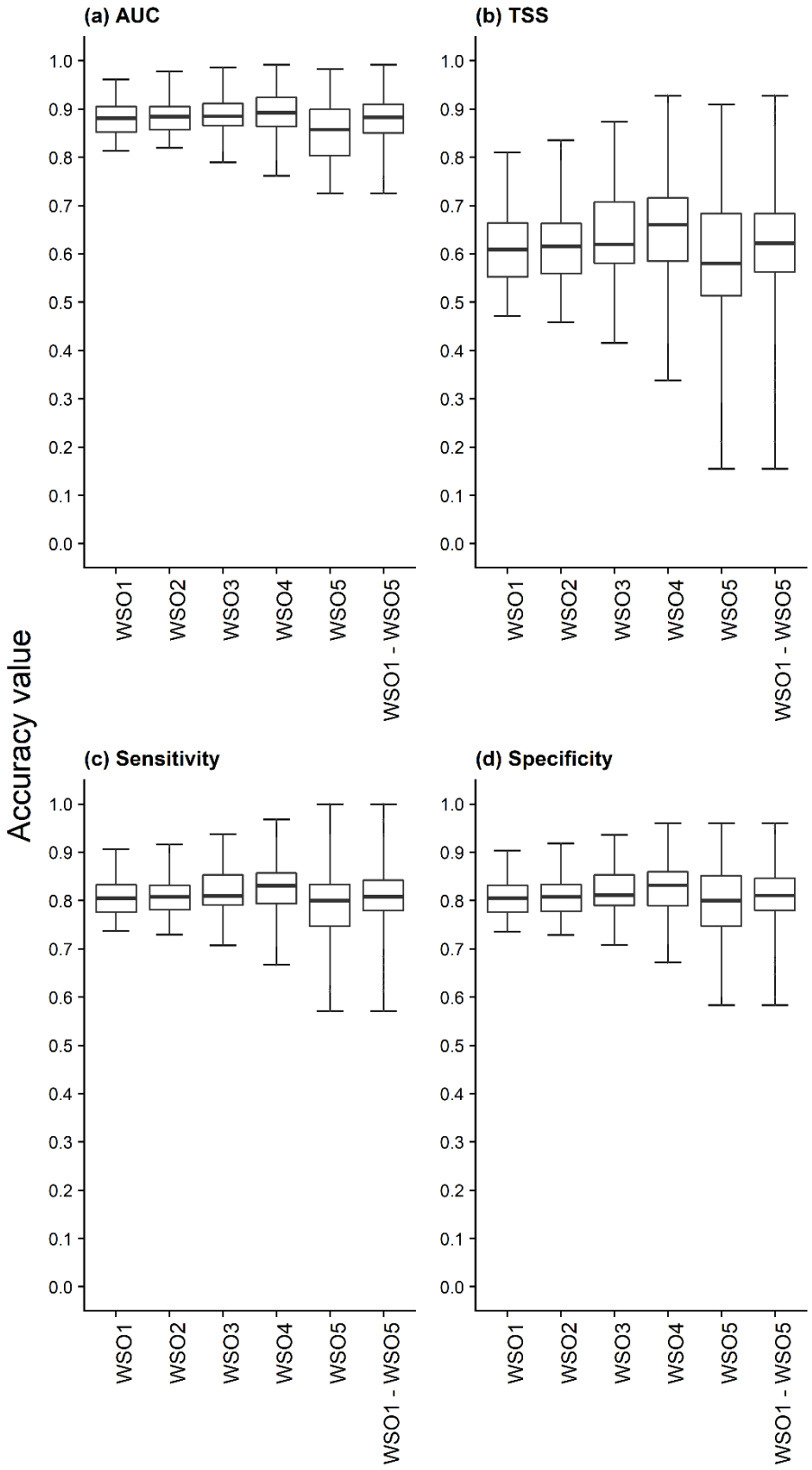

Fig. S6 Distribution of the mean validation performance measures of the multivariate SDMs with keeping the predictor number constant across the five studied scales (WSO1 – WSO5). Performance was assessed by using repeated random splitting (10 times) of the fish data into calibration (70%) and validation (30%) and calculating the (a) AUC, (b) TSS, (c) sensitivity and (d) specificity.

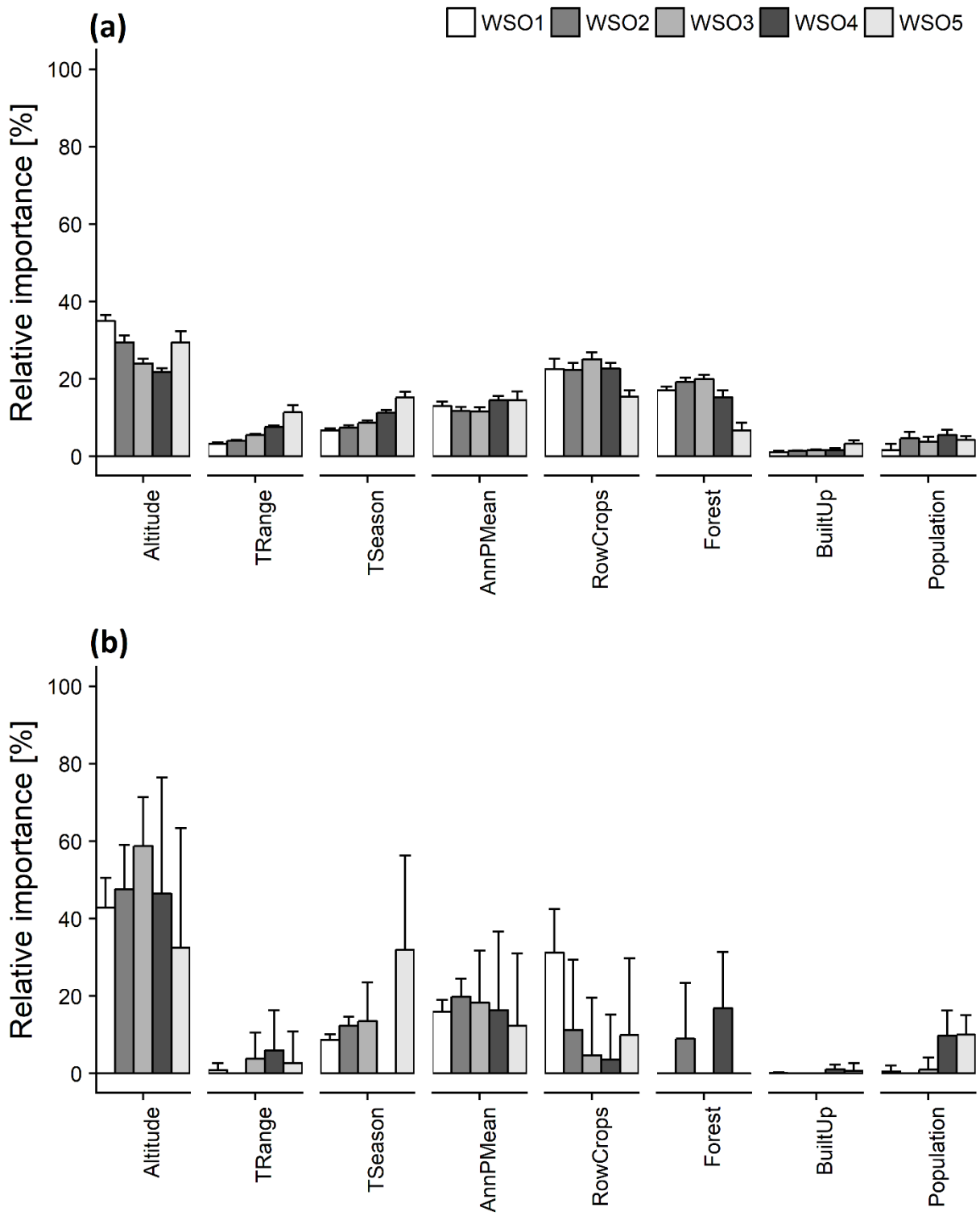

Fig. S7 The mean relative predictor importance of *A. alburnus* resulting from the SDMs across all studied scales (WSO1-WSO5) for two distinct model fitting approaches: (a) with keeping the predictor number constant across the scales, and (b) with simultaneous forward and backward predictor selection. Error bars represent one standard deviation of the estimates. We note that the figure represents the mean relative predictor importance based on all model runs per catchment order.

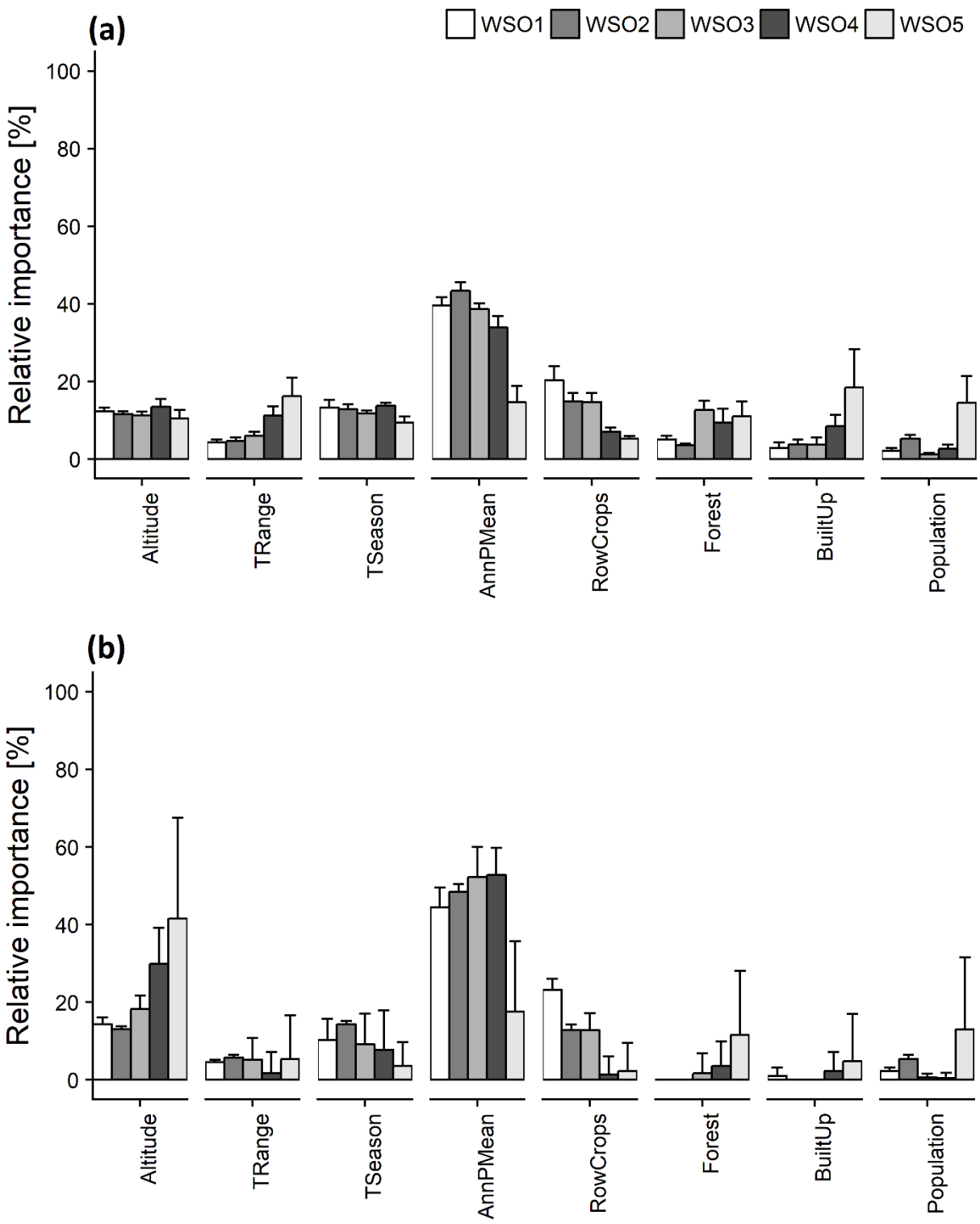

Fig. S8 The mean relative predictor importance of *B. barbatula* resulting from the SDMs across all studied scales (WSO1-WSO5) for two distinct model fitting approaches: (a) with keeping the predictor number constant across the scales, and (b) with simultaneous forward and backward predictor selection. Error bars represent one standard deviation of the estimates. We note that the figure represents the mean relative predictor importance based on all model runs per catchment order.

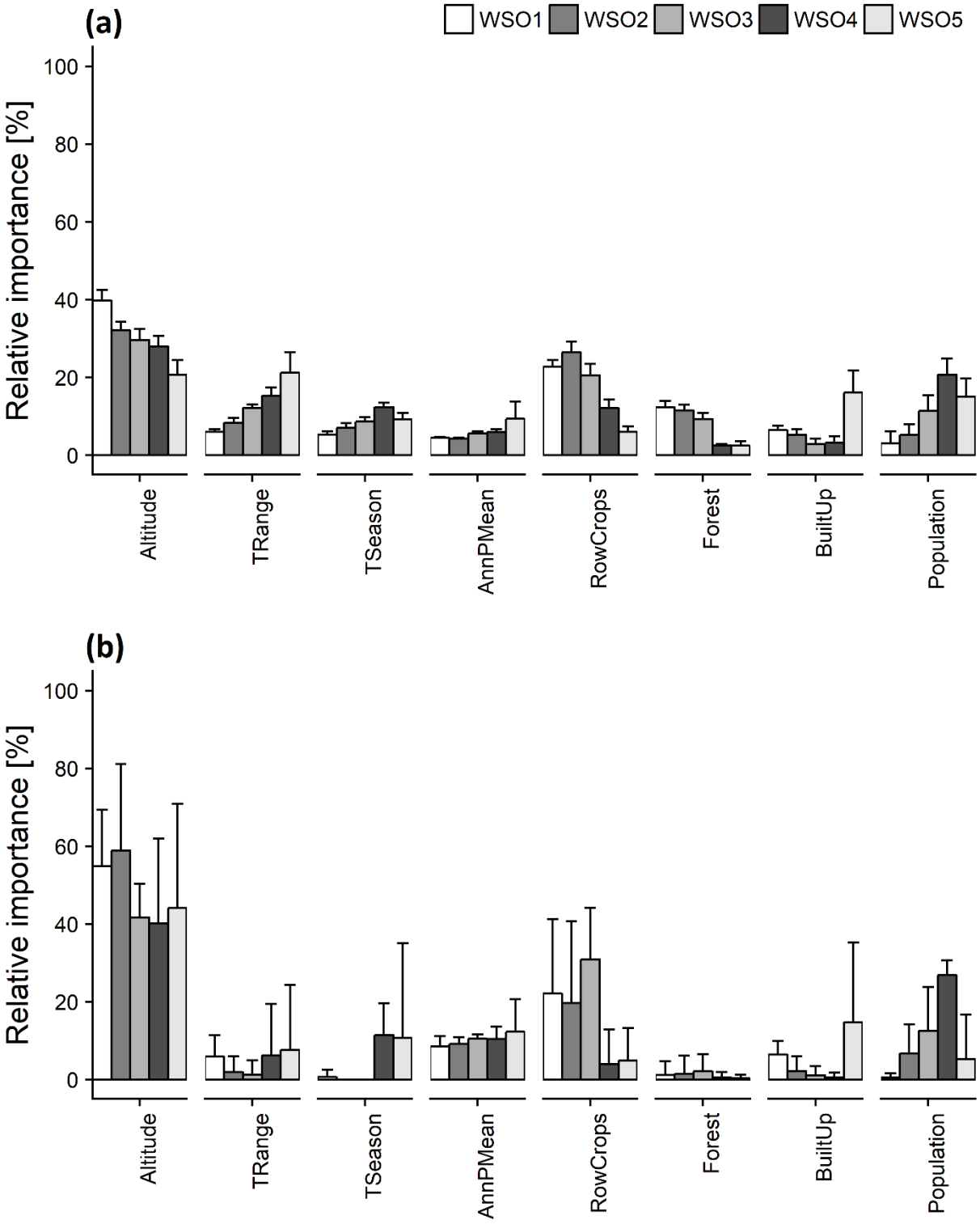

Fig. S9 The mean relative predictor importance of *B. barbus* resulting from the SDMs across all studied scales (WSO1-WSO5) for two distinct model fitting approaches: (a) with keeping the predictor number constant across the scales, and (b) with simultaneous forward and backward predictor selection. Error bars represent one standard deviation of the estimates. We note that the figure represents the mean relative predictor importance based on all model runs per catchment order.

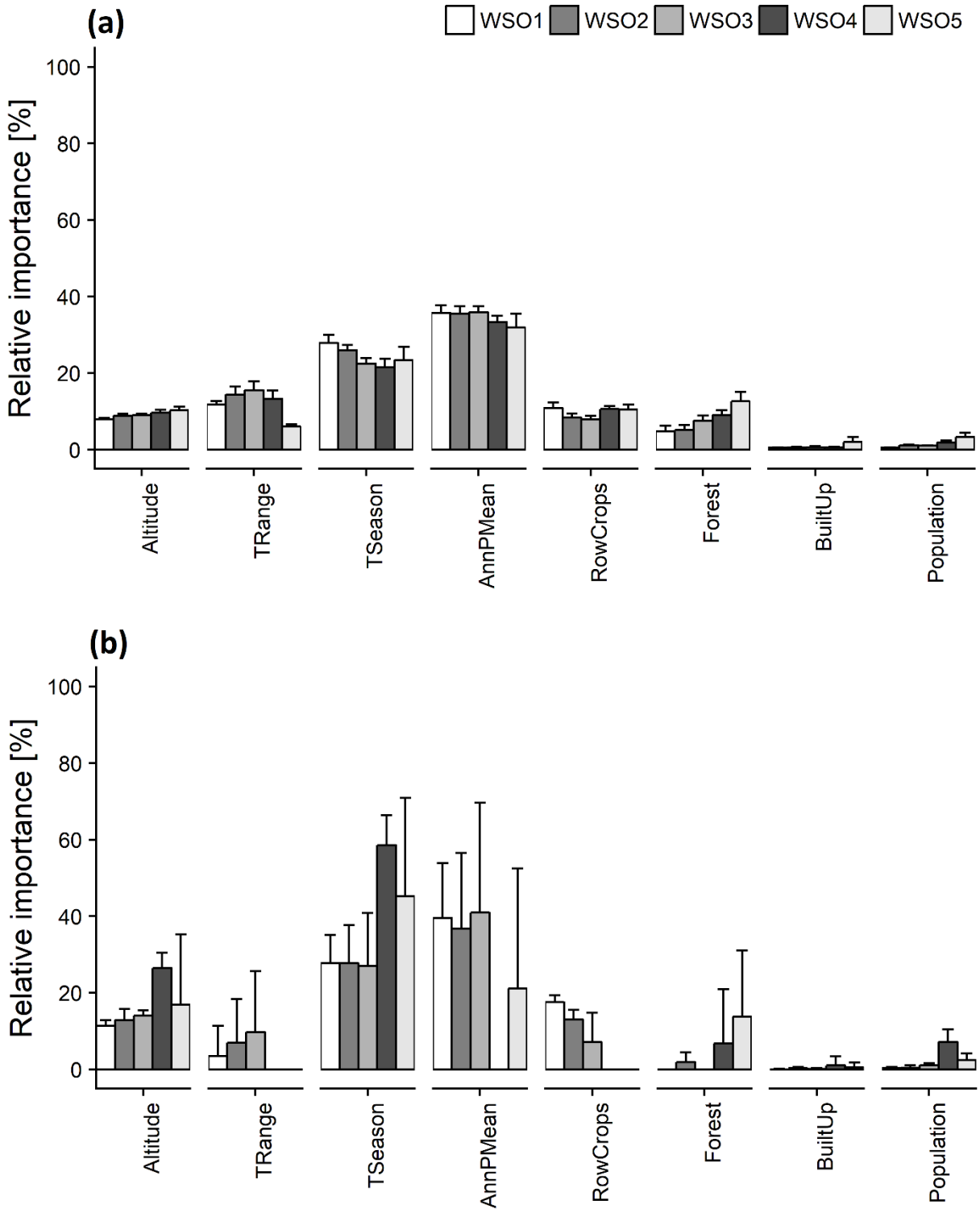

Fig. S10 The mean relative predictor importance of *C. gobio* resulting from the SDMs across all studied scales (WSO1-WSO5) for two distinct model fitting approaches: (a) with keeping the predictor number constant across the scales, and (b) with simultaneous forward and backward predictor selection. Error bars represent one standard deviation of the estimates. We note that the figure represents the mean relative predictor importance based on all model runs per catchment order.

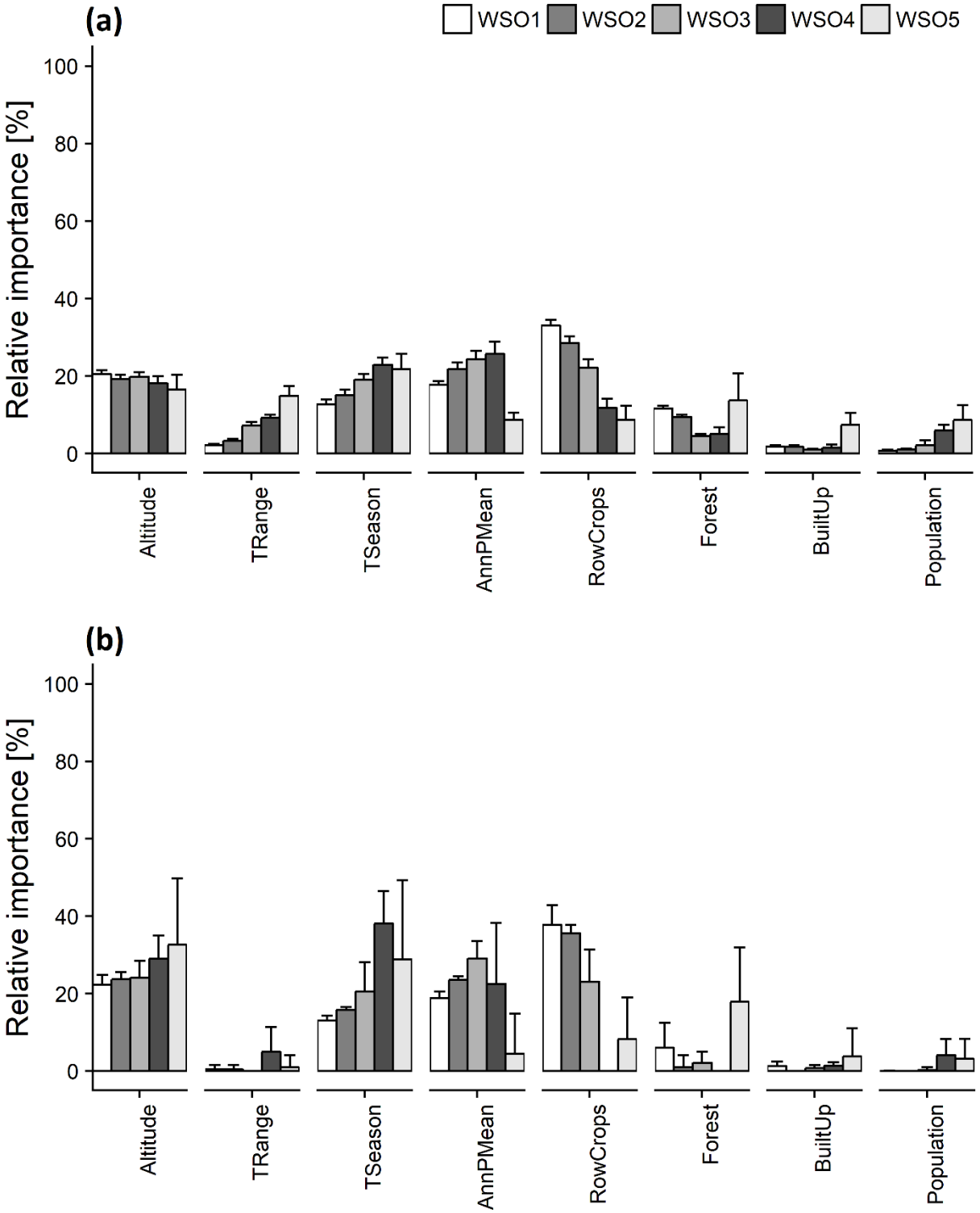

Fig. S11 The mean relative predictor importance of *G. obtusirostris* resulting from the SDMs across all studied scales (WSO1-WSO5) for two distinct model fitting approaches: (a) with keeping the predictor number constant across the scales, and (b) with simultaneous forward and backward predictor selection. Error bars represent one standard deviation of the estimates. We note that the figure represents the mean relative predictor importance based on all model runs per catchment order.

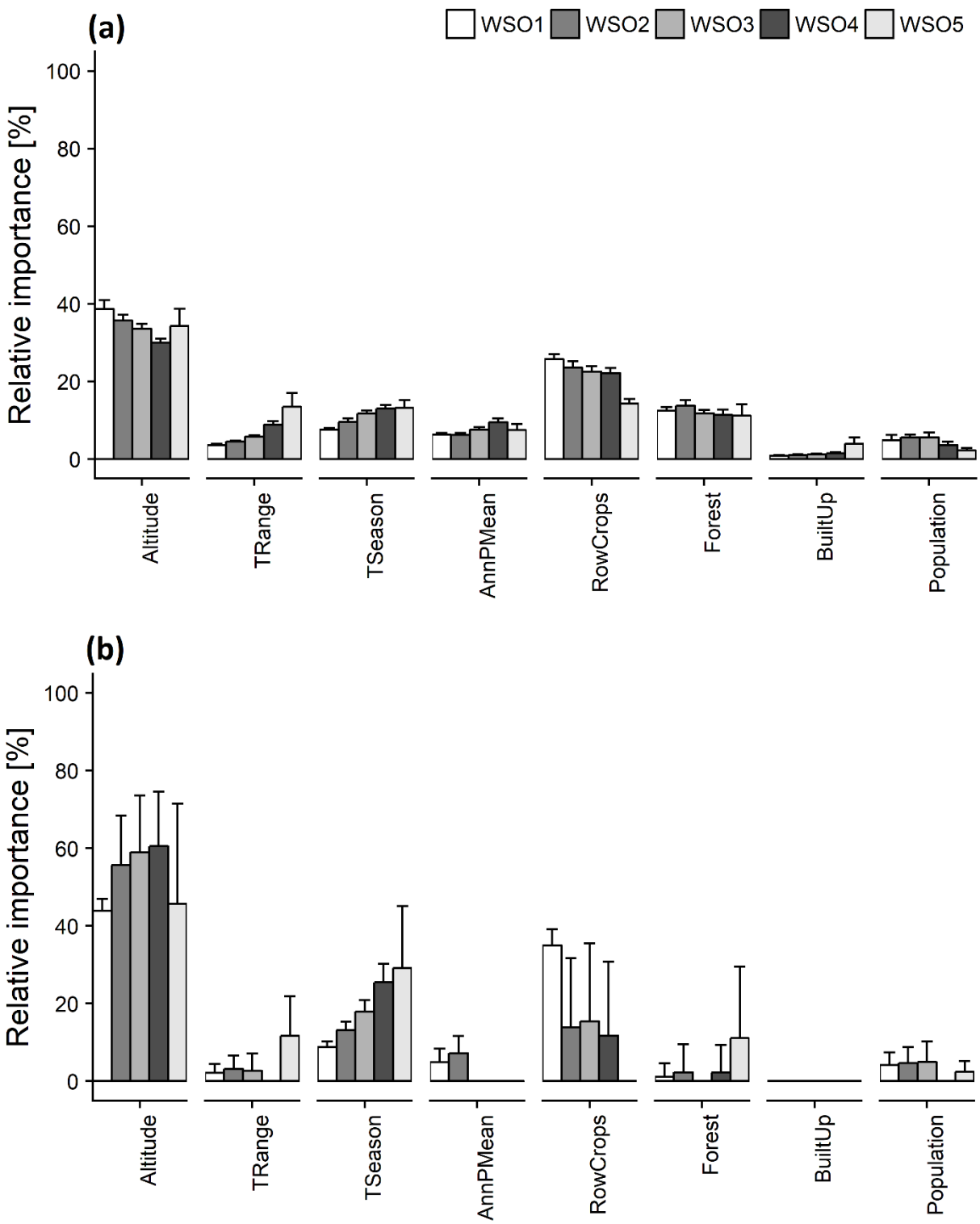

Fig. S12 The mean relative predictor importance of *R. rutilus* resulting from the SDMs across all studied scales (WSO1-WSO5) for two distinct model fitting approaches: (a) with keeping the predictor number constant across the scales, and (b) with simultaneous forward and backward predictor selection. Error bars represent one standard deviation of the estimates. We note that the figure represents the mean relative predictor importance based on all model runs per catchment order.

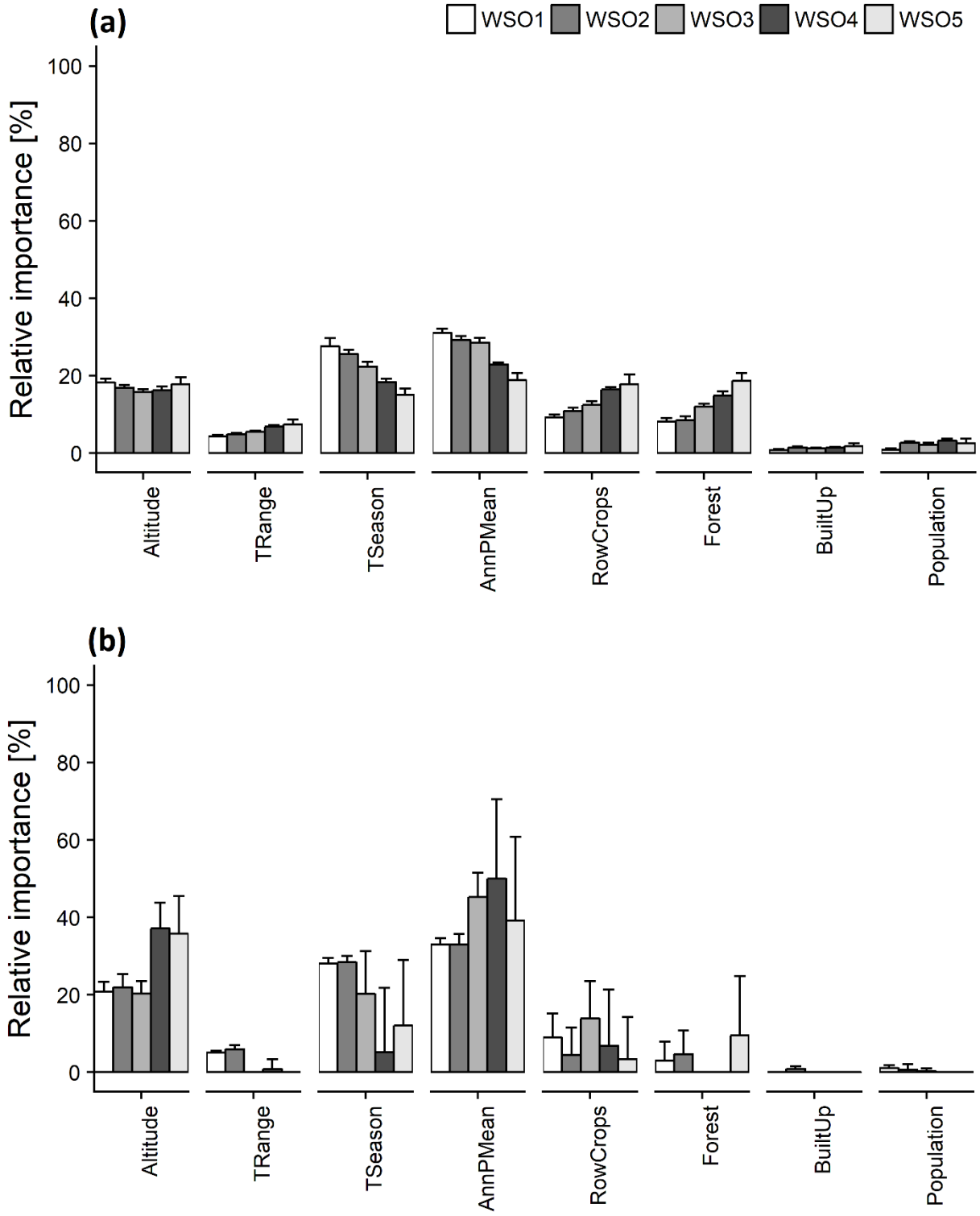

Fig. S13 The mean relative predictor importance of *S. trutta* resulting from the SDMs across all studied scales (WSO1-WSO5) for two distinct model fitting approaches: (a) with keeping the predictor number constant across the scales, and (b) with simultaneous forward and backward predictor selection. Error bars represent one standard deviation of the estimates. We note that the figure represents the mean relative predictor importance based on all model runs per catchment order.

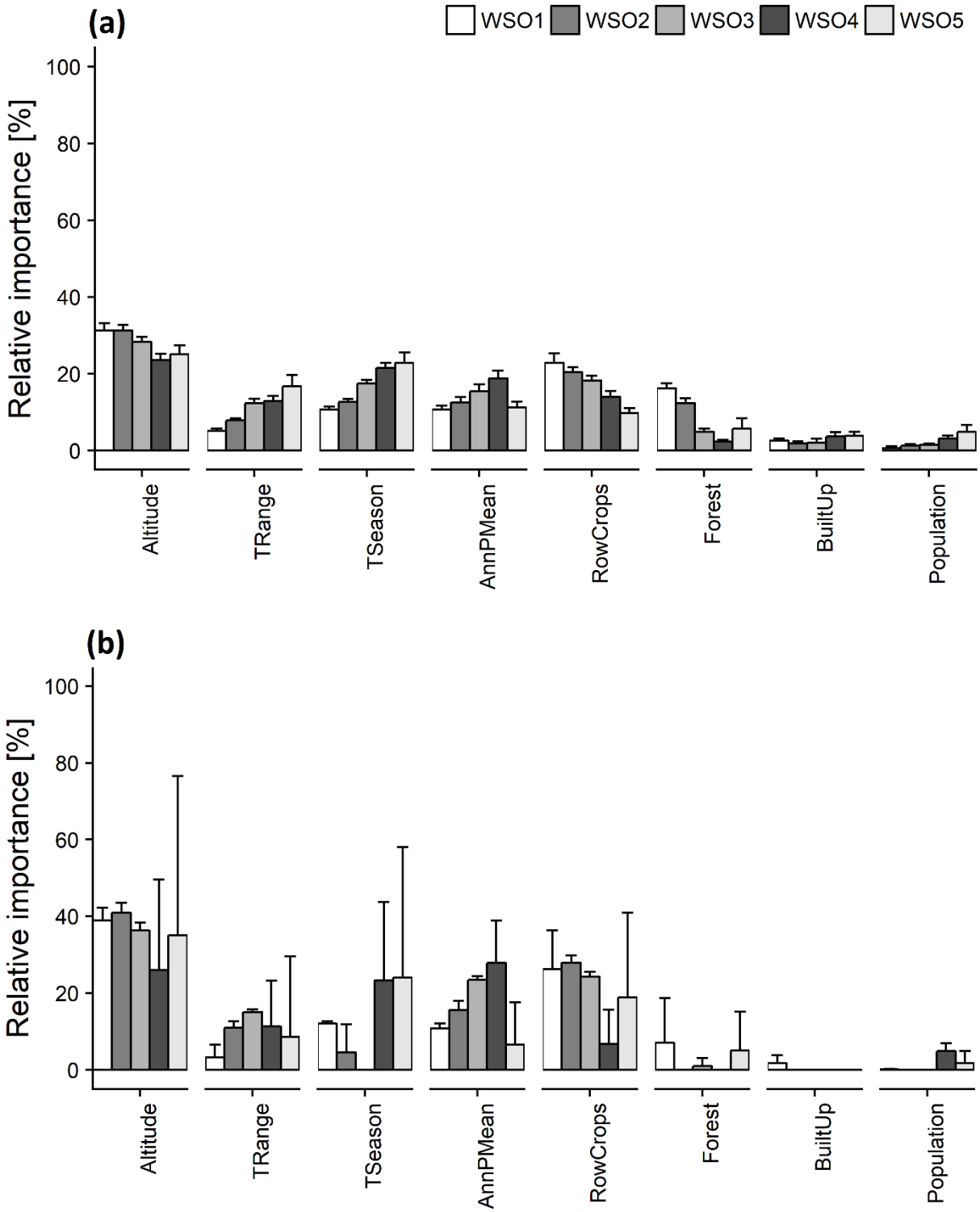

Fig. S14 The mean relative predictor importance of *S. cephalus* resulting from the SDMs across all studied scales (WSO1-WSO5) for two distinct model fitting approaches: (a) with keeping the predictor number constant across the scales, and (b) with simultaneous forward and backward predictor selection. Error bars represent one standard deviation of the estimates. We note that the figure represents the mean relative predictor importance based on all model runs per catchment order.

Table S1 Information value as a measure of the univariate strength of all environmental predictor variables derived across the corresponding catchment areas (ordered according to the mean values). For each of the five spatial scales the information value was calculated as an average predictive strength of the environmental predictor across all studied species; the overall information value of an environmental predictor was calculated as an average predictive strength across all scales and all considered species.

Parameter	Information value					
	WSO1	WSO2	WSO3	WSO4	WSO5	Mean
Altitude	1.87	1.70	1.64	1.85	1.63	1.74
TAprSep	1.59	1.58	1.65	1.83	1.28	1.59
TMaiAug	1.61	1.55	1.63	1.83	1.27	1.58
AnnTMean	1.59	1.48	1.67	1.74	1.29	1.56
WettTMean	1.50	1.57	1.66	1.75	1.27	1.55
Slope	1.46	1.38	1.68	1.77	1.29	1.52
AnnTMax	1.39	1.39	1.66	1.67	1.44	1.51
PMaiAug	1.37	1.50	1.40	1.60	1.24	1.42
RowCrops	1.16	1.22	1.61	2.08	1.01	1.41
PAprSep	1.32	1.26	1.41	1.62	1.17	1.35
Gradient	1.26	1.01	1.36	1.72	1.38	1.35
AnnPMean	1.27	1.32	1.48	1.52	0.91	1.30
TSeason	0.85	1.09	1.20	1.54	1.35	1.21
Agriculture	0.58	0.75	1.15	1.39	1.15	1.00
Population	0.68	0.90	0.95	1.11	0.80	0.89
Forest	0.65	0.67	0.76	0.77	0.61	0.69
TRange	0.25	0.38	0.51	0.70	0.78	0.52
BuiltUp	0.28	0.37	0.55	0.75	0.66	0.52
Grassland	0.04	0.11	0.44	0.80	0.86	0.45
PSeason	0.20	0.30	0.41	0.65	0.60	0.43
Length	0.49	0.45	0.35	0.44	0.28	0.40
Pastures	0.36	0.33	0.21	0.21	0.46	0.32

Table S2 Mean and range of the selected environmental predictors describing catchment influences across the studied scales (WSO1-WSO5).

Variable	WSO1	WSO2	WSO3	WSO4	WSO5
Altitude [m]	582.8 (9.0-2360.8)	652.9 (17.6-2629.7)	741.8 (33.2-2595.2)	818.0 (80.4-2434.1)	709.7 (81.1-2272.5)
TRange [°C]	9.7 (5.8-10.7)	9.6 (5.2-10.6)	9.4 (5.2-10.6)	9.3 (5.5-10.4)	9.4 (6.1-10.3)
TSeason [°C]	7.3 (5.3-8.6)	7.3 (5.1-8.6)	7.2 (5.2-8.6)	7.1 (5.3-8.5)	7.2 (5.5-8.5)
AnnPMean [mm]	870.3 (476.4-1485.7)	887.8 (482.6-1522.5)	924.3 (494.4-1537.3)	956.7 (511.3-1537.5)	907.9 (523.2-1479.1)
RowCrops [%]	26.6 (0-100)	24.6 (0-94.8)	23.3 (0-86.0)	23.0 (0-86.0)	28.3 (0-86.0)
Forest [%]	43.0 (0-100)	46.4 (0-100)	46.3 (0-100)	44.3 (0-94.4)	40.7 (3.1-84.0)
BuiltUp [%]	9.0 (0-100)	7.8 (0-100)	6.3 (0-78.8)	5.6 (0-78.8)	5.4 (0.1-18.1)
Population [No. inh.]	2042 (0-3.2·10^5)	6198 (0-3.6·10^5)	18129 (22-5.9·10^5)	60115 (214-18.8·10^5)	219284 (528-26.8·10^5)

Table S3 Mean and standard deviation (sd) for validation AUCs and TSSs of the multivariate SDMs with keeping the predictor number constant across the five studied scales (WSO1 – WSO5). Performance was assessed by using repeated random splitting (10 times) of the fish data into calibration (70%) and validation (30%).

Species	Accuracy measure		WSO1	WSO2	WSO3	WSO4	WSO5
A. alburnus	AUC	mean	0.90	0.90	0.91	0.91	0.90
		sd	0.02	0.02	0.02	0.02	0.05
	TSS	mean	0.61	0.64	0.69	0.69	0.64
		sd	0.05	0.03	0.05	0.06	0.12
B. barbatula	AUC	mean	0.84	0.85	0.87	0.86	0.78
		sd	0.01	0.01	0.03	0.03	0.04
	TSS	mean	0.54	0.56	0.61	0.61	0.47
		sd	0.03	0.03	0.06	0.05	0.13
B. barbus	AUC	mean	0.86	0.86	0.85	0.88	0.84
		sd	0.02	0.02	0.03	0.03	0.06
	TSS	mean	0.56	0.54	0.54	0.60	0.54
		sd	0.04	0.06	0.07	0.06	0.14
C. gobio	AUC	mean	0.84	0.87	0.88	0.88	0.87
		sd	0.02	0.02	0.03	0.03	0.05
	TSS	mean	0.55	0.60	0.60	0.66	0.63
		sd	0.05	0.05	0.06	0.07	0.08
G. obtusirostris	AUC	mean	0.89	0.90	0.89	0.88	0.85
		sd	0.01	0.02	0.02	0.03	0.06
	TSS	mean	0.64	0.64	0.61	0.63	0.54
		sd	0.02	0.04	0.04	0.07	0.20
R. rutilus	AUC	mean	0.90	0.90	0.91	0.91	0.86
		sd	0.01	0.01	0.01	0.03	0.04
	TSS	mean	0.68	0.67	0.72	0.71	0.65
		sd	0.03	0.04	0.04	0.08	0.12
S. trutta	AUC	mean	0.93	0.95	0.97	0.98	0.89
		sd	0.01	0.02	0.01	0.01	0.07
	TSS	mean	0.73	0.77	0.81	0.86	0.71
		sd	0.04	0.05	0.04	0.04	0.13
S. cephalus	AUC	mean	0.87	0.85	0.85	0.86	0.85
		sd	0.01	0.02	0.02	0.05	0.05
	TSS	mean	0.58	0.54	0.56	0.52	0.53
		sd	0.03	0.04	0.04	0.11	0.12

Table S4 Relative predictor importance resulting from the multivariate SDMs with keeping the predictor number constant across the five studied scales (WSO1 – WSO5). Performance was assessed by using repeated random splitting (10 times) of the fish data into calibration (70%) and validation (30%).

Remark: The values in the table represent the mean relative predictor importance based on all model runs per species and catchment order.

Species	Variable	WSO1	WSO2	WSO3	WSO4	WSO5
Albual	Altitude	34.92%	29.40%	23.97%	21.75%	29.40%
	TRange	3.21%	4.02%	5.47%	7.58%	11.38%
	TSeason	6.61%	7.38%	8.59%	11.27%	15.12%
	AnnPMean	12.98%	11.68%	11.62%	14.48%	14.52%
	RowCrops	22.57%	22.34%	25.11%	22.63%	15.37%
	Forest	17.06%	19.22%	19.94%	15.21%	6.67%
	BuiltUp	1.07%	1.34%	1.53%	1.57%	3.30%
	Population	1.59%	4.63%	3.76%	5.51%	4.24%
Barbbr	Altitude	12.34%	11.60%	11.28%	13.52%	10.42%
	TRange	4.36%	4.61%	5.99%	11.24%	16.25%
	TSeason	13.31%	12.83%	11.82%	13.74%	9.45%
	AnnPMean	39.64%	43.34%	38.64%	33.86%	14.62%
	RowCrops	20.32%	14.89%	14.70%	7.07%	5.29%
	Forest	5.11%	3.56%	12.64%	9.40%	10.99%
	BuiltUp	2.81%	3.86%	3.72%	8.51%	18.41%
	Population	2.13%	5.32%	1.21%	2.65%	14.58%
Barbba	Altitude	39.72%	32.11%	29.60%	27.94%	20.61%
	TRange	6.03%	8.36%	12.18%	15.31%	21.21%
	TSeason	5.31%	7.02%	8.65%	12.37%	9.18%
	AnnPMean	4.41%	4.20%	5.54%	5.97%	9.34%
	RowCrops	22.73%	26.40%	20.55%	12.10%	6.00%
	Forest	12.26%	11.51%	9.27%	2.48%	2.44%
	BuiltUp	6.42%	5.20%	2.84%	3.13%	16.12%
	Population	3.11%	5.19%	11.38%	20.72%	15.10%
Cottgo	Altitude	7.99%	8.86%	8.96%	9.69%	10.25%
	TRange	11.73%	14.40%	15.51%	13.28%	6.04%
	TSeason	27.89%	25.97%	22.51%	21.47%	23.40%
	AnnPMean	35.71%	35.55%	35.88%	33.35%	31.93%
	RowCrops	10.91%	8.39%	7.88%	10.63%	10.46%

	Forest	4.80%	5.12%	7.55%	9.03%	12.66%
	BuiltUp	0.46%	0.58%	0.65%	0.63%	1.96%
	Population	0.50%	1.13%	1.05%	1.91%	3.30%
Gobris	Altitude	20.46%	19.12%	19.80%	18.12%	16.46%
	TRange	2.17%	3.32%	7.15%	9.18%	14.85%
	TSeason	12.71%	15.08%	19.07%	22.91%	21.72%
	AnnPMean	17.68%	21.82%	24.35%	25.67%	8.70%
	RowCrops	32.98%	28.50%	22.05%	11.73%	8.63%
	Forest	11.59%	9.40%	4.48%	5.03%	13.69%
	BuiltUp	1.77%	1.69%	0.98%	1.48%	7.34%
	Population	0.63%	1.06%	2.12%	5.89%	8.61%
Rutiru	Altitude	38.67%	35.66%	33.58%	30.00%	34.26%
	TRange	3.66%	4.54%	5.85%	8.89%	13.52%
	TSeason	7.57%	9.56%	11.76%	12.99%	13.15%
	AnnPMean	6.29%	6.23%	7.60%	9.46%	7.48%
	RowCrops	25.73%	23.58%	22.54%	22.17%	14.27%
	Forest	12.45%	13.77%	11.84%	11.39%	11.14%
	BuiltUp	0.80%	1.06%	1.19%	1.47%	3.96%
	Population	4.84%	5.61%	5.64%	3.63%	2.22%
Saltta	Altitude	18.19%	16.90%	15.85%	16.22%	17.80%
	TRange	4.32%	4.86%	5.50%	6.82%	7.42%
	TSeason	27.57%	25.52%	22.32%	18.36%	15.12%
	AnnPMean	31.01%	29.20%	28.52%	22.88%	18.81%
	RowCrops	9.14%	10.89%	12.44%	16.40%	17.82%
	Forest	8.06%	8.51%	11.99%	14.79%	18.68%
	BuiltUp	0.79%	1.45%	1.21%	1.37%	1.81%
	Population	0.91%	2.66%	2.17%	3.16%	2.55%
Squace	Altitude	31.28%	31.24%	28.24%	23.62%	25.08%
	TRange	5.09%	7.85%	12.28%	12.90%	16.76%
	TSeason	10.67%	12.60%	17.45%	21.55%	22.88%
	AnnPMean	10.66%	12.56%	15.40%	18.84%	11.18%
	RowCrops	22.87%	20.36%	18.24%	13.99%	9.79%
	Forest	16.20%	12.34%	4.89%	2.30%	5.69%
	BuiltUp	2.57%	1.83%	2.02%	3.66%	3.77%
	Population	0.65%	1.21%	1.48%	3.14%	4.85%

Table S5 Relative predictor importance resulting from the multivariate SDMs with simultaneous forward and backward predictor selection across all studied scales (WSO1-WSO5). Performance was assessed by using repeated random splitting (10 times) of the fish data into calibration (70%) and validation (30%).

Remark: The values in the table represent the mean relative predictor importance based on all model runs per species and catchment order.

Species	Variable	WSO1	WSO2	WSO3	WSO4	WSO5
Albual	Altitude	42.82%	47.60%	58.72%	46.43%	32.46%
	TRange	0.83%	0.00%	3.82%	5.97%	2.72%
	TSeason	8.63%	12.33%	13.47%	0.00%	31.93%
	AnnPMean	15.92%	19.84%	18.31%	16.36%	12.37%
	RowCrops	31.22%	11.25%	4.70%	3.64%	9.87%
	Forest	0.00%	8.97%	0.00%	16.81%	0.00%
	BuiltUp	0.08%	0.00%	0.00%	1.06%	0.65%
	Population	0.49%	0.00%	0.98%	9.72%	10.01%
Barbbr	Altitude	14.38%	13.06%	18.25%	29.88%	41.61%
	TRange	4.53%	5.75%	5.20%	1.72%	5.36%
	TSeason	10.20%	14.36%	9.17%	7.77%	3.65%
	AnnPMean	44.42%	48.50%	52.28%	52.82%	17.64%
	RowCrops	23.21%	12.92%	12.84%	1.44%	2.27%
	Forest	0.00%	0.00%	1.66%	3.60%	11.63%
	BuiltUp	1.00%	0.00%	0.00%	2.31%	4.83%
	Population	2.27%	5.41%	0.60%	0.44%	13.00%
Barbba	Altitude	54.83%	58.84%	41.65%	40.12%	44.09%
	TRange	5.89%	1.91%	1.19%	6.24%	7.59%
	TSeason	0.61%	0.00%	0.00%	11.44%	10.78%
	AnnPMean	8.55%	9.17%	10.52%	10.41%	12.29%
	RowCrops	22.07%	19.68%	30.91%	3.98%	4.90%
	Forest	1.14%	1.47%	2.08%	0.46%	0.30%
	BuiltUp	6.40%	2.18%	1.12%	0.56%	14.73%
	Population	0.51%	6.75%	12.53%	26.79%	5.32%
Cottgo	Altitude	11.36%	12.88%	14.02%	26.49%	16.97%
	TRange	3.50%	6.95%	9.71%	0.00%	0.00%
	TSeason	27.73%	27.77%	27.05%	58.58%	45.22%
	AnnPMean	39.52%	36.70%	40.95%	0.00%	21.12%
	RowCrops	17.54%	13.04%	7.11%	0.00%	0.00%

	Forest	0.00%	1.89%	0.00%	6.74%	13.77%
	BuiltUp	0.04%	0.32%	0.10%	1.04%	0.46%
	Population	0.32%	0.45%	1.07%	7.14%	2.47%
Gobris	Altitude	22.29%	23.71%	24.15%	28.99%	32.61%
	TRange	0.52%	0.40%	0.00%	4.94%	0.98%
	TSeason	13.12%	15.85%	20.53%	38.08%	28.89%
	AnnPMean	18.88%	23.52%	29.06%	22.46%	4.49%
	RowCrops	37.78%	35.55%	23.11%	0.00%	8.22%
	Forest	6.06%	0.98%	2.13%	0.00%	17.88%
	BuiltUp	1.32%	0.00%	0.77%	1.45%	3.82%
	Population	0.04%	0.00%	0.24%	4.09%	3.13%
Rutiru	Altitude	43.94%	55.69%	59.03%	60.54%	45.67%
	TRange	2.18%	3.16%	2.66%	0.00%	11.72%
	TSeason	8.74%	13.16%	17.98%	25.46%	29.13%
	AnnPMean	4.90%	7.21%	0.00%	0.00%	0.00%
	RowCrops	34.98%	13.82%	15.41%	11.76%	0.00%
	Forest	1.10%	2.28%	0.00%	2.23%	11.08%
	BuiltUp	0.00%	0.00%	0.00%	0.00%	0.00%
	Population	4.16%	4.68%	4.93%	0.00%	2.40%
Saltta	Altitude	20.84%	21.95%	20.38%	37.12%	35.82%
	TRange	5.07%	5.96%	0.00%	0.81%	0.00%
	TSeason	28.07%	28.45%	20.23%	5.24%	12.10%
	AnnPMean	33.00%	32.92%	45.27%	49.99%	39.17%
	RowCrops	8.95%	4.43%	13.87%	6.83%	3.43%
	Forest	3.01%	4.68%	0.00%	0.00%	9.48%
	BuiltUp	0.00%	0.92%	0.00%	0.00%	0.00%
	Population	1.07%	0.68%	0.25%	0.00%	0.00%
Squace	Altitude	38.94%	40.95%	36.31%	25.96%	35.08%
	TRange	3.17%	10.97%	15.05%	11.25%	8.60%
	TSeason	12.01%	4.53%	0.00%	23.31%	24.09%
	AnnPMean	10.83%	15.62%	23.39%	27.87%	6.59%
	RowCrops	26.26%	27.93%	24.26%	6.71%	18.92%
	Forest	7.06%	0.00%	0.99%	0.00%	5.04%
	BuiltUp	1.68%	0.00%	0.00%	0.00%	0.00%
	Population	0.06%	0.00%	0.00%	4.88%	1.69%

Appendix 3: Supporting information of Part II, Chapter 5

Freshwater species distributions along thermal gradients

The full version of the Appendix is available at:
https://onlinelibrary.wiley.com/doi/full/10.1002/ece3.4659

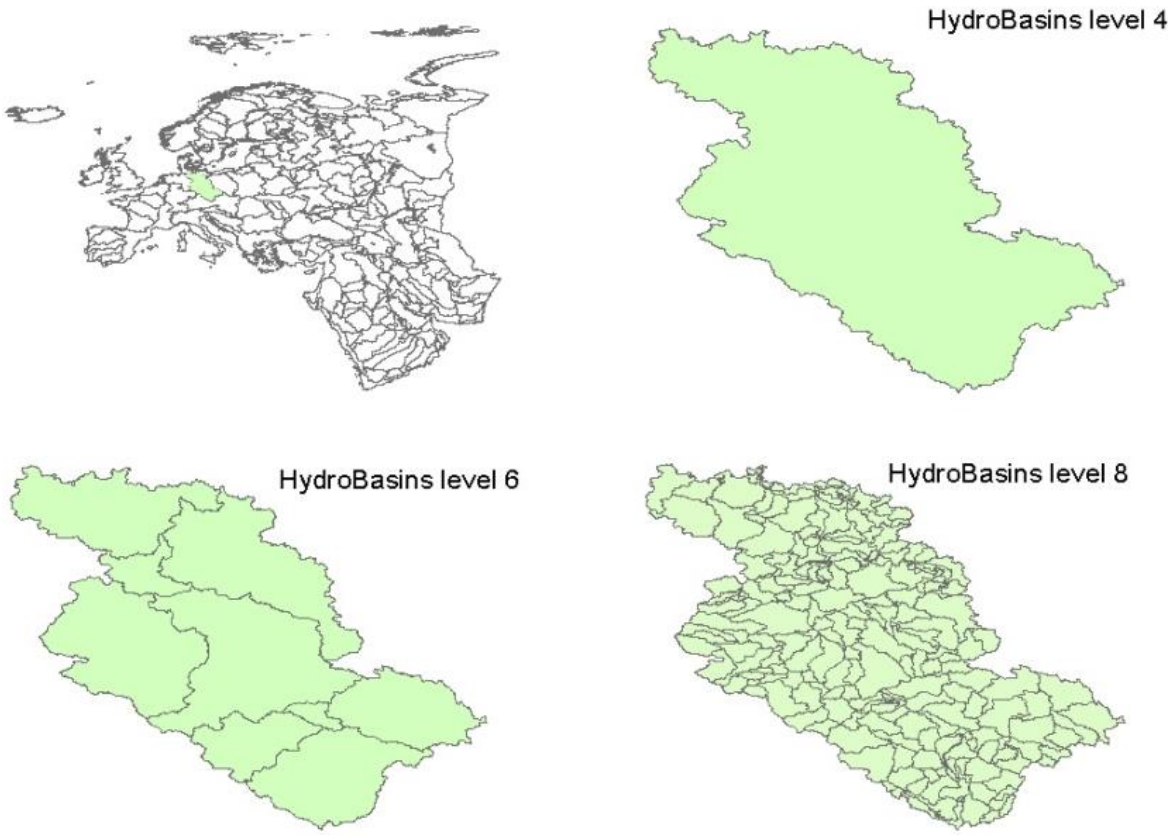

Fig. S1.1 Different HydroBasins data set resolutions for the Elbe River Basin (green).

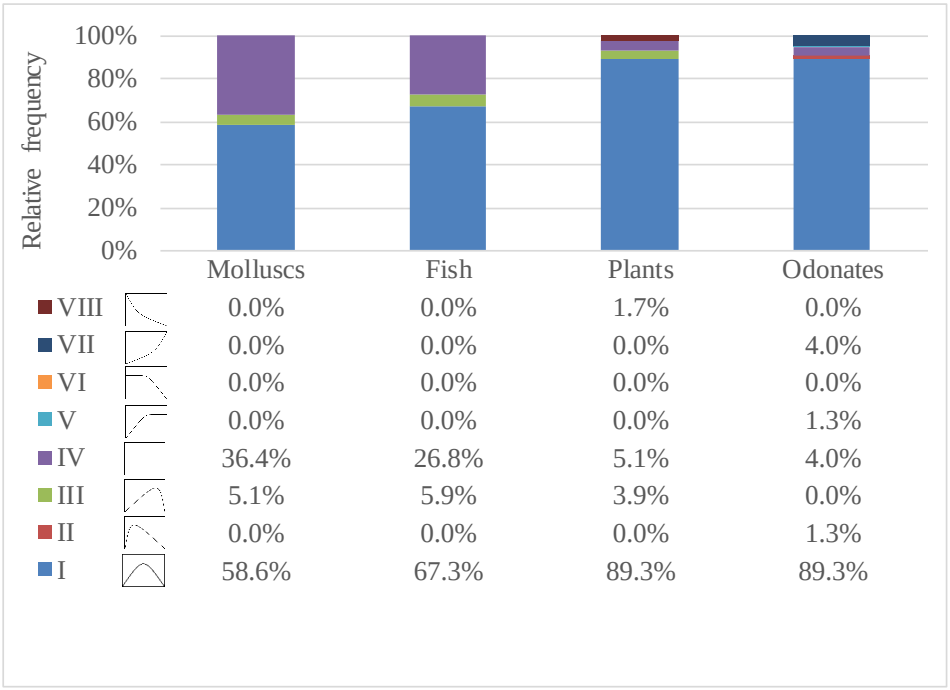

Fig. S1.2 Relative frequency of the different curve types for molluscs, fish, plants and odonates for $Tmean_{air}$. Note that crayfish were excluded because of the low frequency of analyzed species.

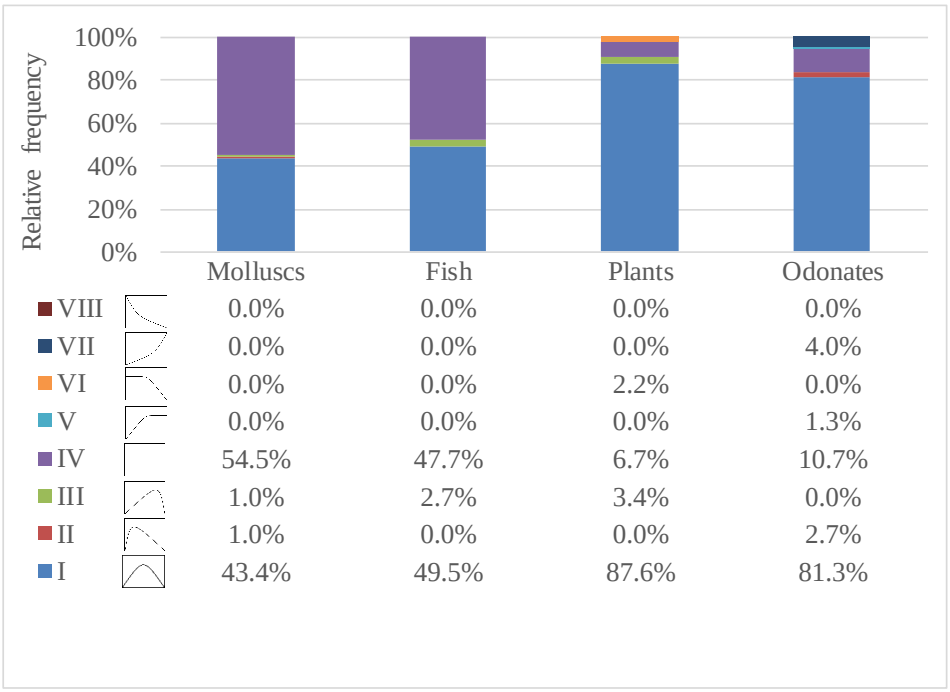

Fig. S1.3 Relative frequency of the different curve types for molluscs, fish, plants and odonates for $Tmax_{air}$. Note that crayfish were excluded because of the low frequency of analyzed species.

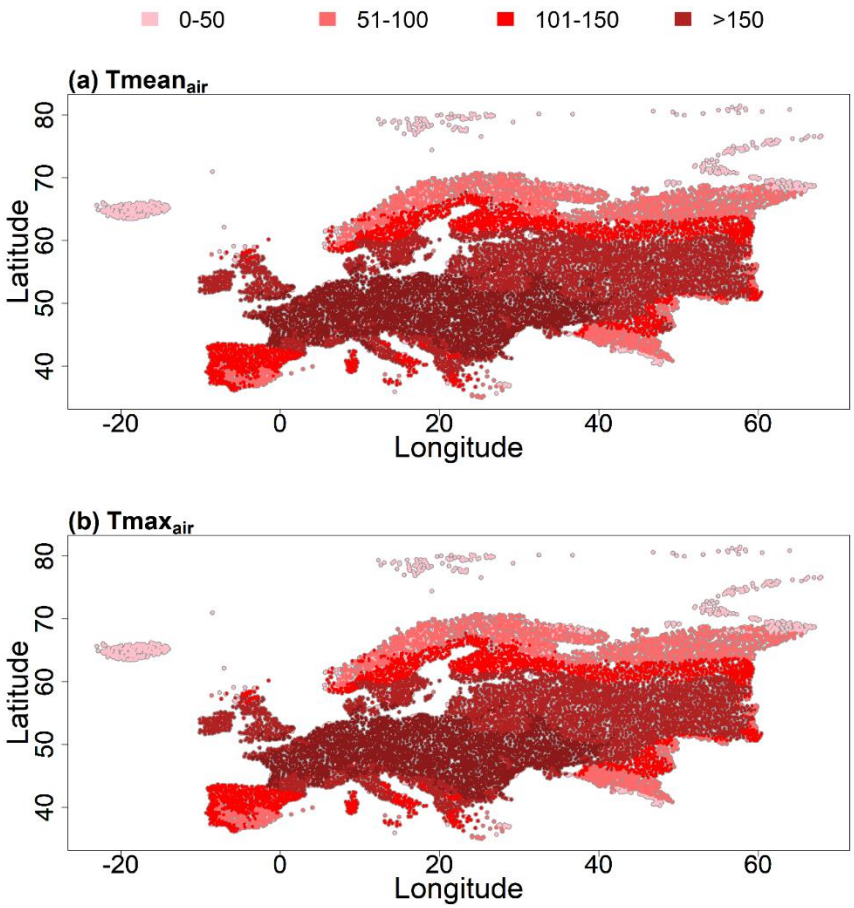

Fig. S1.4 Variation in the number of species with a unimodal response per catchment for (a) Tmean$_{air}$ and (b) Tmax$_{air}$.

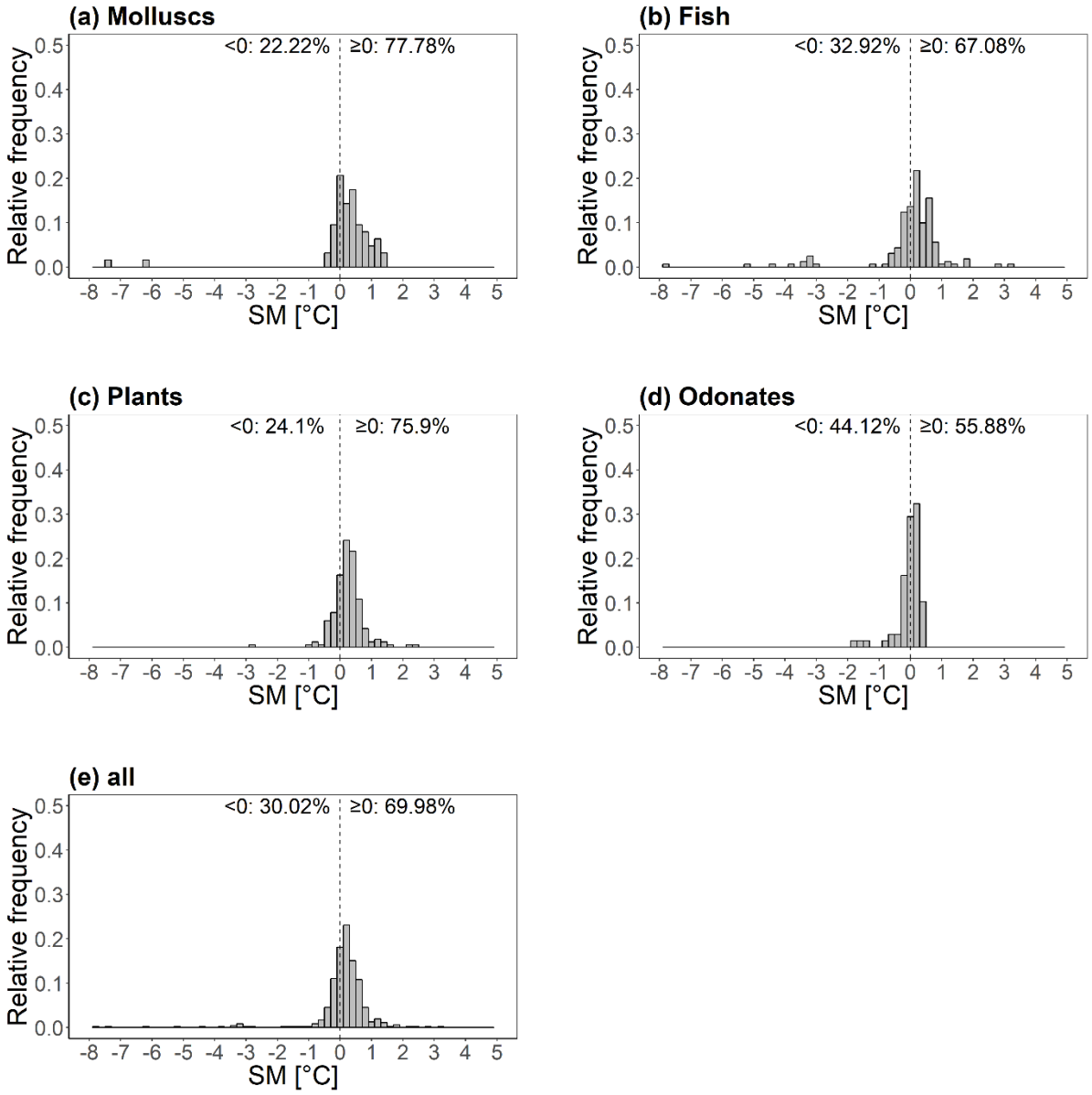

Fig. S1.5 Relative frequencies of the safety margin (SM = T_{pref} – T_{av}) distribution of unimodal species for (a) molluscs, (b) fishes, (c) plants, (d) odonates, and (e) all taxonomic groups combined inferred from $Tmean_{air}$. The dotted line at 0°C separates negative and positive SMs with the relative frequency of the species of the corresponding taxonomic group having a negative or positive SM at the upper end. Note that crayfish were excluded because of the low frequency of analyzed species.

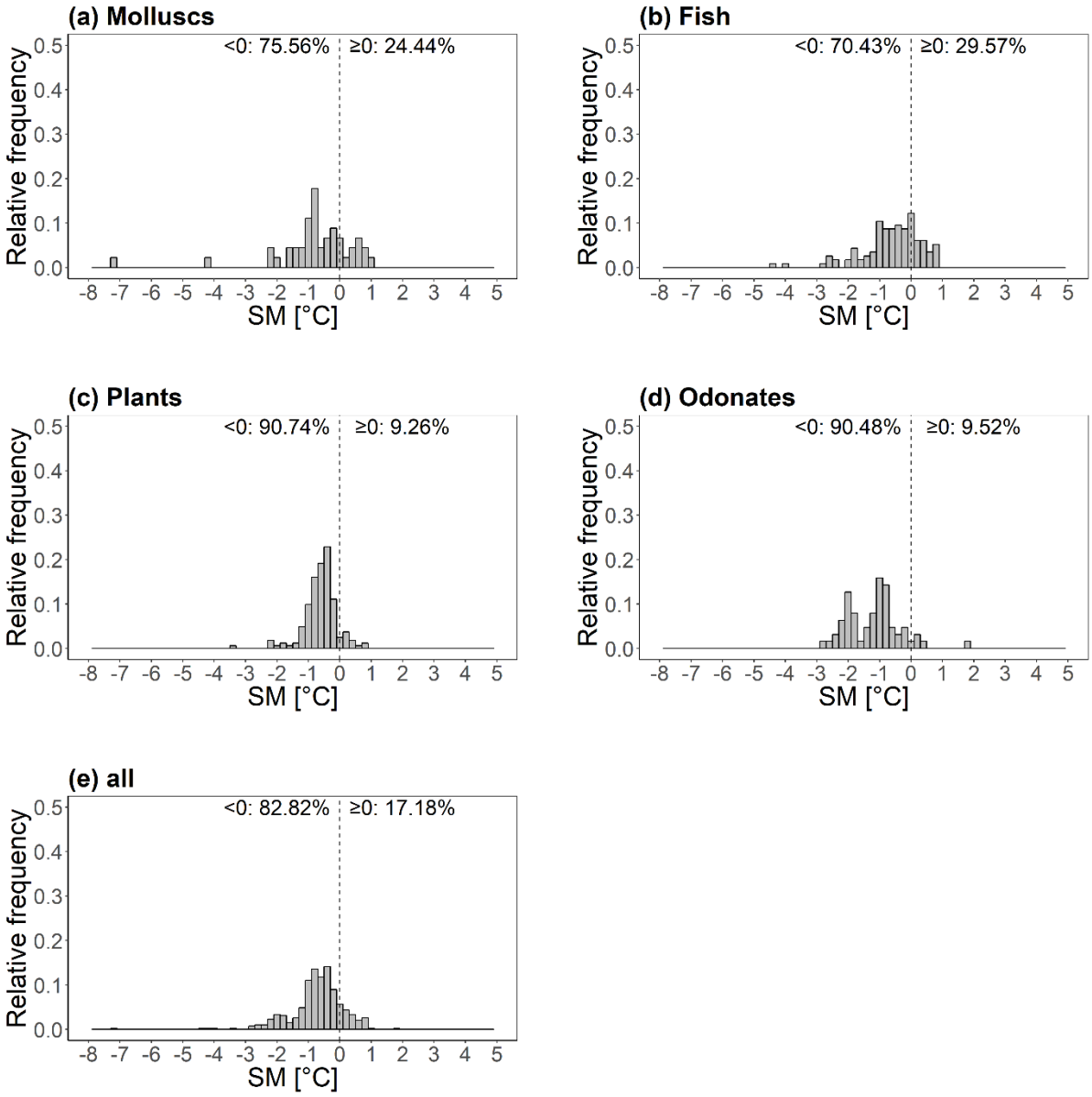

Fig. S1.6 Relative frequencies of the safety margin (SM = T_{pref} – T_{av}) distribution of unimodal species for (a) molluscs, (b) fishes, (c) plants, (d) odonates, and (e) all taxonomic groups combined inferred from $Tmax_{air}$. The dotted line at 0°C separates negative and positive SMs with the relative frequency of the species of the corresponding taxonomic group having a negative or positive SM at the upper end. Note that crayfish were excluded because of the low frequency of analyzed species.

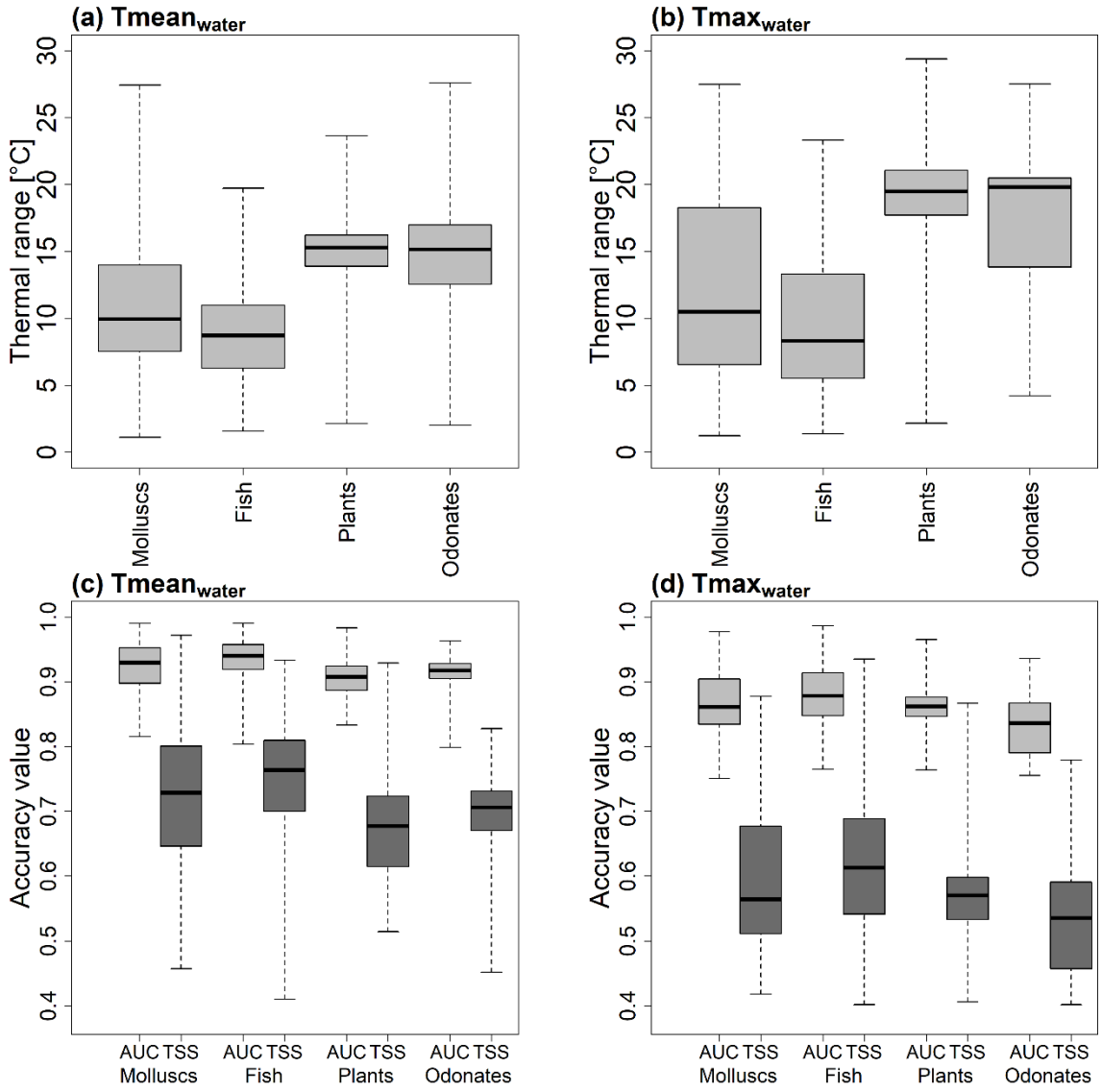

Fig. S1.7 Thermal ranges of the species and the distribution of the accuracy measures per taxonomic group for the respective temperature variable, i.e. for (a, c) $Tmean_{water}$ and (b, d) $Tmax_{water}$. The boxplots illustrate the distribution of the minimum, 25% quantile, median, 75% quantile and maximum of the thermal ranges. The minimum and maximum are displayed by the end of the corresponding whiskers. Note that crayfish were excluded because of the low frequency of analyzed species.

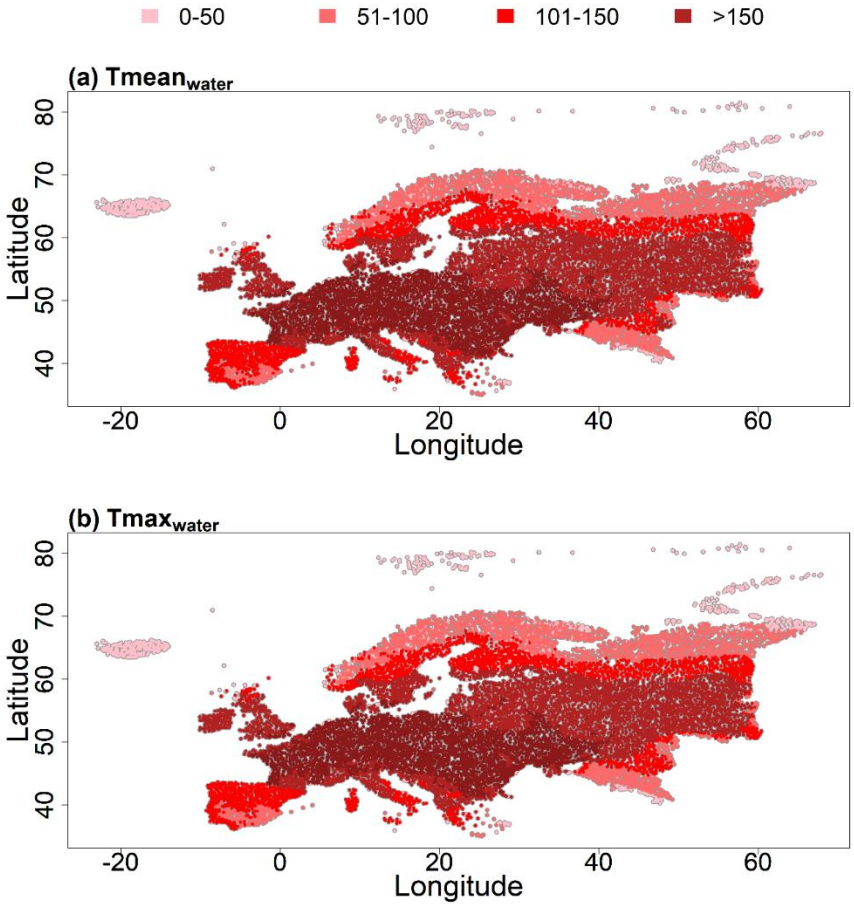

Fig. S1.8 Variation in the number of species with a unimodal response per catchment for (a) $Tmean_{water}$ and (b) $Tmax_{water}$.

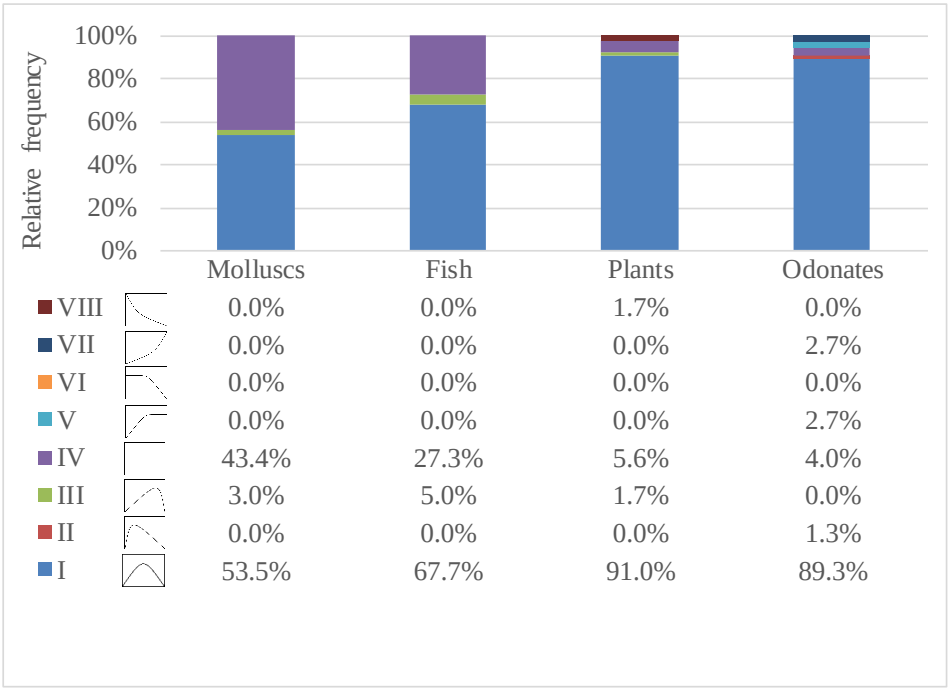

Fig. S1.9 Relative frequency of the different curve types for molluscs, fish, plants and odonates for $Tmean_{water}$. Note that crayfish were excluded because of the low frequency of analyzed species.

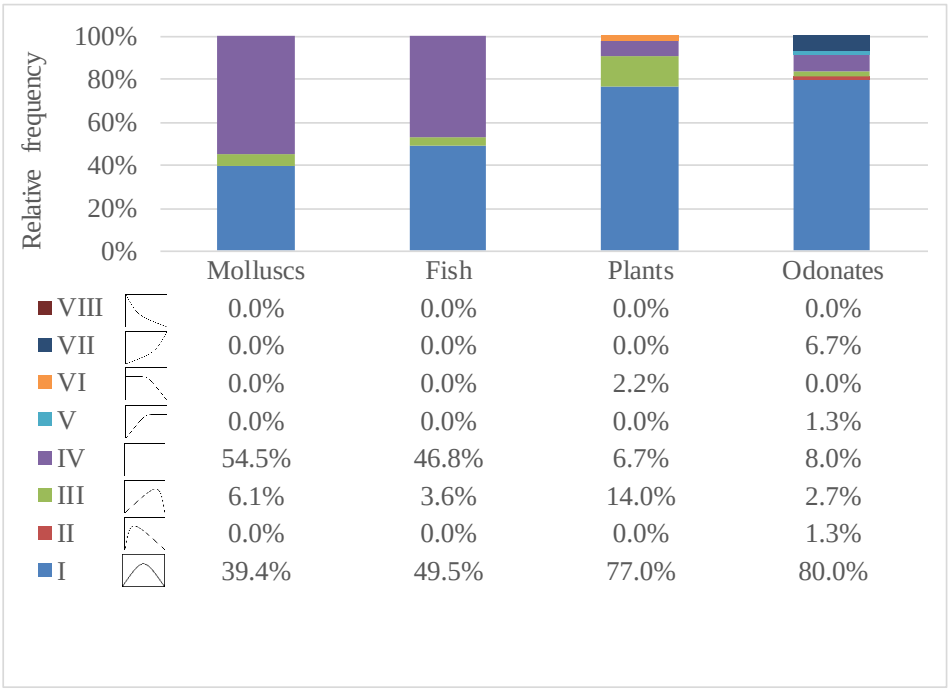

Fig. S1.10 Relative frequency of the different curve types for molluscs, fish, plants and odonates for $Tmax_{water}$. Note that crayfish were excluded because of the low frequency of analyzed species.

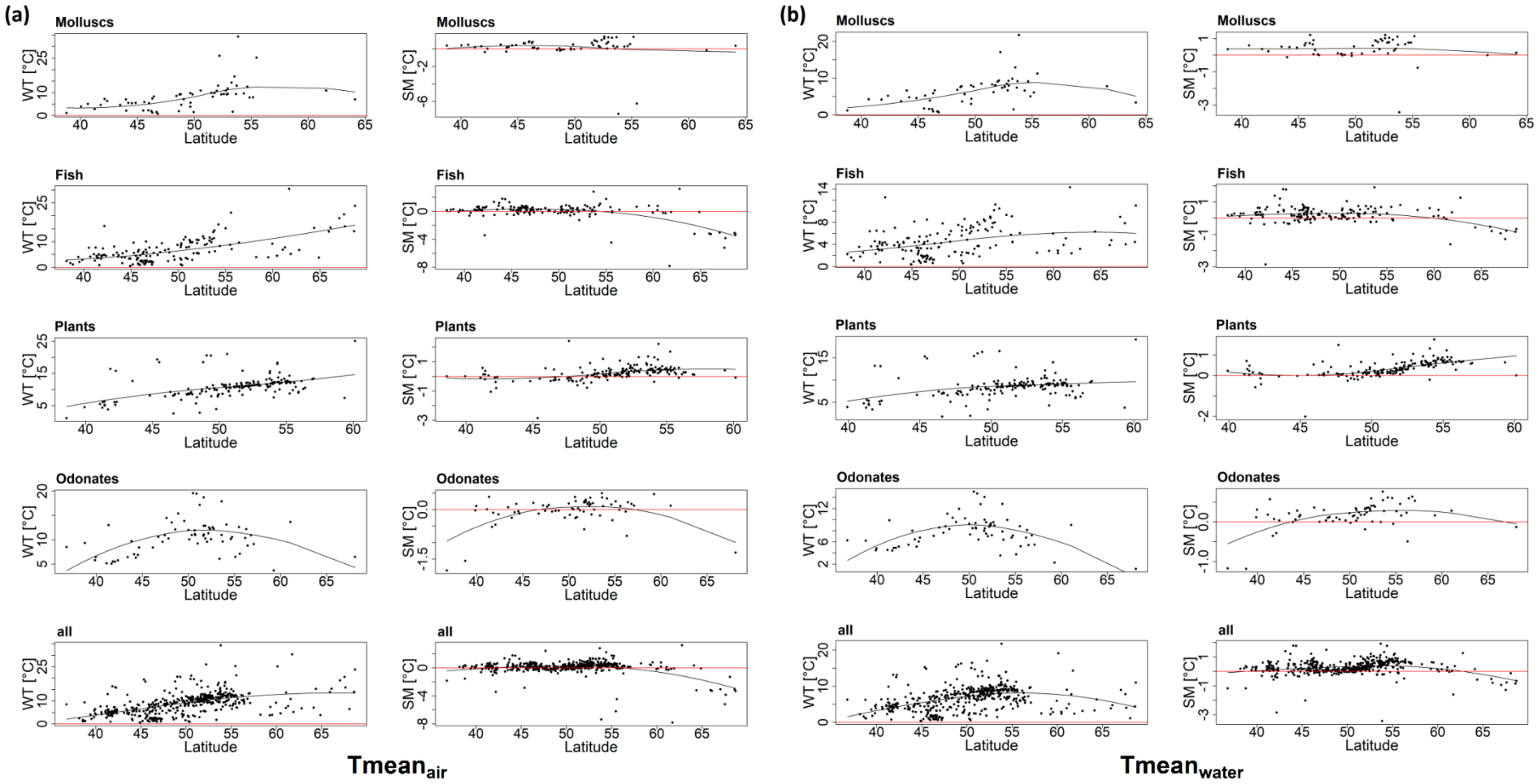

Fig. S1.11 Comparison of the latitudinal distributions and non-linear trend lines of the warming tolerance (WT = CT – T_{pref}) and safety margin (SM = T_{pref} – T_{av}) for freshwater species inferred from the temperature variables (a) $Tmean_{air}$ and (b) $Tmean_{water}$. WT and SM were only computed for species with a unimodal response. Here, latitude values correspond to the average latitude of each species' European latitudinal range. Note that crayfish were excluded because of the low frequency of analyzed species. Each dot represents the WT and SM of one species in the respective figure.

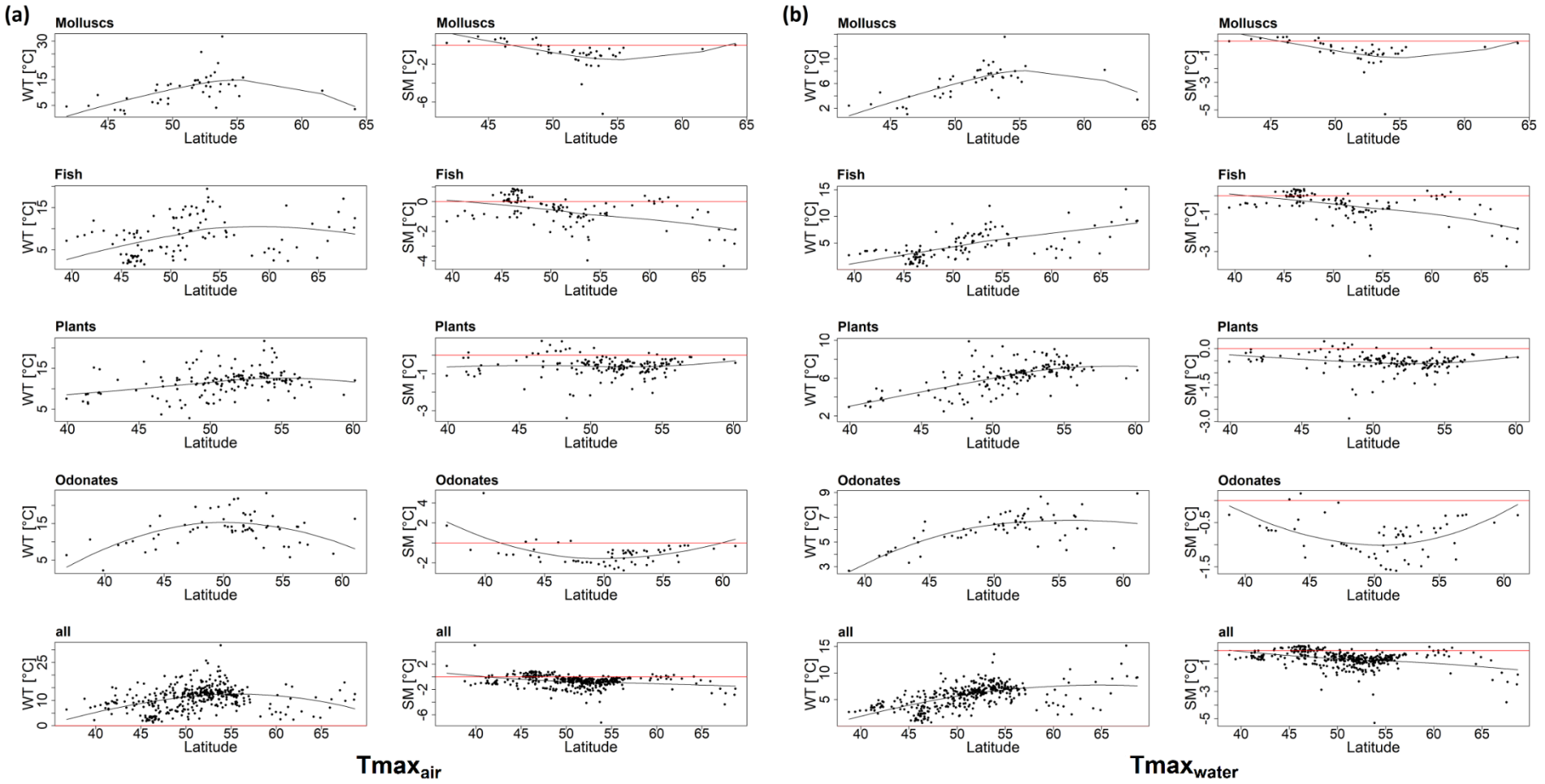

Fig. S1.12 Comparison of the latitudinal distributions and non-linear trend lines of the warming tolerance (WT = CT – T_{pref}) and safety margin (SM = T_{pref} – T_{av}) for freshwater species inferred from the temperature variables (a) $Tmax_{air}$ and (b) $Tmax_{water}$. WT and SM were only computed for species with a unimodal response. Here, latitude values correspond to the average latitude of each species' European latitudinal range. Note that crayfish were excluded because of the low frequency of analyzed species. Each dot represents the WT and SM of one species in the respective figure.

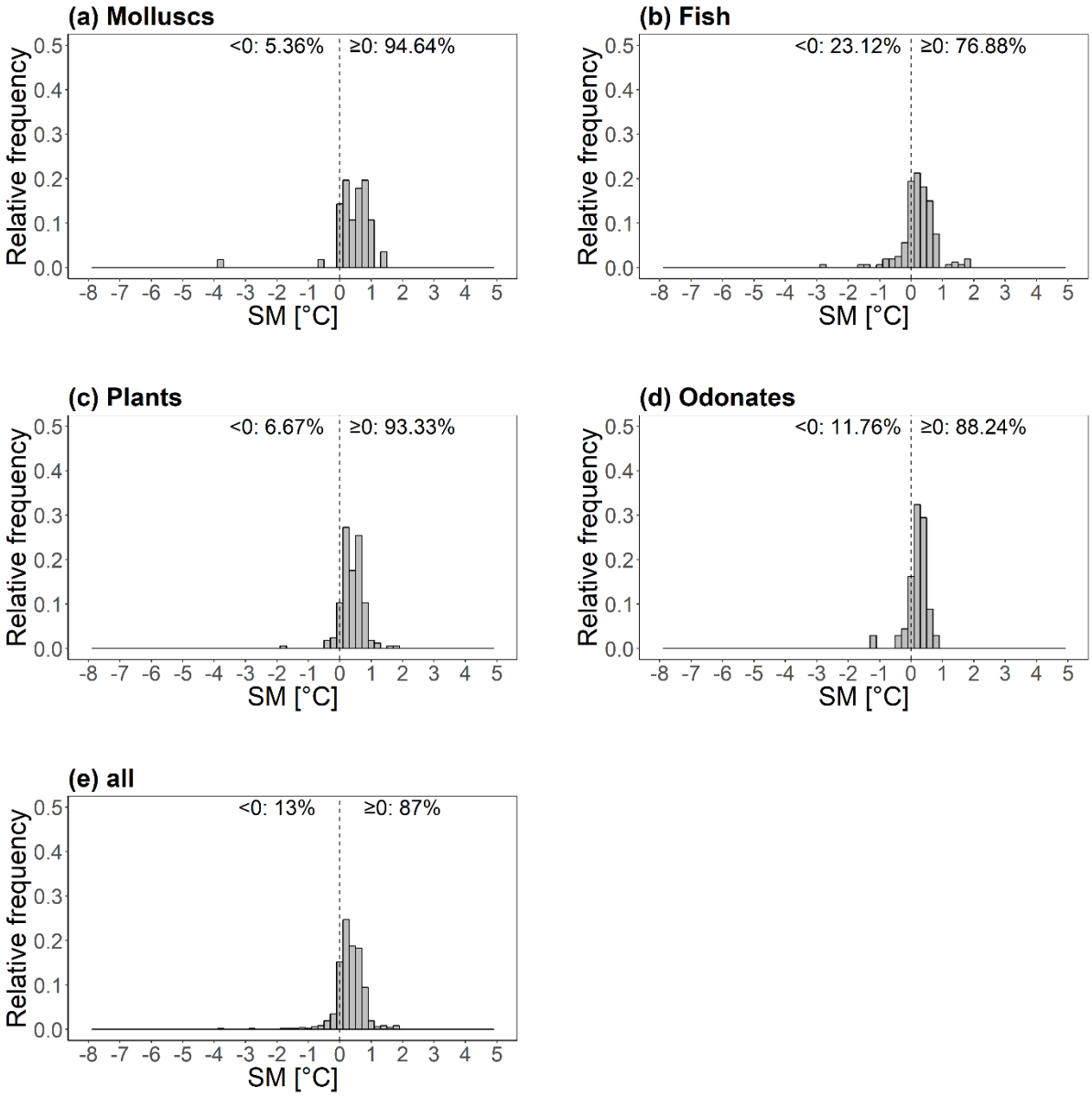

Fig. S1.13 Relative frequencies of the safety margin (SM = T_{pref} – T_{av}) distribution of unimodal species for (a) molluscs, (b) fishes, (c) plants, (d) odonates, and (e) all taxonomic groups combined inferred from $Tmean_{water}$. The dotted line at 0°C separates negative and positive SMs with the relative frequency of the species of the corresponding taxonomic group having a negative or positive SM at the upper end. Note that crayfish were excluded because of the low frequency of analyzed species.

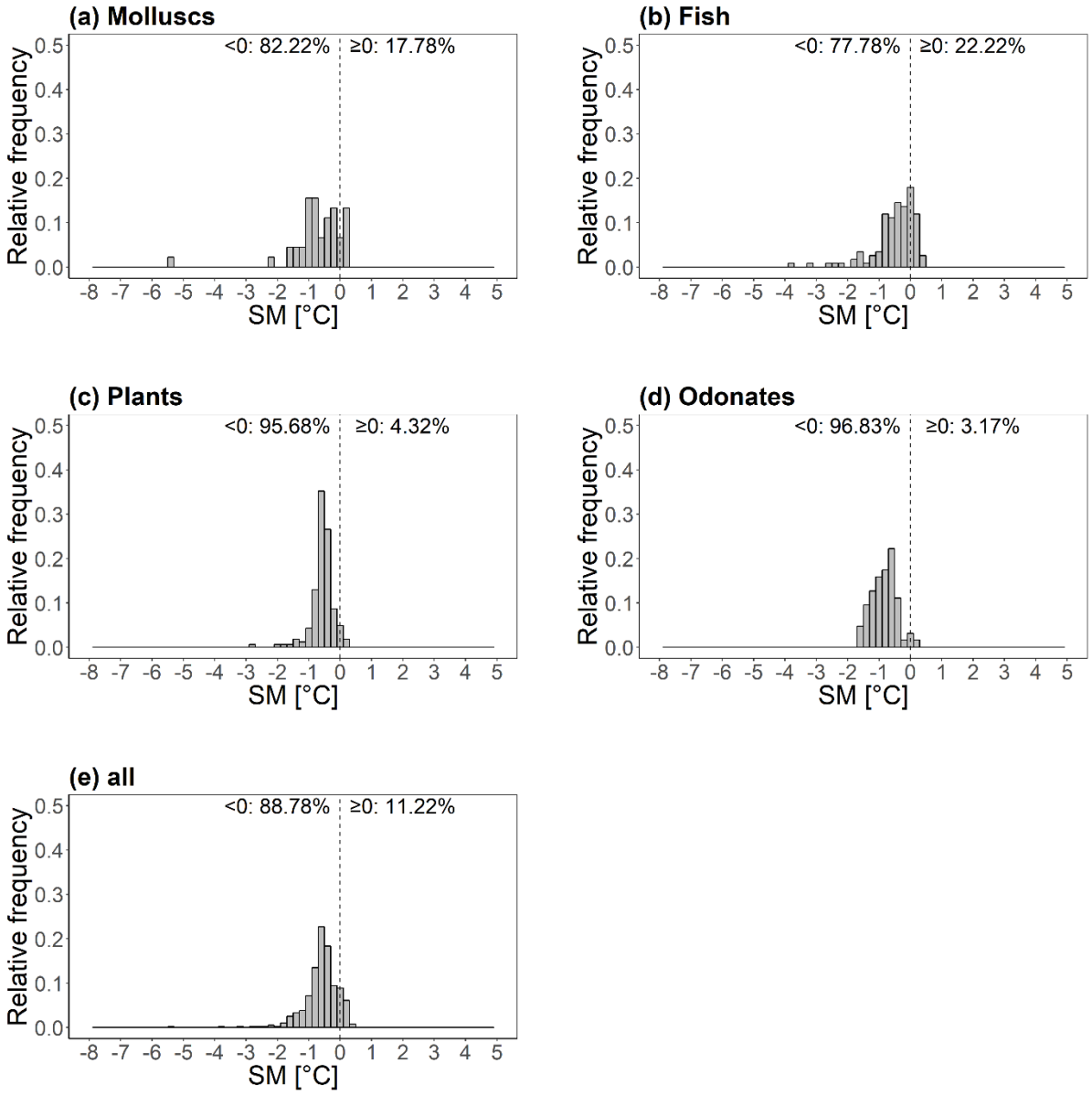

Fig. S1.14 Relative frequencies of the safety margin (SM = T_{pref} – T_{av}) distribution of unimodal species for (a) molluscs, (b) fishes, (c) plants, (d) odonates, and (e) all taxonomic groups combined inferred from $Tmax_{water}$. The dotted line at 0°C separates negative and positive SMs with the relative frequency of the species of the corresponding taxonomic group having a negative or positive SM at the upper end. Note that crayfish were excluded because of the low frequency of analyzed species.

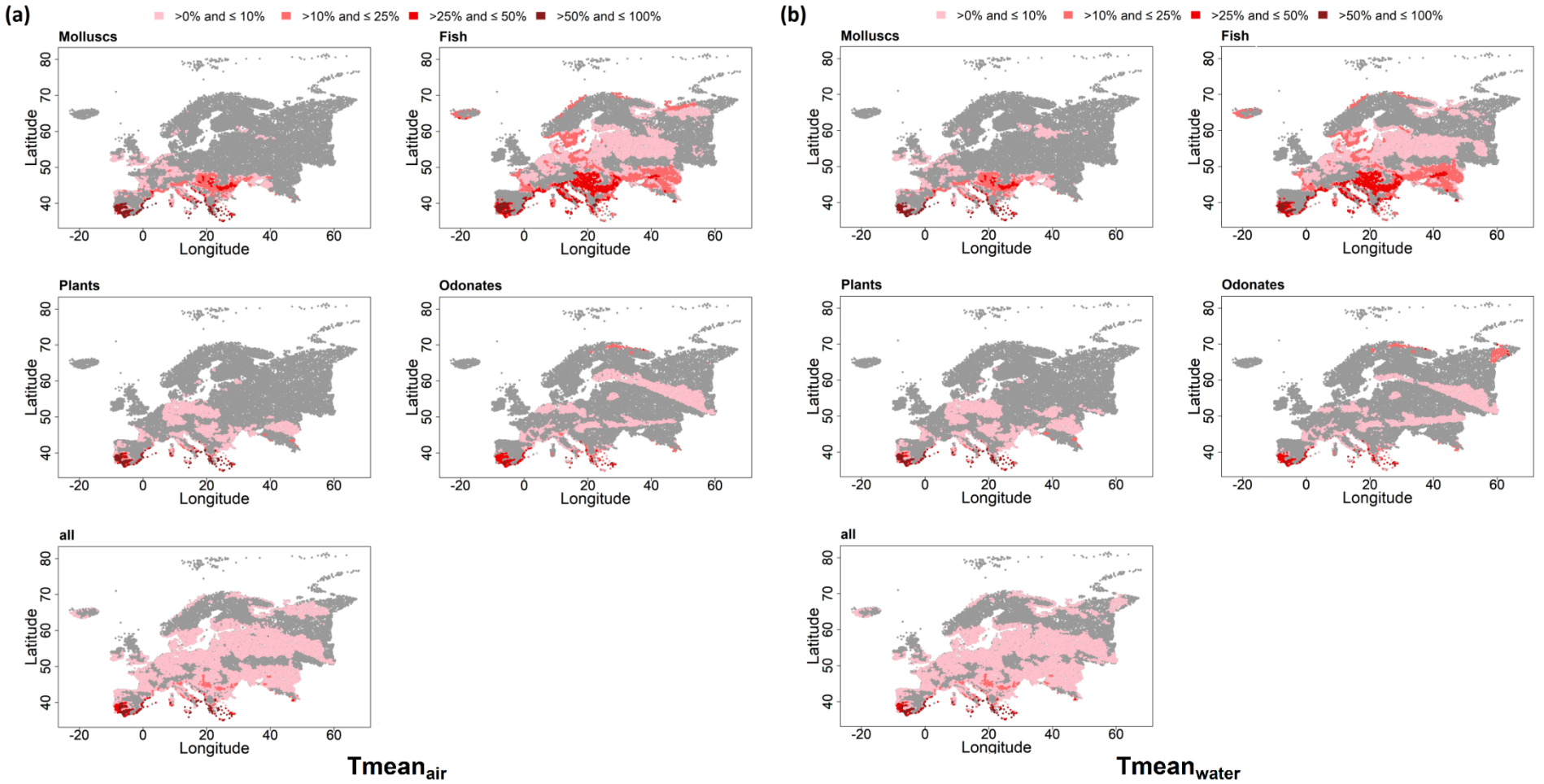

Fig. S1.15 Comparison of the relative frequency per catchment of species with the critical maximum temperature (CT) inferred from (a) $Tmean_{air}$ and (b) $Tmean_{water}$ that is exceeded by the averaged projected temperature of the three climate models MOHC, IPSL and MPI for the 2050s. The grey area represents either no occurrence or catchments in which the CT, i.e. the maximum temperature of a species' occurrence, is not exceeded by the projected temperatures. Note that crayfish were excluded because of the low frequency of analyzed species.

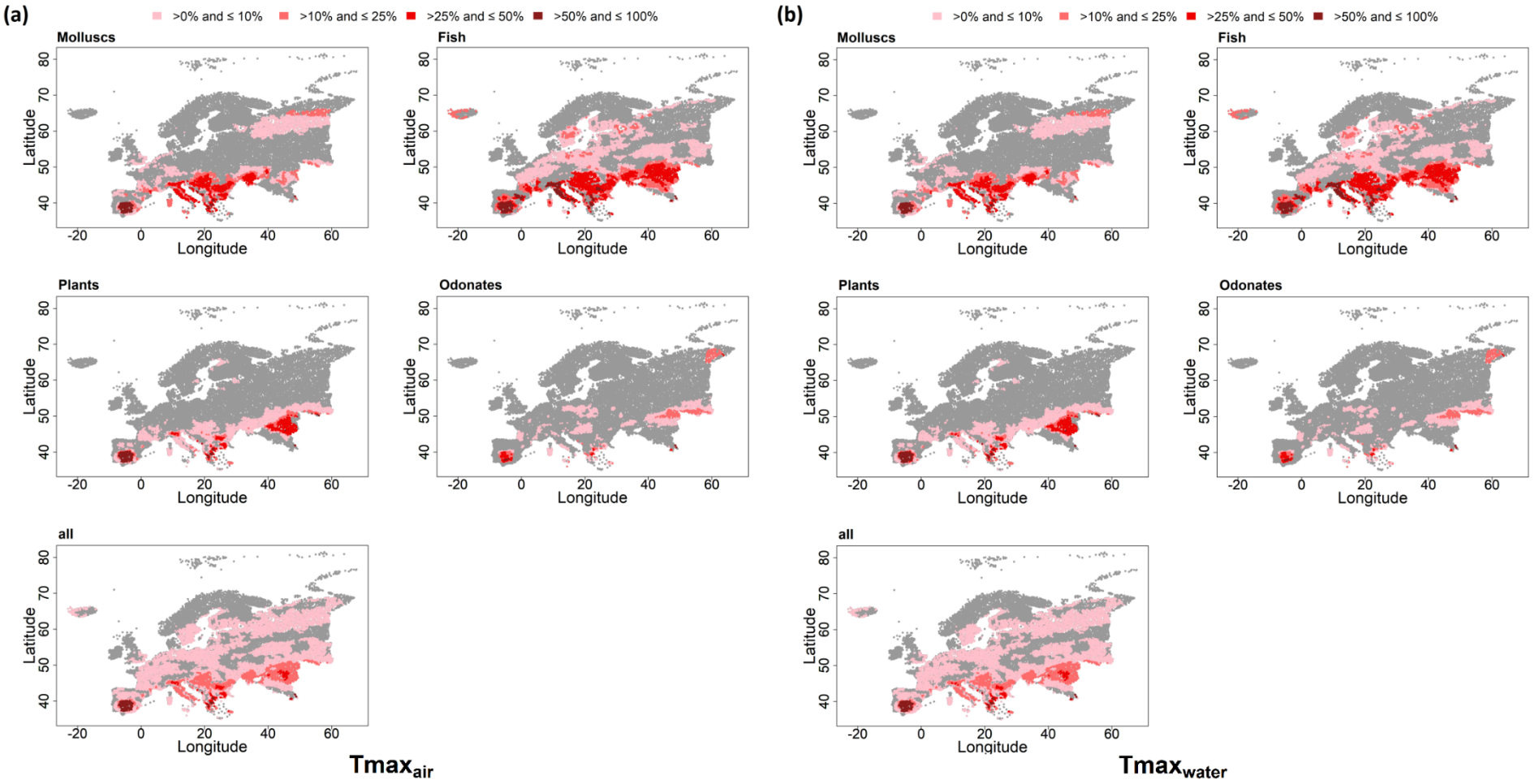

Fig. S1.16 Comparison of the relative frequency per catchment of species with the critical maximum temperature (CT) inferred from (a) $Tmax_{air}$ and (b) $Tmax_{water}$ that is exceeded by the averaged projected temperature of the three climate models MOHC, IPSL and MPI for the 2050s. The grey area represents either no occurrence or catchments in which the CT, i.e. the maximum temperature of a species' occurrence, is not exceeded by the projected temperatures. Note that crayfish were excluded because of the low frequency of analyzed species.

Table S1.1 Pairwise Pearson correlation coefficients among the used temperature variables ($Tmean_{air}$ – Annual mean air temperature; $Tmax_{air}$ – Maximum air temperature of the warmest month; $Tmean_{water}$ – Annual mean water temperature; $Tmax_{water}$ – Maximum water temperature of the warmest month).

Variable	$Tmean_{air}$	$Tmax_{air}$	$Tmean_{water}$	$Tmax_{water}$
$Tmean_{air}$	1.00	0.88	0.98	0.86
$Tmax_{air}$		1.00	0.86	0.96
$Tmean_{water}$			1.00	0.81
$Tmax_{water}$				1.00

Table S1.2 Thermal responses according to the univariate GAM using the annual mean water temperature ($Tmean_{water}$) and the maximum water temperature of the warmest month ($Tmax_{water}$). n is the total number of species with the respective TRC and the corresponding percentage. Note that crayfish were excluded because of the low frequency of analyzed species.

No.	Thermal response curve type		Taxonomic groups							
			Molluscs		Fish		Plants		Odonates	
			$Tmean_{water}$	$Tmax_{water}$	$Tmean_{water}$	$Tmax_{water}$	$Tmean_{water}$	$Tmax_{water}$	$Tmean_{water}$	$Tmax_{water}$
I	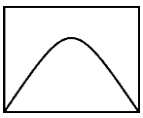	n	53	39	149	109	162	137	67	60
		%	53.5	39.4	67.7	49.5	91.0	77.0	89.3	80.0
II	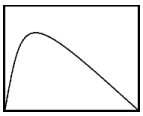	n	0	0	0	0	0	0	1	1
		%	0.0	0.0	0.0	0.0	0.0	0.0	1.3	1.3
III	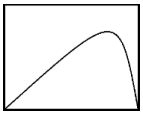	n	3	6	11	8	3	25	0	2
		%	3.0	6.1	5.0	3.6	1.7	14.0	0.0	2.7
IV	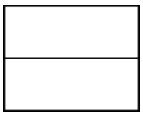	n	43	54	60	103	10	12	3	6
		%	43.4	54.5	27.3	46.8	5.6	6.7	4.0	8.0
V	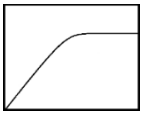	n	0	0	0	0	0	0	2	1
		%	0.0	0.0	0.0	0.0	0.0	0.0	2.7	1.3
VI	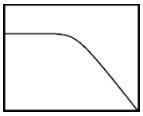	n	0	0	0	0	0	4	0	0
		%	0.0	0.0	0.0	0.0	0.0	2.2	0.0	0.0
VII	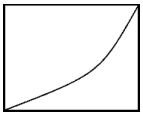	n	0	0	0	0	0	0	2	5
		%	0.0	0.0	0.0	0.0	0.0	0.0	2.7	6.7
VIII	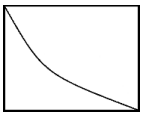	n	0	0	0	0	3	0	0	0
		%	0.0	0.0	0.0	0.0	1.7	0.0	0.0	0.0
$\sum$			99		220		178		75	

Appendix 4: Supporting information of Part II, Chapter 6

European vs. global analyses of species' thermal response curves: pessimistic or optimistic regarding species' future?

Supplementary text

Statistical model

The validation mean AUC and TSS values with $0.82 \leq AUC \leq 0.99$ and $0.47 \leq TSS \leq 0.92$ were moderate to high for both the global and European scale (Table S3). The uncertainty of the modelled occurrence probabilities was low for global scale models; however, uncertainty increased to the lower edges of the thermal gradient for European scale models, especially for *Coregonus sardinella*, *Pungitius pungitius* and *Salvelinus alpinus* (Fig. 1).

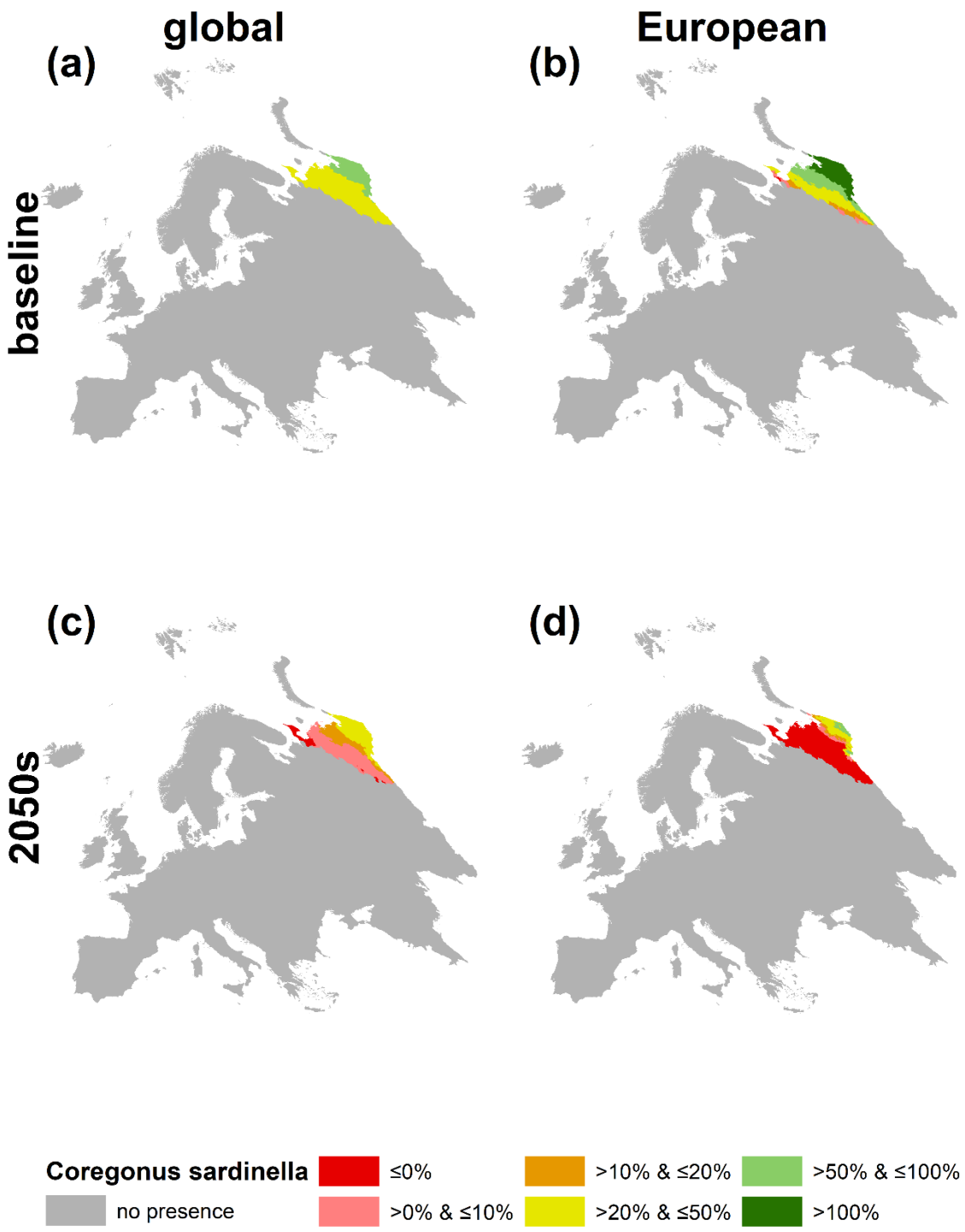

Fig. S1 Percentage of the remaining warming tolerance (WT) for the (a, c) global and (b, d) European distribution of *Coregonus sardinella*. (a, b) and (c, d) represent the percentage for the baseline and 2050s scenario, respectively. The percentage for a species and a catchment *i* was calculated as $\frac{T_{max}-T_{scenario,i}}{WT}$, whereas T_{max} is the maximum temperature of the species' distribution range either extracted from global or European data. Warming tolerance was computed as the difference between T_{max} and the preferred temperature deduced from the respective scale.

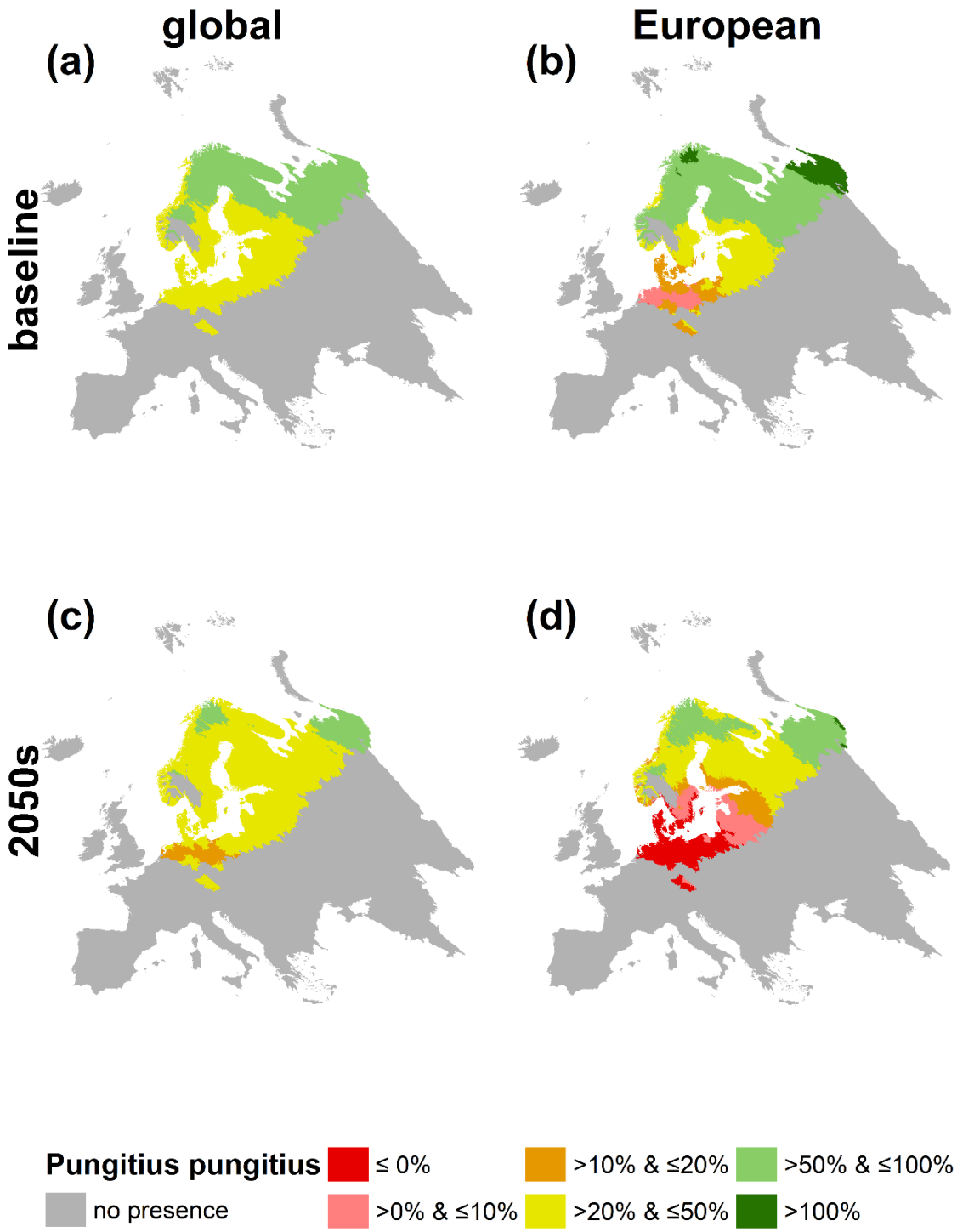

Fig. S2 Percentage of the remaining warming tolerance (WT) for the (a, c) global and (b, d) European distribution of *Pungitius pungitius*. (a, b) and (c, d) represent the percentage for the baseline and 2050s scenario, respectively. The percentage for a species and a catchment *i* was calculated as $\frac{T_{max}-T_{scenario,i}}{WT}$, whereas T_{max} is the maximum temperature of the species' distribution range either extracted from global or European data. Warming tolerance was computed as the difference between T_{max} and the preferred temperature deduced from the respective scale.

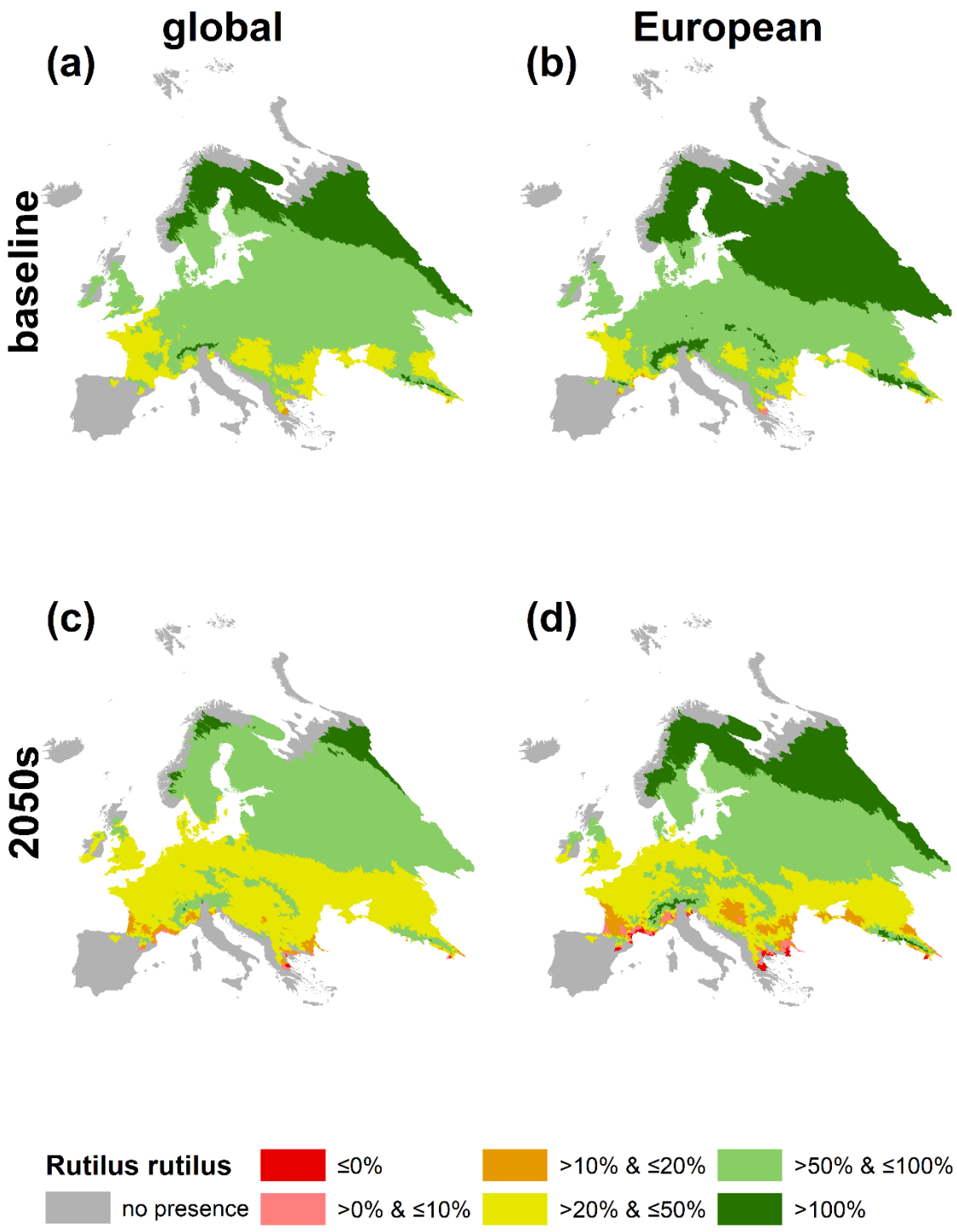

Fig. S3 Percentage of the remaining warming tolerance (WT) for the (a, c) global and (b, d) European distribution of *Rutilus rutilus*. (a, b) and (c, d) represent the percentage for the baseline and 2050s scenario, respectively. The percentage for a species and a catchment *i* was calculated as $\frac{T_{max}-T_{scenario,i}}{WT}$, whereas T_{max} is the maximum temperature of the species' distribution range either extracted from global or European data. Warming tolerance was computed as the difference between T_{max} and the preferred temperature deduced from the respective scale.

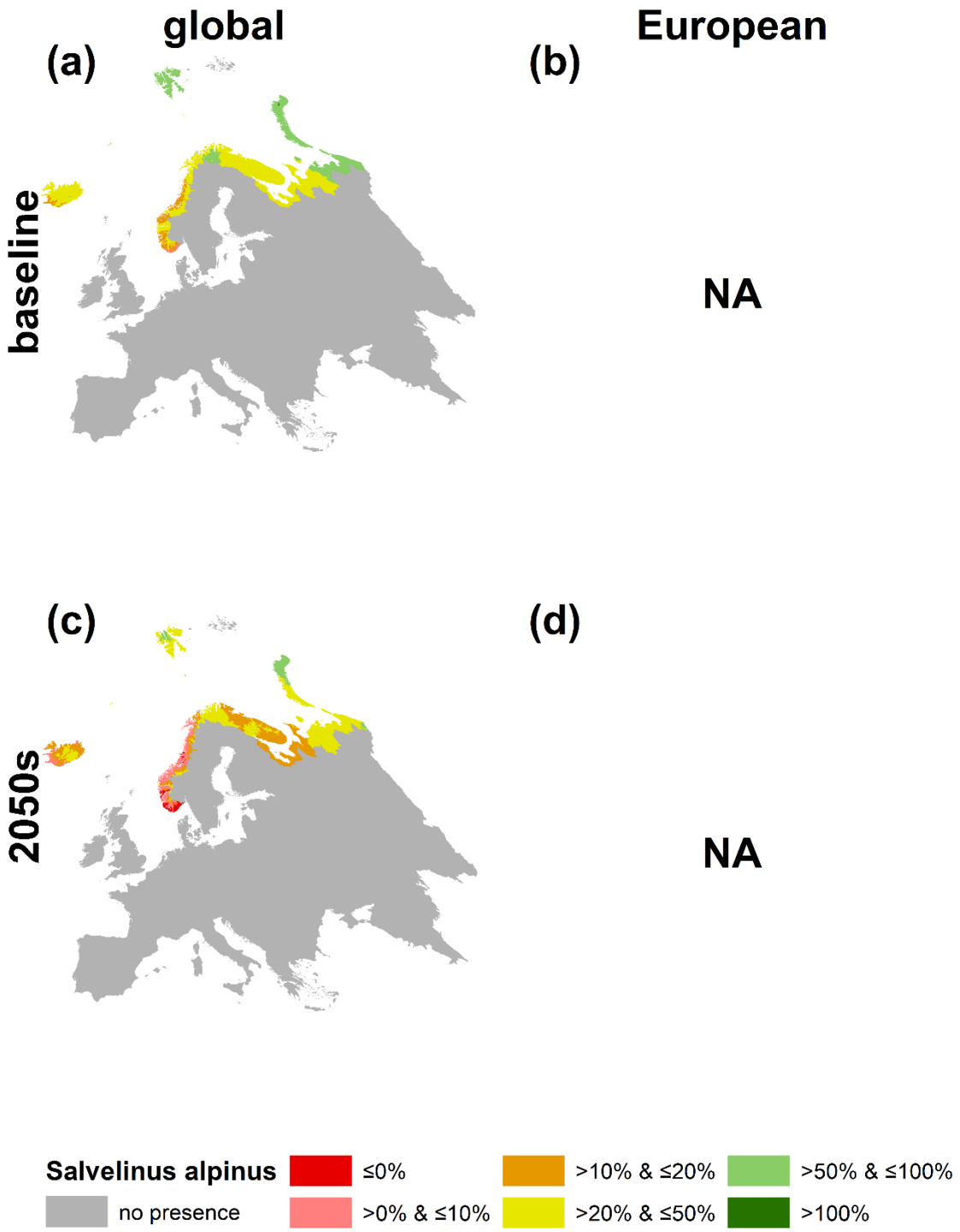

Fig. S4 Percentage of the remaining warming tolerance (WT) for the (a, c) global and (b, d) European distribution of *Salvelinus alpinus*. (a, b) and (c, d) represent the percentage for the baseline and 2050s scenario, respectively. The percentage for a species and a catchment *i* was calculated as $\frac{T_{max}-T_{scenario,i}}{WT}$, whereas T_{max} is the maximum temperature of the species' distribution range either extracted from global or European data. Warming tolerance was computed as the difference between T_{max} and the preferred temperature deduced from the respective scale.

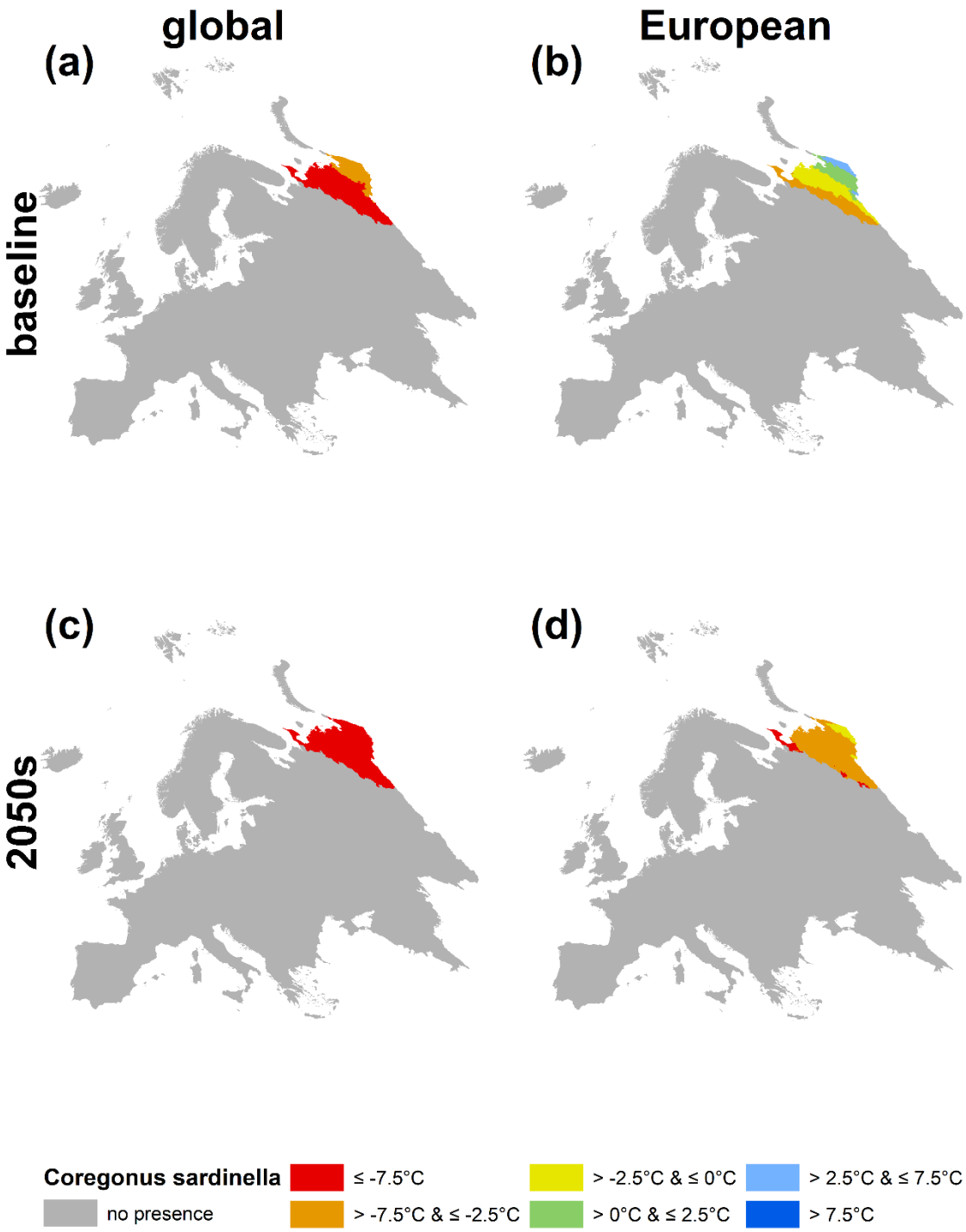

Fig. S5 Catchment-specific safety margins (SMs) for the (a, c) global and (b, d) European analysis of *Coregonus sardinella*. (a, b) and (c, d) represent the results for the baseline and 2050s scenario, respectively. The catchment-specific safety margin for a species and a catchment *i* was calculated as $T_{pref} - T_{scenario,i}$, whereas T_{pref} is the preferred temperature of the species either extracted from the global or European thermal response curve.

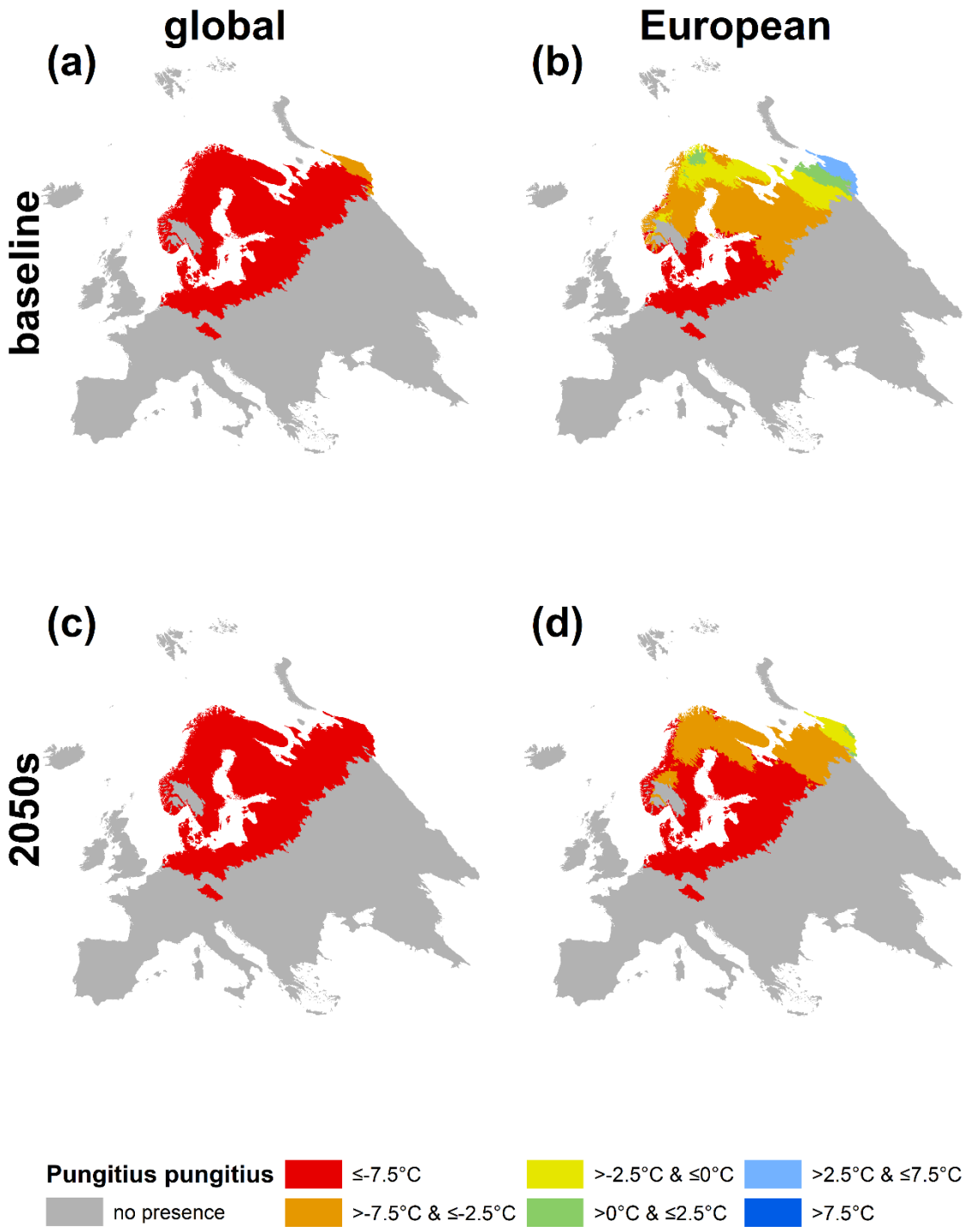

Fig. S6 Catchment-specific safety margins (SMs) for the (a, c) global and (b, d) European analysis of *Pungitius pungitius*. (a, b) and (c, d) represent the results for the baseline and 2050s scenario, respectively. The catchment-specific safety margin for a species and a catchment *i* was calculated as $T_{pref} - T_{scenario,i}$, whereas T_{pref} is the preferred temperature of the species either extracted from the global or European thermal response curve.

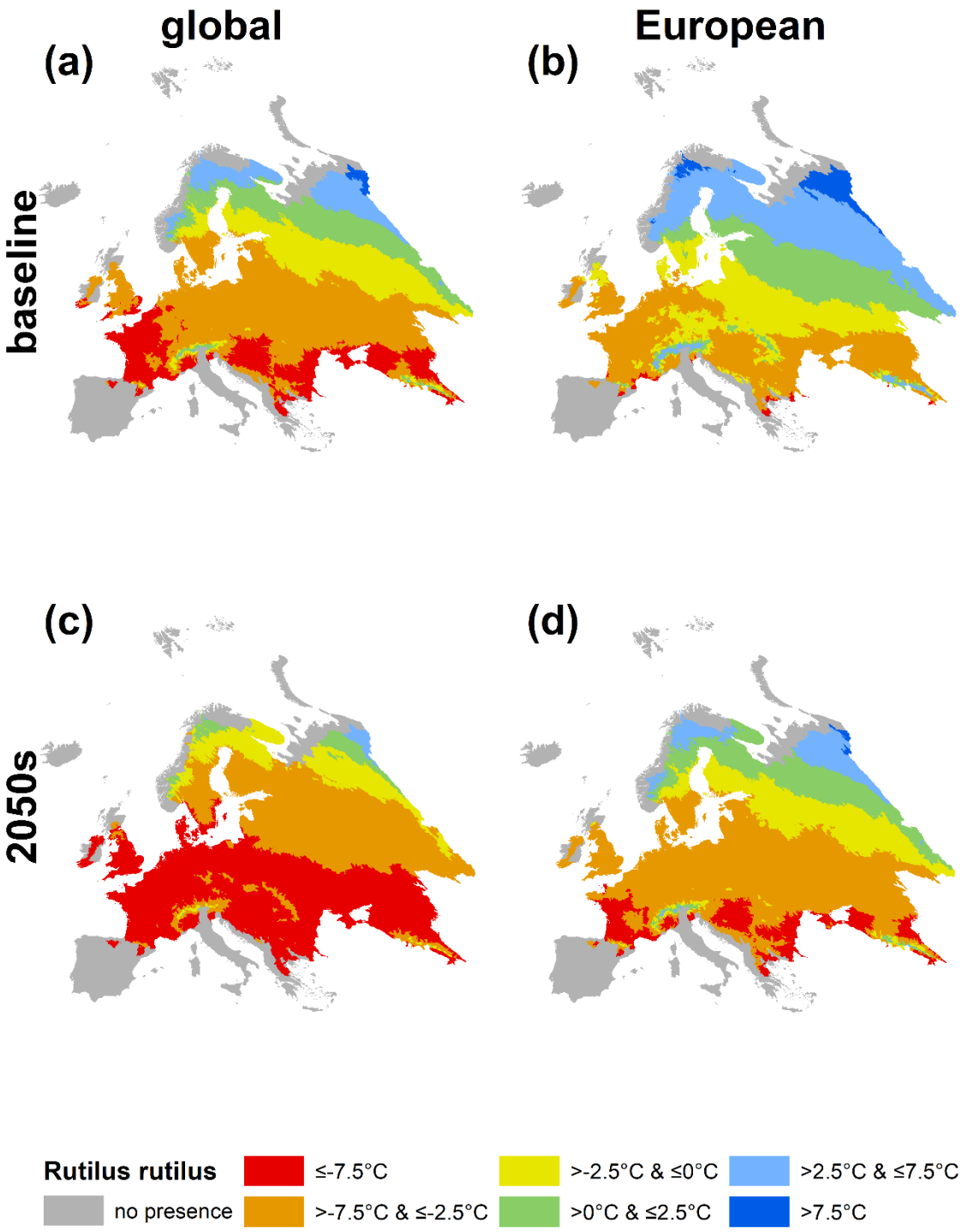

Fig. S7 Catchment-specific safety margins (SMs) for the (a, c) global and (b, d) European analysis of *Rutilus rutilus*. (a, b) and (c, d) represent the results for the baseline and 2050s scenario, respectively. The catchment-specific safety margin for a species and a catchment *i* was calculated as $T_{pref} - T_{scenario,i}$, whereas T_{pref} is the preferred temperature of the species either extracted from the global or European thermal response curve.

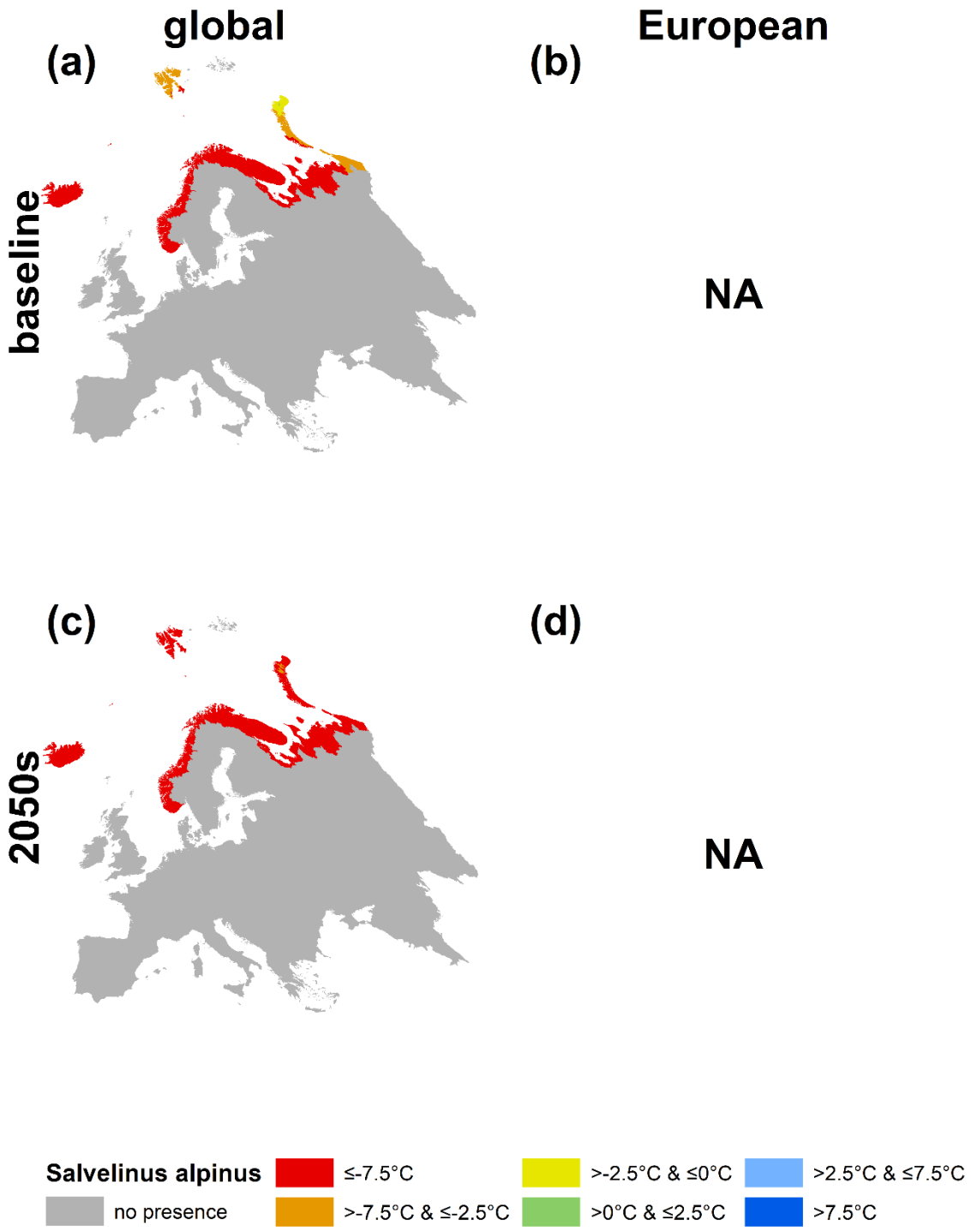

Fig. S8 Catchment-specific safety margins (SMs) for the (a, c) global and (b, d) European analysis of *Salvelinus alpinus*. (a, b) and (c, d) represent the results for the baseline and 2050s scenario, respectively. The catchment-specific safety margin for a species and a catchment *i* was calculated as $T_{pref} - T_{scenario,i}$, whereas T_{pref} is the preferred temperature of the species either extracted from the global or European thermal response curve.

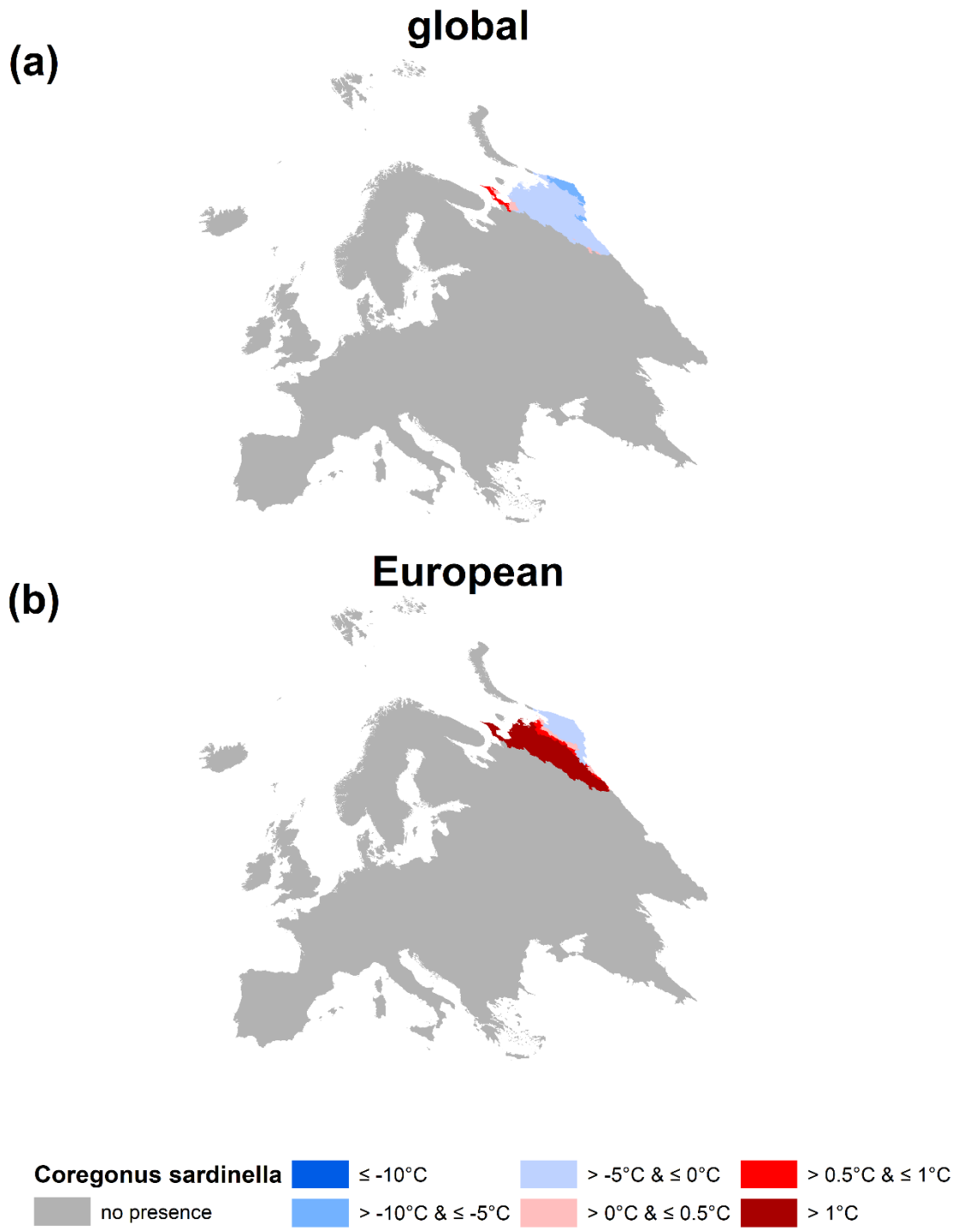

Fig. S9 Catchment-specific future climatic impact inferred from the (a) global and (b) European scale analysis for *Coregonus sardinella*. The impact was calculated as the difference between the projected temperature for the 2050s and T_{max}, the maximum temperature of the species' range at the respective scale.

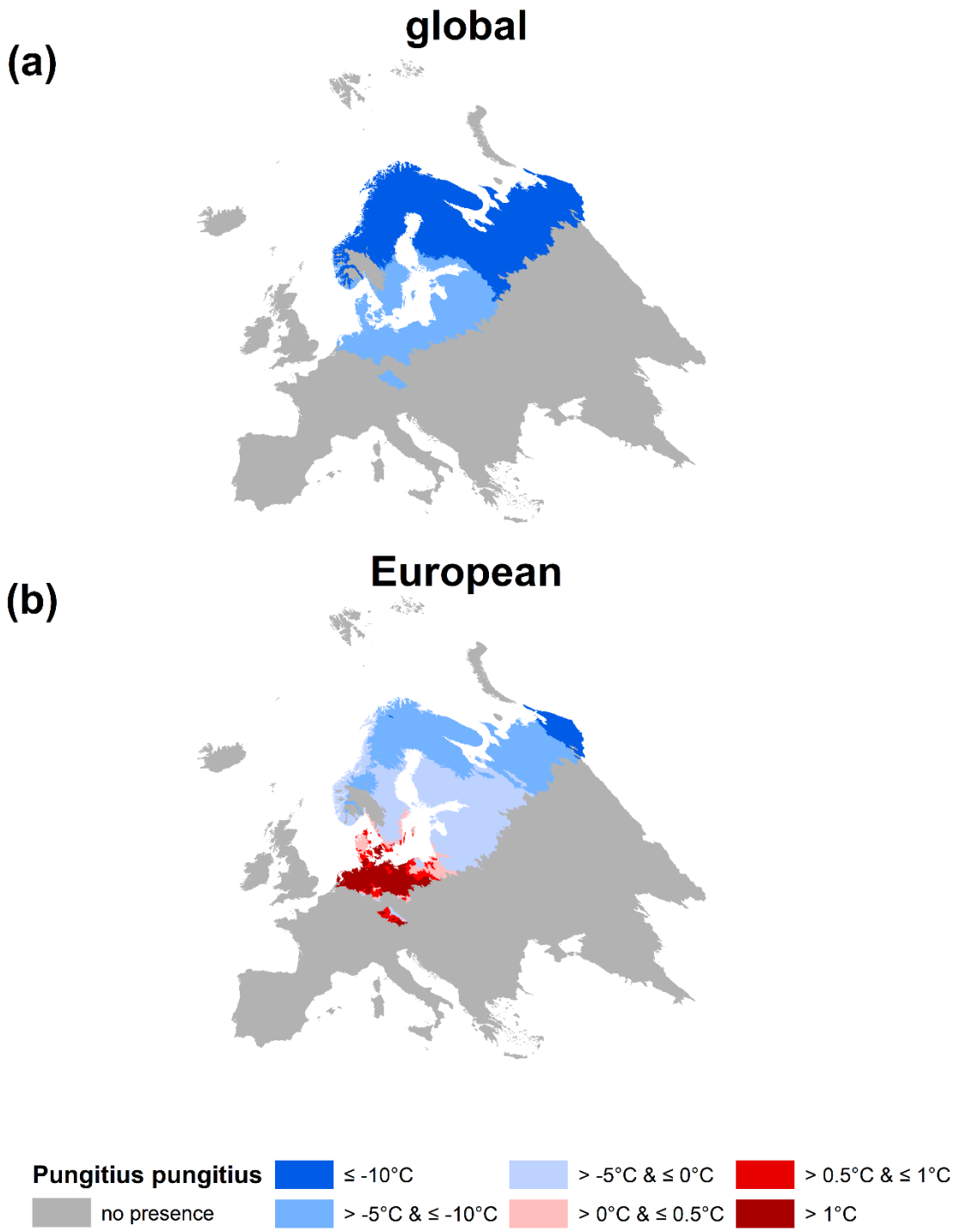

Fig. S10 Catchment-specific future climatic impact inferred from the (a) global and (b) European scale analysis for *Pungitius pungitius*. The impact was calculated as the difference between the projected temperature for the 2050s and T_{max}, the maximum temperature of the species' range at the respective scale.

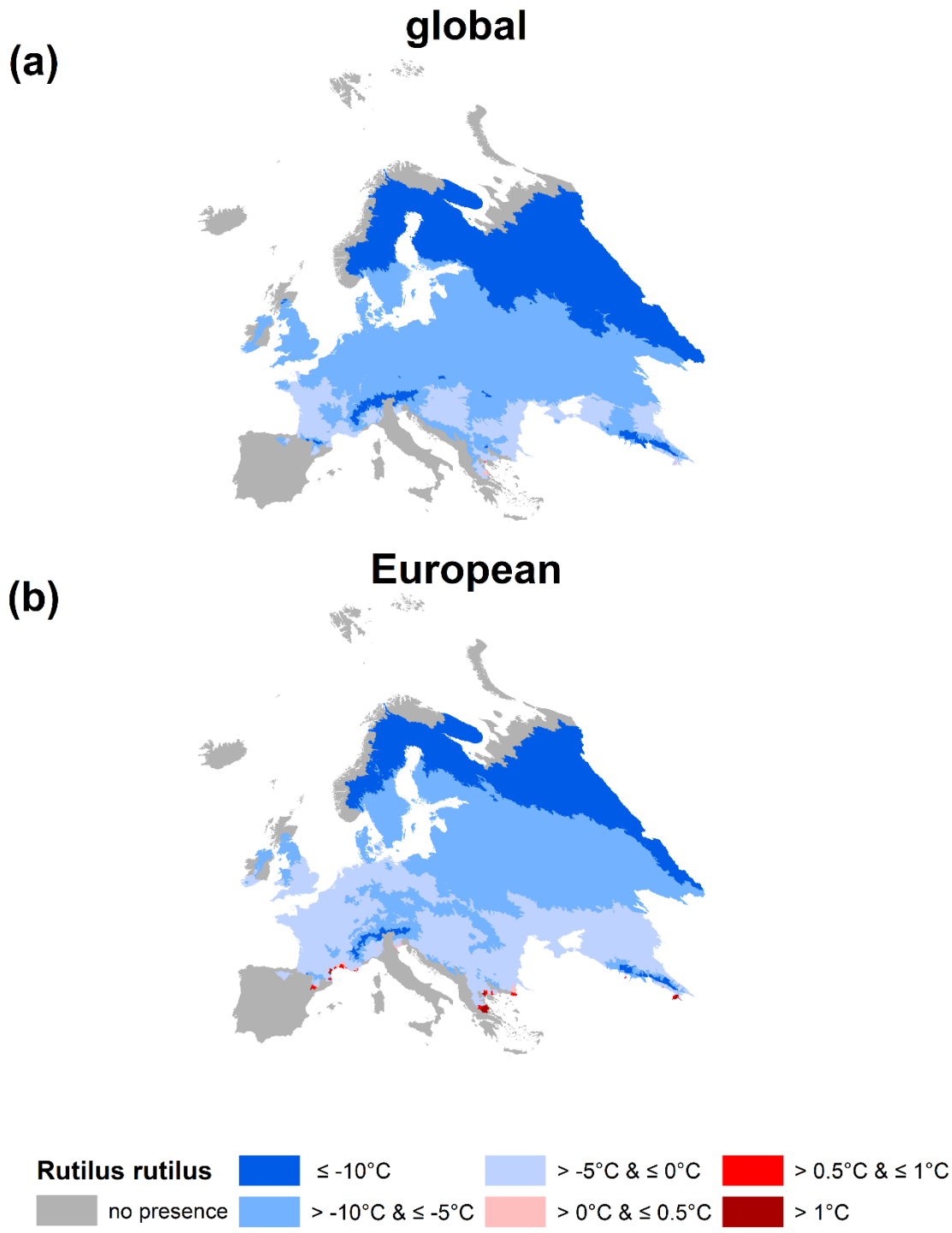

Fig. S11 Catchment-specific future climatic impact inferred from the (a) global and (b) European scale analysis for *Rutilus rutilus*. The impact was calculated as the difference between the projected temperature for the 2050s and T_{max}, the maximum temperature of the species' range at the respective scale.

Fig. S12 Catchment-specific future climatic impact inferred from the (a) global and (b) European scale analysis for *Salvelinus alpinus*. The impact was calculated as the difference between the projected temperature for the 2050s and T_{max}, the maximum temperature of the species' range at the respective scale.

Table S1 Data characteristics of the global and European data set.

Characteristic	Global data	European data
Catchment number	228,465	18,783
Temperature observations	228,064	18,767
Maximum temperature (°C)	31.9	18.4
Minimum temperature (°C)	-24.3	-14.7
Temperature range (°C)	56.2	33.1

Temperature characteristics refer to the annual mean air temperature.

Table S2 Occurrence numbers in the global and European data set without considering catchments with no available temperature data.

Species	Global data	European data	Difference
Coregonus sardinella	19,662	745	18,917
Pungitius pungitius	21,309	6,653	14,656
Rutilus rutilus	33,756	15,478	18,278
Salvelinus alpinus	17,055	1,778	15,277

Table S3 Accuracy measures from the model validation for global and European ranges.

Range	Accuracy measure (mean)	Species			
		Coregonus sardinella	*Pungitius pungitius*	*Rutilus rutilus*	*Salvelinus alpinus*
Global	AUC	0.95	0.86	0.82	0.91
	TSS	0.76	0.52	0.47	0.64
European	AUC	0.99	0.83	0.82	0.91
	TSS	0.92	0.47	0.48	0.65

The validation was conducted by bootstrapping, i.e. dividing the data into a calibration (80%) and validation data set (20%) 100 times. Mean accuracy measures were determined for the validation data set.

Appendix 5: Supporting information of Part II, Chapter 7

Combining species distribution modelling techniques with species thermal performance curves

Fig. S1 Global map of continental catchment regions. Only catchments with an area of >3000 km² were considered. The African region is displayed in brown colour, the Asian region in red, the Australian region in yellow, the European region in green, the North American region in blue and the South American region in orange.

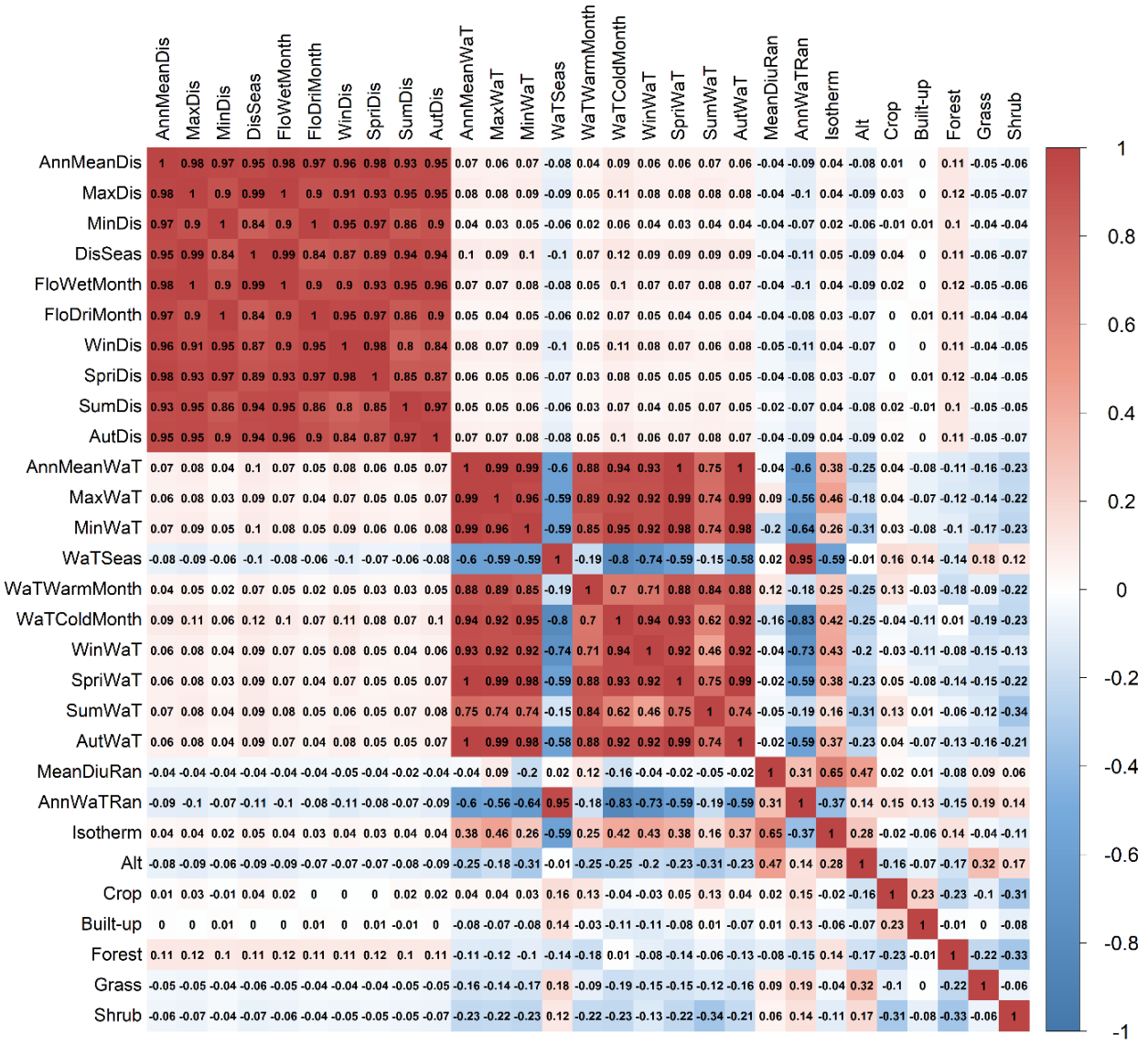

Fig. S2 Correlation matrix indicating the value of the pairwise Bravais-Pearson correlation coefficient of the environmental predictor variables.

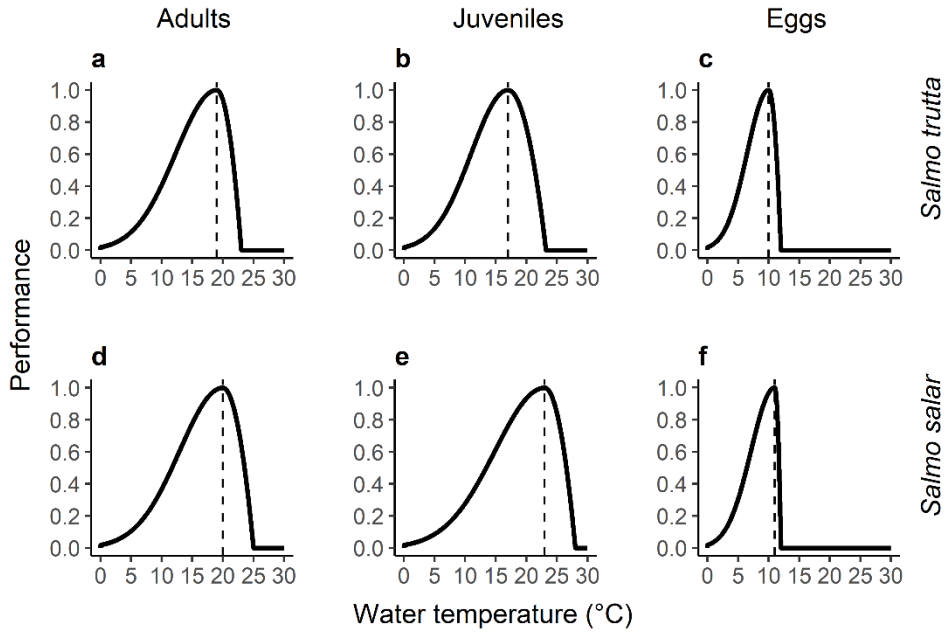

Fig. S3 Thermal performance curves for the life stages adults, juveniles and eggs of *Salmo trutta* (a-c) and *Salmo salar* (d-f). The dashed lines mark the optimum temperatures.

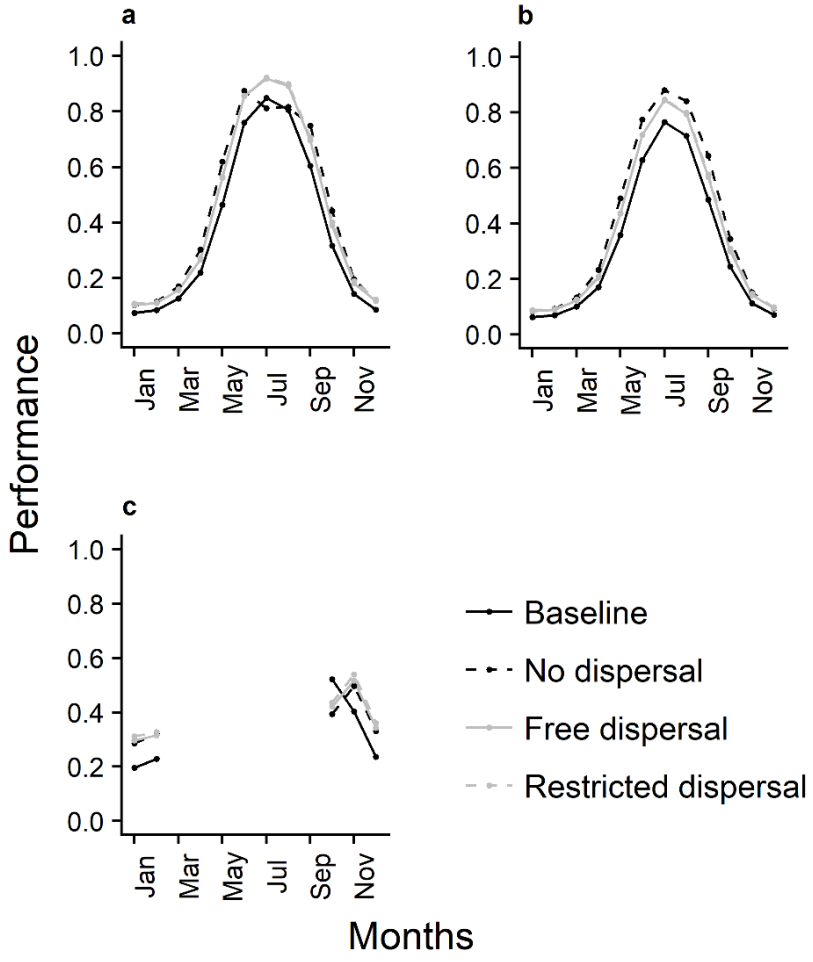

Fig. S4 Baseline and 2050s monthly mean performance for the life stages (a) adults, (b) juveniles and (c) eggs of *Salmo salar* under consideration of different dispersal scenarios in the northern hemisphere. Analyses of the southern hemisphere were excluded because of few observations.

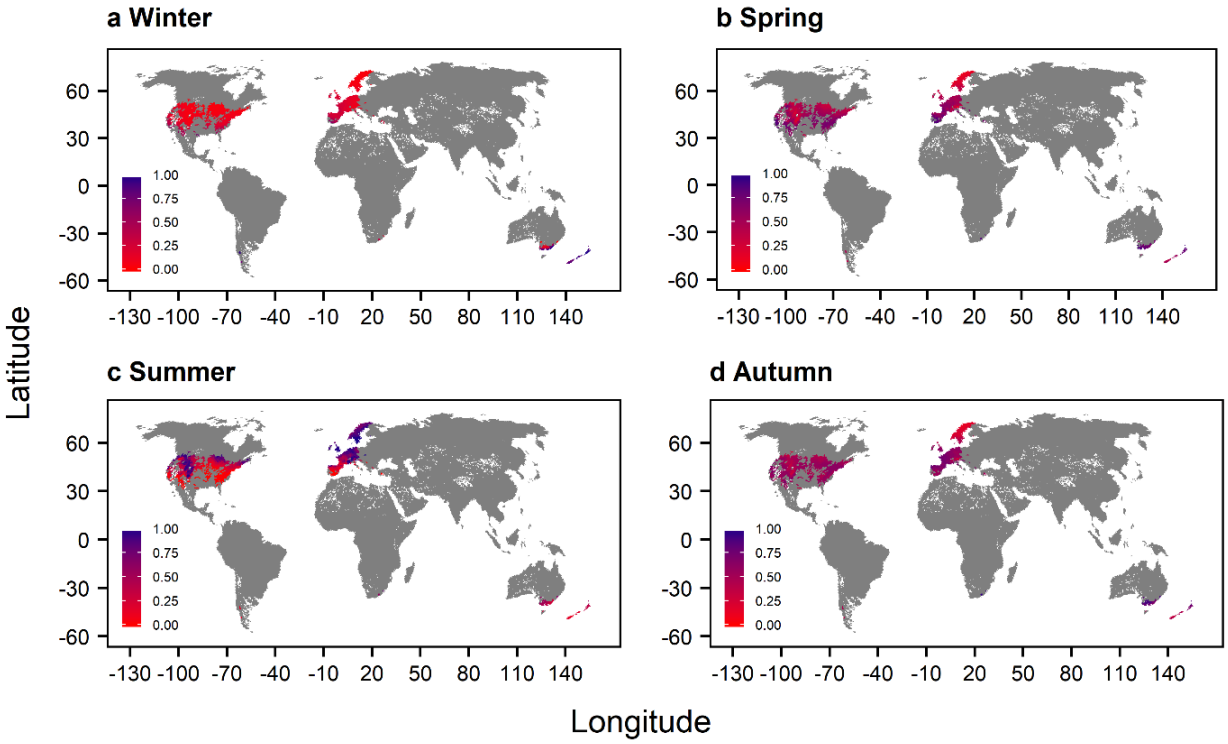

Fig. S5 Global map of the seasonal performances of adult *Salmo trutta* for the "no dispersal" scenario. Note that seasons were defined according to the northern hemisphere.

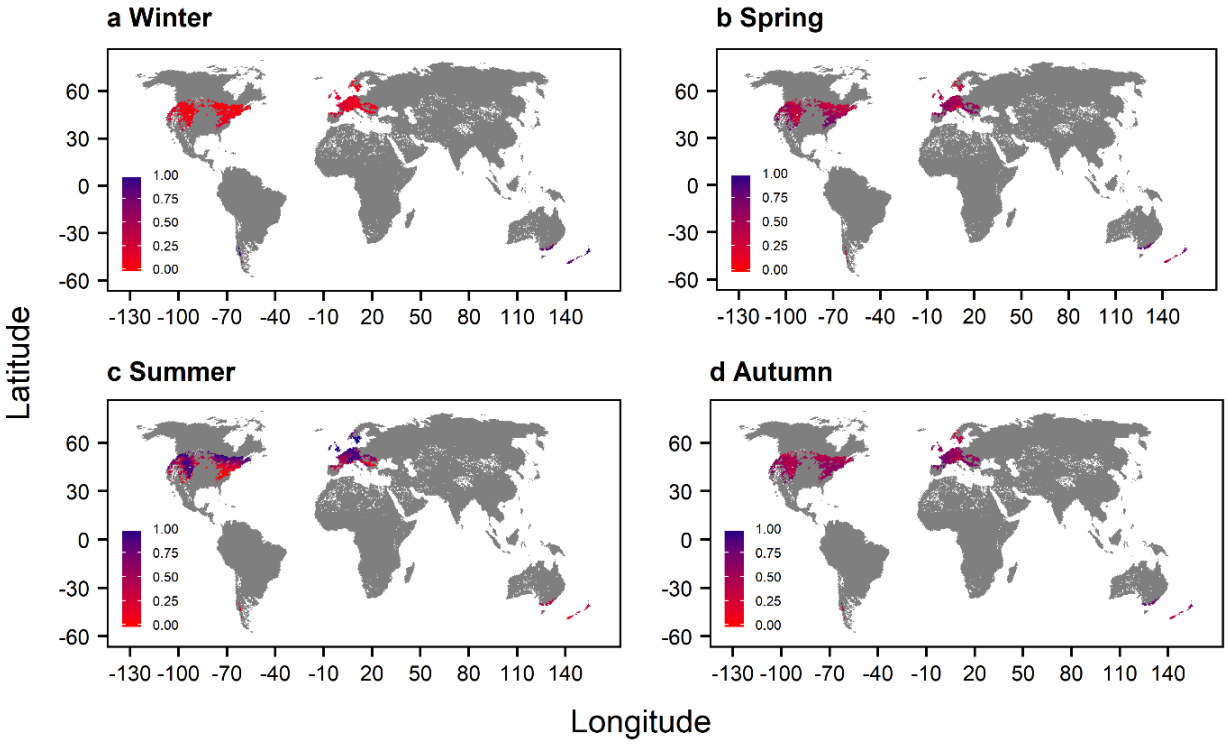

Fig. S6 Global map of the seasonal performances of adult *Salmo trutta* for the "free dispersal" scenario. Note that seasons were defined according to the northern hemisphere.

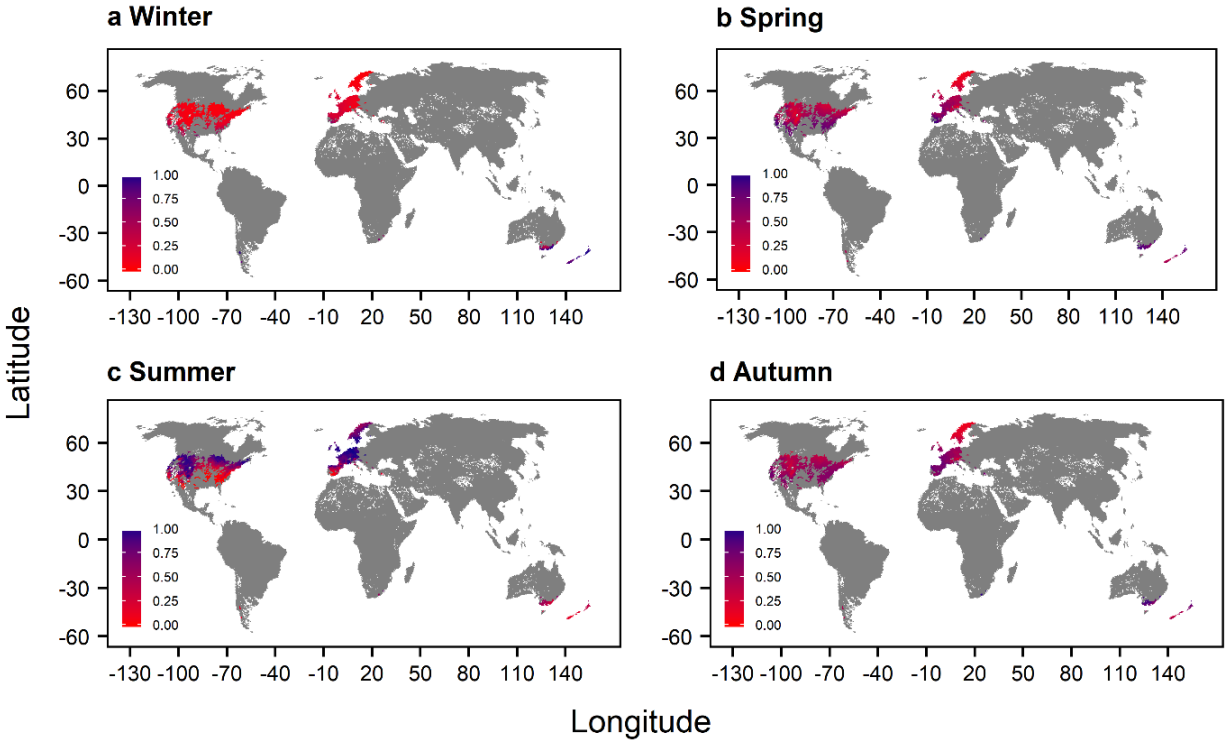

Fig. S7 Global map of the seasonal performances of juvenile *Salmo trutta* for the baseline scenario. Note that seasons were defined according to the northern hemisphere.

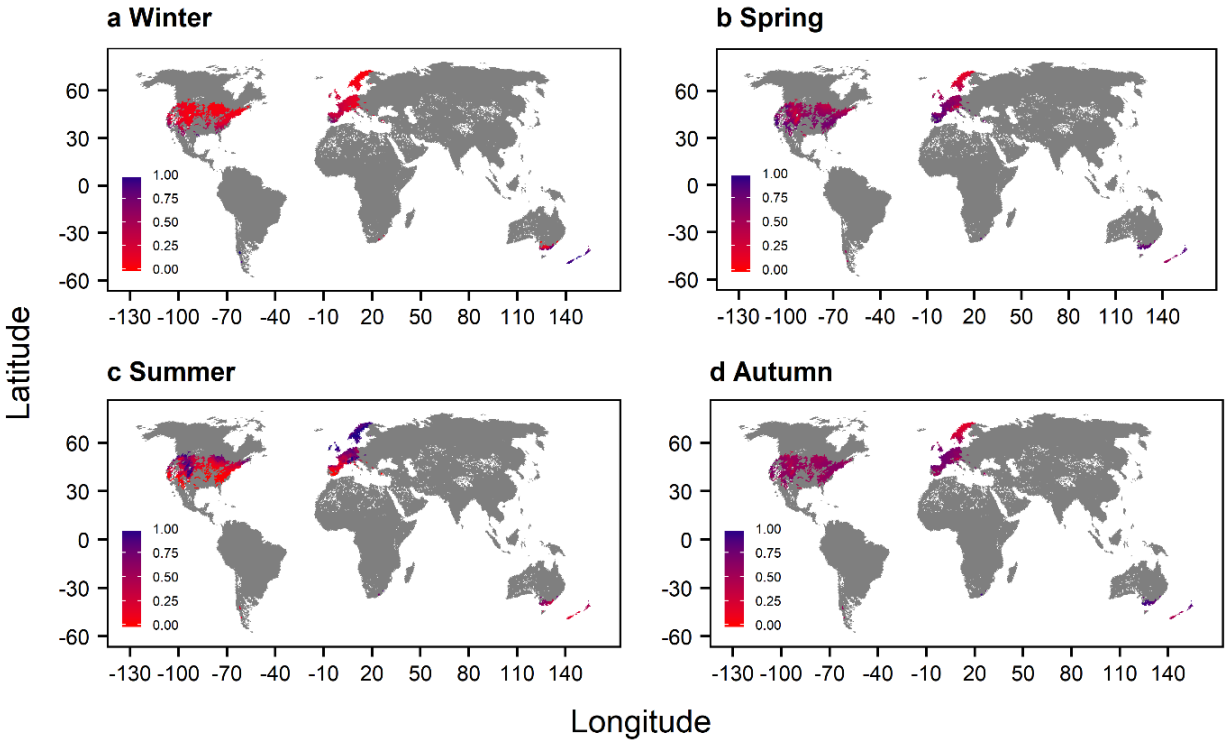

Fig. S8 Global map of the seasonal performances of juvenile *Salmo trutta* for the "no dispersal" scenario. Note that seasons were defined according to the northern hemisphere.

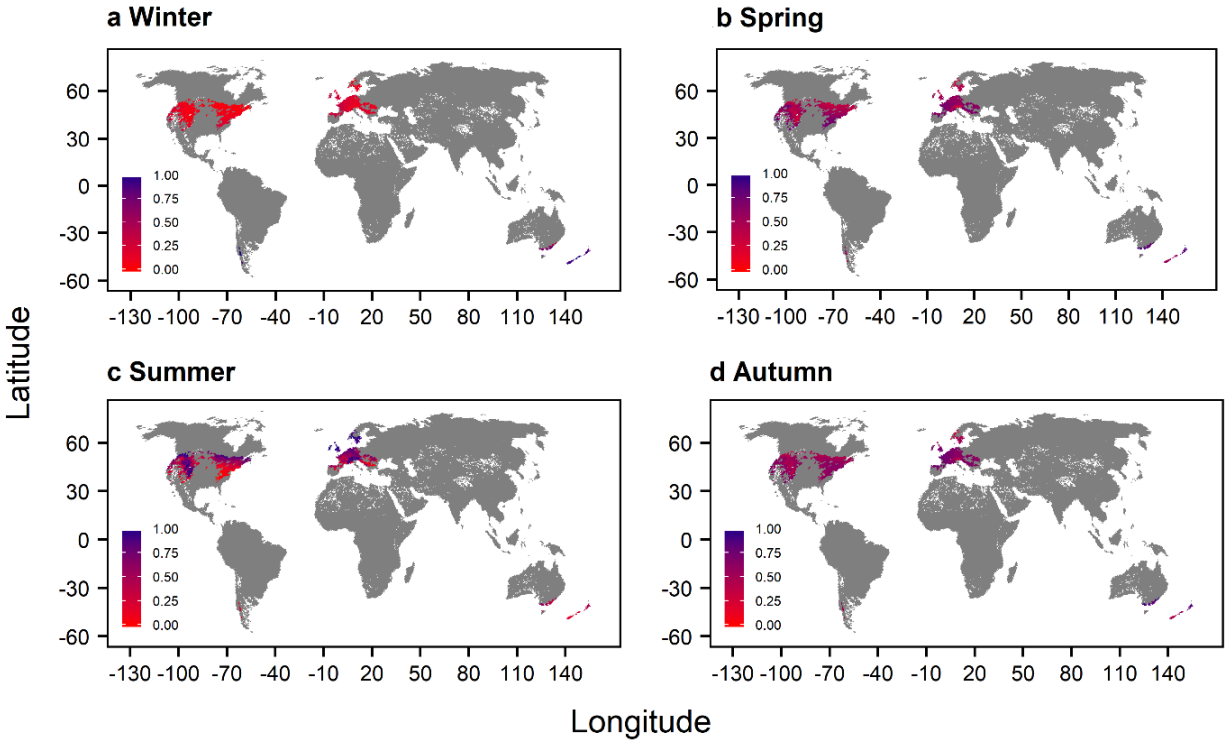

Fig. S9 Global map of the seasonal performances of juvenile *Salmo trutta* for the "free dispersal" scenario. Note that seasons were defined according to the northern hemisphere.

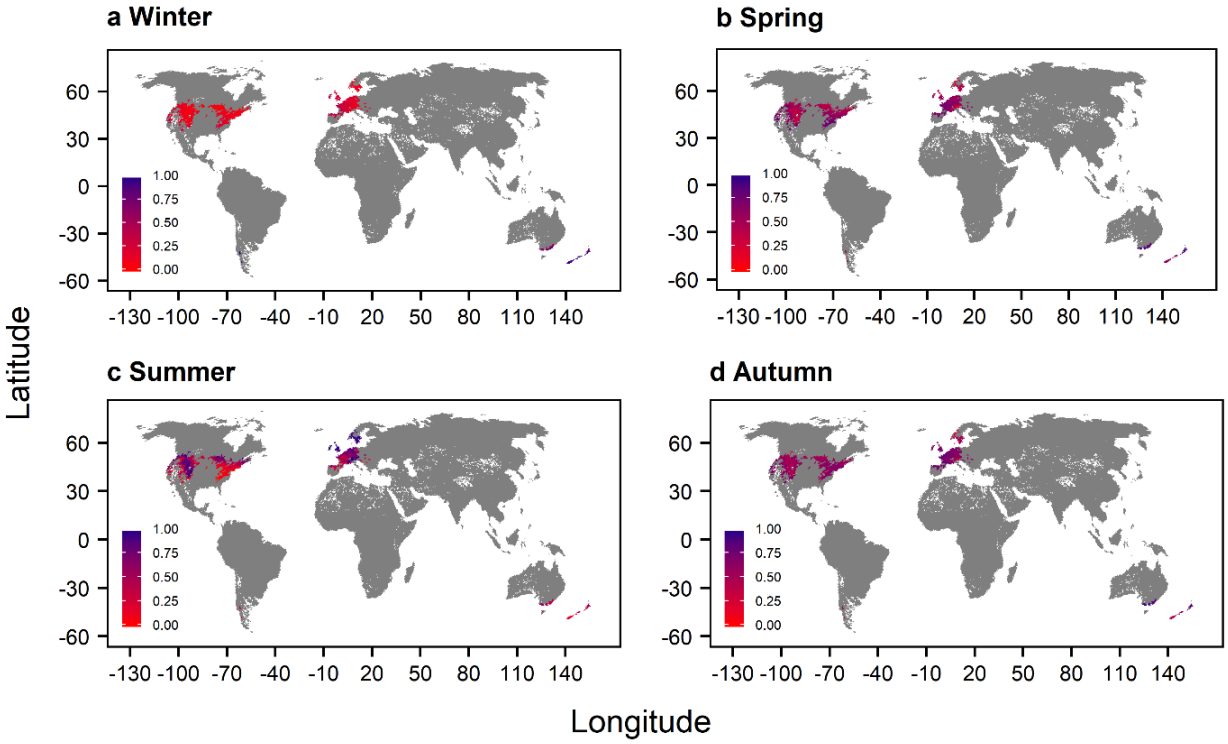

Fig. S10 Global map of the seasonal performances of juvenile *Salmo trutta* for the "restricted dispersal" scenario. Note that seasons were defined according to the northern hemisphere.

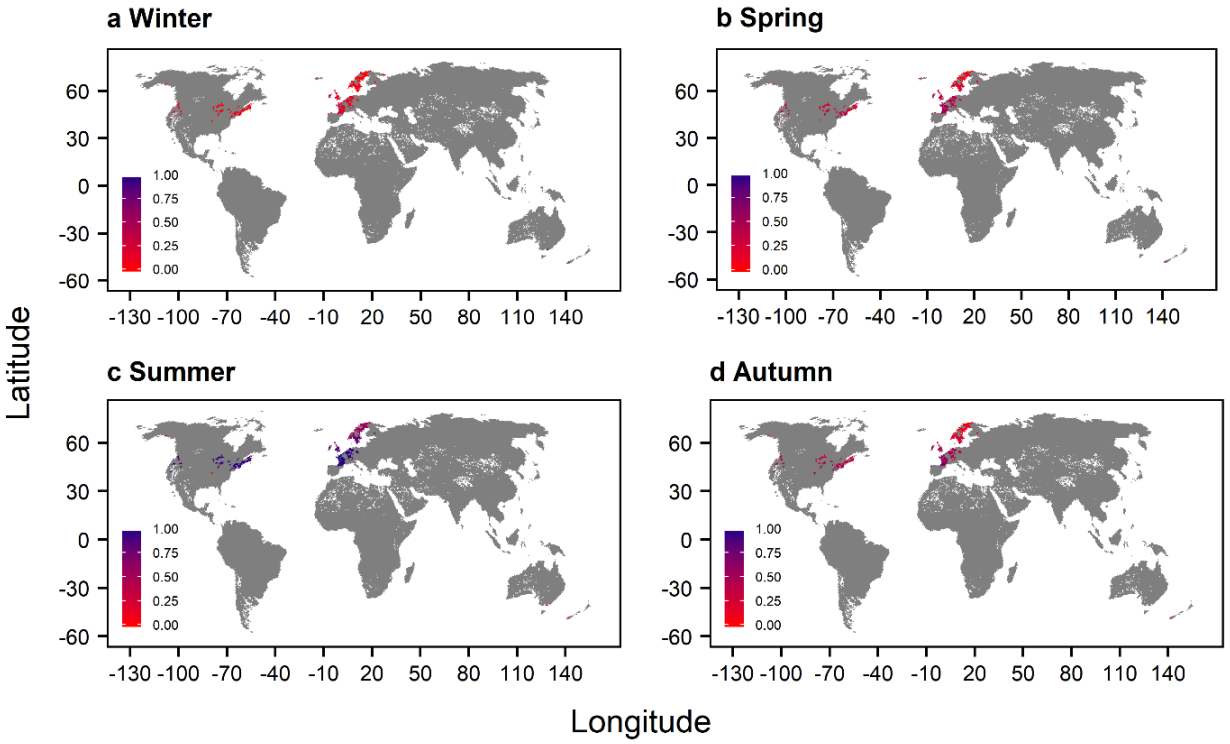

Fig. S11 Global map of the seasonal performances of adult *Salmo salar* for the baseline scenario. Note that seasons were defined according to the northern hemisphere.

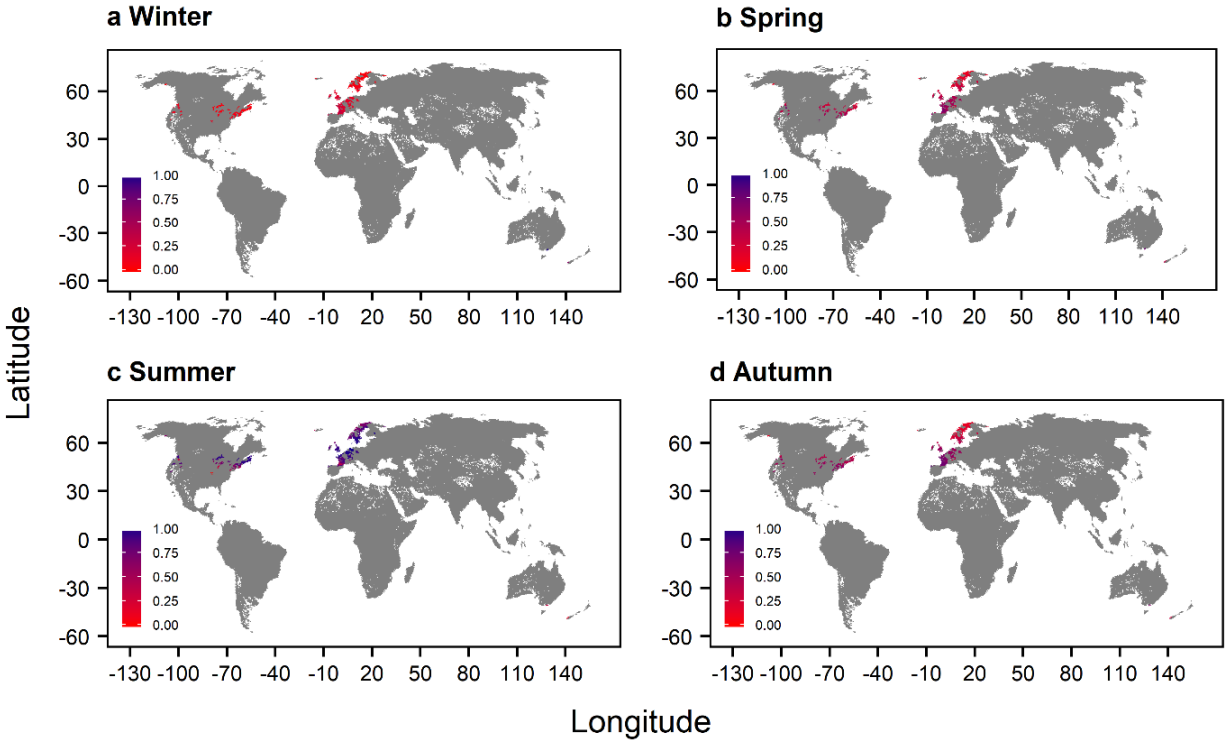

Fig. S12 Global map of the seasonal performances of adult *Salmo salar* for the "no dispersal" scenario. Note that seasons were defined according to the northern hemisphere.

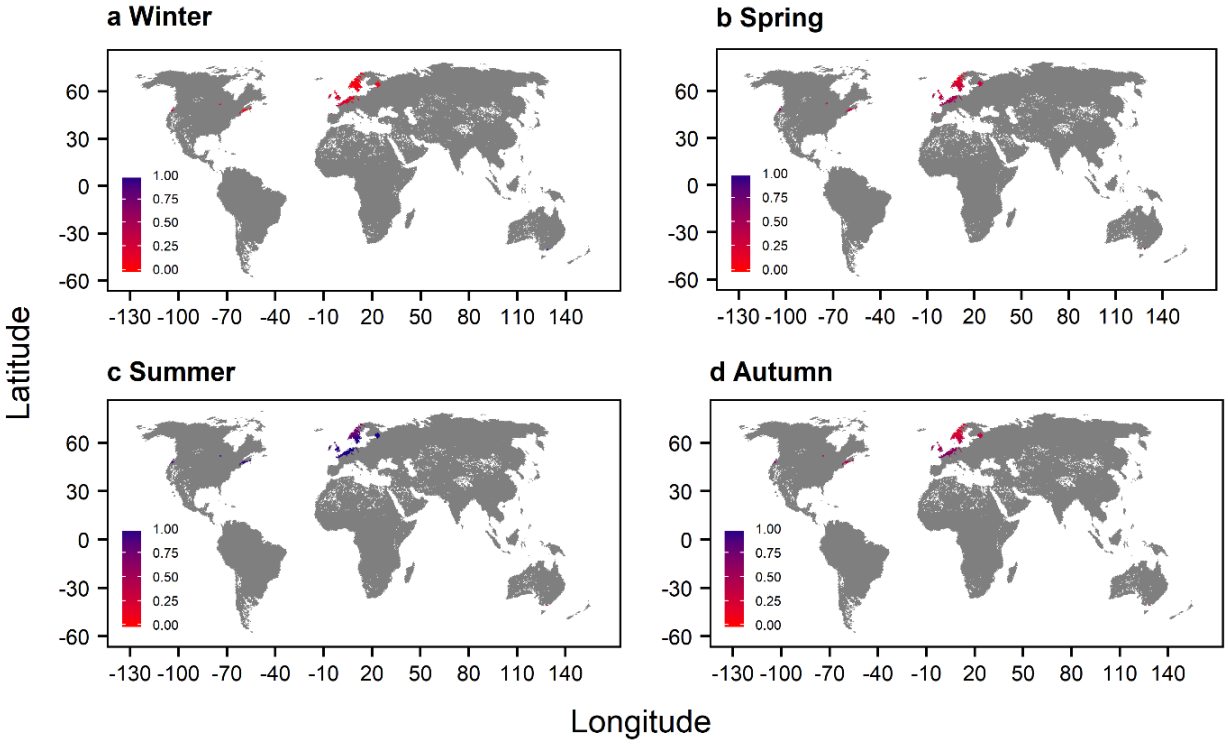

Fig. S13 Global map of the seasonal performances of adult *Salmo salar* for the "free dispersal" scenario. Note that seasons were defined according to the northern hemisphere.

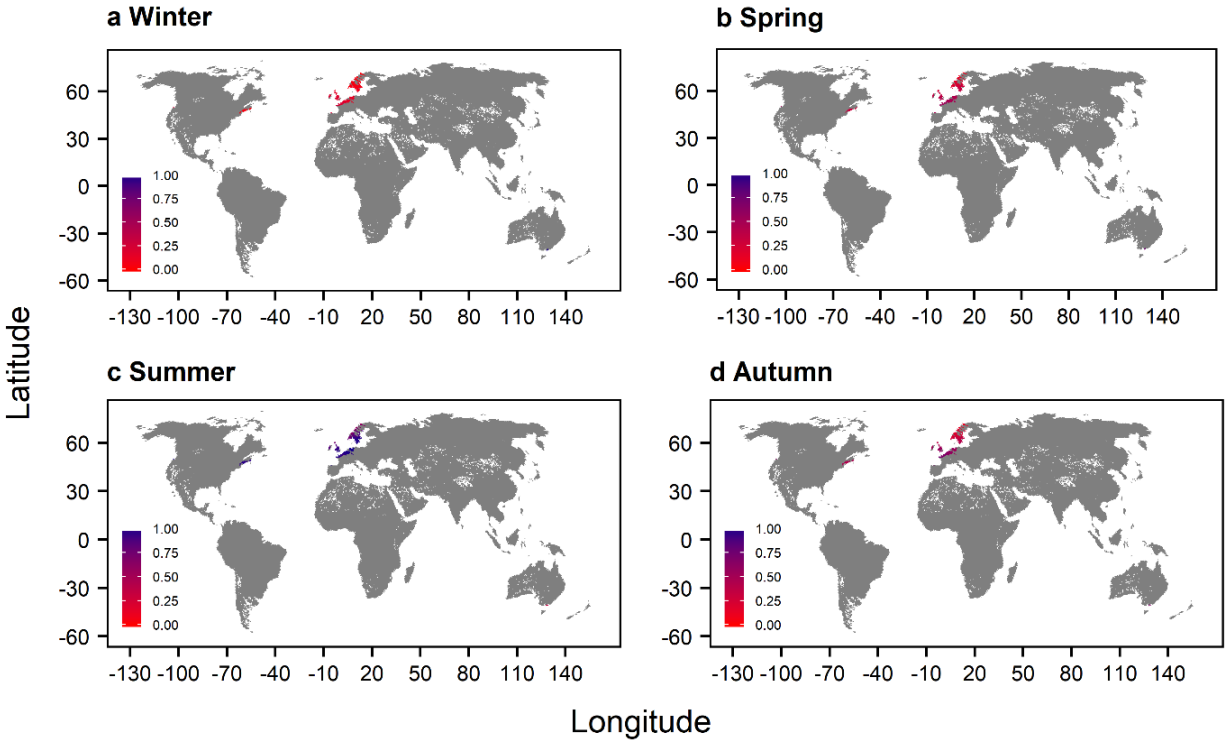

Fig. S14 Global map of the seasonal performances of adult *Salmo salar* for the "restricted dispersal" scenario. Note that seasons were defined according to the northern hemisphere.

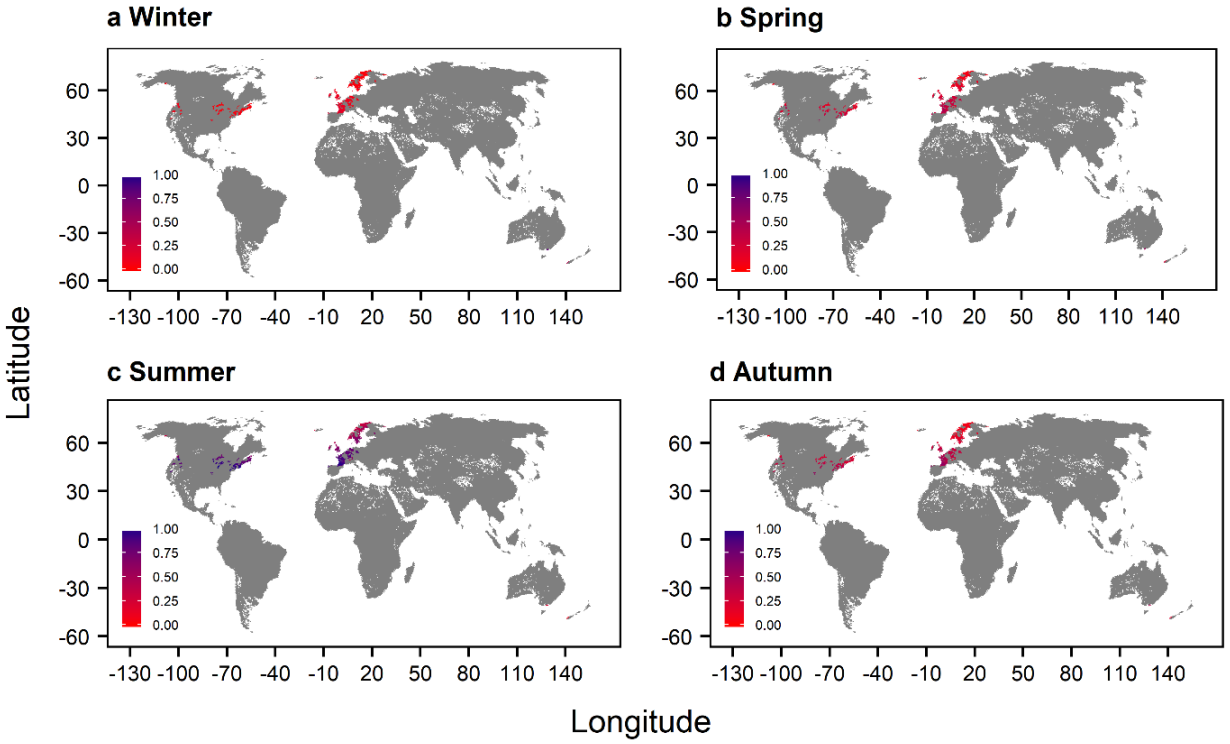

Fig. S15 Global map of the seasonal performances of juvenile *Salmo salar* for the baseline scenario. Note that seasons were defined according to the northern hemisphere.

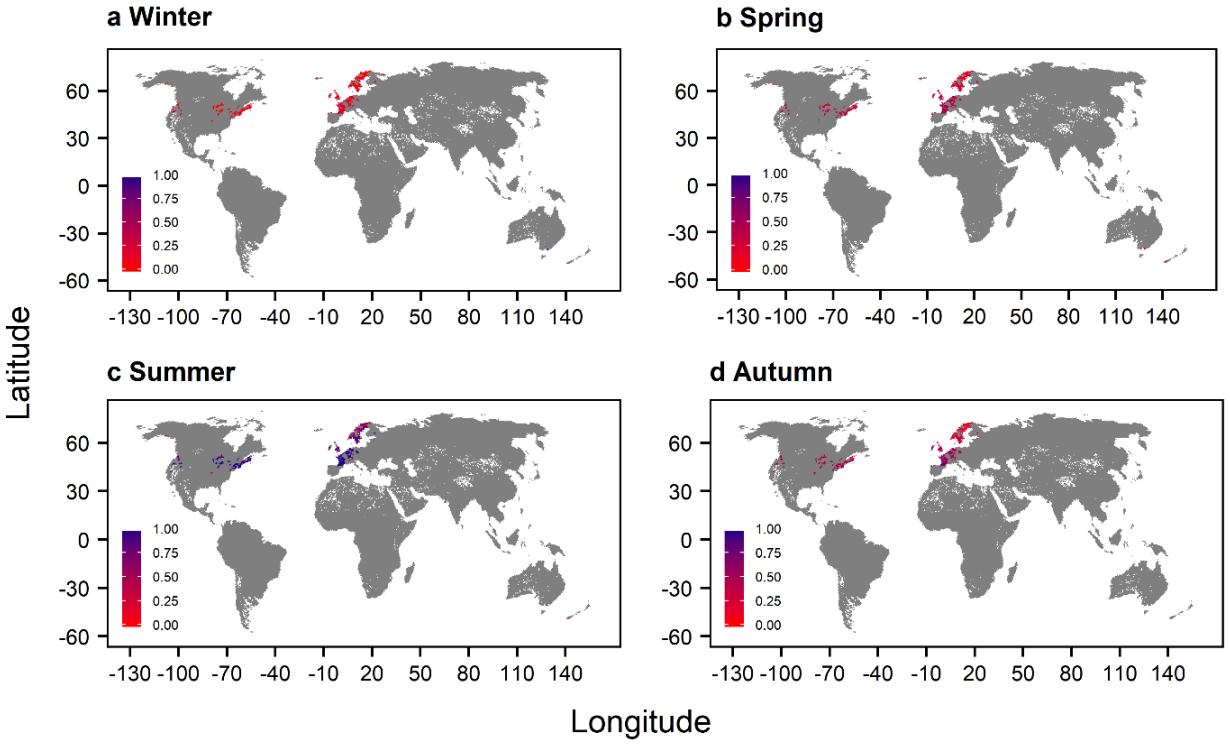

Fig. S16 Global map of the seasonal performances of juvenile *Salmo salar* for the “no dispersal” scenario. Note that seasons were defined according to the northern hemisphere.

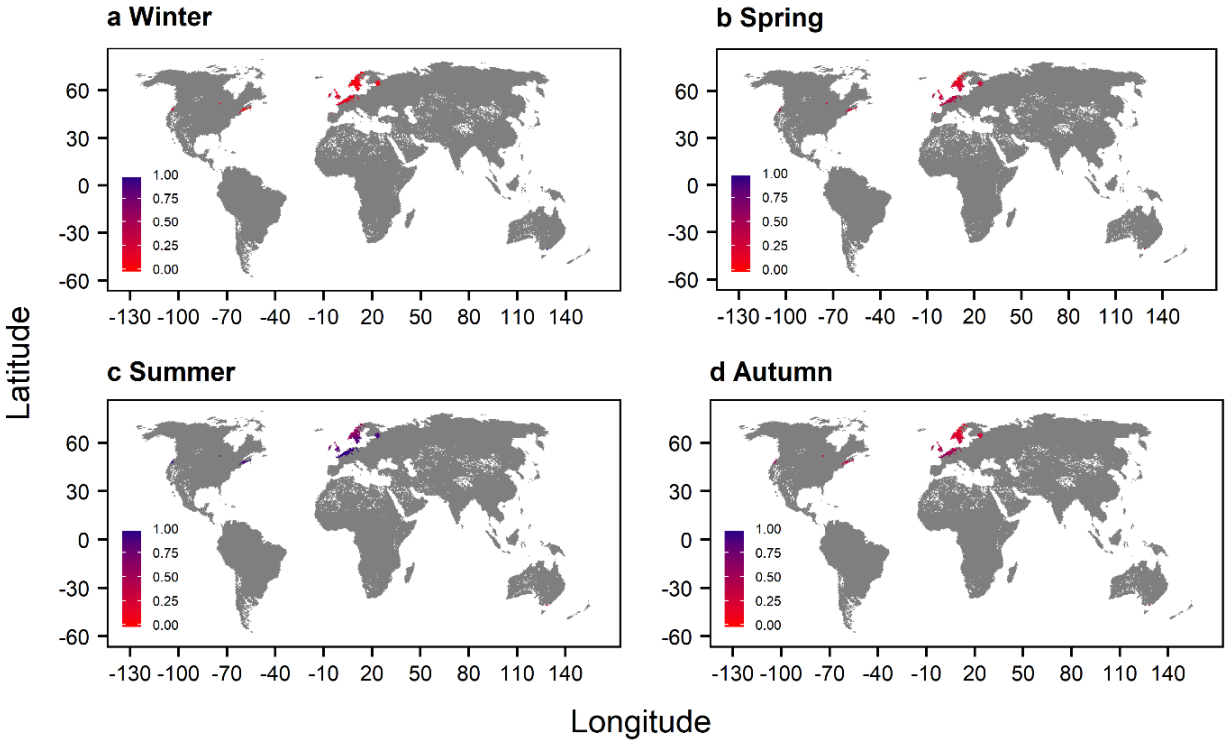

Fig. S17 Global map of the seasonal performances of juvenile *Salmo salar* for the "free dispersal" scenario. Note that seasons were defined according to the northern hemisphere.

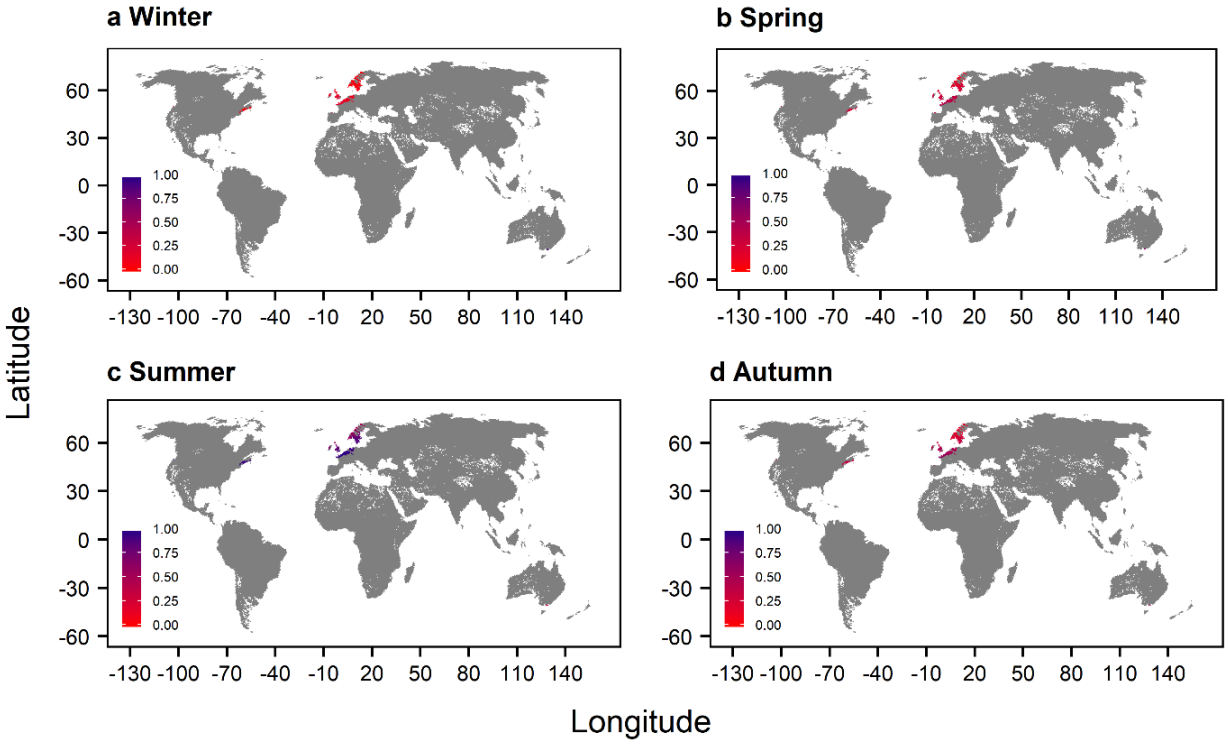

Fig. S18 Global map of the seasonal performances of juvenile *Salmo salar* for the "restricted dispersal" scenario. Note that seasons were defined according to the northern hemisphere.

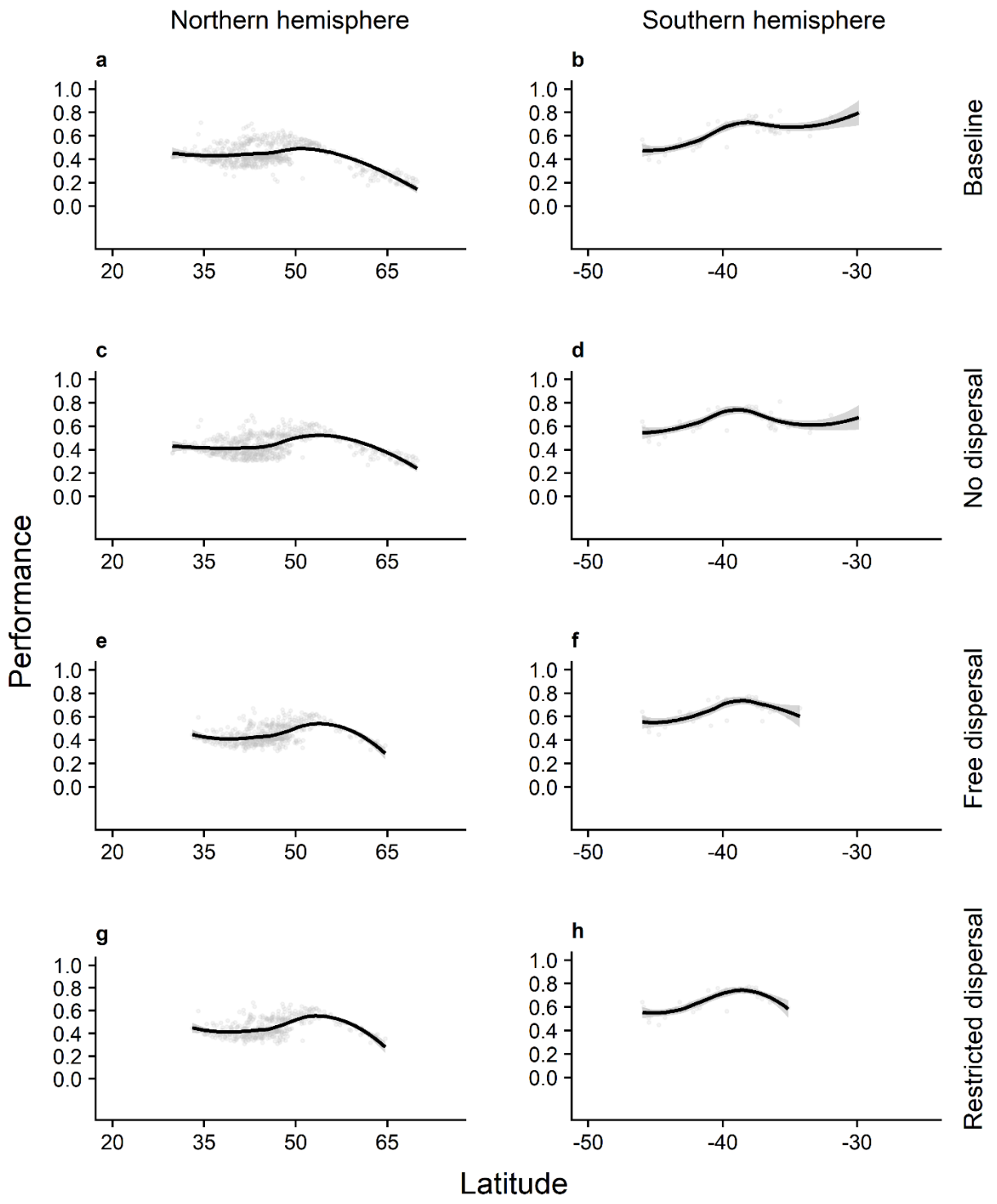

Fig. S19 Latitudinal trends of annual mean performance for juvenile *Salmo trutta* under consideration of different dispersal scenarios. Annual mean performance is based on monthly performance values.

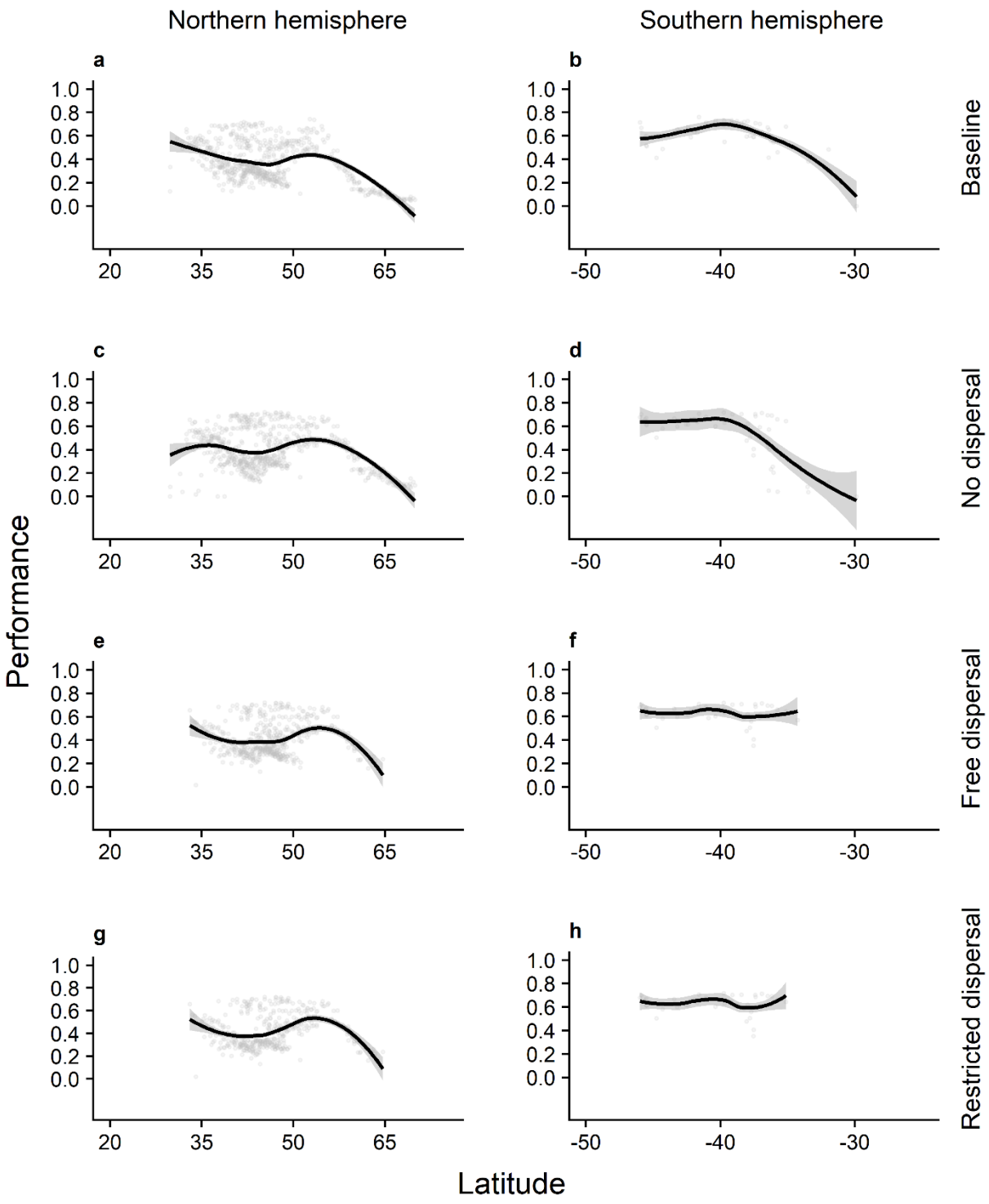

Fig. S20 Latitudinal trends of the performance during the spawning seasons for *Salmo trutta* eggs under consideration of different dispersal scenarios. Performance is based on monthly performance values.

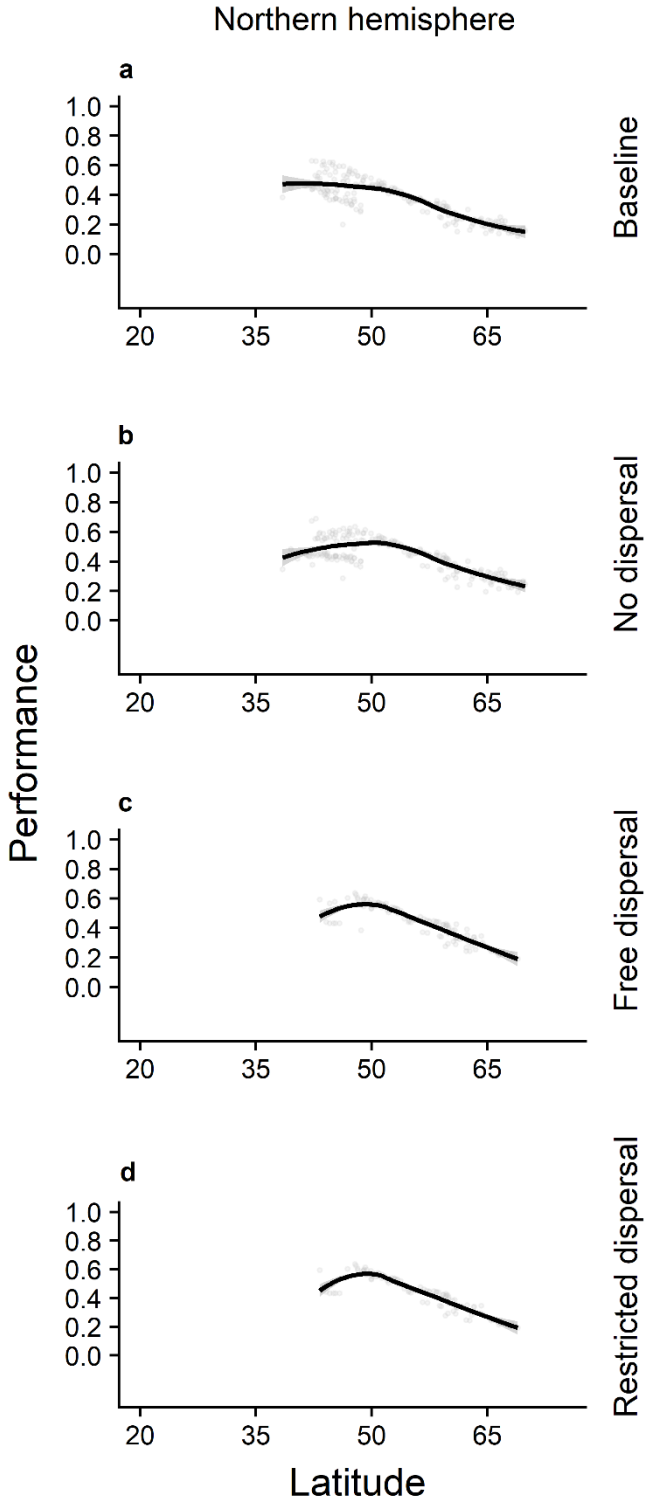

Fig. S21 Latitudinal trends of annual mean performance for adult *Salmo salar* under consideration of different dispersal scenarios in the northern hemisphere. Annual mean performance is based on monthly performance values. Analyses of the southern hemisphere were excluded because of few observations.

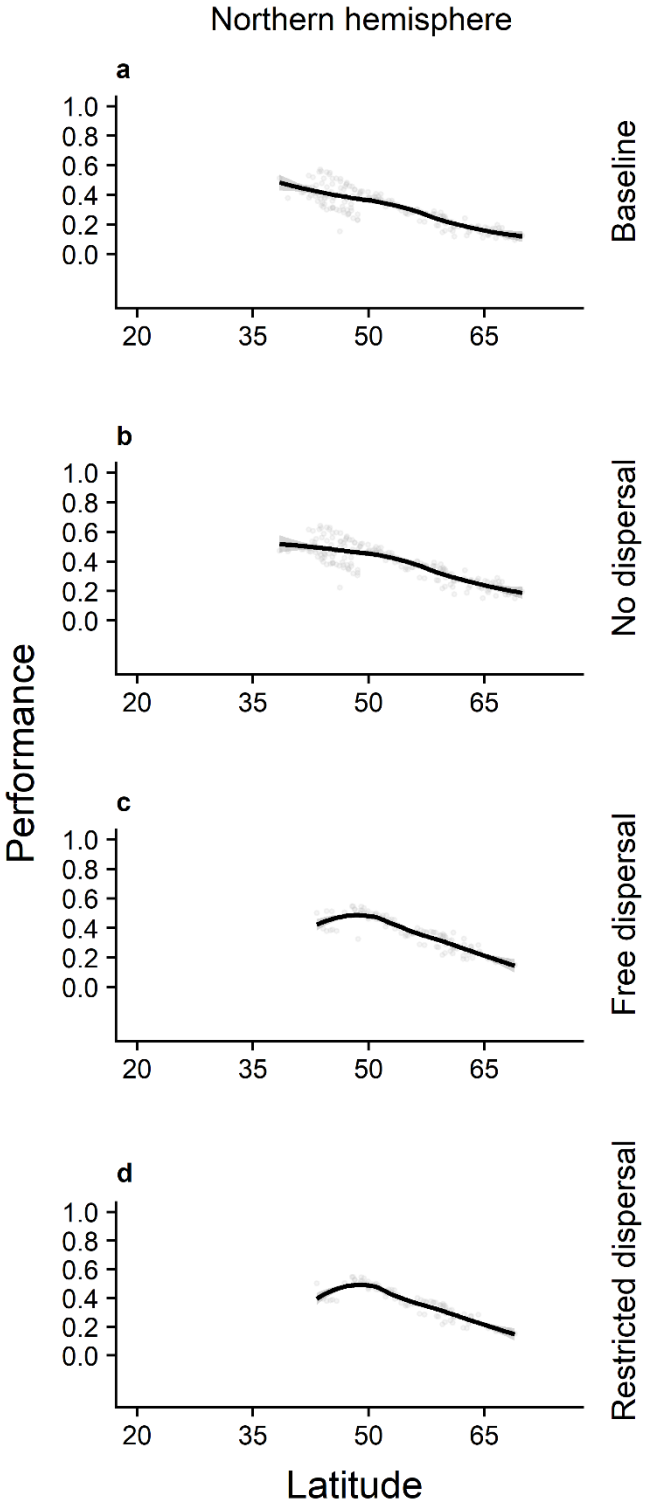

Fig. S22 Latitudinal trends of annual mean performance for juvenile *Salmo salar* under consideration of different dispersal scenarios in the northern hemisphere. Annual mean performance is based on monthly performance values. Analyses of the southern hemisphere were excluded because of few observations.

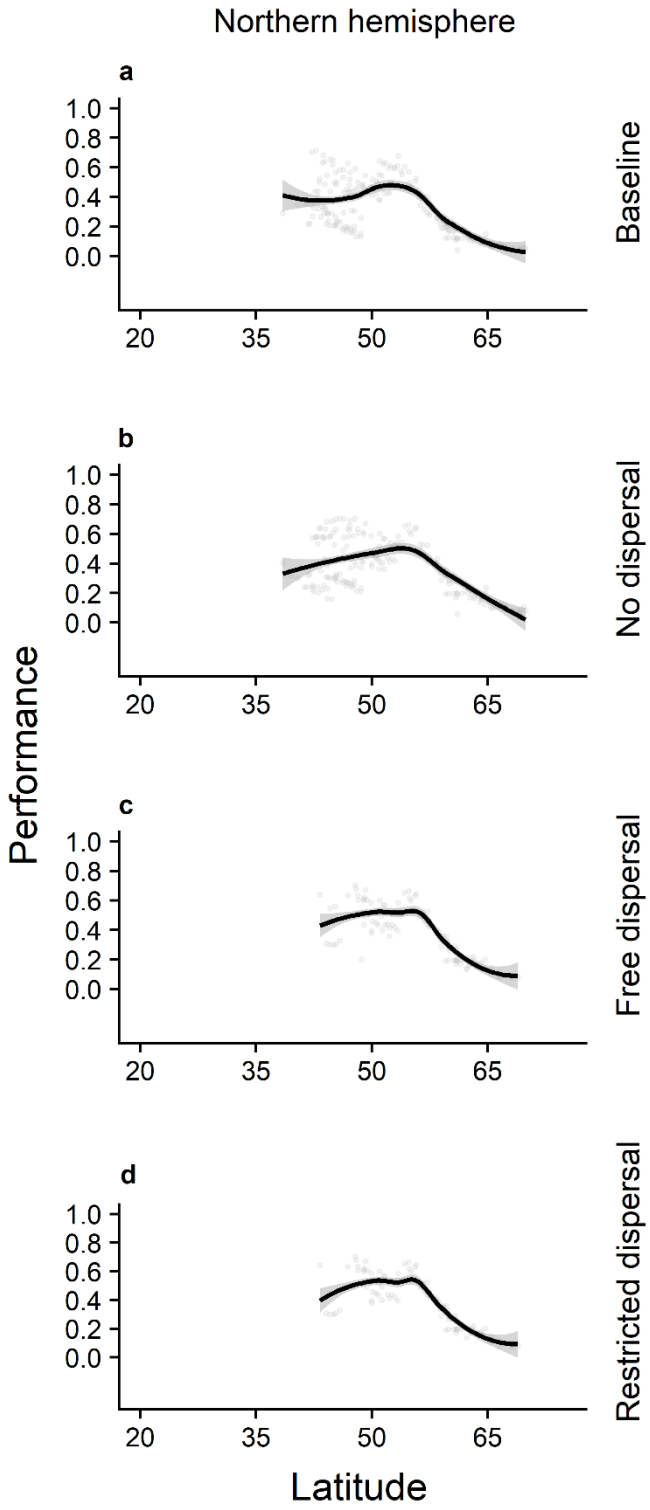

Fig. S23 Latitudinal trends of the performance during the spawning season for *Salmo salar* eggs under consideration of different dispersal scenarios in the northern hemisphere. Performance is based on monthly performance values. Analyses of the southern hemisphere were excluded because of few observations.

Table S1 Data characteristics of the global and European data set.

Region	Total catchment number	Species occurrence number	
		Salmo trutta	***Salmo salar***
Africa	2,687	2	0
Asia	3,981	0	0
Australia	725	49	2
Europe	921	293	147
North America	1,829	384	50
South America	1,552	2	0
Sum	11,695	730	199

Table S2 Overview of the initially considered environmental variables.

Category	Variable (abbreviation)	Description	Literature
Climatic (discharge)	Annual mean discharge (AnnMeanDis)	Average of the annual mean discharges	e.g. Laizé et al., 2014; Markovic et al., 2017
	Maximum discharge (MaxDis)	Average of the annual maximum discharges	
	Minimum discharge (MinDis)	Average of the annual minimum discharges	
	Discharge seasonality (DisSeas)	Average of the annual standard deviation of discharges	
	Flow of the wettest month (FloWetMonth)	Maximum of the monthly discharges	
	Flow of the driest month (FloDriMonth)	Minimum of the monthly discharges	
	Mean winter discharge (WinDis)	Mean discharge for the months December – February	e.g. Wenger et al., 2011a; Wenger et al., 2011b
	Mean spring discharge (SpriDis)	Mean discharge for the months March – May	
	Mean summer discharge (SumDis)	Mean discharge for the months June – August	
	Mean autumn discharge (AutDis)	Mean discharge for the months September – November	
Climatic (water temperature)	Annual mean water temperature (AnnMeanWaT)	Average of the annual mean water temperatures	e.g. Markovic et al. 2012; Markovic et al. 2014
	Maximum water temperature (MaxWaT)	Average of the annual maximum water temperatures	
	Minimum water temperature (MinWaT)	Average of the annual minimum water temperatures	
	Water temperature seasonality (WaTSeas)	Average of the annual standard deviation of water temperatures	
	Water temperature of the warmest month (WaTWarmMonth)	Maximum of the monthly water temperatures	
	Water temperature of the coldest month (WaTColdMonth)	Minimum of the monthly water temperatures	
	Mean winter water temperature (WinWaT)	Mean water temperature for the months December – February	
	Mean spring water temperature (SpriWaT)	Mean water temperature for the months March – May	
	Mean summer water temperature (SumWaT)	Mean water temperature for the months June – August	
	Mean autumn water temperature (AutWaT)	Mean water temperature for the months September – November	
	Mean diurnal range (MeanDiuRan)	Mean of monthly (maximum – minimum water temperature)	
	Annual water temperature range (AnnWaTRan)	Maximum water temperature – minimum water temperature	
	Isothermality (Isotherm)	Mean diurnal range / Annual water temperature range	
Topographic	Altitude (Alt)	Mean catchment elevation	e.g. McNyset, 2005
Land cover	Cropland (Crop)	Percentage of catchment area covered by cropland	e.g. Trautwein et al., 2012
	Built-up area (Built-up)	Fraction of sealed areas within the catchment	
	Forest (Forest)	Percentage of catchment area covered by forest	
	Grassland (Gras)	Percentage of catchment area covered by grassland	
	Shrubland (Shrub)	Percentage of catchment area covered by shrubland	

Table S3 Thermal traits of *Salmo trutta* for different life stages in °C.

Life stage	CT_{min}	CT_{max}	T_{opt}	Literature
adults	0	30.0	17	Küttel et al., 2002
		26.0	19	Otto & Zahn, 2008
		29.0		Lee & Rinne, 1980
		29.9		Lee & Rinne, 1980
	0	24.7		Jonsson & Jonsson, 2009
		23.0	19	Otto & Zahn, 2008
		25.0		Otto & Zahn, 2008
	0	30.0	17	Küttel et al., 2002
		29.0		Beitinger et al., 2000
		29.8		Beitinger et al., 2000
		30.0		Beitinger et al., 2000
		24.6		Todd et al., 2008
		29		Lee & Rinne, 1980
		29.9		Lee & Rinne, 1980
juveniles		26.3		Grande & Andersen, 1991
		27.8		Grande & Andersen, 1991
	0	28.0	14	Küttel et al., 2002
		23.2		Yoder et al., 2012
		26.0		Yoder et al., 2012
		26.4		Yoder et al., 2012
			17	Jonsson & Jonsson, 2009
	0	28.0	14	Küttel et al., 2002
		27.8		Grande & Andersen, 1991
eggs	0	15.0	7	Küttel et al., 2002
	0	12.0	9	Küttel et al., 2002
		16.0		Ojanguren & Braña, 2003
		18.0		Ojanguren & Braña, 2003
			8	Ojanguren & Braña, 2003
			10	Ojanguren & Braña, 2003
	0	15.0	7	Küttel et al., 2002

Table S4 Thermal traits of *Salmo salar* for different life stages in °C.

Life stage	CT_{min}	CT_{max}	T_{opt}	Literature
adults		29.0	17	Küttel et al., 2002
			20	Küttel et al., 2002
				Küttel et al., 2002
	-0.5	25.0	17	Wallace, 1993
		29.0	15	Otto & Zahn, 2008
	0	27.8		Jonsson & Jonsson, 2009
		28.0	15	Otto & Zahn, 2008
		34.0	17	Küttel et al., 2002
juveniles	0	28.0	23	Küttel et al., 2002
		32.9		Beitinger et al., 2000
		32.8		Beitinger et al., 2000
		32.6		Beitinger et al., 2000
		32.7		Beitinger et al., 2000
			20	Jonsson & Jonsson, 2009
		28.7		Grande & Andersen, 1991
		29.2		Grande & Andersen, 1991
		30.0		Garside, 1973
		28.5		Garside, 1973
		29.0		Garside, 1973
eggs	0	16.0	11	Küttel et al., 2002
	0	12.0		Otto & Zahn, 2008
	0	16.0		Elliott, 1981

Table S5 Parameter tuning specifications for Artificial Neural Networks (ANN, manual and ADADELTA), Random Forest (RF), Gradient Boosting Machines (GBM), Multivariate Adaptive Regression Splines (MARS) and Elastic Net (ELNET).

Method	Parameter	Min	Max	Steps	Explanation
ANN (manual)	Activation function				Activation functions define the output of a neuron. Three different functions were tested: Rectifier, Tanh, Maxout.
	Number of nodes	5	500	"+" 5	Number of nodes within the single hidden layer.
	Learning rate	0.001	0.1	"+" 0.001	The learning rate defines the step size during gradient descent.
	Learning rate annealing	1.00E-08	1.00E-05	"×" 10	The annealing of the learning rate avoids the risk of jumping around local minima.
	Learning rate decay factor	0.8	1	"+" 0.05	Decay factor of the learning rate between layers.
	Initial momentum	0	0.8	"+" 0.1	Accelerates the gradient descent by using gradient information from previous iterations.
	Final momentum	0.9	0.99	"+" 0.01	Final momentum after a certain number of training samples for which the momentum increases.
	Dropout ratio	0	0.2	"+" 0.05	Input layer dropout ratio.
	L1-regularization	0	1.00E-04	"+" 1.0E-06	Lambda value for Lasso regularization.
	L2-regularization	0	1.00E-04	"+" 1.0E-06	Lambda value for Ridge regularization.
	Epochs	10	1.00E+03		Number of iterations of the whole data set. The following values were used: 10, 250, 500, 750, 1000.
	MaxW²	10	3.40E+38		Constraint for squared sum of incoming weights per unit. Following values were used: 10, 100, 1000, 3.4028235e+38 (default).
	Balanced classes				Balanced classes set to TRUE in order to balance the class distribution by either oversample or undersample the minority class.
ANN (ADADELTA)	Activation function				Activation functions define the output of a neuron. Three different functions were tested: Rectifier, Tanh, Maxout.
	Number of nodes	5	500	"+" 5	Number of nodes within the single hidden layer.
	Rho	0.9	0.999	"+" 0.001	Rho is similar to prior weight updates (similar to momentum).
	Epsilon	1.00E-09	1.00E-03	"×" 10	Epsilon is similar to learning rate annealing during initial training and at later stages to momentum.
	Dropout ratio	0	0.2	"+" 0.05	Input layer dropout ratio.
	L1-regularization	0	1.00E-04	"+" 1.0E-06	Lambda value for Lasso regularization.

	L2-regularization	0	1.00E-04	"+" 1.0E-06	Lambda value for Ridge regularization.
	Epochs	10	1.00E+03		Number of iterations of the whole data set. Following values were used: 10, 250, 500, 750, 1000.
	MaxW²	10	3.40E+38		Constraint for squared sum of incoming weights per unit. The following values were used: 10, 100, 1000, 3.4028235e+38 (default).
	Balanced classes				Balanced classes set to TRUE in order to balance the class distribution by either oversample or undersample the minority class.
RF	Number of trees	1000	20000	"+" 100	Number of trees used to build the random forest.
	Tree depth	2	30	"+" 1	Maximum tree depth of a single tree.
	Random variable selection	1	#predictors	"+" 1	Number of variables randomly sampled as candidates at each split.
	Sample rate	0.1	1	"+" 0.02	Row sample rate for building a tree.
	Balanced classes				Balanced classes set to TRUE in order to balance the class distribution by either oversample or undersample the minority class.
GBM	Number of trees	1000	20000	"+" 100	Number of trees used for the additive sequence.
	Tree depth	2	#predictors	"+" 1	Maximum tree depth of a single tree.
	Learning rate	0.001	0.1	"+" 0.001	The learning rate defines the weight of each tree in the additive sequence.
	Learning rate annealing	0.9	0.999	"+" 0.001	Scaling factor of the learning rate after each tree.
	Sample rate	0.1	1	"+" 0.02	Row sample rate for building a tree.
	Balanced classes				Balanced classes set to TRUE in order to balance the class distribution by either oversample or undersample the minority class.
MARS	nprune	2	100	"+" 1	Maximum number of terms (including intercept) in the pruned model.
ELNET	Alpha	0	1	"+" 0.01	Parameter for the distribution of regularization between the L1 (Lasso) and L2 (Ridge) penalties.
	Lambda				R package "h2o" compiles an own sequence of potential lambda values, i.e. the regularization strength (max. n = 100).

Table S6 Univariate analysis of *Salmo trutta* distributions using generalized additive models (GAM).

Variable	AUC
Mean autumn water temperature	0.90
Water temperature of the coldest month	0.90
Maximum water temperature	0.89
Mean winter water temperature	0.89
Annual mean water temperature	0.89
Mean spring water temperature	0.89
Minimum water temperature	0.88
Water temperature of the warmest month	0.82
Built-up area	0.81
Annual water temperature range	0.79
Water temperature seasonality	0.76
Mean summer water temperature	0.75
Forest	0.73
Mean diurnal range	0.67
Minimum discharge	0.65
Discharge seasonality	0.65
Mean winter discharge	0.65
Flow of the driest month	0.65
Cropland	0.64
Grassland	0.64
Mean spring discharge	0.64
Mean autumn discharge	0.61
Isothermality	0.60
Annual mean discharge	0.59
Altitude	0.59
Shrubland	0.57
Maximum discharge	0.51
Flow of the wettest month	0.50
Mean summer discharge	0.49

Table S7 Univariate analysis of *Salmo salar* distributions using generalized additive models (GAM).

Variable	AUC
Mean winter water temperature	0.89
Maximum water temperature	0.87
Water temperature of the coldest month	0.87
Mean autumn water temperature	0.87
Water temperature of the warmest month	0.87
Mean spring water temperature	0.86
Annual mean water temperature	0.86
Minimum water temperature	0.85
Mean summer water temperature	0.81
Water temperature seasonality	0.79
Built-up area	0.79
Annual water temperature range	0.78
Forest	0.74
Minimum discharge	0.73
Flow of the driest month	0.72
Mean winter discharge	0.70
Isothermality	0.66
Altitude	0.64
Mean diurnal range	0.62
Shrubland	0.60
Cropland	0.60
Grassland	0.57
Discharge seasonality	0.51
Maximum discharge	0.49
Flow of the wettest month	0.47
Mean summer discharge	0.45
Annual mean discharge	0.41
Mean autumn discharge	0.40
Mean spring discharge	0.36

Table S8 Final tuning parameters for *Salmo trutta* distribution models (Artificial Neural Networks (ANN, manual and ADADELTA), Random Forest (RF), Gradient Boosting Machines (GBM), Multivariate Adaptive Regression Splines (MARS), Elastic Net (ELNET)) and the corresponding performance measures. 5-fold cross validation (cv) using 80% of the data was used for the parameter tuning. After final parameter selection, the final model prediction performance was tested for the remaining 20% of the data (test).

Method	Parameter	Final selection	AUC (cv)	AUC (test)
ANN (manual)	Activation function	Rectifier	0.9787	0.9795
	Number of nodes	475		
	Learning rate	0.037		
	Learning rate annealing	1.00E-05		
	Learning rate decay factor	0.85		
	Initial momentum	0.4		
	Final momentum	0.97		
	Dropout ratio	0.2		
	L1-regularization	9.30E-05		
	L2-regularization	4.40E-05		
	Epochs	1003		
	MaxW²	3.40E+38		
	Balanced classes	TRUE		
ANN (ADADELTA)	Activation function	Maxout	0.9753	0.9754
	Number of nodes	165		
	Rho	0.997		
	Epsilon	1.00E-09		
	Dropout ratio	0.05		
	L1-regularization	3.70E-05		
	L2-regularization	6.00E-05		
	Epochs	754		
	MaxW²	100		
	Balanced classes	TRUE		
RF	Number of trees	12,200	0.9816	0.9795
	Tree depth	25		
	Random variable selection	3		
	Sample rate	0.94		
	Balanced classes	TRUE		
GBM	Number of trees	4,900	0.9787	0.9859
	Tree depth	8		
	Learning rate	0.027		
	Learning rate annealing	0.997		
	Sample rate	0.52		
	Balanced classes	TRUE		
MARS	nprune	58	0.9518	0.9388
ELNET	Alpha	0.01	0.8235	0.8002
	Lambda	0.00145		

Table S9 Final tuning parameters for *Salmo salar* distribution models (Artificial Neural Networks (ANN, manual and ADADELTA), Random Forest (RF), Gradient Boosting Machines (GBM), Multivariate Adaptive Regression Splines (MARS), Elastic Net (ELNET)) and the corresponding performance measures. 5-fold cross validation (cv) using 80% of the data was used for the parameter tuning. After final parameter selection, the final model prediction performance was tested for the remaining 20% of the data (test).

Method	Parameter	Final selection	AUC (cv)	AUC (test)
ANN (manual)	Activation function	Rectifier	0.9728	0.9778
	Number of nodes	410		
	Learning rate	0.002		
	Learning rate annealing	1.00E-06		
	Learning rate decay factor	0.85		
	Initial momentum	0.2		
	Final momentum	0.94		
	Dropout ratio	0.05		
	L1-regularization	8.00E-06		
	L2-regularization	0		
	Epochs	252		
	MaxW²	10		
	Balanced classes	TRUE		
ANN (ADADELTA)	Activation function	Rectifier	0.9649	0.9834
	Number of nodes	75		
	Rho	0.998		
	Epsilon	1.00E-08		
	Dropout ratio	0.1		
	L1-regularization	8.60E-05		
	L2-regularization	6.80E-05		
	Epochs	502		
	MaxW²	10		
	Balanced classes	TRUE		
RF	Number of trees	4,700	0.9802	0.9779
	Tree depth	27		
	Random variable selection	3		
	Sample rate	0.24		
	Balanced classes	TRUE		
GBM	Number of trees	10,600	0.9773	0.9560
	Tree depth	8		
	Learning rate	0.094		
	Learning rate annealing	0.971		
	Sample rate	0.1		
	Balanced classes	TRUE		
MARS	nprune	96	0.9581	0.9734
ELNET	Alpha	0.38	0.8448	0.8668
	Lambda	0.00018		

References

Beitinger, T.L., Bennett, W.A., & McCauley, R.W. (2000). Temperature tolerances of North American freshwater species exposed to dynamic changes in temperature. *Environmental Biology of Fishes*, **58**, 237–275.

Elliott, J.M. (1981). Some aspects of thermal stress on freshwater teleosts. In Stress and Fish (A. D. Pickering, ed), pp. 209-245. Academic Press, London.

Garside, E.T. (1973). Ultimate upper lethal temperature of Atlantic salmon (Salmo salar L.). *Canadian Journal of Zoology*, **51**, 898–900.

Grande, M., & Andersen, S. (1991). Critical thermal maxima for young salmonids. *Journal of Freshwater Ecology*, **6**, 275–279.

Jonsson, B., & Jonsson, N. (2009). A review of the likely effects of climate change on anadromous Atlantic salmon Salmo salar and brown trout Salmo trutta, with particular reference to water temperature and flow. *Journal of Fish Biology*, **75**, 2381– 2447.

Küttel, S., Peter, A., & Wüest, A. (2002). Temperaturpräferenzen und-limiten von Fischarten Schweizerischer Fliessgewässer, Rhône Revitalisierung, Publikation Nummer 1, März, 41 p (in German).

Laize, C.L.R., Acreman, M.C., Schneider, C., Dunbar, M.J., Houghton-Carr, H., Flörke, M., & Hannah, D.M. (2014). Projected flow alteration and ecological risk for pan-European rivers. *River Research and Applications*, **30**, 299–314.

Lee, R.M., & Rinne, J.N. (1980). Critical thermal maximum of five trout species in the southwestern United States. *Transactions of the American Fisheries Society*, **109**, 632–635.

Markovic, D., Freyhof, J., & Wolter, C. (2012). Where Are All the Fish: Potential of Biogeographical Maps to Project Current and Future Distribution Patterns of Freshwater Species. *PLoS ONE*, **7**(7): e40530.

Markovic, D., Carrizo, S., Freyhof, J., Cid, N., Szabolcs, L., Scholz, M., Kasperdius, H., & Darwall, W. (2014). Europe's freshwater biodiversity under climate change: distribution shifts and conservation needs. *Diversity and Distributions*, **20**, 1097–1107.

Markovic, D., Carrizo, S.F., Kärcher, O., Walz, A., & David, J.N.W. (2017). Vulnerability of European freshwater catchments to climate change. *Global Change Biology*, **23**, 3567–3580.

McNyset, K.M. (2005). Use of ecological niche modelling to predict distributions of freshwater fish species in Kansas. *Ecology of Freshwater Fish*, **14**, 243–255.

Ojanguren, A.F., & Braña, F. (2003). Thermal dependence of embryonic growth and development in brown trout. *Journal of Fish Biology*, **62**, 580–590.

Otto, S.A., & Zahn, S. (2008). Temperatur- und Sauerstoff-Toleranz ausgewählter Wanderfischarten der Elbe. Potsdam: Institut für Binnenfischerei e.V (in German).

Todd, C.D., Hughes, S.L., Marshall, T., MacLean, J.C., Lonergan, M.E., & Biow, E.M. (2008). Detrimental effects of recent ocean surface warming on growth condition of Atlantic salmon. *Global Change Biology*, **14**, 1–13.

Trautwein, C., Schinegger, R., Schmutz, S. (2012). Cumulative effects of land use on fish metrics in different types of running waters in Austria. *Aquatic Sciences*, **74**, 329– 341.

Wallace, J. (1993). Environmental considerations. pp. 127–143. In: K. Heen, R. Monahan and F. Utter (eds). Salmon aquaculture. Fishing News Books. Oxford.

Wenger, S.J., Isaak, D.J., Dunham, J.B., Fausch, K.D., Luce, C.H., Neville, H.M., Rieman, B.E., Young, M.K., Nagel, D.E., Horan, D.L. & Chandler, G.W. (2011a). Role of climate and invasive species in structuring trout distributions in the Interior Columbia Basin. *Canadian Journal of Fisheries and Aquatic Sciences*, **68**, 988–1008.

Wenger, S.J., Isaak, D.J., Luce, C.H., Neville, H.M., Fausch, K.D., Dunham, J.B., Dauwalter, D.C., Young, M.K., Elsner, M.M., Rieman, B.E., Hamlet, A.F. & Williams, J.E. (2011b). Flow regime, temperature, and biotic interactions drive differential declines of trout species under climate change. *Proceedings of the National Academy of Sciences of the United States of America*, **108**, 14175–14180.

Yoder, C.O. (2012). Development of a Database for Upper Thermal Tolerances for New England Freshwater Fish Species. MBI Technical Report MBI/2012-4-6.

List of figures

PART II – Application Studies

Chapter 3: Chlorophyll *a* – nutrient and temperature relationships, and predictions for lakes across mountain regions

Chapter 4: Scale effects on the performance of niche-based models of freshwater fish distributions

Chapter 5: Freshwater species distributions along thermal gradients

Chapter 6: European vs. global analyses of species' thermal response curves: pessimistic or optimistic regarding species' future?

Chapter 7: Combining species distribution modelling techniques with species thermal performance curves

List of tables

PART I – Introduction, Methodology and Data

Chapter 2: Methodology and data

PART II – Application Studies

Chapter 3: Chlorophyll *a* – nutrient and temperature relationships, and predictions for lakes across mountain regions

Chapter 4: Scale effects on the performance of niche-based models of freshwater fish distributions

Chapter 5: Freshwater species distributions along thermal gradients

Chapter 6: European vs. global analyses of species' thermal response curves: pessimistic or optimistic regarding species' future?

Chapter 7: Combining species distribution modelling techniques with species thermal performance curves

Bibliography

Abell, J.M., Ozkundakci, D., Hamilton, D.P., & Jones, J.R. (2012). Latitudinal variation in nutrient stoichiometry and chlorophyll-nutrient relationships in lakes: A global study. *Fundamental and Applied Limnology*, **181**, 1–14.

Albrecht, C., & Wilke, T. (2008). Ancient Lake Ohrid: biodiversity and evolution. *Hydrobiologia*, **615**, 103–140.

Allan, J.D., Erickson, D., & Fay, J. (1997). The influence of catchment land use on stream integrity across multiple spatial scales. *Freshwater Biology*, **37**, 149–161.

Allouche, O., Tsoar, A., & Kadmon, R. (2006). Assessing the accuracy of species distribution models: Prevalence, kappa and the true skill statistic (TSS). *Journal of Applied Ecology*, **43**, 1223–1232.

Angert, A.L., Sheth, S.N., & Paul, J.R. (2011). Incorporating population-level variation in thermal performance into predictions of geographic range shifts. *Integrative and Comparative Biology*, **51**, 733–750.

Angilletta, M.J., Niewiarowski, P.H., & Navas, C.A. (2002). The evolution of thermal physiology in ectotherms. *Journal of Thermal Biology*, **27**, 249–268.

Angilletta, M.J. (2006). Estimating and comparing thermal performance curves. *Journal of Thermal Biology*, **31**, 541–545.

Angilletta, M.J. (2009). Thermal adaptation: a theoretical and empirical synthesis. UK, Oxford University Press, Oxford.

Araújo, M.B., & Guisan, A. (2006). Five (or so) challenges for species distribution modelling. *Journal of Biogeography*, **33**, 1677–1688.

Arismendi, I., Safeeq, M., Johnson, S.L., Dunham, J.B., & Haggerty, R. (2012). Increasing synchrony of high temperature and low flow in western North American streams: Double trouble for coldwater biota? *Hydrobiologia*, **712**, 61–70.

Bachmann, R.W, & Hoyer, M.V. (2003). Predicting the frequencies of high chlorophyll levels in Florida lakes from average chlorophyll or nutrient data. *Lake and Reservoir Management*, **19**, 229–241.

Bachmann, R.W., Bigham, D.L., Hoyer, M.V., & Canfield D.E. Jr. (2012). Factors determining the distributions of total phosphorus, total nitrogen, and chlorophyll a in Florida lakes. *Lake and Reservoir Management*, **28**, 10–26.

Barnagaud, J.Y., Devictor, V., Jiguet, F., Barbet-Massin, M., Le Viol, I., & Archaux, F. (2012). Relating Habitat and climatic niches in birds. *PLoS ONE*, **7**, e32819.

Battarbee, R.W., Kernan, M., & Rose, N. (2009). Threatened and stressed mountain lakes of Europe: Assessment and progress. *Aquatic Ecosystem Health & Management*, **12**, 118–128.

Beck, H.E., van Dijk, A.I.J.M., de Roo, A., Dutra, E., Fink, G., Orth, R., & Schellekens, J. (2017) Global evaluation of runoff from 10 state-of-the-art hydrological models. *Hydrology and Earth System Sciences*, **21**, 2881–2903.

Beitinger, T.L., Bennett, W.A., & McCauley, R.W. (2000). Temperature tolerances of North American freshwater species exposed to dynamic changes in temperature. *Environmental Biology of Fishes*, **58**, 237–275.

Bergstra, J., & Bengio Y. (2012). Random search for hyper-parameter optimization. *Journal of Machine Learning Research*, **13**, 2817–305.

Bernhardt, E.S., Palmer, M.A., Allan, J.D., Alexander, G., Barnas, K., Brooks, S., … Sudduth, E. (2005). Synthesizing U.S. river restoration efforts. *Science*, **308**, 636–637.

Bishop, C.M. (1995) Neural networks for pattern recognition, Oxford University Press, Inc., New York.

Blackburn, T.M., & Gaston, K.J. (2002). Scale in macroecology. *Global Ecology and Biogeography*, **11**, 185-189.

Bracken, M.E.S., Hillebrand, H., Borer, E.T., Seabloom, E.W., Cebrian, J., Cleland, E.E., ... Smith, J.E. (2015). Signatures of nutrient limitation and co-limitation: responses of autotroph internal nutrient concentrations to nitrogen and phosphorus additions. *Oikos*, **124**, 113–121.

Brauman, K.A., Richter, B.D., Postel, S., Malsy, M., & Flörke, M. (2016). Water depletion: An improved metric for incorporating seasonal and dry-year water scarcity into water risk assessments. *Elementa: Science of Anthropocene*, **4**, 000083.

Brazner, J.C., Tanner, D.K., Detenbeck, N.E., Batterman, S.L., Stark, S.L., Jagger, L.A., & Snarski, V.M. (2005). Regional, watershed, and site-specific environmental influences on fish assemblage structure and function in western Lake Superior tributaries. *Canadian Journal of Fisheries and Aquatic Sciences*, **62**, 1254–1270.

Breiman, L. (2001a). Random forests. *Machine learning*, **45**(1), 5–32.

Breiman, L. (2001b). Statistical modelling: the two cultures. *Statistical Science*, **16**, 199–215.

Brett, J.R. (1952). Temperature tolerance in young Pacific salmon genus Oncorhynchus. *Journal of the Fisheries Research Board of Canada*, **9**, 265–323.

Brotons, L., Thuiller, W., Araújo, M.B., & Hirzel, A.H. (2004). Presence-absence versus presence-only modelling methods for predicting bird habitat suitability. *Ecography*, **27**, 437–448.

Buisson, L., Blanc, L., & Grenouillet, G. (2008). Modelling stream fish species distribution in a river network: the relative effects of temperature versus physical factors. *Ecology of Freshwater Fish*, **17**, 244–257.

Buisson, L., & Grenouillet, G. (2009). Contrasted impacts of climate change on stream fish assemblages along an environmental gradient. *Diversity and Distributions*, **15**, 613–626.

Buisson, L., Thuiller, W., Casajus, N., Lek, S., & Grenouillet, G. (2010). Uncertainty in ensemble forecasting of species distribution. *Global Change Biology*, **16**, 1145–1157.

Burrows, M.T., Schoeman, D.S., Buckley, L.B., Moore, P., Poloczanska, E.S., Brander, K.M., … Richardson, A.J. (2011). The pace of shifting climate in marine and terrestrial ecosystems. *Science*, **334**, 652–655.

Bush, A., Catullo, R.A., Mokany, K., Thornhill, A.H., Miller, J.T., & Ferrier, S. (2018). Truncation of thermal tolerance niches among Australian plants. *Global Ecology and Biogeography*, **27**, 22–31.

Campbell, J.S. (1977). Spawning characteristics of brown trout and sea trout Salmo trutta L. in Kirk Burn, River Tweed, Scotland. *Journal of Fish Biology*, **11**, 217–229.

Cardinale, B.J., Hillebrand, H., Harpole, W.S., Gross, K., & Ptacnik, R. (2009). Separating the influence of resource 'availability' from resource 'imbalance' on productivity-diversity relationships. *Ecology Letters*, **12**, 475–487.

Carlson, S.M., & Seamons, T.R. (2008). A review of quantitative genetic components of fitness in salmonids: implications for adaptation to future change. *Evolutionary Applications*, **1**, 222–238.

Carrascal, L.M., Villén-Pérez, S., & Palomino, D. (2016). Preferred temperature and thermal breadth of birds wintering in peninsular Spain: The limited effect of temperature on species distribution. *PeerJ*, **4**, e2156.

Carvalho, L., Solimini, A.G., Phillips, G., Pietiläinen, O.P., Moe, J., Cardoso, A.C., … Rekolainen, S. (2009). Site-specific chlorophyll reference conditions for lakes in Northern and Western Europe. *Hydrobiologia*, **633**, 59–66.

Chen, I.C., Hill, J.K., Ohlemueller, R., Roy, D.B., & Thomas, C.D. (2011). Rapid range shifts of species associated with high levels of climate warming. *Science*, **333**, 1024–1026.

Childress, E.S., & Letcher, B.H. (2017). Estimating thermal performance curves from repeated field observations. *Ecology*, **98**, 1377–1387.

Comte, L., & Grenouillet, G. (2013). Do stream fish track climate change? Assessing distribution shifts in recent decades. *Ecography*, **36**, 1236–1246.

Comte, L., Buisson, L.T., Daufresne, M., & Grenouillet, G. (2013). Climate-induced changes in the distribution of freshwater fish: observed and predicted trends. *Freshwater Biology*, **58**, 625–639.

Comte, L., Murienne, J., & Grenouillet, G. (2014). Species traits and phylogenetic conservatism of climate-induced range shifts in stream fishes. *Nature Communications*, **5**, 5023.

Coudon, C., & Gégout, J.C. (2007). Quantitative prediction of the distribution and abundance of Vaccinium myrtillus with climatic and edaphic factors. *Journal of Vegetation Science*, **18**, 517–524.

Croissant, Y., & Millo, G. (2008). Panel Data Econometrics in R: The plm package. *Journal of Statistical Software*, **27**(2), 1–43.

D'Amen, M., Bombi, P., Pearman, P.B., Schmatz, D.R., Zimmermann, N.E., & Bologna, M.A. (2011). Will climate change reduce the efficacy of protected areas for amphibian conservation in Italy? *Biological Conservation*, **144**, 989–997.

Daily, G.C. (1997). Nature's Services: Societal dependence on natural ecosystems. Island Press, Washington, DC.

Dawson, T.P., Jackson, S.T., House, J.I., Prentice, I.C., & Mace, G.M. (2011). Beyond predictions: biodiversity conservation in a changing climate. *Science*, **332**, 53–58.

De Frenne, P., Rodríguez-Sánchez, F., Coomes, D.A., Baeten, L., Verstraeten, G., Vellend, M., … Verheyen, K. (2013). Microclimate moderates plant responses to macroclimate warming. *Proceedings of the National Academy of Sciences of the United States of America*, **110**(46), 18561–18565.

De Jager, A.L., & Vogt, J.V. (2010). Development and demonstration of a structured hydrological feature coding system for Europe. *Hydrological Sciences Journal*, **55**, 661–675.

De Jong, P., & Heller, G.Z. (2008). Generalized linear models for insurance data. Cambridge University Press, Cambridge, UK.

DEFRA. 2013. Catchment Based Approach: Improving the quality of our water environment. Department for Environment, Food & Rural Affairs. Policy paper available at: https://www.gov.uk/government/publications/catchment-based-approach-improving-the-quality-of-our-water-environment.

Dell, A., Pawar, S., & Savage, V.M. (2011). Systematic variation in the temperature dependence of physiological and ecological traits. *Proceedings of the National Academy of Sciences of the United States of America*, **108**, 10591–10596.

Deutsch, C.A., Tewksbury, J.J., Huey, R.B., Sheldon, K.S., Ghalambor, C.K., Haak, D.C., & Martin, P.R. (2008). Impacts of climate warming on terrestrial ectotherms across latitude. *Proceedings of the National Academy of Sciences of the United States of America*, **105**, 6668–6672.

Deutsch, C., Ferrel, A., Seibel, B., Pörtner, H.O., & Huey, R.B. (2015). Climate change tightens a metabolic constraint on marine habitats. *Science*, **348**, 1132–1135.

Dillon, P.J., & Rigler, F.H. (1974). The phosphorus-chlorophyll relationship in lakes. *Limnology and Oceanography*, **19**, 767–773.

Domisch, S., Araújo, M.B., Bonada, N., Pauls, S.U., Jähnig, S.C., & Haase, P. (2013a). Modelling distribution in European stream macroinvertebrates under future climates. *Global Change Biology*, **19**, 752–762.

Domisch, S., Kuemmerlen, M., Jähning, S.C., & Haase, P. (2013b). Choice of study area and predictors affect habitat suitability projections, but not the performance of species distribution models of stream biota. *Ecological Modelling*, **257**, 1–10.

Domisch, S., Jähnig, S.C., Simaika, J.P., Kuemmerlen, M., & Stoll, S. (2015). Application of species distribution models in stream ecosystems: the challenges of spatial and temporal scale, environmental predictors and species occurrence data. *Fundamental and Applied Limnology*, **186**, 45–61.

Dormann, C.F., Purschke, O., Márquez, J.R.G., Lautenbach, S., & Schröder, B. (2008). Components of uncertainty in species distribution analysis: A case study of the great grey shrike. *Ecology*, **89**, 3371–3386.

Dormann, C.F., Elith, J., Bacher, S., Buchmann, C., Carl, G., Carré, G., … Lautenbach, S. (2013). Collinearity: A review of methods to deal with it and a simulation study evaluating their performance. *Ecography*, **36**, 27–46.

Duda, R., Hart, P., & Stork, D. (2001). Pattern Classification. Wiley-Interscience, New York.

Durant, J.M., Hjermann, D.O., Ottersen, G., & Stenseth, N.C. (2007). Climate and the match or mismatch between predator requirements and resource availability. *Climate Research*, **33**, 271–83.

EEA (European Environment Agency): Corine Land Cover 2000 (2004). Mapping a decade of change Document Actions, Tech. Rep. Brochure No 4/2004.

EEA. CORINE Land Cover. (2011). Version 13, Copenhagen: European Environmental Agency (EEA), available at www.eea.europa.eu/publications/COR0-landcover.

Efron, B.,& Hastie, T. (2016). Computer age statistical inference. Cambridge University Press, Cambridge, UK.

Eisner, S. (2016). Comprehensive evaluation of the WaterGAP3 model across climatic, physiographic, and anthropogenic gradients, dissertation, KOBRA Dokumentenserver, University of Kassel, Germany, available at: http://nbn-resolving. de/urn:nbn:de:hebis:34-2016031450014 (last access: 10 January 2019).

Eisner, S., Flörke, M., Chamorro, A., Daggupati, P., Donnelly, C., Huang, J., … Krysanova, V. (2017). An ensemble analysis of climate change impacts on streamflow seasonality across 11 large river basins, *Climatic Change*, **141**, 401–417.

El-Gabbas, A., & Dormann, C.F. (2017). Improved species-occurrence predictions in data-poor regions: using large-scale data and bias correction with down-weighted Poisson regression and Maxent. *Ecography*, **41**, 1161–1172.

Elith, J., Leathwick, J.R., & Hastie, T. (2008). A working guide to boosted regression trees. *Journal of Animal Ecology*, **77**, 802–813.

Elith, J., & Graham, C.H. (2009). Do they? How do they? WHY do they differ? On finding reasons for differing performances of species distribution models. *Ecography*, **32**, 66–77.

Elliott, J.A., Jones, I.D., & Thackeray, S.J. (2006). Testing the sensitivity of phytoplankton communities to changes in water temperature and nutrient load, in a temperate lake. *Hydrobiologia*, **559**, 401–411.

Elliott, J.M. (1993). A 25-year study of production of juvenile sea-trout, Salmo trutta, in an English Lake District stream, p. 109-122. In R. J. Gibson and R. E. Cutting [ed.] Production of juvenile Atlantic salmon, Salmo salar, in natural waters. *Canadian Special Publication of Fisheries and Aquatic Sciences*, **118**.

Elliott, J.M. (1994). Quantitative ecology and the brown trout. Oxford Series in Ecology and Evolution, Oxford University Press, Oxford.

Elliott, J.M., & Elliott, J.A. (2010). Temperature requirements of Atlantic salmon Salmo salar, brown trout Salmo trutta and Arctic charr Salvelinus alpinus: predicting the effects of climate change. *Journal of Fish Biology*, **77**, 1793–1817.

Elliott, J.M., & Allonby, J.D. (2013). An experimental study of ontogenetic and seasonal changes in the temperature preferences of unfed and fed brown trout, Salmo trutta. *Freshwater Biology*, **58**, 1840–1848.

Elmendorf, S., & Moore, K. (2008). Use of community composition data to predict the fecundity and abundance of species. *Conservation Biology*, **22**, 1523–1532.

Elser, J.J., Bracken, M.E.S., Cleland, E.E., Gruner, D.S., Harpole, W.S., Hillebrand, H., … Smith, J.E. (2007). Global analysis of nitrogen and phosphorus limitation of primary producers in freshwater, marine and terrestrial ecosystems. *Ecology Letters*, **10**, 1135–1142.

Enders, E.C., Boisclair, D., & Roy, A.G. (2005). A model of total swimming costs in turbulent flow for juvenile Atlantic salmon (Salmo salar). *Canadian Journal of Fisheries and Aquatic Sciences*, **62**, 1079–1089.

Esselman, P.C., & Allan, J.D. (2010). Relative influences of catchment- and reach-scale abiotic factors on freshwater fish communities in rivers of northeastern Mesoamerica. *Ecology of Freshwater Fish*, **19**, 439–454.

Fagan, W.F. (2002). Connectivity, fragmentation, and extinction risk in dendritic metapopulations. *Ecology*, **83**, 3243–3249.

Fausch, K.D., Torgersen, C.E., Baxter, C.V., & Li, H.W. (2002). Landscapes to riverscapes: bridging the gap between research and conservation of stream fishes. *BioScience*, **52**, 483–498.

Field, C., et al., eds (2014). Climate Change 2014 - Impacts, adaptation and vulnerability: Part A: Global and sectoral aspects. Cambridge University Press, New York.

Fielding, A.H., & Bell, J.F. (1997). A review of methods for the assessment of prediction errors in conservation presence/ absence models. *Environmental Conservation*, **24**, 38–49.

Filipe, A., Markovic, D., Pletterbauer, F., Tisseuil, C., De Wever, A., Schmutz, S., … Freyhof, J. (2013). Forecasting fish distribution along stream networks: brown trout (Salmo trutta) in Europe. *Diversity and Distributions*, **8**, 1059–1071.

Filstrup, C.T., Wagner, T., Soranno, P.A., Stanley, E.H., Stow, C.A., Webster, K.E., & Downing, J.A. (2014). Regional variability among nonlinear chlorophyll—phosphorus relationships in lakes. *Limnology and Oceanography*, **59**(5), 1691–1703.

Filstrup, C.T., & Downing, J.A. (2017). Relationship of chlorophyll to phosphorus and nitrogen in nutrient-rich lakes. *Inland Waters*, **7**(4), 385–400.

Fitzpatrick, M.C., & Hargrove, W.W. (2009). The projection of species distribution models and the problem of non-analog climate. *Biodiversity and Conservation*, **18**, 2255–2261.

Fleming, I.A., Lamberg, A. & Jonsson, B. (1997). Effects of early experience on the reproductive performance of Atlantic salmon. *Behavioural Ecology*, **8**, 470–480.

Floury, M., Usseglio-Polatera, P., Delattre, C., & Souchon, Y. (2017). Assessing long-term effects of multiple, potentially confounded drivers in ecosystems from species traits. *Global Change Biology*, **23**, 2297–2307.

Forseth, T., Larsson, S., Jensen, A.J., Jonsson, B., Näslund, I., & Berglund, I. (2009). Thermal performance of juvenile brown trout, Salmo trutta L.: no support for thermal adaptation hypotheses. *Journal of Fish Biology*, **74**, 133–149.

Franklin, J. (2009). Mapping species distributions: Spatial inference and prediction. Cambridge University Press, New York.

Frazier, M.R., Huey, R.B., & Berrigan, D. (2006). Thermodynamics constrains the evolution of insect population growth rates: ''Warmer is better.''. *American Naturalist*, **168**, 512–520.

Friedman, J.H. (1991). Multivariate adaptive regression splines (with discussion). *The Annals of Statistics*, **19**, 1–141.

Friedman, J.H., & Meulman, J.J. (2003). Multiple additive regression trees with application in epidemiology. *Statistics in Medicine*, **22**, 1365–1381.

Friedman, J.H., & Popescu, B.E. (2008). Predictive learning via rule ensembles. *The Annals of Applied Statistics*, **2**, 916–954.

Friedman, J.H., Hastie, T., & Tibshirani, R. (2010). Regularization paths for generalized linear models via coordinate descent. *Journal of Statistical Software*, **33**(1), 1–22.

Frost, A.J., Thomson, J.S., Smith, C., Burton, H.C., Davis, B., Watts, P.C., & Sneddon, L.U. (2013). Environmental change alters personality in the rainbow trout, Oncorhynchus mykiss. *Animal Behaviour*, **85**, 1199–1207.

Gauch, H.G., & Whittaker, R.H. (1972). Coenocline Simulation. *Ecology*, **53**, 446–451.

Glebe, B.D., & Leggett, W.C. (1981). Temporal, intra-population differences in energy allocation and use by American shad (Alosa sapidissima) during the spawning migration. *Canadian Journal of Fisheries and Aquatic Sciences*, **38**, 795–805.

Green, P.A., Vörösmarty, C.J., Harrison, I., Farrell, T., Sáenz, L., & Fekete, B.M. (2015). Freshwater ecosystem services supporting humans: pivoting from water crisis to water solutions. *Global Environmental Change*, **34**, 108–118.

Greene, W.H. (2012). Econometric analysis (7th ed.). Pearson, Boston, London.

Greig, S.M., Sear, D., & Carling, P.A. (2005). Fine sediment accumulation in salmon spawning gravels and the survival of incubating salmon progeny: implications for spawning habitat management. *Science of the Total Environment,* **344**, 241–258.

Grenouillet, G., Buisson, L., Casajus, N., & Lek, S. (2011). Ensemble modelling of species distribution: the effects of geographical and environmental ranges. *Ecography*, **34**, 9–17.

Grömping, U. (2006). Relative importance for linear regression in R: The Package relaimpo. *Journal of Statistical Software*, **17**, 1–27.

Guildford, S.J., & Hecky, R.E. (2000). Total nitrogen, total phosphorus, and nutrient limitation in lakes and oceans: Is there a common relationship? *Limnology and Oceanography*, **45**, 1213–1223.

Guisan, A., & Thuiller W. (2005). Predicting species distribution: offering more than simple habitat models. *Ecology Letters*, **8**, 993–1009.

Guisan, A., Graham, C.H., Elith, J., Huettmann, F., & the NCEAS Species Distribution Modelling Group (2007). Sensitivity of predictive species distribution models to change in grain size. *Diversity and Distributions*, **13**, 332–340.

Gunkel, G., & Casallas, J. (2002). Limnology of an equatorial high mountain lake - Lago San Pable, Ecuador: The significance of deep diurnal mixing for lake productivity. *Limnologica*, **32**, 33–43.

Hastie, T., & Tibshirani, R. (1986). Generalized additive models. *Statistical Science*, **1**, 297–310.

Hastie, T., Tibshirani, R., & Friedman, J. (2001). The elements of statistical learning. Springer New York Inc., New York.

Hastie, T. (2016). gam: Generalized Additive Models R package version 1.15.

He, B., Oki, T., Sun, F., Komori, D., Kanae, S., Wang, Y., … & Yamazaki, D. (2011). Estimating monthly total nitrogen concentration in streams by using artificial neural network. *Journal of Environmental Economics and Management*, **92**, 172–177.

Heggberget, T.G. (1988). Timing of spawning of Norwegian Atlantic salmon (Salmo salar). *Canadian Journal of Fisheries and Aquatic Sciences*, **45**, 845–849.

Heggenes, J., Krog, O.M.W., Lindås, O.R., Dokk, J.G., & Bremnes, T. (1993). Homeostatic behavioural responses in a changing environment: Brown trout (Salmo trutta) become nocturnal during winter. *Journal of Animal Ecology*, **62**, 295–308.

Hempel, S., Frieler, K., Warszawski, L., Schewe, J., & Piontek, F. (2013). A trend-preserving bias correction – the ISI-MIP approach. *Earth System Dynamics*, **4**, 49–92.

Henle, K., Dick, D., Harphaske, A., Kühn, I., Schweiger, O., & Settele, J. (2010). Climate change impacts on European amphibians and reptiles. Biodiversity and climate change: Reports and guidance developed under the Bern Convention Volume 1 Nature and environment, No 156. Strasbourg Cedex: Council of Europe Publishing. pp. 225–306.

Hereford, J. (2009). A quantitative survey of local adaptation and fitness trade-offs. *American Naturalis*t, **173**, 579–88.

Hester, E.T., & Doyle, M.W. (2011). Human impacts to river temperature and their effects on biological processes: A quantitative synthesis. *Journal of the American Water Resources Association*, **47**, 571–587.

Hickling, R., Boy, D.B., Hill, J.K., & Thomas, C.D. (2005). A northward shift of range margins in British Odonata. *Global Change Biology*, **11**, 502–506.

Hijmans, R.J., Cameron, S. E., Parra, J.L., Jones, P.G., & Jarvis, A. (2005). Very high resolution interpolated climate surfaces for global land areas. *International Journal of Climatology*, **25**, 1965–1978.

Hijmans, R.J., Cameron, S.E., & Parra, J.L. (2007). WorldClim version 1.4. Museum of Vertebrate Zoology, University of California. Available at: http://www.worldclim.org/.

Hijmans, R.J., Phillips, S., Leathwick, J., & Elith, J. (2017). Package 'dismo', R package version 1.1-1. Available online at: http://cran.r-project.org/web/packages/dismo/index.html.

Hochachka, P.W., & Somero, G.N. (2002). Biochemical adaptation: mechanism and process in physiological evolution. Oxford University Press, New York.

Hoegh-Guldberg, O., & Bruno, J.F. (2010). The impact of climate change on the world's marine ecosystems. *Science*, **328**, 1523–1528.

Hollister, J.W., Milstead, W.B., & Kreakie, B.J. (2016). Modeling lake trophic state: a random forest approach. *Ecosphere*, **7**(3), e01321.

Hopkins, R.L., & Burr, B.M. (2009). Modeling freshwater fish distributions using multiscale landscape data: a case study of six narrow range endemics. *Ecological Modelling*, **220**, 2024–2034.

Hosmer, D.W., & Lemeshow, S. (2000). Applied logistic regression. Wiley, New York.

Huber, U.M., Bugmann, H.K.M., & Reasoner, M.A. (2005). Global change and mountain regions: an overview of current knowledge. The Netherlands: Springer, Dordrecht.

Huey, R.B., & Stevenson, R.D. (1979). Integrating thermal physiology and ecology of ectotherms: a discussion of approaches. *American Zoologist*, **19**(1), 357–366.

Huey, R., & Kingsolver, J.G. (1989). Evolution of thermal sensitivity of ectotherm performance. *Trends in Ecology & Evolution*, **4**, 131–135.

Huisman, J., Olff, H., & Fresco, L.F.M. (1993). A hierarchical set of models for species response analysis. *Journal of Vegetation Science*, **4**, 37–46.

Hurlbert, A.H., & Jetz, W. (2007). Species richness, hotspots, and the scale dependence of range maps in ecology and conservation. *Proceedings of the National Academy of Sciences of the United States of America*, **104**, 13384–13389.

ICPDR (2009). The Danube River Basin: Facts and figures. International Commission for the Protection of the Danube River (ICPDR), Vienna.

IPCC (2013). Climate Change 2013: The Physical Science Basis. Contribution of Working Group I to the Fifth Assessment Report of the Intergovernmental Panel on Climate Change. Cambridge University Press, New York.

Isaak, D.J., Wollrab, S., Horan, D., & Chandler, G. (2012). Climate change effects on stream and river temperatures across the northwest U.S. from 1980–2009 and implications for salmonid fishes. *Climatic Change*, **113**, 499–524.

Isaak, D.J., Wenger, S.J., & Young, M.K. (2017). Big biology meets microclimatology: Defining thermal niches of ectotherms at landscape scales for conservation planning. *Ecological Applications*, **27**, 977–990.

IUCN (2013). IUCN Red List of Threatened Species. Version 2013.2.

IUCN (2014). Guidelines for Using the IUCN Red List Categories and Criteria. Version 11. Prepared by the Standards and Petitions Subcommittee.

Jackson, D., Peres-Neto, P.R., & Olden, J.D. (2001). What controls who is where in freshwater fish communities: The roles of biotic, abiotic and spatial factors? *Canadian Journal of Fisheries and Aquatic Sciences*, **58**, 157–170.

Jain, A.K., Mao, J., & Mohiuddin, K.M. (1996). Artificial neural networks: a tutorial. *Computer*, **29**(3), 31–44.

Jansen, F., & Oksanen, J. (2013). How to model species responses along ecological gradients – Huisman–Olff–Fresco models revisited. *Journal of Vegetation Science*, **24**, 1108–1117.

Jatteau, P., Drouineau, H., Charles, K., Carry, L., Lange, F., & Lambert, P. (2017). Thermal tolerance of allis shad (Alosa alosa) embryos and larvae: Modeling and potential applications. *Aquatic Living Resources*, **30**, 2.

Jensen, D.W., Steel, E.A., Fullerton, A.H., & Pess, G.R. (2009). Impact of fine sediment on egg-to-fry survival of Pacific salmon: a meta-analysis of published studies. *Reviews in Fisheries Science*, **17**, 348–359.

Jeppesen, E., Mehner, T., Winfield, I.J., Kangur, K., Sarvala, J., Gerdeaux D., … Meerhoff, M. (2012). Impacts of climate warming on the long-term dynamics of key fish species in 24 European lakes. *Hydrobiologia*, **694**, 1–39.

Jimenez-Valverde, A., & Lobo, J.M. (2007). Threshold criteria for conversion of probability of species presence to either-or presence-absence. *Acta Oecologica*, **31**(3), 361–369.

Jobling, M. (1981). Temperature tolerance and the final preferendum – rapid methods for the assessment of optimum growth temperatures. *Journal of Fish Biology*, **19**, 439–455.

Johnson, J.A., & Kelsch, S.W. (1998). Effects of evolutionary thermal environment on temperature-preference relationships in fishes. *Environmental Biology of Fishes*, **53**, 447–458.

Jonsson, B., & Jonsson, N. (1993). Partial migration: niche shift versus sexual maturation in fishes. *Reviews in Fish Biology and Fisheries*, **3**, 348–365.

Jonsson, B., & L'Abée-Lund, J. H. (1993). Latitudinal clines in life history variables of anadromous brown trout in Europe. *Journal of Fish Biology*, **43**, 1–16.

Jonsson, B., Forseth, T., Jensen, A.J., & Naesje, T.F. (2001). Thermal performance of juvenile Atlantic salmon, Salmo salar L. *Functional Ecology*, **15**, 701–711.

Jonsson, B., & Jonsson, N. (2009). A review of the likely effects of climate change on anadromous Atlantic salmon Salmo salar and brown trout Salmo trutta, with particular reference to water temperature and flow. *Journal of Fish Biology*, **75**, 2381–2447.

Jonsson, B., & Jonsson, N. (2011). Ecology of Atlantic Salmon and Brown Trout: Habitat as a template for life histories. Springer Science & Business Media, Dordrecht.

Jonsson, B., & Jonsson, N. (2014). Early environments affect later performances in fishes. *Journal of Fish Biology*, **85**, 155–188.

Kärcher, O., Frank, K., Walz, A., and Markovic, D. (2019). Scale effects on the performance of niche-based models of freshwater fish distributions. *Ecological Modelling*, **405**, 33–42 (= Chapter 4 in Part II of this thesis).

Kärcher, O., Hering, D., Frank, K., & Markovic D. (2019). Freshwater species distributions along thermal gradients. *Ecology and Evolution*, **9**, 111–124. (= Chapter 5 in Part II of this thesis)

Kasprzak, P., Padisák, J., Koschel, R., Krienitz, L., & Gervais, F. (2008). Chlorophyll a concentration across a trophic gradient of lakes: An estimator of phytoplankton biomass? *Limnologica*, **38**, 327–338.

Kelsch, S.W. (1996). Temperature selection and performance by bluegills: Evidence for selection in response to available power. *Transactions of the American Fisheries Society*, **125**, 948–955.

Kingsolver, J.G., Woods, H.A., Buckley, L.B., Potter, K.A., MacLean, H.J., & Higgins, J.K. (2011). Complex life cycles and the responses of insects to climate change. *Integrative and Comparative Biology*, **51**, 719–732.

Kletou, D., Hall-Spencer, J.M. & Kleitou, P. (2016). A lionfish (pterois miles) invasion has begun in the Mediterranean Sea. *Marine Biodiversity Records*, **9**, 46.

Knowler, D.J., MacGregor, B.W., Bradford, M.J., & Pereman, R.M. (2004). Valuing freshwater salmon habitat on the west coast of Canada. *Journal of Environmental Management*, **69**, 261–273.

Kottelat, M., & Freyhof, J. (2007). Handbook of European Freshwater Fishes. Cornol; Kottelat, Berlin: Freyhof, 646 p.

Kraemer, B.M., Mehner, T., & Adrian, R. (2017). Reconciling the opposing effects of warming on phytoplankton biomass in 188 large lakes. *Scientific Reports*, **7**, 10762.

Krenek, S., Berendonk, T.U., & Petzoldt, T. (2011). Thermal performance curves of Paramecium caudatum: A model selection approach. *European Journal of Protistology*, **47**, 124–137.

Kuemmerlen, M., Schmalz, B., Guse, B., Cai, Q., Fohrer, N., & Jähning, S.C. (2014). Integrating catchment properties in small scale species distribution models of stream macroinvertebrates. *Ecological Modelling*, **277**, 77–86.

Kuemmerlen, M., Reichert, P., Siber, R., & Schuwirth, N. (2019). Ecological assessment of river networks: from reach to catchment scale. *Science of the Total Environment*, **650**, 1613–1627.

Lampa, E., Lind, L., Lind, P.M., & Bornefalk-Hermansson, A. (2014). The identification of complex interactions in epidemiology and toxicology: a simulation study of boosted regression trees. *Environmental Health*, **13**, 57.

Lapointe, M.F., Bergeron, N.E., Bérubé, F., Pouliot, M.A., & Johnston P. (2004). Interactive effects of substrate sand and silt contents, redd-scale hydraulic gradients, and interstitial velocities on egg-to-emergence survival of Atlantic salmon (Salmo salar). *Canadian Journal of Fisheries and Aquatic Sciences*, **61**, 2271–2277.

Larsen, K. (2016). R package 'Information'. version 0.0.9.

Lassalle, G., Béguer, M., Beaulaton, L., & Rochard, E. (2008). Diadromous fish conservation plans need to consider global warming issues: An approach using biogeographical models. *Biological Conservation*, **141**(4), 1105–1118.

Lassalle, G., Crouzet, P., Gessner, J., & Rochard, E. (2010). Global warming impacts and conservation responses for the critically endangered European Atlantic sturgeon. *Biological Conservation*, **143**, 2441–2452.

Lauzeral, C., Grenouillet, G., & Brosse, S. (2013). Spatial range shape drives the grain size effects in species distribution models. *Ecography*, **36**, 778–787.

Lawesson, J.E., Fosaa, A.M., & Olsen, E. (2003). Calibration of Ellenberg indicator values for the Faroe Islands. *Applied Vegetation Science*, **6**, 53–62.

Lawson, C.R., Hodgson, J.A., Wilson, R.J., & Richards, S.A. (2014). Prevalence, thresholds and the performance of presence-absence models. *Methods in Ecology and Evolution*, **5**, 54–64.

Lee, K.Y., Chung, N., & Hwang, S. (2016). Application of an artificial neural network (ANN) model for predicting mosquito abundances in urban areas. *Ecological Informatics*, **36**, 172–180.

Lee-Yaw, J. A., Kharouba, H.M., Bontrager, M., Mahony, C., Csergő, A.M., Noreen, A.M., … Angert, A.L. (2016). A synthesis of transplant experiments and ecological niche models suggests that range limits are often niche limits. *Ecology Letters*, **19**, 710–722.

Lehner, B., Liermann, C.R., Revenga, C., Vörösmarty, C., Fekete, B., Crouzet P, … Wisser, D. (2011). High-resolution mapping of the world's reservoirs and dams for sustainable river-flow management. *Frontiers in Ecology and the Environment*, **9**, 494–502.

Lehner, B., & Grill, G. (2013). Global river hydrography and network routing: baseline data and new approaches to study the world's large river systems. *Hydrological Processes*, **27**, 2171–2186.

Lejeusne, C., Chevaldonne, P., Pergent-Martini, C., Boudouresque, C.F., & Perez, T. (2010). Climate change effects on a miniature ocean: The highly diverse, highly impacted Mediterranean. *Sea Trends in Ecology & Evolution*, **25**(4), 250–260.

Lévêque, C., Oberdorff, T., Paugy, D., Stiassny, M.L.J., & Tedesco, P.A. (2008). Global diversity of fish (Pisces) in freshwater. *Hydrobiologia*, **595**, 545–567.

Li, X., & Wang, Y. (2013). Applying various algorithms for species distribution modelling. *Integrative Zoology*, **8**, 124–135.

Limburg, K.E., & Waldman, J.R. (2009). Dramatic declines in North Atlantic Diadromous Fishes. *BioScience*, **59**, 955–965.

Lindeman, R.H. et al. (1980). Introduction to bivariate and multivariate analysis. Glenview, IL; Scott, Foresman, 444 p.

Linke, S., Norris, R.H., Pressey, R.L. (2008). Irreplaceability of river networks: towards catchment-based conservation planning. *Journal of Applied Ecology*, **45**, 1486–1495.

Lobo, J.M., Jimenez-Valverde, A., & Real. R. (2008). AUC: A misleading measure of the performance of predictive distribution models. *Global Ecology and Biogeography*, **17**, 145–151.

Logez, M., Bady, P., & Pont, D. (2012). Modelling the habitat requirement of riverine fishspecies at the European scale: Sensitivity to temperature and precipitation and associated uncertainty. *Ecology of Freshwater Fish*, **21**, 266–282.

Londe, L.R., Novo, E.M.L.M., Barbosa, C., & Araujo, C.A.S. (2016). Water residence time affecting phytoplankton blooms: study case in Ibitinga Reservoir (São Paulo, Brazil) using Landsat/TM images. *Brazilian Journal of Biology*, **76**(3), 664–672.

Long, J.S., & Ervin, L.H. (2000). Using Heteroscedasticity Consistent Standard Errors in the Linear Regression Model. *The American Statistician*, **54**(3), 217–224.

Lu, F., Chen, Z., Liu, W., & Shao, H. (2016). Modeling chlorophyll-a concentrations using an artificial neural network for precisely eco-restoring lake basin. *Ecological Engineering*, **96**, 422–429.

MacCallum, S.N., & Merchant, C.J. (2013). ARC-Lake v2.0. 1991-2011. University of Edinburgh, School of GeoSciences / European Space Agency; [accessed on April 2017]. http://hdl.handle.net/10283/88.

MacLean, S., & Beissinger, S.R. (2017). Species' traits as predictors of range shifts under contemporary climate change: A review and meta-analysis. *Global Change Biology*, **23**, 4094–4105.

Magnuson, J.J., Crowder, L.B., & Medvick, P.A. (1979). Temperature as an ecological resource. *American Zoologist*, **19**, 331–343.

Magumba, D., Maruyama, A., Michiko, T., Kato, A., & Kikuchi, M. (2013). Relationships between chlorophyll a, phosphorus and nitrogen as fundamentals for controlling phytoplankton biomass in lakes. *Environmental Control in Biology*, **51**(4), 179–185.

Manel, S., Williams, H.C., & Ormerod, S.J. (2001). Evaluating presence-absence models in ecology: The need to account for prevalence. *Journal of Applied Ecology*, **38**, 921–931.

Mantyka-Pringle, C.S., Martin, T.G., Moffatt, D.B., Linke, S., & Rhodes, J.R. (2014). Understanding and predicting the combined effects of climate change and land-use change on freshwater macroinvertebrates and fish. *Journal of Applied Ecology*, **51**, 572–581.

Markovic, D., Freyhof, J., & Wolter, C. (2012). Where are all the fish: Potential of biogeographical maps to project current and future distribution patterns of freshwater species. *PLoS ONE*, **7**(7), e40530.

Markovic, D., Scharfenberger, U., Schmutz, S., Pletterbauer, F., & Wolter, C. (2013). Variability and alterations of water temperatures across the Elbe and Danube River Basins. *Climatic Change*, **119**, 375–389.

Markovic, D., Carrizo, S.F., Freyhof, J., Cid, N., Szabolcs, L., Scholz, M., Kasperdius, H., & Darwall, W. (2014). Europe's freshwater biodiversity under climate change: distribution shifts and conservation needs. *Diversity and Distributions*, **20**, 1097–1107.

Markovic, D., Carrizo, S.F., Kärcher, O., Walz, A., & David, J.N.W. (2017). Vulnerability of European freshwater catchments to climate change. *Global Change Biology*, **23**, 3567–3580.

Marmion, M., Parviainen, M., Luoto, M., Heikkinen, R.K., & Thuiller, W. (2009). Evaluation of consensus methods in predictive species distribution modelling. *Diversity and Distributions*, **15**, 59–69.

Martin, B.T., Pike, A., John, S.N., Hamda, N., Roberts, J., Lindley, S.T., & Danner, E.M. (2016). Phenomenological vs. biophysical models of thermal stress in aquatic eggs. *Ecology Letters*, **20**, 50–59.

Matzinger, A., Jordanoski, M., Veljanoska-Sarafiloska, E., Sturm, M., Müller, B., & Wüest, A. (2006). Is Lake Prespa jeopardizing the ecosystem of ancient Lake Ohrid? *Hydrobiologia*, **553**, 89–109.

McCauley, E., Downing, J.A., & Watson, S. (1989). Sigmoid relationships between nutrients and chlorophyll among lakes. *Canadian Journal of Fisheries and Aquatic Sciences*, **46**, 1171–1175.

McCulloch, W.S., & Pitts, W. (1943). A logical calculus of the ideas imminent in nervous activity. *Bulletin of Mathematical Biology*, **5**, 115–133.

McPhearson, P.T., & Wallace, O.C. (2008). Remote sensing applications to biodiversity conservation, [accessed on April 2017]. http://ncep.amnh.org

Meller, L., Cabeza, M., Pironon, S., Barbet-Massin, M., Maiorano, L., Georges, D., … Thuiller, W. (2014). Ensemble distribution models in conservation prioritization: from consensus predictions to consensus reserve networks. *Diversity and Distributions*, **20**, 309–321.

Milborrow, S. (2018). Derived from mda:mars by T. Hastie and R. Tibshirani. earth: Multivariate adaptive regression splines, R package version 4.4.7. http://www.milbo.users.sonic.net/earth.

Mohseni, O., Stefan, H.G., & Eriksson, T.R. (1998). A nonlinear regression model for weekly stream temperatures. *Water Resources Research*, **34**, 2685–2692.

Morán-Ordóñez, A., Lahoz-Monfort, J.J., Elith, J., & Wintle, B.A. (2016). Evaluating 318 continental-scale species distribution models over a 60 year prediction horizon: what factors influence the reliability of predictions? *Global Ecology and Biogeography*, **26**, 371–384.

Nagaraju, S.K., Gudasalamani, R., Barve, N., Ghazoul, J., Narayanagowda, G.K., & Ramanan, U.S. (2013). Do ecological niche model predictions reflect the adaptive landscape of species? A test using Myristica malabarica Lam., an endemic tree in the Western Ghats, India. *PLoS ONE*, **8**, e82066.

Nowakowski, A.J., Thompson, M.E., Donnelly, M.A., & Todd, B.D. (2017). Amphibian sensitivity to habitat modification is associated with population trends and species traits. *Global Ecology and Biogeography*, **26**, 700–712.

Nussey, D.H., Postma, E., Gienapp, P., & Visser, M. (2005). Selection on heritable phenotypic plasticity in wild birds. *Science*, **310**, 304–307.

Økland, R.H. (1992). Studies in SE Fennoscandian mires: Relevance to ecological theory. *Journal of Vegetation Science*, **3**, 279–284.

Oksanen, J., & Minchin, P.R. (2002). Continuum theory revisited: What shape are species responses along ecological gradients? *Ecological Modelling*, **157**, 119–129.

Östergren, J., & Rivinoja, P. (2008). Overwintering and downstream migration of Sea sea trout (Salmo trutta L.) kelts under regulated flows – northern Sweden. *River Research and Applications*, **24**, 551–563.

Pachauri, R.K., Mayer, L., & editors (2015). Climate change 2014. Synthesis report. Geneva, Switzerland: Intergovernmental panel on climate change. 151 p.

Pankhurst, N.W., & King, H.R. (2010). Temperature and salmonid reproduction: implications for aquaculture. *Journal of Fish Biology*, **76**, 69–85.

Parmesan, C., Root, T.L., & Willig, M.R. (2000). Impacts of extreme weather and climate on terrestrial biota. *Bulletin of the American Meteorological Society*, **81**, 443–450.

Parmesan, C. (2006). Ecological and evolutionary responses to recent climate change. *Annual Review of Ecology, Evolution, and Systematics*, **37**, 637–669.

Pearson, R.G., & Dawson, T.P. (2003). Predicting the impacts of climate change on the distribution of species: are bioclimate envelope models useful? *Global Ecology and Biogeography*, **12**, 361–371.

Pereira, H.M., Leadley, P.W., Proença, V., Alkemade, R., Scharlemann, J.P., Fernandez-Manjarrés, J.F., … & Chini, L. (2010). Scenarios for global biodiversity in the 21st century. *Science*, **330**, 1496–1501.

Peterson, D.L., & Parker, V.T. (1998). Ecological scale: Theory and applications. Columbia Universtiy Press, New York.

Phillips, G., Pietiläinen, O.P., Carvalho, L., Solimini, A., Solheim, A.L., & Cardoso, A.C. (2008). Chlorophyll-nutrient relationships of different lake types using a large European dataset. *Aquatic Ecology*, **42**, 213–226.

Phillips, S.J., Anderson, R.P., & Schapire, R.E. (2006). Maximum entropy modeling of species geographic distributions. *Ecological Modelling*, **190**, 231–259.

Phillips, S.J., & Dudík, M. (2008). Modeling of species distributions with Maxent: new extensions and a comprehensive evaluation. *Ecography*, **31**, 161–175.

Poikane, S., Portielje, R., van den Berg, M., Phillips, G., Brucet, S., Carvalho, L., … Van Wichelen, J. (2014). Defining ecologically relevant water quality targets for lakes in Europe. *Journal of Applied Ecology*, **51**, 592–602.

Prairie, Y., Duarte, C.M., & Kalff, J. (1989). Unifying nutrient–chlorophyll relationships in lakes. *Canadian Journal of Fisheries and Aquatic Sciences*, **46**, 1176–1182.

Premazzi, G., & Chiaudani, G. (1992). Ecological quality of surface waters. Quality assessment schemes for European community lakes. Ispra (Varese), Italy: Commission of the European Communities, Joint Research Centre.

Pried, I.G. (1985). Metabolic scope in fishes. In Fish Energetics New Perspectives (Tytler, P. & Calow, P., eds), pp. 33–64. Croom Helm, London.

Punzet, M., Voß, F., Voß, A., Kynast, E., & Bärlund, I. (2012). A global approach to assess the potential impact of climate change on stream water temperatures and related in-stream first-order decay rates. *Journal of Hydrometeorology*, **13**, 1052–1065.

Pyne, M.I., & Poff, N.L. (2017). Vulnerability of stream community composition and function to projected thermal warming and hydrologic change across ecoregions in the western United States. *Global Change Biology*, **23**, 77–93.

R Development Core Team. (2017). R: A Language and environment for statistical computing. R Foundation for Statistical Computing, Vienna.

R Development Core Team (2018). R: A Language and environment for statistical computing. R Foundation for Statistical Computing, Vienna.

Rapport, D.J., Costanza, R., & McMichael, A.J. (1998). Assessing ecosystem health. *Trends in Ecology & Evolution*, **13**, 397–402.

Riahi, K., Rao, S., Krey, V., Cho, C., Chirkov, V., Fischer, G., … & Rafaj, P. (2011). RCP8.5 – A scenario of comparatively high greenhouse gas emissions. *Climatic Change*, **109**, 33–57.

Ridgeway, G., with contributions from others. (2017). gbm: Generalized Boosted Regression Models. R package version 2.1.3. https://CRAN.R-project.org/package=gbm

Riffler, M., Lieberherr, G.D., & Wunderle, S. (2015). Lake surface water temperatures of European Alpine lakes (1989-2013) based on the Advanced Very High Resolution Radiometer (AVHRR) 1 km data set. *Earth System Science Data*, **7**(1), 1–17.

Rome, L.C., Stevens, E.D., & John-Alder H.B. (1992). The influence of temperature and thermal acclimation on physiological function, pp. 183-205 in M.E. Feder, and W.W. Burggrem, eds. Environmental physiology of the Amphibians. The University of Chicago Press, Chicago.

Sakamoto, M. (1966). Primary production by phytoplankton community in some Japanese lakes and its dependence on lake depth. *Archiv für Hydrobiologie*, **62**, 1–28.

Scheffer, M. (1998). Ecology of Shallow Lakes. Kluwer Academic Publishers, Dordrecht.

Schinegger, R., Borgwardt, F., Melcher, A., & Schmutz, S. (2016). Metadata describing the European Fish Index Plus (EFI+) database. *FMJ*, **17**, 1–12.

Schneider, C., Flörke, M., De Stefano, L., & Petersen-Perlman, J.D. (2017). Hydrological threats for riparian wetlands of international importance — a global quantitative and qualitative analysis. *Hydrology and Earth System Sciences*, **21**, 2799–2815.

Schulte, P.M., Healy, T.M., & Fangue, N.A. (2011). Thermal performance curves, phenotypic plasticity, and the time scales of temperature exposure. *Integrative and Comparative Biology*, **51**, 691–702.

Science for Environment Policy (2015). Ecosystem Services and the Environment. In-depth Report 11 produced for the European Commission, DG Environment by the Science Communication Unit, UWE, Bristol. Available at: http://ec.europa.eu/ science-environment-policy

Scranton, K., & Amarasekare, P. (2017). Predicting phenological shifts in a changing climate. *Proceedings of the National Academy of Sciences of the United States of America*, **114**, 13212–13217.

Shuter, B.J., & Post, J.R. (1990). Climate, population variability, and the zoogeography of temperate fishes. *Transactions of the American Fisheries Society*, **119**, 314–336.

Sinclair, B.J., Marshall, K.E., Sewell, M.A., Levesque, D.L., Willett, C.S., Slotsbo, S., … Huey, R. B. (2016). Can we predict ectotherm responses to climate change using thermal performance curves and body temperatures? *Ecology Letters*, **19**(11), 1372–1385.

Singer, A., Johst, K., Banitz, T., Fowler, M.S., Groeneveld, J., Gutiérrez, A.G., … Travis, J.M.J. (2016). Community dynamics under environmental change: How can next generation mechanistic models improve projections of species distributions? *Ecological Modelling*, **326**, 63–74.

Slatyer, R.A., Hirst, M., & Sexton, J.P. (2013). Niche breadth predict geographical range size: A general ecological pattern. *Ecological Letters*, **16**, 1104–1114.

Soranno, P.A., Cheruvelil, K.S., Bissell, E.G., Bremigan, M.T., Downing, J.A., Fergus, C.E., … Webster, K.E. (2014). Cross-scale interactions: Quantifying multi-scaled cause-effect relationships in macrosystems. *Frontiers in Ecology and the Environment*, **12**, 65–73.

Souchon, Y., & Tissot, L. (2012). Synthesis of thermal tolerances of the common freshwater fish species in large Western Europe rivers. *Knowledge and Management of Aquatic Ecosystems*, **405**, 03.

Soulsby, C., Youngson, A.F., Moir, H.J., & Malcolm, I.A. (2001). Fine sediment influence on salmonid spawning habitat in a lowland agricultural stream: a preliminary assessment. *Science of The Total Environment*, **265**, 295–307.

Strahler, A.N. (1964). Quantitative geomorphology of drainage basins and channel networks. – In: Chow VT (ed) Handbook of Applied Hydrology. New York: McGraw-Hill, pp 4–74.

Strayer, D.L. (2003). Effects of land cover on stream ecosystems: Roles of empirical models and scaling issues. *Ecosystems*, **6**, 407–423.

Strayer, D.L., & Dudgeon, D. (2010). Freshwater biodiversity conservation: Recent progress and future challenges. *Journal of the North American Benthological Society*, **29**, 344–358.

Suleiman, A., Tight, M.R., & Quinn, A.D. (2016). Hybrid neural networks and boosted regression tree models for predicting roadside particulate matter. *Environmental Modeling & Assessment*, **21**(6), 731–750.

Swets, J.A. (1988). Measures of the accuracy of diagnostic systems. *Science*, **240**, 1285–1293.

The H2O.ai team (2018). h2o: R Interface for H2O, R package version 3.20.0.8. https://www.h2o.ai/

Thuiller, W. (2003). BIOMOD – optimizing predictions of species distributions and projecting potential future shifts under global change. *Global Change Biology*, **9**, 1353–1362.

Thuiller, W. (2004). Patterns and uncertainties of species range shifts under climate change. – *Global Change Biology*, **10**, 2020–2027.

Thuiller, W., Brotons, L., Araújo, M.B. & Lavorel, S. (2004). Effects of restricting environmental range of data to project current and future species distributions. *Ecography*, **27**, 165–172.

Thuiller, W., Lafourcade, B., Engler, R., & Araujo, M.B. (2009). BIOMOD–a platform for ensemble forecasting of species distributions. *Ecography*, **32**, 369–73.

Thuiller, W., Albert, C.H., Dubuis, A., Randin, C., & Guisan, A. (2010). Variation in habitat suitability does not always relate to variation in species' plant functional traits. *Biology Letters*, **6**, 120–123.

Tudesque, L., Tisseuil, C., & Lek, S. (2014). Scale-dependent effects of land cover on water physico-chemistry and diatom-based metrics in a major river system, the Adour-Garonne basin (South Western France). *Science of The Total Environment*, **466-467**, 47–55.

Turner, W., Spector, S., Gardiner, N., Fladeland, M., Sterling, E., & Steininger, M. (2003). Remote sensing for biodiversity science and conservation. *Trends in Ecology & Evolution*, **18**(6), 306–314.

Urban, M.C., Bocedi, G., Hendry, A.P., Mihoub, J.B., Pe'er, G., Singer, A., & Travis, J.M.J. (2016). Improving the forecast for biodiversity under climate change. *Science*, **353**(6304), 1293–1310.

USGS: Global Land Cover Characterization (GLCC) (2008). Available at: https://www.usgs.gov/centers/eros/science/usgs-eros-archive-land-cover-products- global-land-cover-characteristics-glcc?qt-science_center_objects=0#qt-science_center_objects

Van Vuuren, D.P., Edmonds, J., Kainuma, M., Riahi, K., Thomson, A., Hibbard, K., … Rose, S.K. (2011). The representative concentration pathways: An overview. *Climatic Change*, **109**, 5–31.

Vasconcelos, R.P., Batista, M.I., & Henriques, S. (2017). Current limitations of global conservation to protect higher vulnerability and lower resilience fish species. *Scientific Reports*, **7**, 7702.

Verberk, W.C.E.P., Durance, I., Vaughan, I.P., & Ormerod, S.J. (2016). Field and laboratory studies reveal interacting effects of stream oxygenation and warming on aquatic ectotherms. *Global Change Biology*, **22**, 1769–1778.

Vetaas, O.R. (2000). Comparing species temperature response curves: Population density versus second-hand data. *Journal of Vegetation Science*, **11**(5), 659–666.

Vetaas, O.R. (2002). Realized and potential climate niches: a comparison of four rhododendron tree species. *Journal of Biogeography*, **29**, 545–554.

Vornanen, M., Haverinen, J., & Egginton, S. (2014). Acute heat tolerance of cardiac excitation in the brown trout (Salmo trutta fario). *The Journal of Experimental Biology*, **217**, 299–309.

Weithoff, G., Lorke, A., & Walz, N. (2000). Effects of water-column mixing on bacteria, phytoplankton, and rotifers under different levels of herbivory in a shallow eutrophic lake. *Oecologia*, **125**(1), 91–100.

Wenger, S.J., Isaak, D.J., Luce, C.H., Neville, H.M., Fausch, K.D., Dunham, J.B., … Williams, J.E. (2011). Flow regime, temperature, and biotic interactions drive differential declines of trout species under climate change. *Proceedings of the National Academy of Sciences of the United States of America*, **108**, 14175–14180.

Wiens, J.J. (2011). The niche, biogeography and species interactions. *Philosophical Transactions of the Royal Society B: Biological Sciences*, **366**(1576), 2336–2350.

Wittmann, M.E., Barnes, M.A., Jerde, C.L., Jones, L.A., & Lodge, D.M. (2016). Confronting species distribution model predictions with species functional traits. *Ecology and Evolution*, **6**, 873–879.

Wood, S.N. (2011). Fast stable restricted maximum likelihood and marginal likelihood estimation of semiparametric generalized linear models. *Journal of the Royal Statistical Society: Series B*, **73**(1), 3–36.

Woodin, S.A., Hilbish, T.J., Helmuth, B., Jones, S.J., & Wethey, D.S. (2013). Climate change, species distribution models, and physiological performance metrics: predicting when biogeographic models are likely to fail. *Ecology and Evolution*, **3**, 3334–3346.

Woodward, G., Perkins, D.M., & Brown, L.E. (2010). Climate change and freshwater ecosystems impacts across multiple levels of organization. *Philosophical Transactions of the Royal Society B: Biological Sciences*, **365**, 2093–2106.

Wootton, R.J. (1998). Ecology of teleost fishes. 2nd ed. Kluwer, London.

Wu, J., & Li, H. (2006). Concepts of scale and scaling. In: J. Wu , K. B. Jones, H. Li & O. L. Loucks (ed) Scaling and Uncertainty Analysis in Ecology: Methods and applications (pp. 3-16). Springer, Dordrecht.

Zeiler, M.D. (2012). ADADELTA: An Adaptive Learning Rate Method. Arxiv.org. N.p. https://arxiv.org/abs/1212.5701

Zhang, W., & Goh, A.T. (2016). Multivariate adaptive regression splines and neural network models for prediction of pile drivability. *Geoscience Frontiers*, **7**, 45–52.

Acknowledgements

Throughout the writing of this thesis over the past years I have received great support from many people in different ways. I am very grateful for each one of them.

In particular, I would like to express my sincere thanks to my supervisor Danijela Markovic-Bredthauer for enabling me to do this research, to gain valuable experience and to learn from her comprehensive expertise. I want to thank her for the constructive and professional discussions as well as her encouragement, which has created a very pleasant working atmosphere and always motivated me to do this work. I am also very grateful for the many opportunities she provided to visit great international meetings and conferences.

Furthermore, I want to thank Karin Frank for being my second supervisor. I am thankful for her helping feedback on this thesis and her valuable advices.

Moreover, I would like to acknowledge Christopher T. Filstrup, Christof Schneider, Daniel Hering, Ariane Walz, Jörg Freyhof, Orhideja Tasevska, Suzana Patceva, and Mario Brauns who provided important help for the creation of the interdisciplinary studies.

Additionally, I am thankful to my family, Viktor, Nelia, Victor and Jan, and my girlfriend who have supported and prayed for me in every situation. I would also like to thank my bible study group for the strong support in prayer. Finally, I am grateful for the whole experience, the people that God brought into my life in this life phase as well as the motivation and strength for everything received through the grace of Jesus Christ.